AFWTR-TR-67-1

3 3679 00060 6915

BNWL-572 VOL II

UC-53, Meteorology

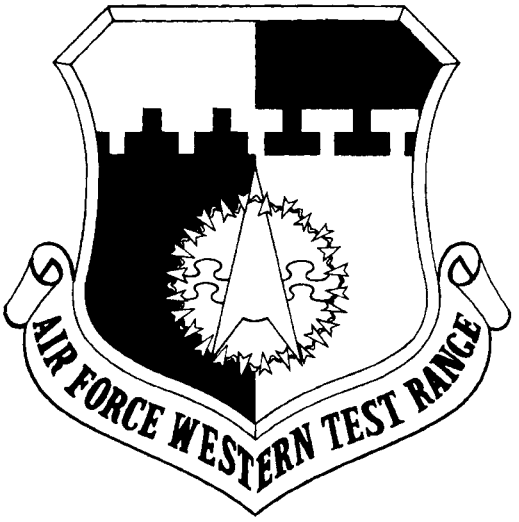

TECHNICAL REPORT

THE MOUNTAIN IRON DIFFUSION PROGRAM: PHASE I SOUTH VANDENBERG: VOLUME II

By

W. T. Hinds and P. W. Nickola

Atmospheric Sciences Section
Environmental and Radiological Sciences Department

January, 1968

PACIFIC NORTHWEST LABORATORY
BATTELLE MEMORIAL INSTITUTE
RICHLAND, WASHINGTON

Printed in the United States of America
Available from
Clearinghouse for Federal Scientific and Technical Information
National Bureau of Standards, U.S. Department of Commerce
Springfield, Virginia 22151
Price: Printed Copy $3.00; Microfiche $0.65

TABLE OF CONTENTS

LIST OF FIGURES

LIST OF TABLES

THE MOUNTAIN IRON DIFFUSION PROGRAM: PHASE I

W. T. Hinds and P. W. Nickola

INTRODUCTION

The advent of Air Force missile operations at South Vandenberg brought the need for prediction of hazards involved in nonroutine circumstances. Although a prediction technique existed for North Vandenberg, no confidence could be placed in predictions using that equation and technique over the substantially more mountainous terrain characterizing the southern portion of the Base. Thus, the need, at South Vandenberg, for an atmospheric diffusion testing program was recognized and Operation Mountain Iron was initiated.

The problems involved in Mountain Iron were numerous and complex; not the least was the rugged terrain, which prohibited striking off sampling arcs concentric about release points--the classic and simplest concept of atmospheric diffusion experimental designs. Furthermore, the understanding desired from these tests seemed likely to require a detailed definition of the varying structure of the atmosphere over South Vandenberg--detail beyond the standard observations of weather conditions.

The purpose of the study was to determine an empirical diffusion equation for South Vandenberg. The scope of the operation included 1) tracer releases from two sites near two launch points and collection of diffusion and meteorological data over South Vandenberg; 2) reduction and analysis of diffusion and meteorological data for South Vandenberg. Beyond this, the analysis yielded additional information on trajectories and WIND* system station suitability.

---

* Weather Information Network and Display

The total amount of data gathered during the Mountain Iron series is overwhelming, and certainly all of it could not be fully utilized for the multiple purposes to which it might apply. Indeed, many aspects of atmospheric behavior, e.g., seabreeze circulation onset and decay and its relation to diffusion, were not even considered for detailed study. Therefore, the data gathered during the testing series were set up for storage in more detail than usual because of their remaining value beyond their initial application.

To enhance the use of Mountain Iron program results, two Volumes have been prepared: Volume I, which mainly presents the operational use of the equation, and this Volume II, which contains a detailed discussion of techniques and data analysis. A description of the physical setting of South Vandenberg is contained in both volumes, * to provide geographical nomenclature and relationships to the readers. Chapter 2 describes the experimental technique, meteorological support, and some of the problems involved in the program. A summary of the test conditions and data reduction methods is also included. In Chapter 3, a brief presentation of the theory of turbulent diffusion is given. Chapter 4 deals with data aquisition and reduction. Chapter 5 presents the diffusion data in summary form, and discusses the methods used for estimating plume growth. The integration of the data into theoretical relationships is discussed in Chapter 6. The results of brief investigations into other aspects of the Mountain Iron data, such as short-term releases and trajectory determination, are discussed in Chapter 7. Finally, to lend confidence to use of the data and resulting equations, the Mountain Iron data are compared in several ways in Chapter 8 to earlier data from North Vandenberg and Hanford. Appendices contain a tabulation of the basic diffusion data, a listing of terminology and units, and aircraft sampling results.

---

* Chapter 3, Volume I and Chapter 1, Volume II

Some brief mention should be made of the choice of experimental procedure. The technique used for Mountain Iron is very nearly identical to that used for Dry Gulch and Ocean Breeze, so the data should be directly comparable. The minor deviations in experimental design for Mountain Iron are described in Chapter 2.

Of more importance is the path chosen for analysis of such a complex set of data. Of several alternatives, two were finally settled upon as most likely to yield useful and profitable results. One was simply to follow the lead of the WIND equation method--statistical determination of the best-fit equation in a product form of equation. The fundamental reason for adopting this method was the guarantee of useful results although the degree of reliability was unpredictable. This last fact led us to parallel the statistical approach with attempts to fit the data into models which were derived from physically based reasoning. In deference to the complexity likely to be induced by the terrain, no guarantee of success or simplicity could be predicted for this "physical" approach, but if successful, this approach was the more likely to yield insights into the processes involved in diffusion over and around hilly terrain. Such insights would be valuable in suggesting courses of action when faced with differing source points, or differing terrain, something lacking completely in the statistical approach. Satisfactory results were achieved with both approaches although the statistical model was slightly better than the "physical" model. However, the later would most certainly improve with continued examination of the mechanisms which act to disperse airborne materials.

SUMMARY

The Mountain Iron diffusion program consisted of 113 tracer releases from two source points on South Vandenberg Air Force Base. The experimental design incorporated a tracer procedure identical to that used during the Ocean Breeze and Dry Gulch programs, but the sampling grid for the Mountain Iron series used existing roads, rather than circular arcs, for sampler access. Meteorological support for the test series consisted of :

- Battery-powered cup-and-vane anemometry at the source point and at eleven outlying sites spread over South Vandenberg
- WIND system sensors at several sites as the sensors were installed
- Wiresonde temperature soundings at the source point
- Radiosonde data from four sites on South Vandenberg.

Diffusion measurements were made by some 300 air samplers at distances from about a half mile to nearly 10 miles, and by an airborne concentration sensor during a portion of the tests.

Analysis of the data led to a reliable method of predicting σ_y, the standard deviation of crosswind plume spread, as a function of lateral turbulent intensity and travel time. No measurements of vertical turbulence were made from which vertical plume spread could be estimated; instead, vertical temperature difference was used to characterize vertical diffusion. However, a physically based model, accounting for lateral and vertical diffusion in the continuity equation, was not more successful than a simpler statistical fit similar to that used for the North Vandenberg Equation. Nevertheless, the statistical fit yielded a functional form which is, itself, physically satisfactory. The recommended equation provides predictions within a factor of two of observed dependent data, 75% of the time, and within a factor of four, 97% of the time. The equation uses distance (feet), standard deviation of 10-second averages of source point wind direction fluctuations (degrees), mean wind speed at 12 feet (knots), temperature difference between 6 and 300 feet ($^{\circ}$F), pollutant concentration (parts per million) and rate of release

(pounds per minute). A similar equation using temperature difference between 6 and 54 feet yields comparable accuracies, except 73% of the predictions are with a factor of 2.

At the 95% confidence level, the recommended equations for NO_2 are

$$\chi/Q = 2.13 \times 10^5 \, X^{-1.85} \, \sigma_t^{-0.355} \, \bar{u}^{-0.868} \, (\Delta T_6^{300} + 10.8)^{1.14}$$

$$\chi/Q = 1.14 \times 10^5 \, X^{-1.82} \, \sigma_\theta^{-0.417} \, \bar{u}^{1.03} \, (\Delta T_6^{54} + 9)^{1.55}$$

$$X = 790 \, (\chi/Q)^{-0.54} \, \sigma_\theta^{-0.192} \, \bar{u}^{-0.470} \, (\Delta T_6^{300} + 10.8)^{0.616}$$

and

$$X = 608 \, (\chi/Q)^{-0.55} \, \sigma_\theta^{-0.229} \, \bar{u}^{-0.566} \, (\Delta T_6^{54} + 9)^{0.852}$$

In terms of an arbitrary gas of molecular weight M, the corresponding equations are

$$\frac{\chi M}{Q} = 98 \times 10^5 \, X^{-1.85} \, \sigma_t^{-0.355} \, \bar{u}^{-0.868} \, (\Delta T_6^{300} + 10.8)^{1.14}$$

$$\frac{\chi M}{Q} = 52.5 \times 10^5 \, X^{-1.82} \, \sigma_\theta^{-0.417} \, \bar{u}^{-1.03} \, (\Delta T_6^{54} + 9)^{1.55}$$

$$X = 6250 \, \left(\frac{M}{Q}\right)^{-0.54} \, \sigma_t^{-0.192} \, \bar{u}^{-0.470} \, (\Delta T_6^{300} + 10.8)^{0.616}$$

and

$$X = 5000 \, \left(\frac{M}{Q}\right)^{-0.55} \, \sigma_t^{-0.229} \, \bar{u}^{-0.566} \, (\Delta T_6^{54} + 9)^{0.852}$$

The recommended equations are applicable only to continuous ground level nonbouyant releases with the source located within the area bounded approximately by Pad A, Palc I, Palc II and Pad D. The data available from the secondary source point, near Pad D, compared favorably with the predictions from the equation developed for the

primary source point near Palc II. Thus, only one equation was recommended for both source points, with the restriction that the equation must not be extrapolated much beyond the sampling distances, about 10 or 11 miles.

Aircraft sampling indicated that an inversion base is usually the upper limit of vertical diffusion but a slightly stable layer may be penetrated. The horizontal limits of the plume aloft are rather well estimated by the limits observed on the ground, which are extrapolated downwind if necessary. In most cases, strong direction shear in winds aloft accompanied a displacement from the surface plume pattern of the aircraft-sampled plume.

The relationship between χ_{ip}, the peak instantaneous concentration aloft, and $\overline{\chi}_p$, the mean concentration at the ground-level plume centerline, is given by the expression

$$\chi_{ip}/\overline{\chi}_p = 2.0\, X^{1.2}$$

where X is the distance from the source in kilometers.

CHAPTER 1.
PHYSICAL AND CLIMATOLOGICAL DESCRIPTION OF SOUTH VANDENBERG

INTRODUCTION

A very brief description of the geography and climatology will be given here, while the relation between terrain and diffusion will be discussed later. Also, the relatively short time available for collection of climatological data precluded any thorough climatological summary. The climatology published by Meteorology Research, Inc., in conjunction with an earlier study [1] is still appropriate and, in many places, provides insight into the meteorological phenomena at South Vandenberg.

THE SITE

South Vandenberg lies on a westward jutting portion of the California coast about a hundred miles west-northwest of Los Angeles (Figure 1). The Coast Range Mountains dwindle into the ocean along this section of the coast, and form the eastward buttresses of the Santa Ynez Mountains which culminate in 4000-foot high ridges several miles east of South Vandenberg. The mountains are characterized by ridges 1000 to 1500 feet high, running generally east-west, with 2000-foot high peaks along the southern portion of South Vandenberg. The most striking feature is probably Honda Canyon, a rather deep and steep-sided canyon, walled on the south by Honda Ridge and on the north by Target Ridge. The canyon is some 700 or 800 feet deep along most of its length, and is generally no more than 1 1/2 miles across. Smaller canyons, which are not so deep but are even narrower (opening mostly north and east), branch from these two main ridges. The result is a broken appearance which is much more rugged than the description in feet and miles implies. The prominent terrain features affecting Mountain Iron Phase I are identified in Figure 2.

The northwest portion of South Vandenberg is the Lompoc Terrace, several square miles of level and rolling grassland only a few hundred feet above the ocean. North of this plateau lies the very flat flood plain

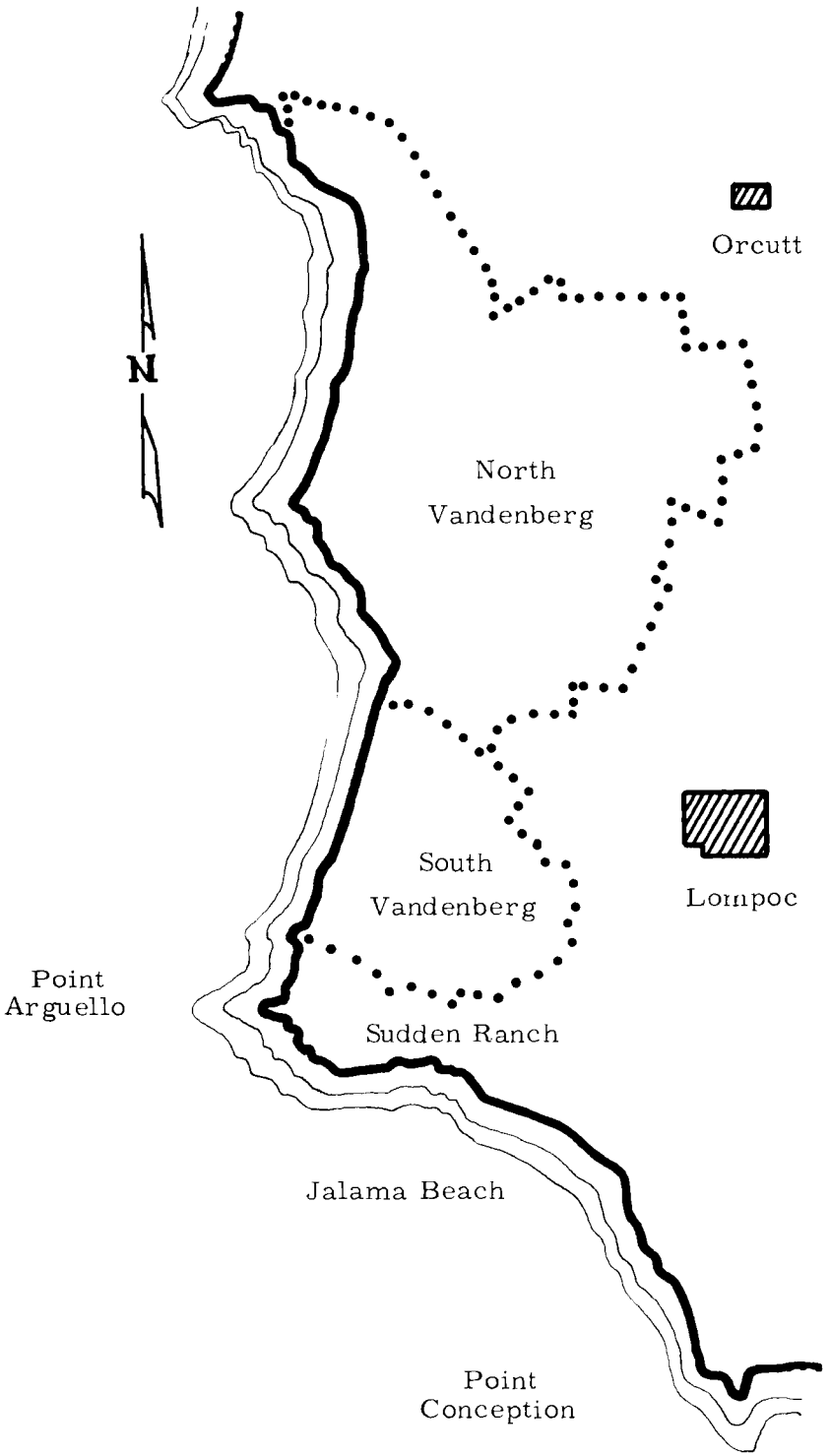

FIGURE 1. Vicinity Map

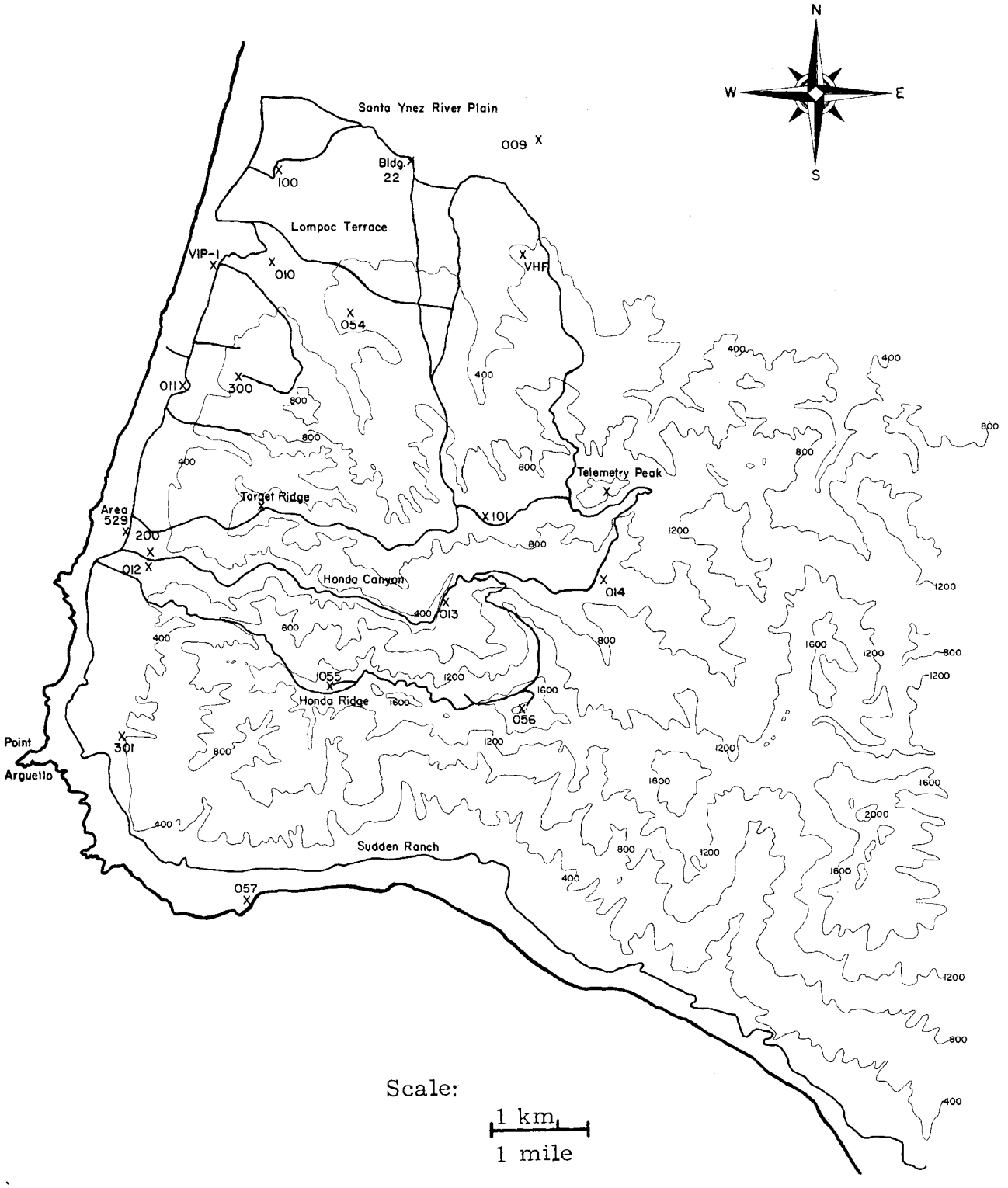

FIGURE 2. Prominent Terrain Features, MI-Phase I

of the old Santa Ynez River; from this smooth river bottom, the Santa Ynez Mountains rise abruptly like a pile of sand on a table top. The coastline lies nearly north-south along the portion of South Vandenberg north of Honda Ridge, then turns more than 90 degrees to east-west along the southern border south of Point Arguello. This abrupt curvature of the coast appears to be related to the common occurrence of northwest winds over South Vandenberg that back to west winds over Point Conception a few miles south of Point Arguello.

The major ridges on South Vandenberg are mostly covered with a dense stand of low growing chapparal and related shrubs, as shown in Figure 3, whereas the low lands are generally grassland--the floor of Honda Canyon, the Sudden Ranch area, and the Lompoc Terrace being examples. Trees occur in scattered clumps only, except east of the head of Honda Canyon and along creek beds. The vegetation types change rather rapidly with increasing distance from the ocean; trees occur in increasing number following the generally increasing average precipitation inland in this area.

CLIMATOLOGY

The period of time during which Mountain Iron Phase I was fully operational spanned only eight months, much too short for a climatological summary. However, wind data from several sites were available for many days of the months between January 1966 and July 1966. The midseason months--January, April and July-- were chosen for complete reduction of all wind data available from several sites: 100, VHF, 200, Target Ridge, 101, 055 and 301 (when available). The wind data were read as 30-minute averages centered on the quarter hours, with direction read to 8 points of the compass and speed in 5 knot increments or calm.

The data were then summarized by averaging over all days of the month and over a given time interval. The time intervals chosen were 1/2, 1, 2, 3, 4, and 6 hours, starting at 0000 hours. A tabulation of the summary is included as an Appendix in Volume I. Included

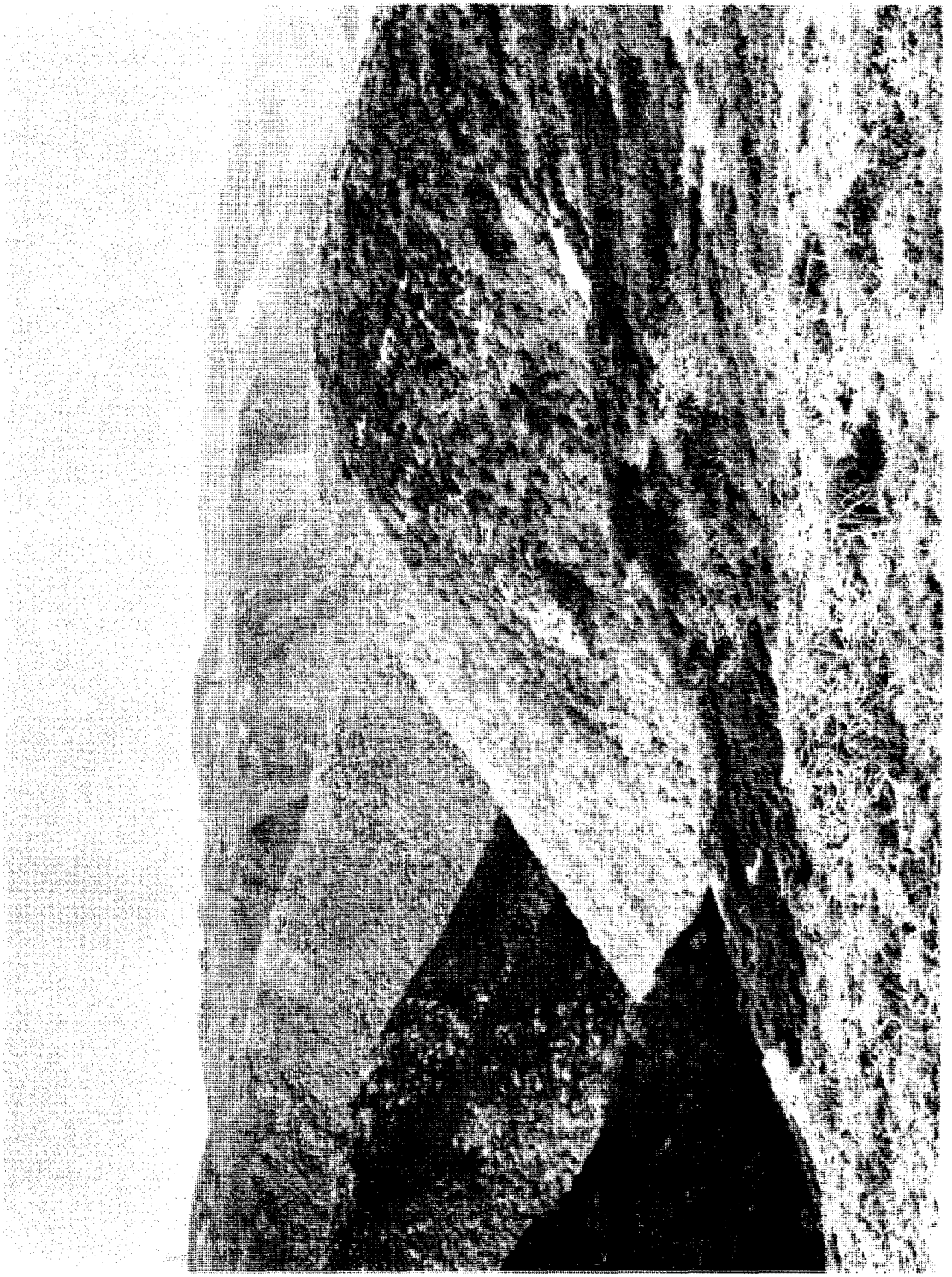

FIGURE 3. Low, Dense, Foliage on Major Ridges of South Vandenberg

in the monthly summary for each site is the highest observed 30 minute average wind speed, the direction from which it came, the percentage distribution of wind directions in the given time period, and the average speed during that time period.

A fairly complete picture of wind patterns over Southern California is given by Demarrais, Holzworth and Hosler[2] for the mid-season months. By use of their regional analysis as a backdrop and the data presented here for details of flow over South Vandenberg, a fairly reliable generalized picture of transport should be possible. To illustrate the expected patterns over South Vandenberg in a general sense, a series of maps are included in Appendix C, Volume I; these maps show the most probable 1-hour average wind directions for day and night conditions during the 3 midseason months.

CHAPTER 2.
EXPERIMENTAL PROCEDURES

The experimental procedures adopted for Operation Mountain Iron were directly descended from procedures used successfully in the past for the Green Glow, Ocean Breeze, and Dry Gulch diffusion programs. The test design embodies a continuous constant-rate release of an inert tracer that follows atmospheric motions. This chapter contains a description of the plume generation and assay techniques, the sampling grid, and meteorological support. A discussion of some problems encountered during the program is also included.

PLUME GENERATION

The atmospheric tracer material used during these experiments was the fluorescent pigment zinc sulfide, U.S. Radium Corporation designation No. 2210. It is a very fine particulate that fluoresces green under ultraviolet light. The particle size distribution is nearly log-normal, with a geometric mean of 2.5 microns and a standard deviation of the logarithms of the diameter of 0.70. The material's specific gravity is 4.1.

To prepare the tracer for release, a small amount of water (about 1/2 gallon) was added to the dry material, and the mixture was thoroughly blended with a paint shaker. The slurry was then transferred to a large formulation tank for further mixing with additional water for at least 20 minutes before release through the dispenser. The suspension was well stirred in the formulation tank during the release period by a propeller-type industrial mixer to assure homogeneity.

The fluorescent pigment slurry was dispensed through standard Todd Insecticidal Fog Applicators, (TIFA). The TIFA is an aerosol fog generator consisting of four primary components:

- An air blower, which delivers 160 cfm to the atomizer cup and which atomizes the liquid carrier
- A combustion chamber, used to heat the air from the blower to aid evaporation of the carrier

- A formulation pump to supply the formulation to the atomizer cup under pressure
- A 7.5 hp gasoline engine, to drive the blower and the pump and, also, to supply a continuous electric spark to fire the combustion chamber.

Two to four generators, operating in unison with a common formulation tank, yielded release rates up to 30 kg per hour, depending upon individual test requirements. The dispensing rate was varied by adjusting the formulation pressure, by adjusting the droplet size selector, by adjusting slurry concentration, or a combination of all three. (Once set, the dispensing rate is essentially constant.) Generally speaking, a volumetric generation rate of 20 gallons per hour and a blower air temperature of 1000 °F produces a spray that essentially evaporates with a few feet of the nozzle. For portability, the TIFA's were mounted on a modified missile trailer. The effective source height was 2 to 6 meters above ground, with the nozzles of the four dispensers aimed to converge at about that height in front of the generators to produce essentially a point source. Figure 4 shows the generation site with the TIFA's in operation.

The generation rate was set prior to each release and not altered after generation was started. The actual amount of pigment emitted during each run was computed by subtracting the amount of formulation remaining in the tank at the end of the generation period from the total at the beginning.

The primary sampler used in Operation Mountain Iron experiments was a membrane filter inserted in a disposable polyethylene holder. Samples collected on a filter were bulk samples intended to collect all pigment passing through the intake zone during a given run.

Figure 5 shows the sampler unit, made up of five parts:

- The base contains a cavity where a disc of creped-paper filter backing is inserted.

FIGURE 4. Source A Generation Site

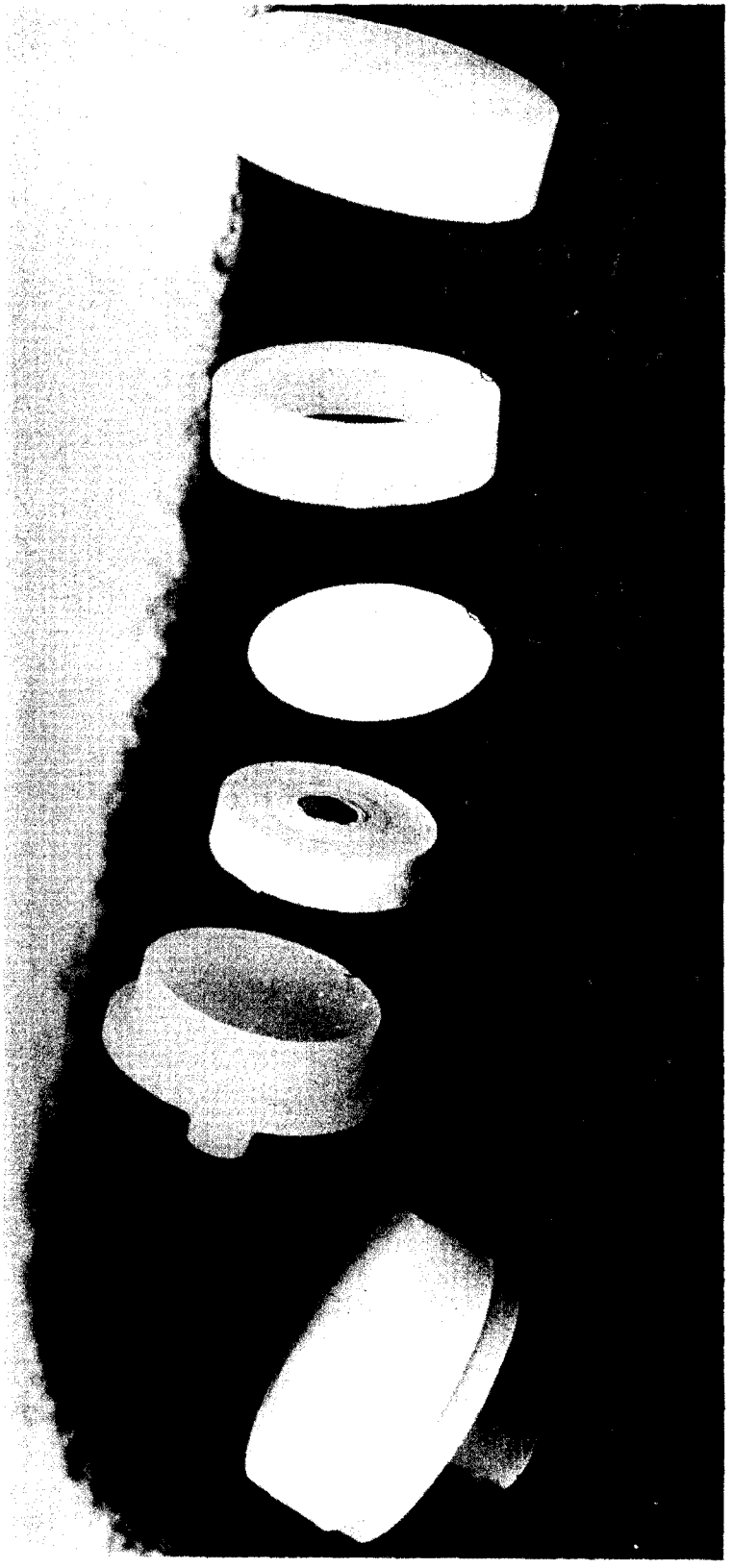

FIGURE 5. Exploded View of Air Sampler

- A molecular membrane filter* is placed on the plane circular surface formed by the base and the filter backing.
- The retaining ring pinches the periphery of the filter tightly against the base, while the circular area of 1 5/8 inch diameter, still exposed, is supported by the porous creped-paper backing.
- The dust cap merely protects the filter surface, both prior to and subsequent to sampler exposure.

Vacuum is applied at the ribbed nozzle of the base, and the dust cap is removed during field operation. Each filter holder was used only once; thus, there was a complete new set of sampling units for each field test, which eliminated any possibility of contamination from the sampling assembly.

The basic vacuum system used throughout consisted of a Gast Model 2565V, heavy duty, vane-type vacuum pump driven by a Clinton Series 290, Model TBA, air-cooled, 4-cycle, 1-cylinder, gasoline engine shown in Figure 6. Each unit can provide 5 cfm of air flow at critical flow and operated for about 4 hours without refueling.

SAMPLE ASSAYING

The filters were assayed for zinc sulfide tracer material with automatic equipment that required the pigment be held on the surface of the filter and not deeply enmeshed in the filtering medium. The filter used provided a compromise between the requirements for a "hard surface" and relatively low resistance to air flow required by the large volumes of air to be sampled. The diameter of the smallest particulates completely (99+%) retained on the surface of this filter was less than 1 micron. In addition, membrane filters are soluble in a variety of solvents, making it possible to assay the pigment in the presence of considerable amounts of dust if necessary.

---

* Membrane Filter, 47 mm diam, Type GM-1 of Gelman Instrument Co., Ann Arbor, Michigan

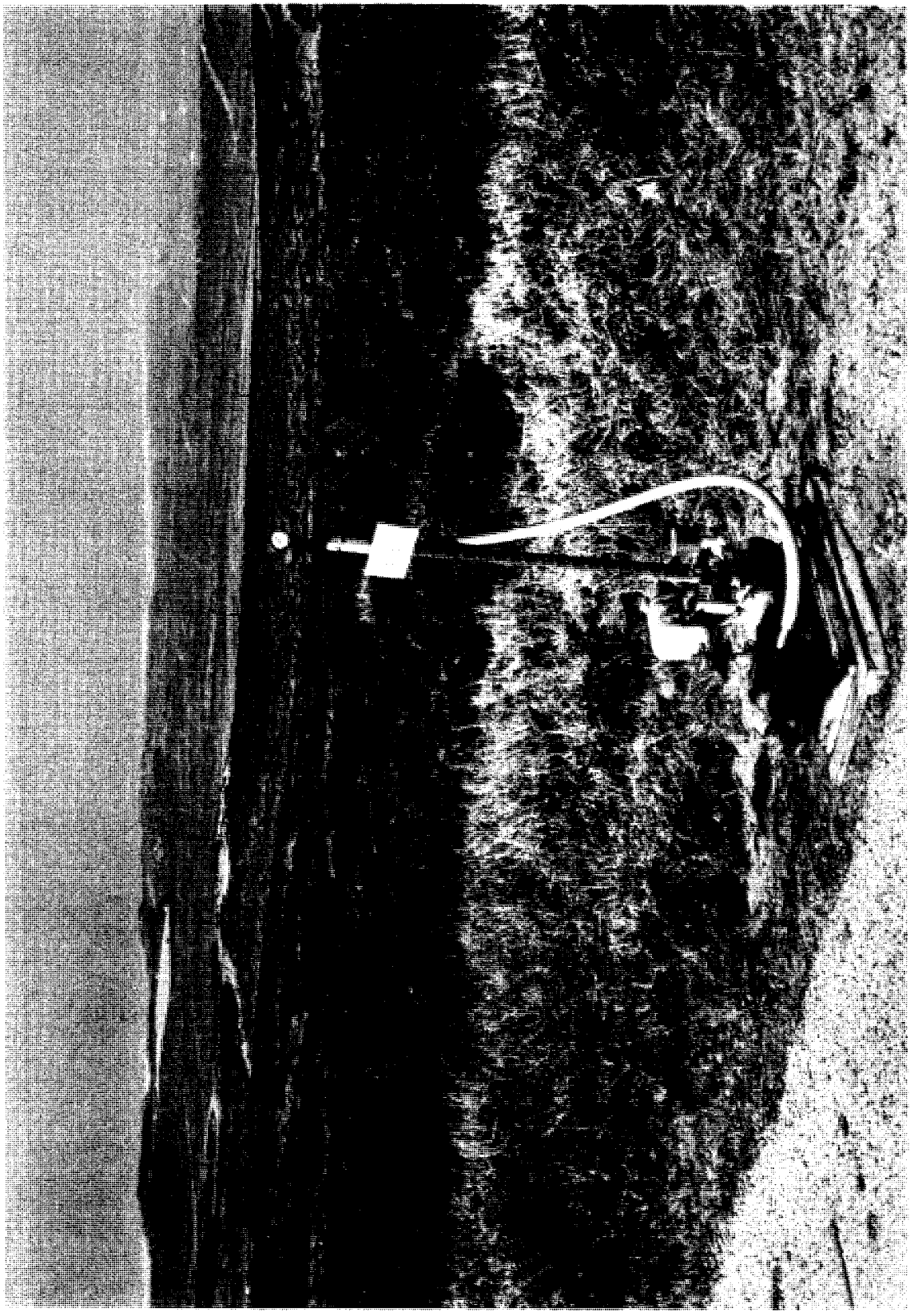

FIGURE 6. Typical Air Sample Site

The bulk samples from the field were assayed by use of the Rankin counter (developed at Hanford), which uses an alpha emitter to activate the fluorescent pigment deposited on the membrane filter.

Figure 7 shows, schematically, the principle of operation. The filter on which the zinc sulfide is deposited is placed beneath a phototube, surrounded by a 200 microcurie plutonium source in the shape of an annulus. The plutonium alpha particles bombard the zinc sulfide resulting in scintillations which are seen by the phototube and tallied on a scaler. Since detailed description of the counter can be found in Barad and Fuquay,[3] it will not be discussed here.

Count reproducibility with the Rankin counter is good. Since the actual count to mass calibration was not far from linear, the same statement can be made regarding mass indicated for repeated assays of a given filter. Table I gives values of $\sigma_x/\bar{x}$ for various count (mass) values for the counter used. The σ_x is the standard deviation on repeat counts of a given filter, and $\bar{x}$ is the mean count.

TABLE I. Values of $\sigma_x/\bar{x}$ for Various Count Values

Counts/min	Mass, g	$\sigma_x/\bar{x}$
100	6.6×10^{-8}	0.16
1,000	5.9×10^{-7}	0.048
10,000	5.3×10^{-6}	0.038
100,000	4.8×10^{-5}	0.012
1,000,000	4.4×10^{-4}	0.011

The standard error increases rapidly for counts near 100, but the analysis was generally restricted to counts greater than about 500, so no great error was introduced here.

THE SAMPLING GRID

Ordinarily, diffusion tests are designed with sampling arcs concentric about the source point and spaced logarithmically to reflect the expected power-law decrease of exposure with distance.

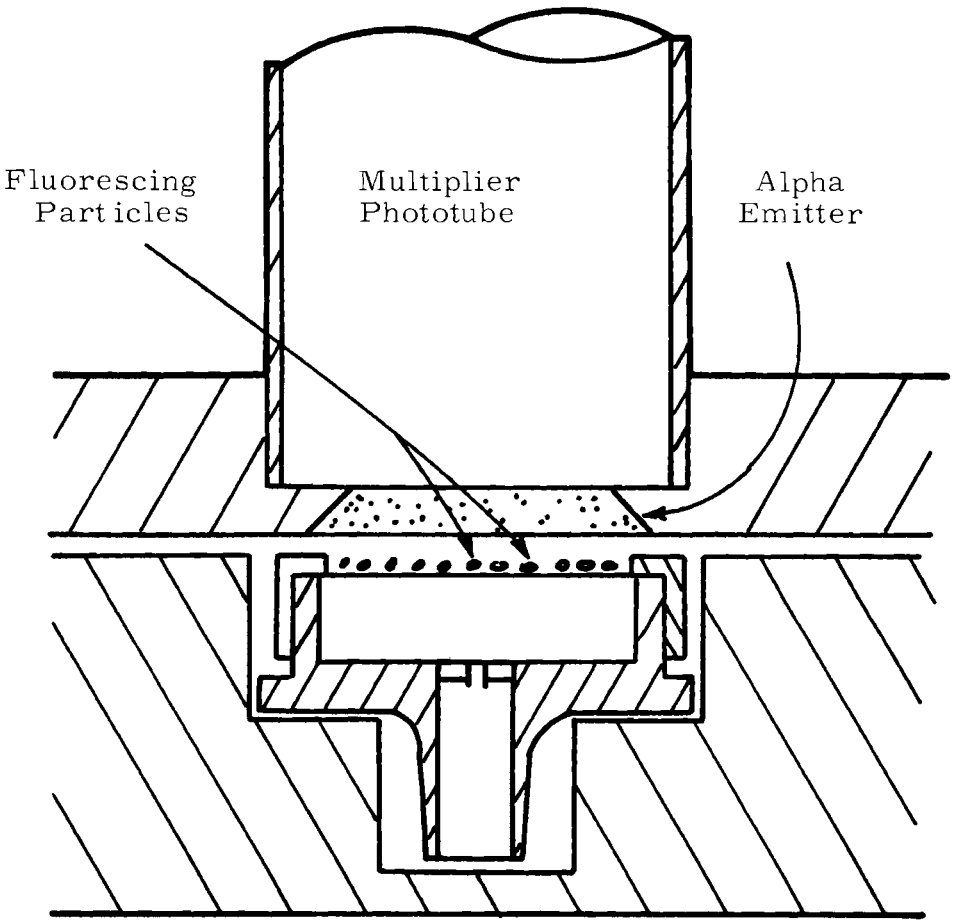

FIGURE 7. Schematic Drawing of Rankin Counter Geometry

This type of design was inconceivable at South Vandenberg, as thoughtful contemplation of a topographical map will show. However, existing roads and jeep trails provided, with a few drawbacks, a suitable network of possible sampling routes. The roads, in general, follow creek banks and ridge tops; the chosen routes are indicated in Figure 8, with many existing roads and trails ignored.

The routes chosen provide adequate sampling from the primary source point [the VIP-1 helicopter pad, near launch complex II (Palc II)], especially in the prevailing winds, northwest and north-northwest. Approximately, sampling distances in these conditions are 1 1/2, 2 1/2, 4, 6, 7, and 10 km. From the source point, with westerly winds, sampling distances approximate 1, 4, and 6 km, which is a somewhat less satisfying set of measurements but still adequate.

The situation was far less satisfactory when sampling from the second source (Area 529, near Scout Pad D) was considered. Located at the foot of Honda Canyon, Area 529 is geographically notable in that all contiguous major topographical features effectively radiate from it, thus roads following the major features are radial, not circumferential. The consequence of this arrangement was to provide poor crosswind plume definition and to leave in question the true peak concentration for releases from this source point, except for winds with a strong northerly or southerly component. The sampling distances from Area 529 were approximately 6 and 7 1/2 km for southwesterly winds; 5 1/2 km in westerly winds; and 1/2, 1, and 5 1/2 km in northwesterly winds.

Occasionally, depending upon wind conditions, tests from both sites yielded samples at distances exceeding 12 or 13 km, usually from the southern end of the Sudden Ranch sampling area. These important data were few because, in general, they are caused by an especially strong curvature of wind flow in the lee of the Santa Ynez mountains.

The samplers along the routes chosen were nominally spaced one-tenth mile apart along Routes 1, 3, 6, and portions of 2 and 10; two-tenths mile apart along Routes 4, 5, 7, and the remainder of 2 and 10; and

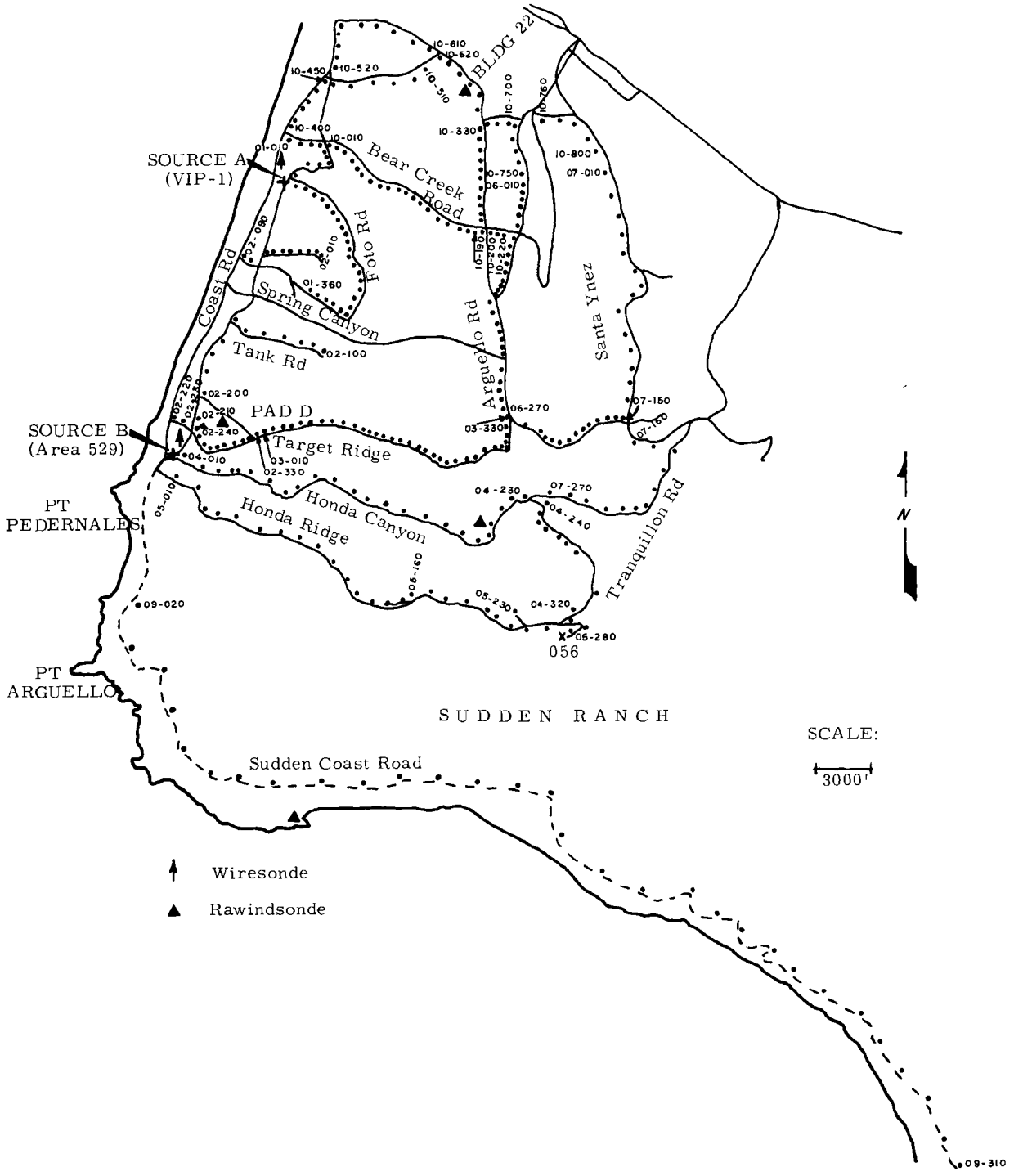

FIGURE 8. Air Sampler Grid and Upper Air Sounding Stations

four-tenths mile apart along Route 9. Figure 8 is a detail map of the sampler network, illustrating the dense network of sampler stations and defining the sampler routes. The occasional uneven spacing indicates a nominal sampler position with a particularly undesirable exposure that could be improved by a small variation in spacing. Rocks, trees, buildings, and brush commonly occasioned such variations. Larger scale factors could not be dealt with so handily; cuts for a roadway along the lee side of ridges induced several cases of poor sampler siting, which were unavoidable without seeking or building new roads. The most striking examples of this situation lay along Honda Ridge between Sites 05-050 and 05-100; a few samplers were placed along the roadway on the lee (south) side of the ridge behind nearly vertical cuts approaching 100 feet high. Meaningful sampling in the wake of a bluff body is no simple task. In an attempt to estimate the effect of this particular example of undesirable sample siting, an old trail along the crest of Honda Ridge was resurrected and five supplementary samplers placed along it during the summer portion of the test series. In general, the effect was noticeable but not crucial.

A similar perplexity arose when sampler orientation was considered. The air samplers used were not particularly sensitive to misorientation, but, undoubtedly, a wind blowing <u>across</u> the filter face or against the sampler back would yield nontypical exposures. Since the same network was to be used for both sources interchangeably, a single orientation could not be entirely correct. However, the details of topographically influenced wind patterns were mostly unknown--leaving the forecast of wind direction at each sampler to guesswork. Therefore, the simplest solution was chosen: the samplers were faced toward the primary source point. This choice has the advantage of consistency, but it is not unassailable. One exception to this unanimity was the route along the floor of Honda Canyon. Since the canyon is generally rather deep and steep, the flow was expected to be along-canyon rather than across-canyon. Therefore, the samplers were placed facing an up-canyon wind, except in a few unusual circumstances.

METEOROLOGICAL SUPPORT

A considerable effort was required to gather the extensive meteorological support called for in the experimental design of Project Mountain Iron. Very few of the meteorological data were available from standard or existing sites, and thus necessitated a lengthy phase of instrumentation setup and personnel orientation. At the beginning of the Mountain Iron testing program, only three sites were reporting in the WIND system mode: Tower 300 at Palc II, Site 010 in Bear Creek Canyon, and Site 011 in Spring Canyon. To supplement these observations, portable battery operated cup-and-vane anemometers were set up at several sites. The positions of all the meteorological observing positions are shown in Figure 9. Many of these supplementary wind sensors were placed in proposed WIND sensors sites, but a few--notably, Target Ridge, VHF, and Telemetry--were new sites altogether.

Source point observations were made by another battery powered equipment cup-and-vane anemometer set up near the trailer bearing the generators. The temperature structure of the atmosphere at the source point was measured by a wiresonde, which was routinely used to heights of 140 meters (460 feet) at hourly or occasionally half-hourly intervals.

Upper air soundings were ultimately made from four sites: Building 22, the Ionospheric Sounder in Honda Canyon, Pad D area, and from the Boathouse in the Sudden Ranch area. The procedure set for the radiosondes called for a frequency of reading twice the standard to a height of 5,000 feet, with one sounding to be followed to 10,000 feet.

PROBLEMS ENCOUNTERED DURING THE EXPERIMENTAL PHASE

A serious experimental difficulty was sampler access. During the winter rains, some portions of the unimproved roads were quite susceptible to washing and flooding, especially in Honda Canyon. In fact, the Honda Canyon sampling route was usable in its entirety only ten days between late November and March. The data available indicate that Honda Canyon causes anomalous diffusion, but due to its inaccessibility

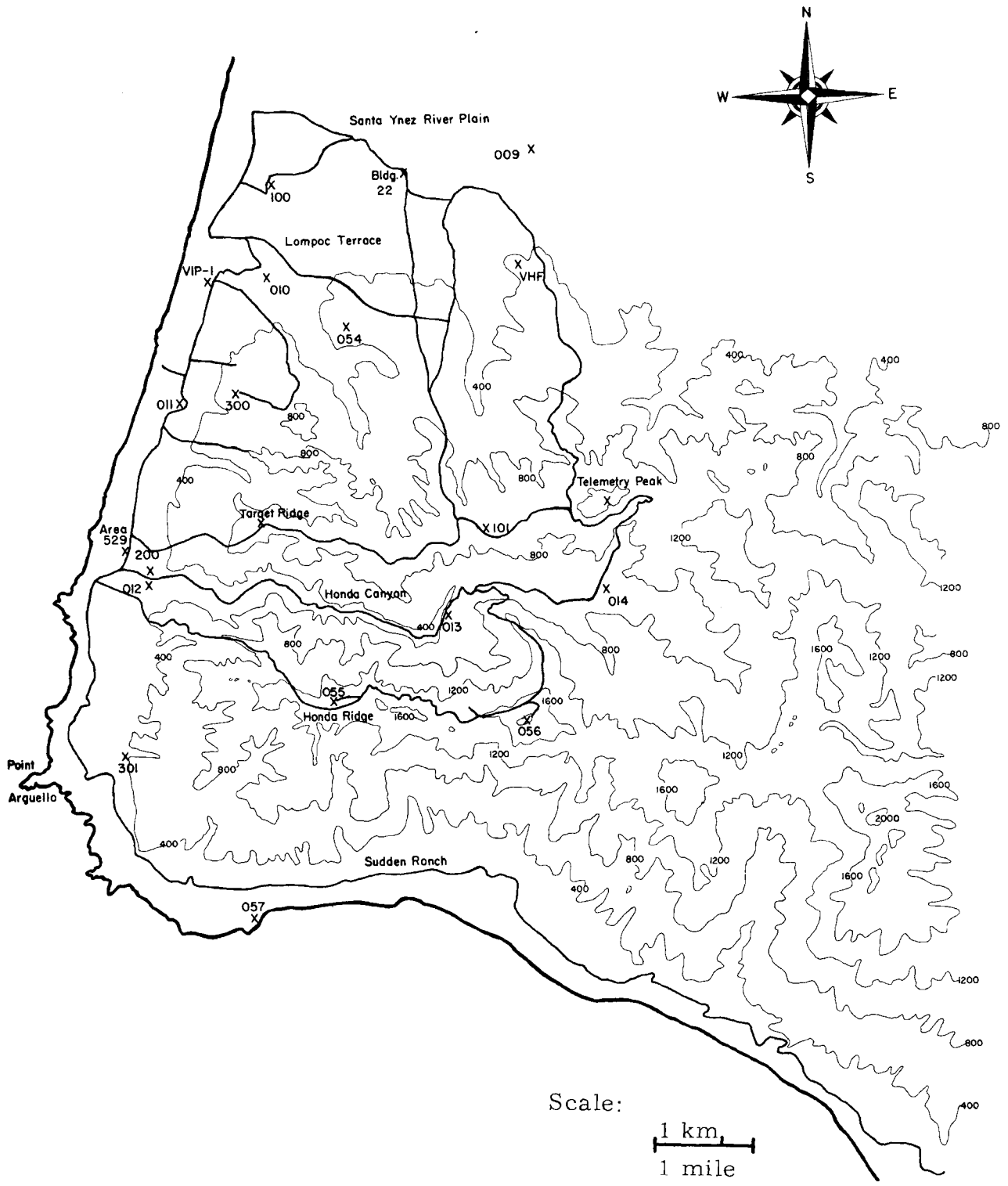

FIGURE 9. Prominent Terrain Features, MI-Phase I

for a substantial fraction of the test series, no positive conclusions can be drawn. Other portions of the network along Target Ridge and Tranquillon Road into the canyon were intermittently impassable for similar reasons, but without such lasting effects on the data gathering effort because access was usually restored in a reasonably short time.

The most serious difficulties were encountered in gathering the meteorological data (as opposed to diffusion data). Since the meteorological effort was large--involving substantial numbers of both men and equipment--a certain amount of difficulty was inevitable.

Meteorological data were of four types, each with its own peculiarities and problems:

- The existing Wind Information Network and Display (WIND) system
- Outlying wind sensors at planned WIND sites and supplementary sites
- Source point data
- Radiosonde data.

The difficulties encountered in each will be briefly outlined, to allow some judgment of the reliability of each.

The radiosonde data were collected according to the best standard procedures. In fact, the radiosonde support was remarkable. Following a relatively slow build-up to the complete data gathering effort, the continuous releases of radiosondes, (each hour for four to six hours each test) provided data deserving of a very extended analysis.

The WIND system was in a continual state of expansion throughout the test series, including the installation of a new computer. Since it was not intended for support of the diffusion testing, the WIND system data was limited in extent and quality for much of the test series and used only in a supplementary sense.

The two remaining categories, forming the fundamental pool of meteorological data used in the analysis, utilized portable equipment. Occasionally, additional attention was necessary to account for

inconsistencies resulting from chart zeroing and chart timing problems. Generally, a rule was adopted that any error of 5% or less would be uncorrected; greater errors required rescaling of charts. In the end, the errors in time probably do not exceed 5% or 6%, and the errors in magnitude are probably not much larger.

CHAPTER 3.
FUNDAMENTAL NOTIONS OF TURBULENT DIFFUSION

Turbulent diffusion is an exceedingly complex phenomenon which has not yet yielded completely to an analytic description. A great deal is known about some aspects of diffusion, particularly in homogeneous conditions--conditions which are invariant with motion in space. In some cases, the real atmosphere does indeed act as a homogeneous fluid but, in general, such simplicity is found only as a limiting case (if at all). Various methods of describing the complexity of atmospheric behavior have been developed in the last generation or two; they fall mainly under two general categories: 1) diffusion proportional to the gradient of the diffusing substance analogous to molecular diffusion, and 2) statistical descriptions of the diffusing substance related to statistical descriptions of concurrent atmospheric motions. The statistical approach has been quite fruitful in the recent past, and forms a reasonably coherent framework upon which experimental measurements may be hung. For our purposes here, the statistical theory will do well enough to describe the results of experimentation.

In this chapter, a fundamental theorem of diffusion will be explained that relates diffusion in homogeneous conditions to meteorological statistics. The distribution of material within a plume will then be discussed, and the form that the equation of continuity takes, according to the distribution in the plume, will be set out for use as a basis for modeling atmospheric behavior. Finally, the complicating effects of the real atmosphere's inhomogeneities will be discussed briefly to provide some feeling for the inevitable lack of precision involved in predictions of diffusion over real terrain.

The relation between concentration and exposure is simply that exposure is the average concentration experienced by the sampler, multiplied by the time the sampler was exposed to the concentration. The ratio of concentration to release rate is equal to the ratio of exposure to total mass released. Since the air samplers used in the Mountain Iron series measured exposure, concentration will not be used in the following analysis.

THEORETICAL BACKGROUND

It seems intuitively reasonable that the atmospheric turbulent motions should be intimately linked with the resulting diffusion of a substance in the atmosphere. This expectation was placed on firm footing by G. I. Taylor[4] in the first of a series of penetrating papers concerning diffusion in turbulent flow. Fundamental to his argument is the correlation coefficient, R, between the displacement of a particle at time t and at time $t + \xi$:

$$R(\xi) = \frac{\overline{y(t)\ y\ (t + \xi)}}{\overline{[y(t)]^2}} \tag{1}$$

The result of his argument is that in homogeneous and stationary conditions (mean values uniform in both space and time) the variance of the lateral particle displacement is

$$\sigma_y^{\ 2} = 2\sigma_v^{\ 2}\int_o^t \int_o^\tau R(\xi)\, d\xi\, d\tau \tag{2}$$

so that the mean-square lateral dispersion of a particle is determined by the variance of the wind fluctuation along the crosswind axis, and the Lagrangian correlation coefficient of particle displacements along that axis at t and $t + \xi$. A detailed discussion can be found in Pasquill.[5] (The Lagrangian type correlation refers to motion in a frame of reference following a particle along its path, as opposed to the Eulerian type, which refers to motion of a sequence of particles passing a given point in space.)

An immediately appealing result can be found from Equation (1) during the time interval in which the correlation is unity:

$$\sigma_y^{\ 2} = \sigma_v^{\ 2} t^2 \tag{3}$$

or

$$\sigma_y = \sigma_v t \tag{4}$$

In words, the growth of a plume from a continuous point source in stationary homogeneous conditions is linearly porportional to travel time near the source. During this time interval, the transford, $X = \bar{u}t$, is accurate. Of course, for a truly useful result, the interval during which the correlation is near unity must be of meaningful length.

The prospect for routine measurement of the Lagrangian spectrum is bleak. Recognizing this, Hay and Pasquill suggested that the Eulerian and Lagrangian correlograms might be related by a simple constant factor, β. Ordinary observations indicate that the Lagrangian correlation must be longer lived than the Eulerian, e.g. smoke from a bonfire or chimney will continue in a straight line from the source long after the wind at the source has changed direction; if so, Hay and Pasquill[5] show how Eulerian measurements can be used as input for the Lagrangian equations given by Taylor's argument.

One particularly interesting result of the Hay-Pasquill postulate is the simple form which results for the dependence of σ_y on σ_v; the detailed derivation found in Pasquill[5] will not be given here. The result of their reasoning is simply

$$\sigma_y^2 = (\sigma_v^2)_{t/\beta}\, t^2 \qquad (5)$$

where v is sampled (i.e., the length of record) over the period of release, and averaged over intervals of length t/β, where t is travel time to a point where σ_y is to be calculated. Thus, the rate of spreading of a plume is related to the corresponding wind fluctuations in a manner very similar to that derived by Taylor.[4] However, Equation (3) required the <u>total</u> variance of wind fluctuations, whereas the Hay-Pasquill technique requires that the fluctuations be increasingly smoothed as travel time t increases, before the variance of the fluctuations is calculated.

The entity β has been related to turbulent structure by reasoning through the characteristics of homogeneous stationary turbulence; the important result is that β is inversely related to the <u>intensity</u> of turbulence,

approximated by $\sigma_v/\bar{u}$. The actual values of β reported by investigators so far have shown a very wide scatter; in general, it seems that β averages about 3 to 5 at most sites. It will be shown later that the Mountain Iron data seem to lead to significantly larger values over the terrain at South Vandenberg. However, the basic result that β is inversely related to turbulent intensity seems consistent with these data.

DISTRIBUTION WITHIN A PLUME

The distribution of matter within a continuous plume is characterized by a maximum which trails off to zero concentration at the edge of the plume. The precise manner in which the concentration decreases determines the form the equation of continuity takes. The equation of continuity--simply a statement of the conservation of mass--states that the mass flux through succeeding vertical planes downwind from the source remains constant and equal to the rate of release. (This statement ignores the depletion caused by interaction with the surface, or other substances in the air; practically all airborne substances can be expected to exhibit such interactions to some degree. Since the Mountain Iron experimental technique was identical with that used for the Ocean Breeze and Dry Gulch programs, for which this depletion was not separated from the vertical diffusion, the same approach will be adopted here to assure that the results from all test series are compatible.) The mass flux through a vertical plane is given by

$$Q_T = \iint Eu \, dydz \qquad (6)$$

Customarily, the surface is treated as a perfect reflector, and the distribution of concentration along the y and z axes is presumed to be Gaussian. This assumption is accurate for the horizontal distribution over uniform terrain; unfortunately, the effect of rough terrain on distribution is not well established. The vertical distribution is roughly Gaussian for plumes released well above the surface, and can be approximated by a reflected Gaussian distribution for releases near the

surface. Here again, the complications induced by rough terrain are not understood. However, with the bivariate normal assumptions, the equation of continuity takes the form

$$\frac{E}{Q_T} = \frac{\chi}{Q} = \frac{1}{\pi \bar{u} \sigma_y \sigma_z} \exp - \left[\frac{y^2}{2\sigma_y^2} + \frac{z^2}{2\sigma_z^2} \right] \tag{7}$$

It is worth noting that if other than the bivariate normal distribution is required for an accurate description, the centerline of the plume [given by the first factor on the right hand side of Equation (7)] is changed only in the constant term, and the constant probably varies less than a factor of two over the range of distributions observed in the atmosphere. A lucid discussion can be found in Pasquill's useful book.[5]

The simple appearance of $\bar{u}$ in Equation (7) belies the complex motions for which it must account. The mean wind speed in the equation is the mean speed over the entire height of the plume and over the time of release, which makes the most representative $\bar{u}$ difficult to determine. Normally, the wind speed at the release height is averaged over the release period for insertion in the equation.

Wind speed, however, is only one of three parameters appearing in the equation; the other two are measures of dispersion of the plume about its mean: σ_y and σ_z. These are of fundamental importance, since they appear explicitly in Equation (2) as the plume parameter tied to turbulent fluctuations and time (or distance). The determination of both σ_y and σ_z allows the direct use of Equation (7) to determine the centerline (maximum) exposure or concentration (which is of course the item of most concern in nearly all applied studies) as a function of travel time or distance.

If Equation (7) is rewritten for centerline exposure with the plume dispersion parameters alone appearing on the right hand side, their importance is clear:

$$\frac{E_p \bar{u}}{Q_T} = \frac{1}{\pi \sigma_y \sigma_z} \tag{8}$$

The choice of which $\bar{u}$ to use is usually forced by lack of appropriate data--data that should ideally include the wind speed appropriate for each sampling station. The experimental design for Mountain Iron included a number of subsidiary wind sensors well scattered over South Vandenberg, so a choice of sites for $\bar{u}$ is possible if desired. Physically, the function of $\bar{u}$ in Equation (8) is to provide a measure of the relative stretching of various portions of the plume. In nondivergent flow, the source point wind speed will suffice; in other conditions no single wind speed is uniquely appropriate. This is just one example of the complicating factors which prevent an accurate determination of centerline exposure as a function of downwind travel.

The mean wind is of more general importance than a measure of plume stretching alone. It was shown in Equation (2) that in stationary and homogeneous conditions, plume growth was dependent on time available for dispersion. However, the commonest method of representing diffusion data has been as a function of distance, not time. This exchange of independent variables does not create a problem in organizing data when the Lagrangian correlation is close to unity. By approximating σ_v with $\sigma_\theta \bar{u}$, Equation (3) then becomes $\sigma_y^2 = \sigma_\theta^2 X^2$. However, if the correlation is less than unity, Equation (2) shows that σ_y is no longer linearly related to time so that an assumed dependence on X ($= \bar{u}t$) retains a residual dependence on $\bar{u}$.

CHAPTER 4.
DATA ACQUISITION AND REDUCTION

TEST CONDITIONS

Since any extensive field program is occasionally plagued by a breakdown in certain portions, it is not surprising that such a large data-gathering effort as this was no exception. The Mountain Iron design incorporated diffusion measurements, micrometeorological measurements, and upper air measurements that provided the possibility for about 160,000 data bits, of which some 130,000 were actually brought for analysis. The relative completeness of the various types of data is shown in Table II.

TABLE II. Completeness of Data

Date Type	Total Possible	% Success
Diffusion	34,000	95
Source winds	31,000	90
Outlying winds	8,000	86
Source temperature soundings	5,000	80
Upper air sounding	72,000	82

Overall, better than 80% of the possible data were successfully measured. The greatest cause of lost data was the relatively slow start of the meteorological network compared to the diffusion tests, but after all systems were in operation, success increased to more than 90%.

A more detailed description of the relative success of each of the 113 tests attempted is given in Table III, where each of the possible types of data is listed explicitly as not available (NA) or available (X). This table readily shows the tests appropriate for detailed analysis, and those that must be used only for the more gross comparative work.

Table III reinforces the statement that after getting under way, the program was marked by few lapses in data gathering efficiency. Also listed in Table III is a brief statement of the test conditions attached to each; length of release, release time, and source point.

TABLE III. Source Point, Length of Release, and Availability of Data

Test	Source Point	Date	Time On	Length of Release	Source Wind	Point Temp.	Out-lying Winds	WIND	Upper Air Source Radiosonde Sites
3	A	1 Dec. 65	1145	30	x	NA	x	NA	1
4	A	10	1201	30	x	NA	x	NA	2
5	A	13	1200	30	x	NA	x	NA	2
6	A	14	1202	30	x	NA	x	NA	2
7	A	15	1210	30	x	NA	x	NA	2
8	A	16	-	-	x	NA	NA	NA	1
9	A	17	1435	30	x	NA	x	NA	1
10	A	20	1200	30	NA	NA	x	NA	1
11	A	3 Jan. 66	1218	34	NA	NA	NA	NA	2
12	A	4	1242	30	x	NA	x	3	3
13	A	5	1145	30	x	NA	x	NA	3
14	A	11	1104	30	x	NA	x	3	3
15	A	11	1345	30	NA	NA	x	3	3
16	A	14	1047	30	x	NA	x	3	3
17	A	17	1055	30	NA	NA	x	3	3
18	A	18	1045	30	x	x	x	NA	3
19	A	24	1040	30	NA	x	NA	4	3
20	A	25	1156	30	NA	NA	x	NA	3
21	A	27	1155	30	x	x	x	4	2
22	A	28	1147	15	NA	NA	NA	4	3
23	A	31	1145	15	x	x	x	4	3
24	A	3 Feb. 66	1130	15	NA	NA	NA	4	3
25	A	7	1045	15	x	x	x	4	3
26	A	7	1255	15	x	x	x	4	3
27	A	8	1159	15	x	x	x	NA	3
28	A	16	1200	15	x	x	x	3	3
29	A	17	1109	15	NA	x	x	3	4
30	A	23	1845	15	x	x	x	NA	4
31	A	24	1845	15	x	x	x	NA	4
32	A	24	2056	15	x	x	x	NA	4
33	A	25	1845	15	x	x	x	3	4
34	A	25	2110	15	x	x	x	3	4
35	A	26	0000	15	x	x	x	3	3
36	A	1 Mar. 66	1900	15	x	NA	x	3	4
37	A	3	0110	15	NA	NA	x	2	4

TABLE III. (contd)

Test	Source Point	Date	Time On	Length of Release	Source Wind	Point Temp.	Out-lying Winds	WIND	Upper Air Source Radiosonde Sites
38	A	7	1146	5	x	x	x	NA	4
39	A	8	1145	15	NA	x	x	3	4
40	A	14	1102	5	x	x	x	3	4
41	A	15	1056	5	x	x	x	3	4
42	A	17	1102	5	x	x	x	3	4
43	A	17	1407	5	x	x	x	4	4
44	A	21	1108	5	x	x	x	4	4
45	A	25	1106	5	x	NA	x	3	4
46	A	28	2310	5	x	x	x	3	4
47	A	29	0253	15	NA	NA	x	3	4
48	A	29	2315	5	NA	x	x	3	4
49	B	6 Apr. 66	1306	15	NA	x	x	2	4
50	A	8	1210	15	x	x	x	NA	4
51	B	11	1302	15	NA	x	x	3	4
52	B	12	1051	30	NA	x	x	3	4
53	A	13	1205	44	x	x	x	3	4
54	B	20	1245	30	x	x	x	5	4
55	B	21	1109	30	NA	x	x	3	4
56	B	22	1115	30	NA	x	x	NA	4
57	B	25	1055	30	NA	x	x	7	4
58	B	25	1407	30	NA	x	x	8	4
59	A	26	1213	48	x	x	x	7	3
60	A	27	1255	29	x	x	x	8	4
61	B	28	1107	30	NA	x	x	NA	4
62	B	2 May 66	1315	30	x	x	x	6	4
63	B	4	1302	20	x	x	x	8	4
64	B	5	1328	30	NA	x	NA	NA	4
65	B	5	1645	30	x	NA	NA	NA	4
66	B	6	1323	30	x	x	x	NA	4
67	B	10	1014	30	NA	x	x	7	4
68	B	11	1007	30	x	x	x	NA	4
69	A	12	1005	30	x	x	x	8	4
70	A	19	1505	30	x	x	x	10	5
71	B	20	1535	30	x	x	x	10	4
72	B	20	1830	30	x	NA	x	10	4
73	A	23	1032	30	x	x	x	8	4
74	A	24	1000	30	x	x	x	11	4
75	A	25	0957	28	NA	x	x	9	4
76	A	26	1100	30	NA	x	x	10	4
77	A	31	1838	30	x	x	x	9	4

TABLE III. (contd)

Test	Source Point	Date	Time On	Length of Release	Source Wind	Point Temp.	Out-lying Winds	WIND	Upper Air Source Radiosonde Sites
78	A	31	2125	30	x	NA	x	9	4
79	A	1 June 66	1834	30	x	x	x	9	4
80	A	1	2145	30	x	NA	x	9	4
81	A	2	2040	30	x	x	x	NA	4
82	B	6	1000	30	x	x	x	9	4
83	B	7	1012	30	NA	x	x	9	4
84	A	10	0942	30	x	NA	x	10	4
85	A	10	1245	30	x	NA	x	10	4
86	A	13	1000	30	x	NA	x	10	4
87	A	13	1310	30	x	NA	x	10	4
88	A	20	2215	30	x	x	x	NA	4
89	A	21	0107	30	x	x	x	NA	4
90	A	21	2300	30	x	x	x	NA	4
91	A	22	0203	30	x	x	x	NA	4
92	B	22	2305	30	x	x	x	NA	4
93	B	23	2215	30	x	x	x	NA	4
94	A	24	0105	30	x	NA	x	NA	4
95	B	28	1112	30	x	x	x	NA	4
96	B	29	1112	30	x	x	x	NA	4
97	B	30	1106	30	NA	x	x	NA	4
98	A	6 Jul 66	1906	30	x	x	x	NA	4
99	A	6	2208	30	x	x	x	NA	4
100	A	7	1900	30	NA	x	x	NA	4
101	A	11	1903	30	NA	x	x	NA	4
102	A	12	1900	30	x	x	x	NA	4
103	A	12	2202	30	x	NA	x	NA	4
104	A	13	1905	25	x	x	x	NA	4
105	A	14	1933	30	NA	NA	x	NA	4
106	A	15	1915	30	x	x	x	NA	3
107	A	18	1102	30	x	x	x	NA	4
108	A	20	1110	30	NA	NA	x	NA	4
109	A	21	1157	30	x	x	x	NA	4
110	A	22	1055	30	x	x	x	NA	4
111	A	25	1400	30	x	x	x	NA	4
112	A	26	1400	30	x	x	x	NA	4
113	A	27	1345	30	x	x	x	NA	4

The distribution of test wind directions is indicated in Figures 10 and 11. These two figures indicate the number of tests in a given direction by the length of the vector extending downwind. The preponderance of testing in northwesterly flow from Source A is obvious (Figure 10), while the Source B tests--much less numerous--were more evenly distributed (Figure 11).

The macroscale conditions of the tests are indicated in Table IV; also listed is a brief summary of meteorological observations during the test period: source point wind speed and direction, the relative humidity, and an approximate geostrophic wind at the beginning and end of the test period. This approximation, being observed winds at 1600 meters height, serves to indicate whether the geostrophic conditions are stationary during the test. If the geostrophic wind is not relatively constant during a particular interval, micrometeorological measurements can be expected not to be stationary, as well. This point was recently developed in some detail by Munn,[6] and provides a possible explanation for some perplexing differences between ostensibly similar conditions. There is little doubt that significant advances in understanding mesoscale diffusion will require cognizance of mesoscale variability of boundary layer flow. There is equally little doubt that the Mountain Iron diffusion data reflect mesoscale diffusion behavior; thus, a most important point is that future work with the data may be expected to be mesoscale in character, rather than microscale, which has in the past characterized the approach to diffusion. It is worth noting that understanding of mesoscale phenomena is by no means as advanced as that of microscale phenomena, a condition arising from the large amount of data thought necessary to properly characterize mesoscale behavior (as presently understood) as well as an inherently more complex theoretical setting.

DIFFUSION DATA REDUCTION

The raw assay data from each of the air samplers were a photomultiplier count of scintillations proportional to the mass of tracer captured on the filter. These counts were each converted to mass, and normalized to the flow rate through the sampler to yield the exposure at that sampler.

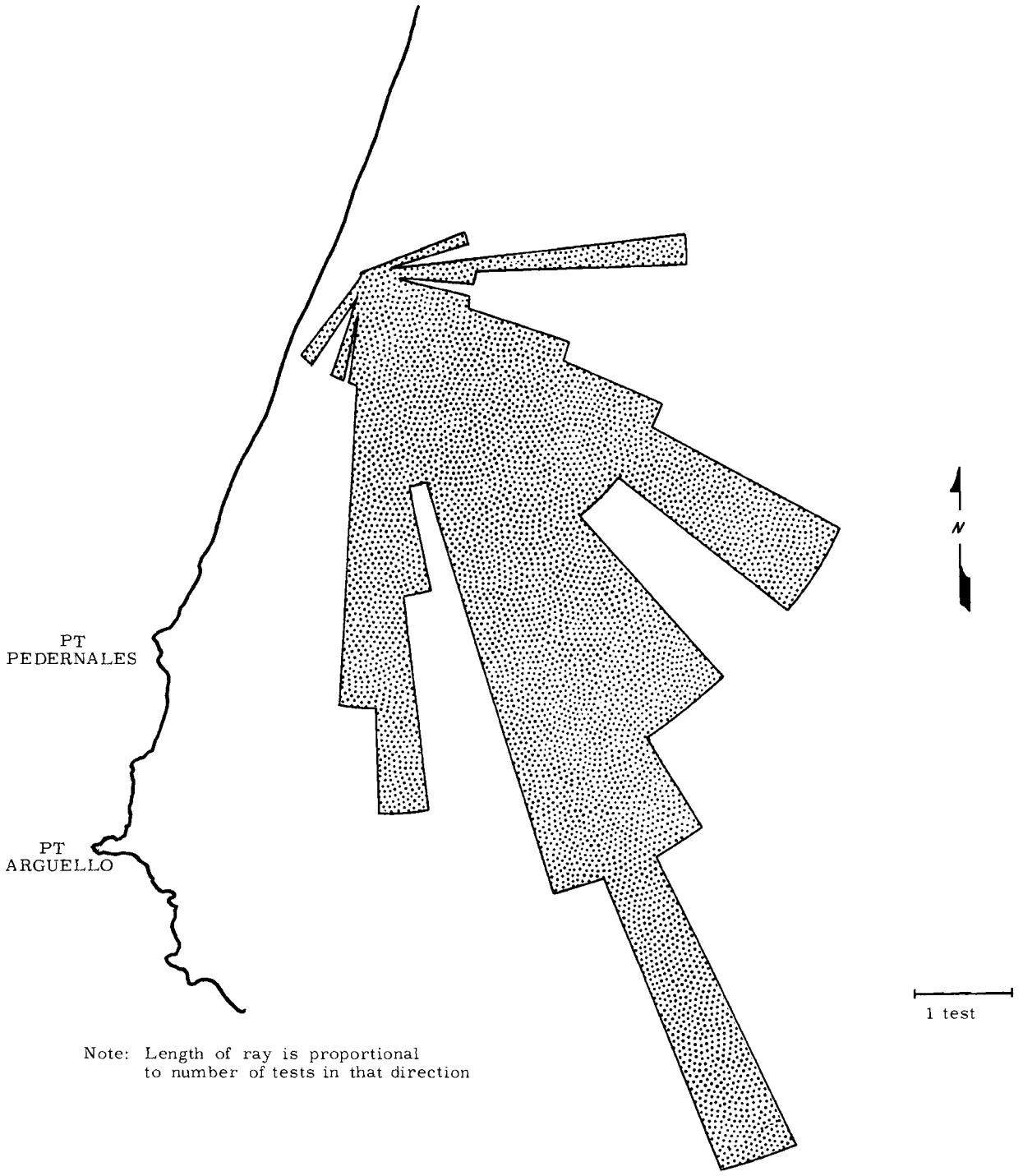

FIGURE 10. Distribution of Test Wind Direction (Site A)

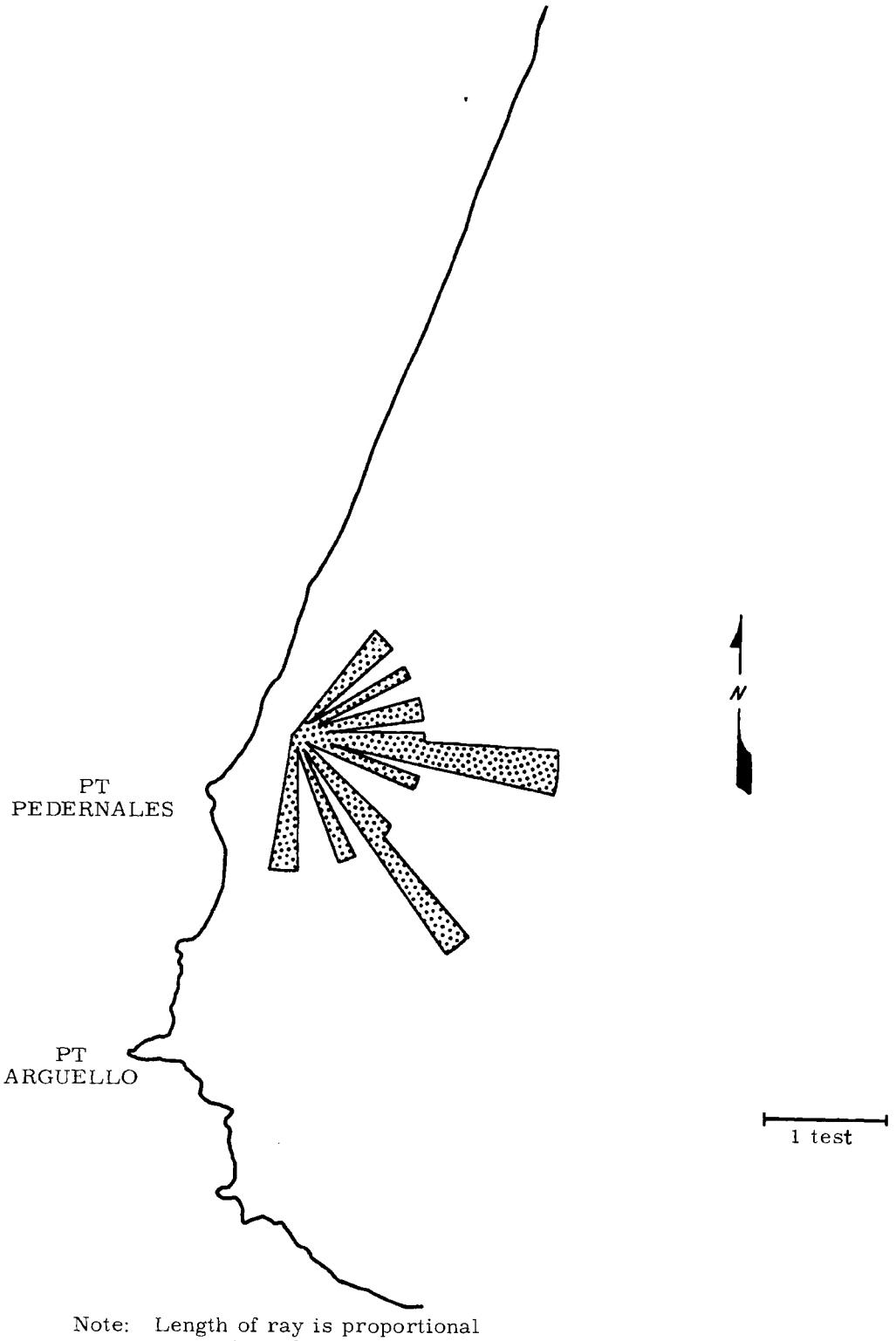

Note: Length of ray is proportional to number of tests in that direction

FIGURE 11. Distribution of Test Wind Direction (Site B)

TABLE IV. Summary of Atmospheric Conditions During MI Tests

Test	Source Point			Geostrophic Condition			
				Beginning		End	
	Speed mps	Direction degrees	Relative Humidity %	Speed mps	Direction degrees	Speed mps	Direction degrees
3	2.7	315	54	5.7	358	5.1	002
4	4.3	325	69	4.6	337	4.6	016
5	5.3	320	57	6.7	337	5.7	348
6	7.1	360	77	9.8	338	8.7	347
7	1.7	035	50	3.6	329	3.6	329
9	2.9	330	40	01.5	041	1.5	002
11	-	350	63	11.3	326	6.7	024
12	2.4	335	67	05.1	310	3.6	309
13	2.1	325	69	04.1	350	7.7	315
14	5.8	355	52	11.0	350	11.6	353
15	-	355	54	8.1	194	11.3	351
16	2.1	360	52	16.1	358	13.1	355
17	-	005	39	16.7	80	10.2	081
18	2.6	340	41	5.9	281	4.3	259
19	-	-	61	6.6	010	11.2	010
20	-	-	62	15.0	136	12.1	145
21	2.7	305	66	-	-	-	-
22	-	-	56	5.4	141	2.3	191
23	3.1	300	72	8.2	324	9.4	325
24	-	-	67	14.5	159	17.6	148
25	4.4	355	56	12.0	335	13.0	331
26	5.7	335	54	13.0	331	11.5	347
27	5.0	335	56	9.2	010	11.0	360
28	2.7	285	67	4.8	217	9.5	190
29	-	340	77	0.8	256	2.9	237
30	2.8	355	90	1.0	223	1.0	238
31	6.6	330		9.0	327	8.1	357
32	5.4	335		8.2	358	7.0	360
33	5.9	310	88	10.3	308	7.6	310
34	5.9	300	81	11.7	325	15.5	310
35	5.5	290	76	13.5	310	6.0	325
36	8.1	315	69	14.0	321	19.1	310
37	-	-	65	15.4	336	14.9	344
38	2.7	295	68	8.0	337	9.5	330
39	-	-	78	9.0	263	7.5	275

TABLE IV. (contd)

Test	Source Point Speed mps	Source Point Direction degrees	Source Point Relative Humidity %	Geostrophic Condition Beginning Speed mps	Geostrophic Condition Beginning Direction degrees	Geostrophic Condition End Speed mps	Geostrophic Condition End Direction degrees
40	4.9	345	76	19.0	337	16.3	350
41	4.7	325	72	7.8	339	7.5	318
42	5.2	005	25	14.2	357	15.0	351
43	4.7	340	44	10.3	015	11.0	007
44	5.2	320	64	19.8	350	19.5	355
45	3.7	265	81	5.7	035	4.2	016
46	3.6	345	-	9.5	013	8.7	005
47	-	-	-	9.0	353	8.5	351
48	-	-	95	7.6	015	5.9	030
49	-	-	-	9.0	142	7.5	147
50	4.7	320	98	15.0	320	2.7	360
51	-	-	-	11.7	310	7.2	003
52	-	-	78	8.2	325	6.1	347
53	3.2	290	72	5.5	121	6.2	124
54	3.7	280	71	9.9	120	9.7	130
55	-	-	68	4.7	343	7.3	355
56	-	270	78	4.5	035	3.2	055
57	-	315	75	0.6	135	1.2	192
58	-	-	75	2.3	245	1.8	216
59	3.9	320	80	19.4	355	14.6	356
60	3.9	300	80	7.8	160	11.5	139
61	-	275	79	5.6	093	5.0	099
62	3.9	320	78	6.1	136	4.9	135
63	2.9	280	63	8.8	159	9.1	151
64	-	-	59	9.0	175	9.6	187
65	-	290	80	8.5	217	5.2	205
66	-	-	65	0.2	005	1.7	254
67	-	265	72	1.6	100	1.9	050
68	4.0	335	72	4.2	287	6.6	310
69	3.8	300	76	3.8	192	3.7	187
70	3.4	315	82	3.7	125	1.7	103
71	4.4	240	78	7.1	153	6.4	152
72	2.8	220	78	5.5	175	5.5	180
73	4.7	265	77	6.2	027	6.5	022
74	3.3	305	89	4.2	100	5.7	113
75	-	295	92	4.3	119	3.8	134
76	-	310	89	6.1	046	8.2	036
77	5.5	305	84	4.0	023	4.0	067
78	4.9	310	87	5.0	054	5.2	019
79	2.5	335	76	1.5	271	1.1	055

TABLE IV. (contd)

Test	Source Point Speed mps	Source Point Direction degrees	Source Point Relative Humidity %	Geostrophic Condition Beginning Speed mps	Geostrophic Condition Beginning Direction degrees	Geostrophic Condition End Speed mps	Geostrophic Condition End Direction degrees
80	2.4	340	85	Calm	Calm	2.5	131
81	4.8	335	77	6.0	046	6.3	037
82	4.1	225	70	7.0	220	7.0	210
83	-	255	65	3.0	115	3.0	110
84	2.9	330	84	14.0	010	7.9	009
85	2.8	295	94	-	-	-	-
86	3.0	320	82	2.0	094	1.0	135
87	5.2	250	84	0.5	270	2.0	055
88	3.9	335	90	6.0	340	3.0	325
89	4.4	330	92	4.0	318	13.0	320
90	3.9	325	89	12.0	325	15.0	330
91	3.3	360	94	16.0	339	24.0	345
92	4.5	360	99	11.0	359	8.0	360
93	5.5	005	91	5.0	018	10.0	342
94	3.9	340	96	6.0	314	6.0	328
95	2.2	260	80	3.0	094	2.0	087
96	2.8	320	80	2.0	215	3.0	204
97	-	275	76	4.0	270	2.0	304
98	3.2	355	91	3.0	255	3.0	240
99	2.7	350	94	3.0	349	3.0	238
100	-	335	87	4.0	196	6.0	216
101	-	340	89	1.0	227	1.0	292
102	2.0	335	87	7.0	359	5.0	357
103	2.0	360	12	4.0	015	6.0	002
104	2.0	325	86	3.0	024	4.0	065
105	-	-	89	7.0	070	2.0	014
106	2.5	350	92	5.0	162	3.0	158
107	3.2	330	81	10.0	009	3.0	027
108	-	-	80	12.0	308	5.0	330
109	2.8	300	80	4.0	117	14.0	151
110	2.7	270	-	6.0	128	7.0	123
111	3.2	305	83	4.0	315	3.0	006
112	3.2	305	90	1.0	012	1.0	164
113	4.3	330	84	2.0	020	3.0	359

METEOROLOGICAL DATA REDUCTION

Meteorological data requiring reduction were the outlying winds (supplementary to the incomplete WIND system), and source point winds. The outlying wind data were read in 7 1/2 minute averages of both wind speed and direction, then averaged for half-hour intervals for the first 1 1/2 hours of each test. The source point data were read as 10-second averages of both speed and direction during the time of release, from which standard deviations were calculated.

The WIND system data, when available, were averaged for half-hour intervals for the first hour of each test. Wiresonde data were reduced to temperature differences between 6 and 54 feet or 300 feet. The radiosonde data were already available in summary sheet form and did not require further reduction or tabulation.

CHAPTER 5.
GROUND LEVEL OBSERVATIONS OF DIFFUSION

Although provisions were made for both ground-level and airborne measurements of diffusion, the greater importance was attached to the ground-level measurements during this phase of Operation Mountain Iron. The basic test design was, in fact, planned to yield a fairly detailed description of each test from ground-level data alone. This chapter, then, will discuss the ground-level data only, with the results of the airborne measurements presented for extended discussion in Appendix B.

The basic data in the Operation were exposures measured at each of some 300 sites well scattered over South Vandenberg. The first section will explain how the data were handled to yield the greatest benefit for pictorial and quantitative understanding of diffusion over South Vandenberg. The exposure data are then presented in terms of the ambient meteorology, to indicate the various effects of atmospheric condition and geographic placement of source points. The methods adopted for estimating parameters required for a rational model of atmospheric diffusion are then explained.

THE DIFFUSION DATA

As the very first step, the list of exposures measured at the various sampling positions was converted to a map of the exposures over which contours of exposure were drawn. This rather laborious task was necessary, since the sampling was confined to existing roads which were not related in any reasonable fashion to the source points. The resulting isopleths of exposure gave a fairly reliable picture of the intersection of the plume with the ground. Generally, the plumes can be classified as one of three types:

- A modified cigar
- A canyon low
- A multiple maximum type.

The modified cigar is only slightly different than the ordinary plumes from sources over flat terrain; they may be characterized by bending or

turning, but represent a monotonic decline of exposure with distance. The canyon low type results from flow over two ridges with a deep, steep canyon between; the exposures found in the canyon are significantly lower than on either ridge. The multiple maximum is really an elaborate canyon low type, resulting from flow over two, three, or even more ridges and valleys. As might be expected, tests over South Vandenberg showed a strong bias toward the canyon low type--especially releases made from Source A--since the prevailing flow was directed at the Target-Honda Ridge system. Of the 102 tests termed successful, 78 were from Source A--52 were the canyon low type and only 21 were the modified cigar type. The Source B releases were somewhat more ordinary since the prevailing flow carried the plume over Sudden Ranch and the ocean. Table V lists the various types from the two sources. It is clear that techniques applicable to homogeneous terrain will not fit the data exactly, but the difficulty may not be overwhelming.

TABLE V. Plume Types

Plume Type	Modified Cigar	Canyon Low	Multiple Maximum
Source A	21	52	5
Source B	15	1	8

It appears that the canyon low type can be expected to occur most of the time with northwest flow from a source near the north side of South Vandenberg. It is unfortunate that Source A was so far removed from Palc II because this complex will inevitably be strongly affected by its close connection with the slopes of Target Ridge; releases may not react in the same manner as releases from Source A, so forecasting canyon low types may be difficult.

In spite of the difficult access to Honda Canyon during the rainy season, many tests have documented the occurrence of the canyon low. As an example of the clear-cut character of this phenomenon, Figure 12 presents the isopleths for Test 48 along with the measured values of

FIGURE 12. Canyon Low Type of Plume (MI Test Number 48)

exposure at some of the samplers yielding significant exposures. The reduction of exposure in the Canyon is sometimes dramatic.

One difficulty inherent in using existing roads for sampling routes is the probability that some of the tests will not be adequately sampled when the plume axis is aligned with, instead of crossing, the sampling route. This was particularly true for releases from Source B (as mentioned earlier); however, the same problem occurred (although not frequently) with Source A releases in westerly winds. Isopleths of exposure certainly aid in the choice of centerline exposure; however, one problem is the spacing of samplers. Near the source, a spacing of one-tenth mile is coarse enough that the maximum exposure may be significantly underestimated due to the plume being only slightly wider than the sampler spacing. This problem is more pertinent to Source B releases (since the sampler spacing was two-tenths mile in that area, and four-tenths on Sudden Ranch), but exists also for Source A tests. Narrow plumes, associated with night releases and short release times, are especially sensitive to sampler spacing.

After the plume contours were drawn, the centerline exposures were picked off. The plume contours were used to indicate which samplers should be chosen, and which apparent centerline exposures were, in fact, removed slightly but significantly from the centerline. These exposure data then formed the nucleus for the analysis and equation.

The fundamental data for each test are listed in Appendix A:

- Centerline exposure (normalized to unit source strength)
- Distance to the exposure
- Estimated travel time to that distance
- An estimate of σ_y where possible
- Source point σ_θ
- Temperature differences from 6 to 54 feet and from 6 to 300 feet.

The procedures adopted for estimating σ_y and travel time are outlined in the following sections.

A broad picture of the diffusion results is presented in Figures 13, 14, and 15. These illustrate the envelope of data that fit in the description of each figure; only the envelope is shown to simplify the presentation. In the following paragraphs, these generalized envelopes are used to present a clear picture of the relation between source points and gross meteorological conditions.

The Source A data were derived from 67 successful tests with a release time of 15 or 30 minutes, of which 26 were classified as night tests. The relation between the night and day tests is clearly seen in Figure 13. The wide variation in results from the day tests overlap almost completely the relatively narrow grouping found for the night tests. The lack of complete separation between the day and night groups, among other evidence, is indicative that atmospheric conditions are not the primary source of variability between tests. Interesting, also, is the noticeable change in slope of the curves at about 5000 meters, which is about the average distance to the northern edge of Honda Canyon to the south, or to Arguello Ridge to the east of the source point. The relatively smooth wind fields blowing over the Lompoc Terrace are apparently disrupted rapidly by the ridge-canyon formations. This disruption causes a sudden increase in rate of diffusion, or lifting of the plume.

The data from Source B came from 25 tests, 4 of which were classed as night tests. Of particular interest is the complete overlap between day and night tests (Figure 14). The slope of the night tests is distorted rather badly by the small number of tests; one test, MI-72 particularly contributed to the very shallow slope indicated. This test, the only night test from Source B with a southwest wind, produced the slowest diffusion observed in the test series and yielded the highest exposures observed at distances of 5 to 7 miles (the limit of this test). Test 72 is shown in Figure 14 where the slow decrease of exposure with distance is obvious. Several tests from Source B produced trajectories directly up the canyon, but, unfortunately, tended to hug the walls and were sampled only along the edge of the plume. Since the sampling arcs paralleled the axis of the plume, there was no hope of determining plume width growth rates.

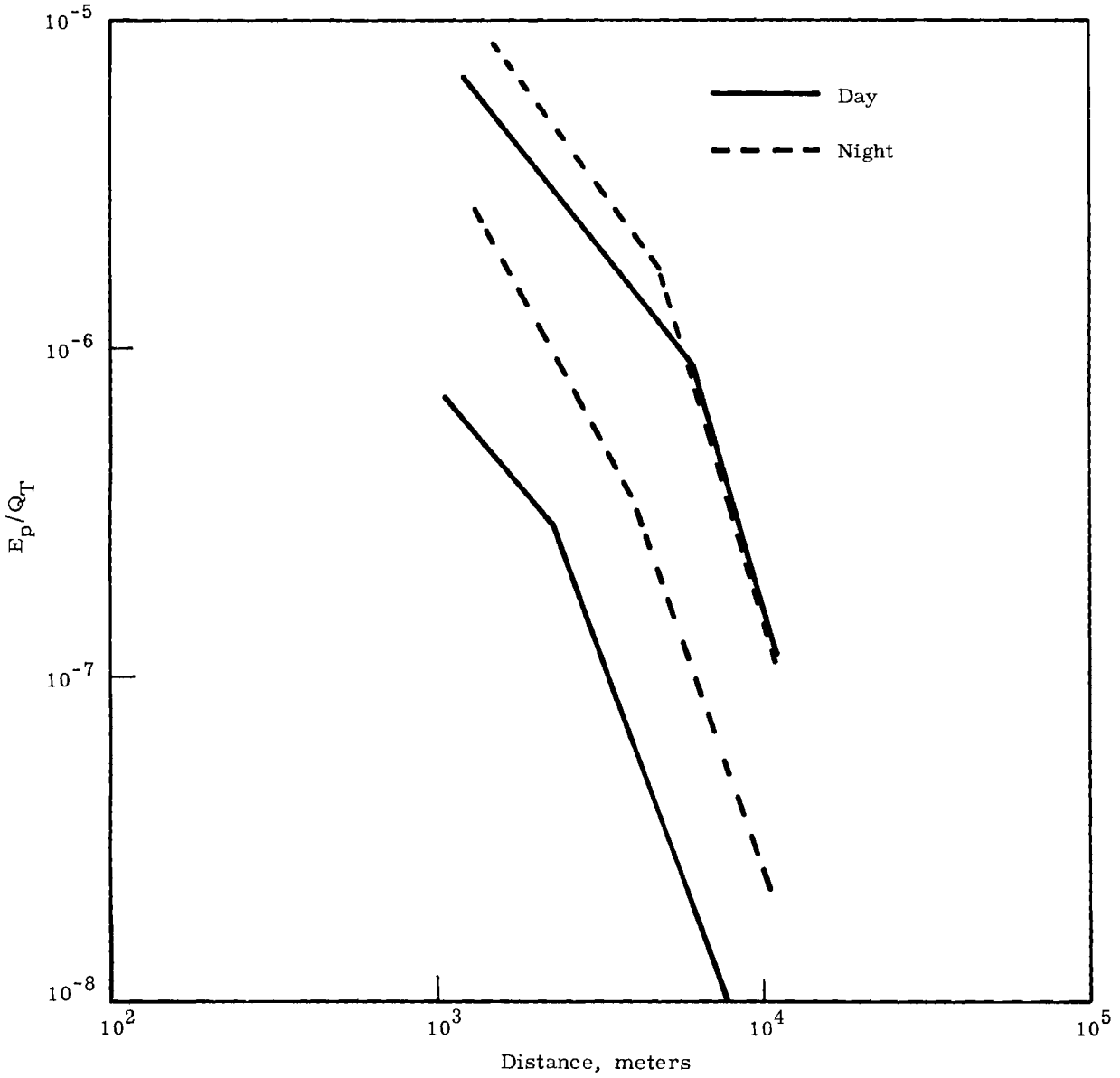

FIGURE 13. E_p/Q_T Versus Distance (Source A)

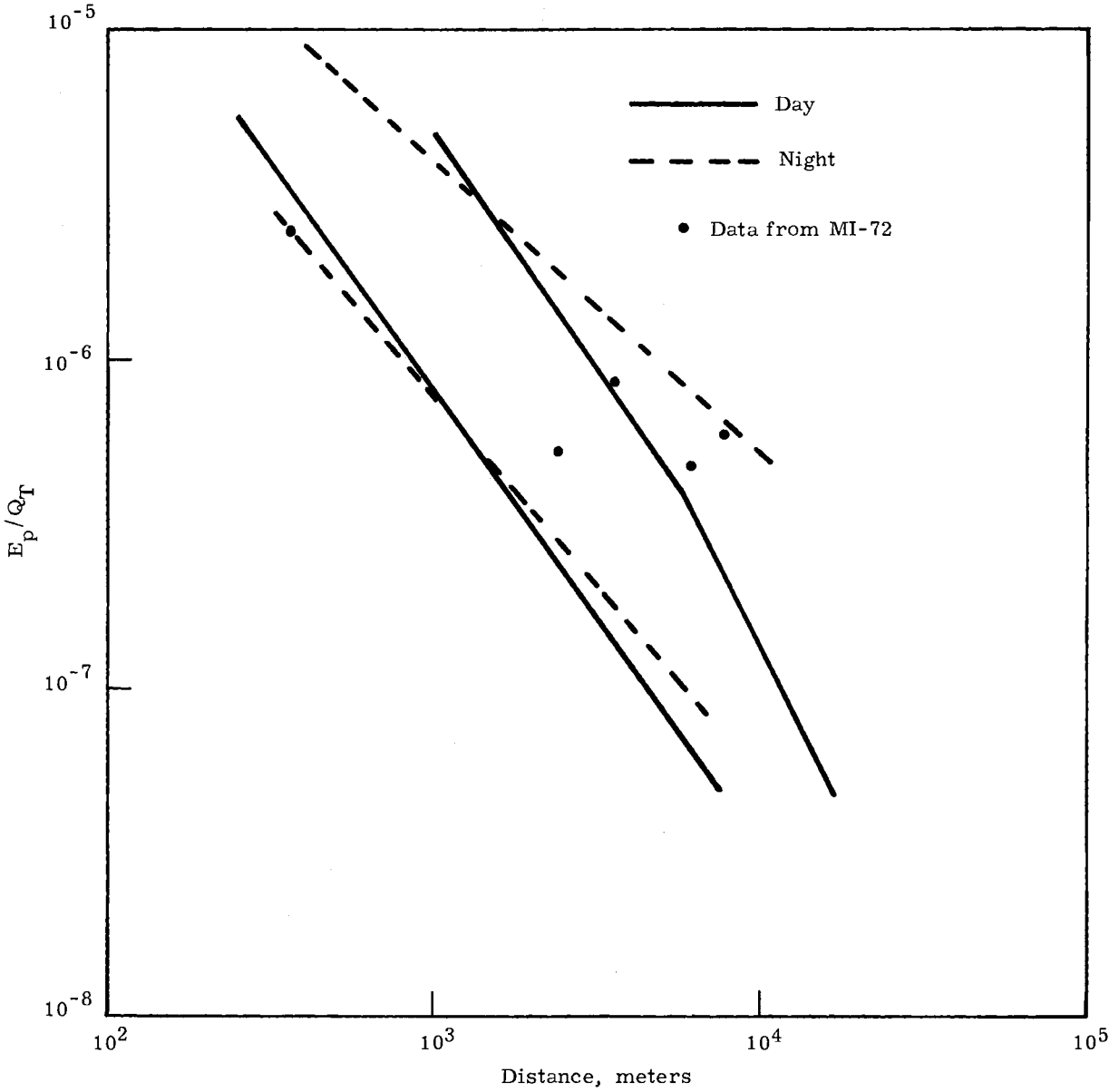

FIGURE 14. E_p/Q_T Versus Distance (Source B)

A comparison between results from Sources A and B is shown in Figure 15. In general, the Source B data are comparable to the Source A data, except near the source where the oft-mentioned difficulty in estimating centerline exposure for Source B releases prevents firm statements. During the day, exposures from the two sources are quite comparable at distances beyond 8 or 9 km, out to the sampling limit of about 15 km (nearly 10 miles).

TRAVEL TIME

The time available to a particle for dispersion from its neighbors plays a fundamental role in diffusion and is a determining factor for the smoothing in the Hay-Pasquill technique for estimating σ_y. Over smooth terrain, the calculation of travel time is relatively straightforward. Since the wind speed probably changes only slowly with distance, the assumption of homogeneity is justified. Unfortunately, such is not the case at South Vandenberg; flow over the ridges characteristic of this area is normally at a significantly higher speed than over the sea-level lowlands, and frequently the Sudden Ranch area experiences higher speeds than the ridges.[1] Therefore, the best estimate of the time actually available to the plume requires a changing wind speed with distance. A simple x/u approximation is only good for a limited span of time or distance, after which the wind speed must be altered to another more appropriate speed. It is incorrect to use the arithmetic average of wind speed to the point in question; since time is inversely proportional to speed, an inverse averaging process is required. However, any real averaging technique leads immediately to the problem of boundary specification between regions and to the treatment of data points lying close to the boundary.

The boundaries chosen in the South Vandenberg area were specified according to available wind speed sensors and representativeness of the siting of the sensors. Boundaries will of course be different for differing release points because for Source B tests, no sensor was available at the Source A position, and the WIND system sensor at site 300 (a possible alternative) was not available for many tests.

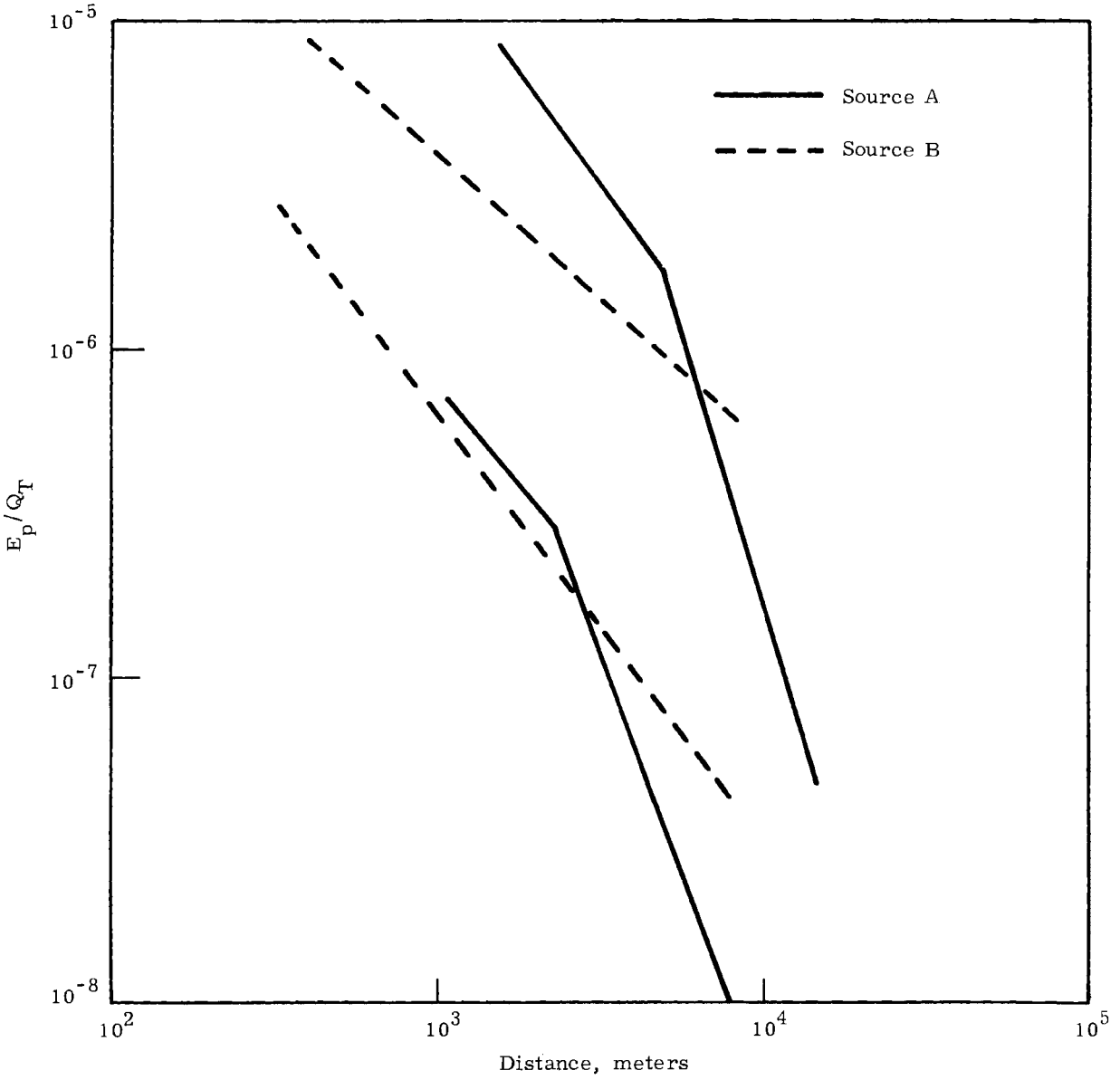

FIGURE 15. E_p/Q_T Versus Distance

The "spheres of influence" of the various sensors are indicated in Figures 16 and 17 for Source A and B releases, respectively. The position of the sensor providing data for each sphere is named in each area, with a description of each area given in Tables VI and VII. From these areas and from isopleths of exposure contours, the appropriate wind speed could readily be used to calculate the travel time between the boundary of any given area and the sampler in question. Successive calculation of times along the plume path yielded the total time to each of the centerline exposures and, correspondingly, the time to each of the σ_y measurements.

Since, in general, the winds in Honda Canyon were significantly less than over either of the bounding ridges, the travel time to Honda Ridge was calculated directly from Target Ridge by use of Remote Radar speeds from the downwind boundary of the Target Ridge area. The travel time to Honda Canyon sites was calculated from the Ionospheric Sounder data, but the time to Canyon points was not factored into the travel time to other points. This procedure sometimes gave shorter travel times to Honda Ridge exposures than to Honda Canyon exposures, which seems physically plausible when the large difference in speed between the canyon floor and the ridge tops is considered.

The set of travel times resulting from these calculations gave a new set of downwind variables that are readily usable in the Hay-Pasquill technique for estimating plume width at various downwind points.

Because the area of influence of the source speed is necessarily large, the source point wind speed plays a significant part in the travel time calculations, thus measurements of wind speed at the source are necessary.

PLUME WIDTH ESTIMATES

The discussion of the relation between distribution of material within the plume and the form of the equation of continuity made a point that will be amplified here. Regardless of the distribution, the standard deviation of the distribution appears as a fundamental parameter in the equation. For this reason, the task of determining the plume standard

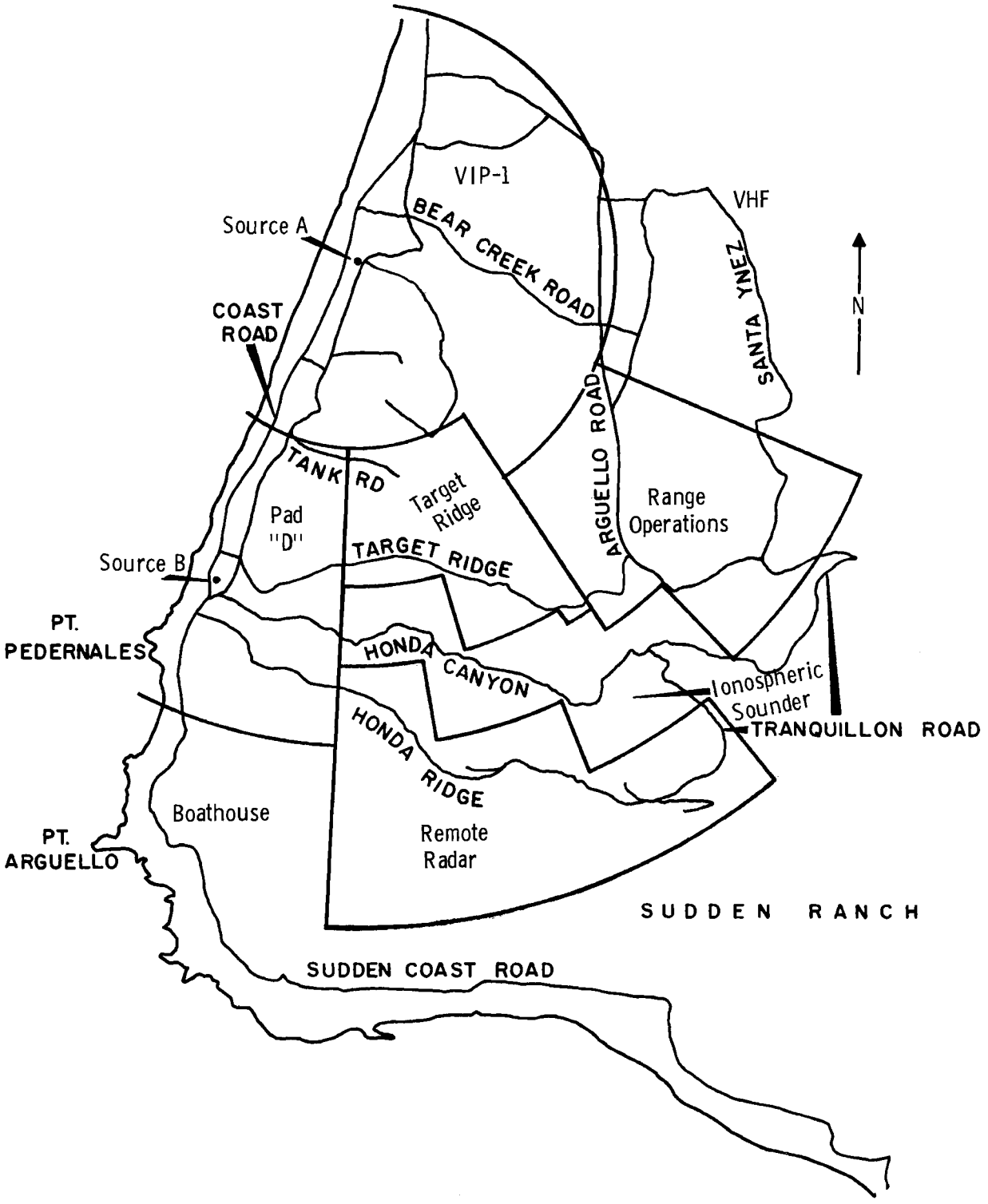

FIGURE 16. Spheres of Influence Source A

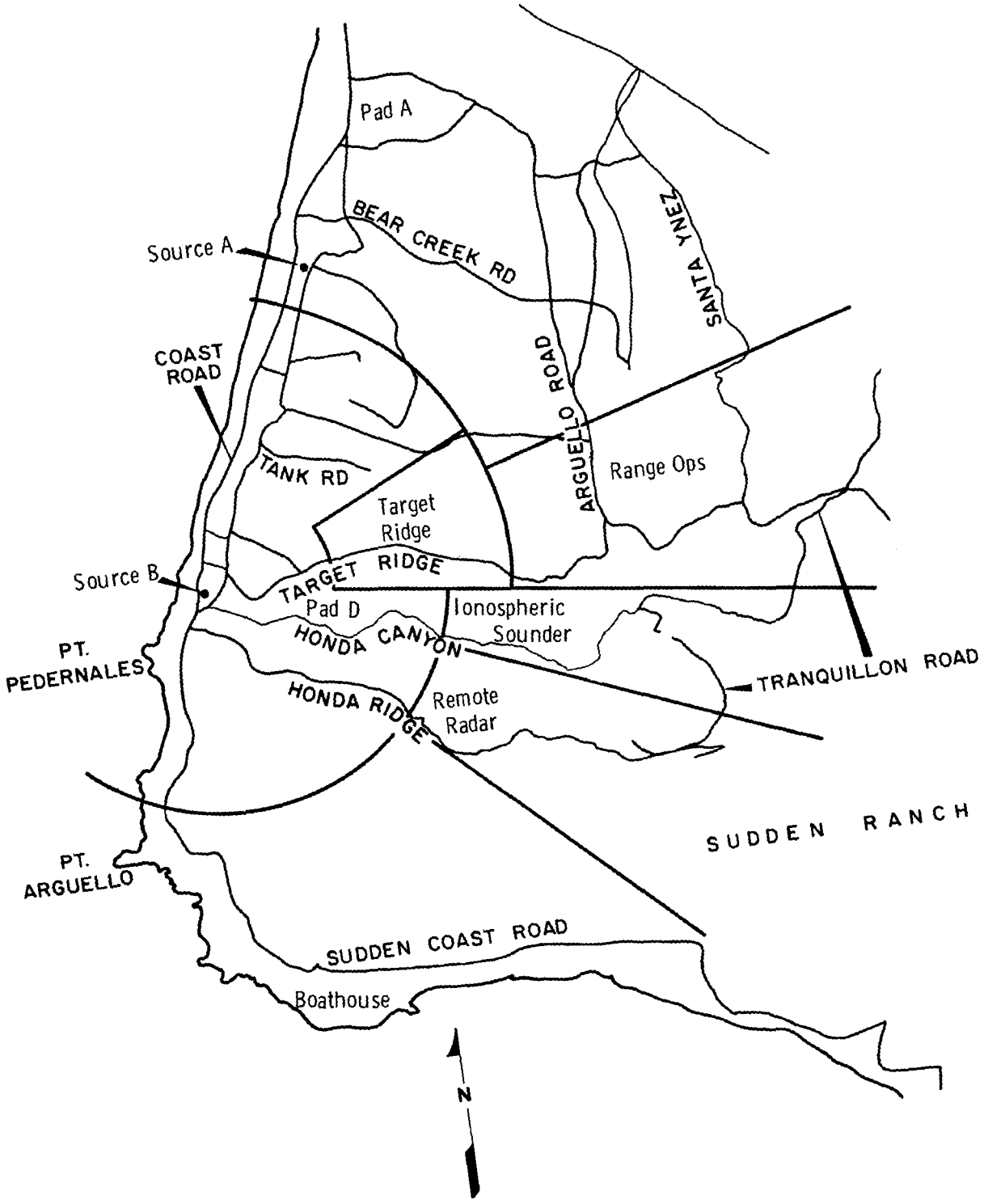

FIGURE 17. Spheres of Influence Source B

TABLE VI. Source A - Spheres of Influence

Area	Sensor Location	Radii		Azimuth Limits	
		Inner	Outer	Northern	Southern
Lower Honda Canyon	Pad D	2500	6500	183	---
Target Ridge	Target Ridge	2500	4500	165	183
		2500	5500	145	165
Upper Arguello Ridge	Range Ops	3500	6000	139	145
		3500	7500	112	137
Lower Arguello Ridge	VHF	3500	----	---	112
Honda Canyon	Ion. Sounder	4500	5500	171	183
		4500	6500	165	171
		5500	6500	155	165
		5700	7500	145	155
		6000	7500	141	145
		6000	----	137	141
		7500	----	---	137
Honda Ridge	Remote Radar	5500	9000	171	183
		6500	9000	155	171
		7500	9000	141	155
Sudden Ranch	Boathouse	6500	----	183	---
		9000	----	---	183
Source	VIP-1	----	2500	145	---
		----	3500	---	145

TABLE VII. Source B - Spheres of Influence

Area	Sensor Location	Radii		Azimuth Limits	
		Inner	Outer	Northern	Southern
Source	Area 529	----	4000	---	65
		----	1500	65	97
		----	3000	97	---
Lompoc Plateau	Pad A	4000	----	---	74
Upper Arguello Ridge	Range Ops	4000	----	74	97
Honda Canyon	Ion. Sounder	3000	----	97	111
Honda Ridge	Remote Radar	3000	----	111	134
Sudden Ranch	Boathouse	3000	----	134	---

deviation as some function of meteorological conditions or measurements required considerable effort. If a reasonably precise method can be found for estimating σ_y, not only is the estimation of centerline exposure made easier but the area affected by the plume is more or less readily estimated.

Given the amorphous geometry of the sampling routes, however, direct calculation of σ_y was in general impossible. Fortunately, in a very limited number of cases, the sampling routes were perpendicular (or nearly so) to the plume so that meaningful σ_y calculations were conceivable. After all tests were screened, the best examples of monomodal tests crossing sampling routes at near right angles were chosen for σ_y calculations. Table VIII lists the test and route number chosen in each case; the calculated σ_y and the estimated σ_y measured directly from the maps of exposure contours are listed also. The technique of estimating σ_y involved measuring the distance across the plume between exposure contours which were one-tenth the centerline exposure at that distance. This distance is 4.3 σ_y if the distribution within the plume is Gaussian. Although the standard deviation of a distribution is somewhat sensitive to the form of the distribution, the data in Table VIII show that the estimated values of σ_y are not greatly different from the calculated values, especially in view of the difficulty in assuring good distributions for the calculations. The overestimation involved in the estimated σ_y values is clearly shown in Figure 18. On the average, the estimated values exceed the calculated values by 10%, with a reasonable amount of scatter. The overestimation is apparently due to the unsymmetrical distribution common to most tests; whereas, the average kurtosis was 3.1 (close to the Gaussian value of 3.0), the average skewness was 0.65 instead of the Gaussian value of zero. Since a skew distribution is characterized by a larger σ_y than a normal distribution with the same maximum value, a large part of the difference must be attributed to skewness. One point of interest is the difficulty in estimating σ_y encountered for the 5-minute tests. There is no obvious reason for the scatter indicated by the outlying two 5-minute tests.

TABLE VIII. Comparison of Calculated and Estimated σ_y

Test	Route	Calculated σ_y	Estimated σ_y	Remarks
16	3	358	435	
25	3	357	367	
28	6	330	385	
35	6	278	263	
36	6	258	280	
40	3	382	470	5-minute test
42	3	316	220	5-minute test
43	3	407	453	5-minute test
46	3	279	405	5-minute test
50	3	321	350	
60	6	442	545	
60	7	846	870	
64	6	280	370	
64	7	438	475	
69	6	545	620	
69	7	748	830	

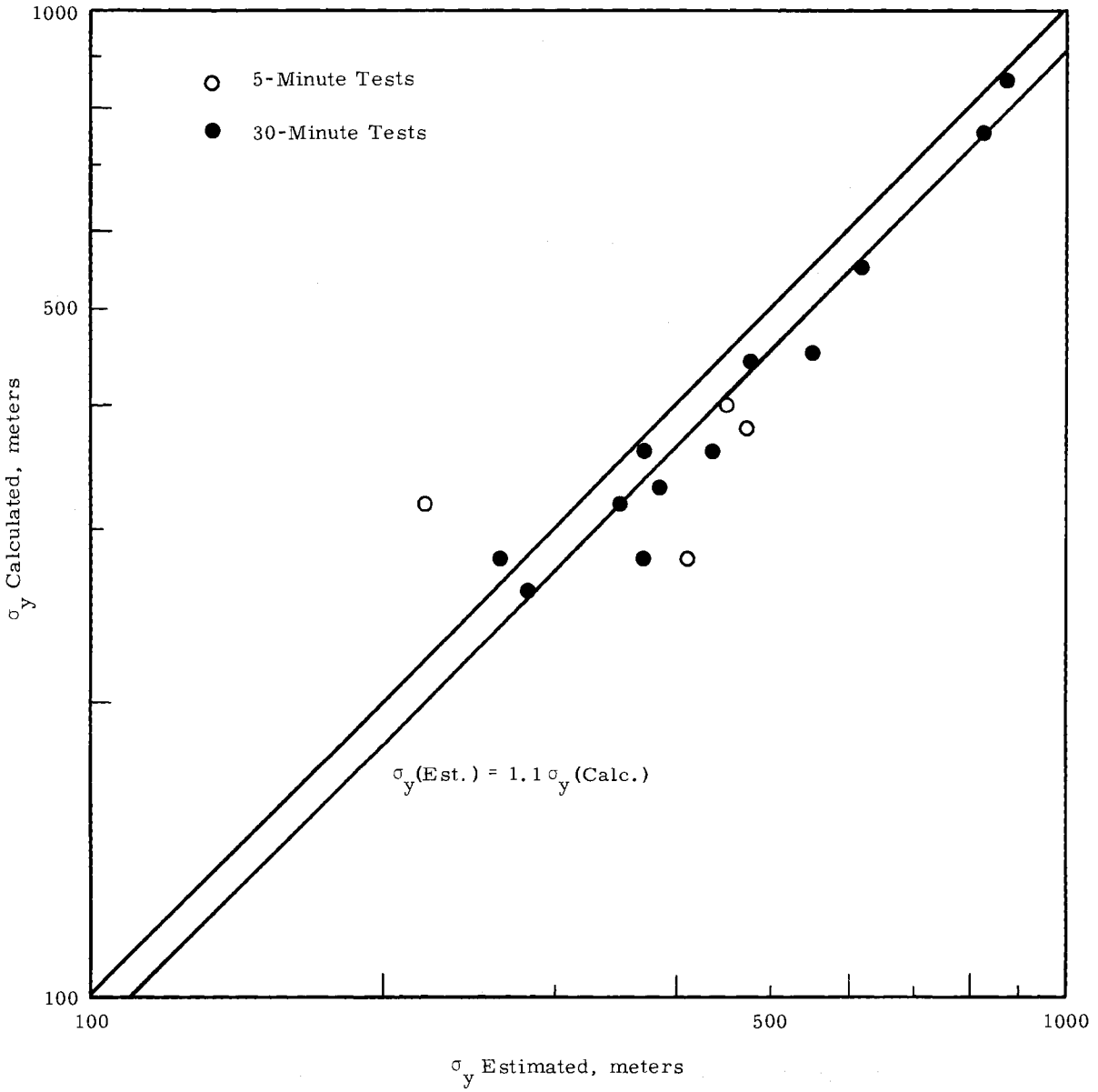

FIGURE 18. Estimated σ_y Values

Because only 10% error was indicated, the estimates of σ_y from measurement of plume width were presumed reliable and σ_y was measured at all points possible for the test series. The resulting data are included in Appendix A. It must be noted that some of the values were deduced from slightly bimodal or noticeably skewed tests, and may not be correct to within 10%; the necessity for a wide sample of data made some compromise mandatory. Because plume width data from Source B were scanty and difficult to procure, only Source A data were used.

Traditional presentations of plume width data rely on a simple power-law dependence of σ_y on distance. If the Mountain Iron data are plotted in this fashion, such a dependence is indeed discernible (Figure 19). The scatter about the mean is rather large with the limits shown being a factor of two removed from the mean.

The relation between Taylor's analysis (Lagrangian in nature) and ordinary meteorological measurements was discussed in Chapter 3. The Hay-Pasquill suggestions and hypotheses, based on this relation offer another tack clearly worth an attempt. The success of the Hay-Pasquill technique lies in the correct choice of β, a simple matter ex post facto but not all clearly possible to forecast. After some experimentation, the relation

$$\beta = 3.46/\sigma_\theta \quad (\sigma_\theta \text{ in radians})$$

or (9)

$$\beta = 200/\sigma_\theta \quad (\sigma_\theta \text{ in degrees})$$

was chosen as the best indicated by the data, although $\beta = 100/\sigma_\theta$ was little different. This relation for β yields considerably larger values than other workers have reported, even in stable conditions where one might expect β to be large. The larger β produces considerably less smoothing than was found to be appropriate elsewhere, a fact that no doubt reflects a structure of turbulence differing strongly from other sites.

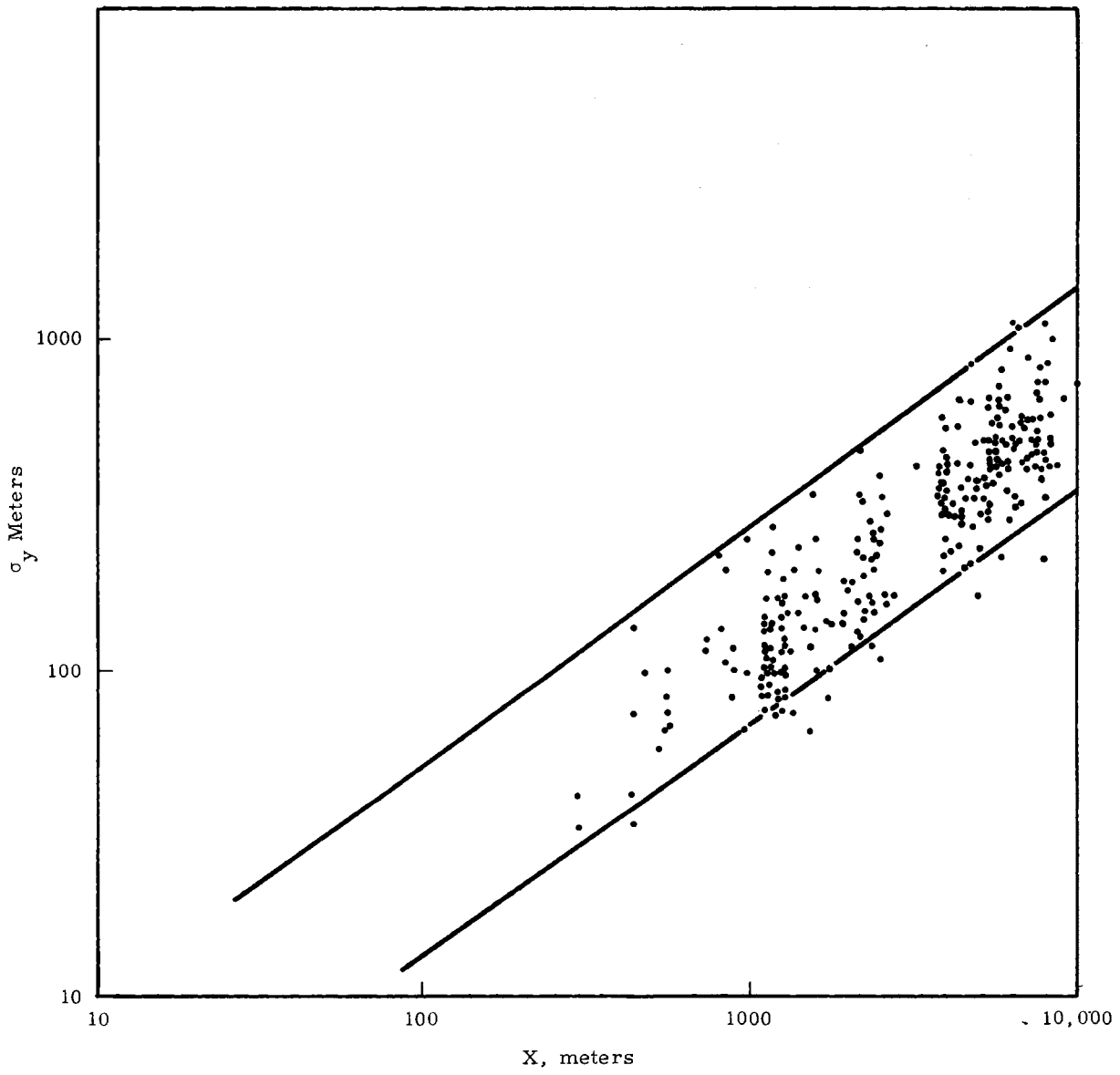

FIGURE 19. σ_y Versus Distance, all Tests

By use of the β calculated from Equation (9), σ_θ was calculated for each of the σ_y values in Appendix A. The σ_y values were normalized to $\sigma_\theta u$ (approximately equal to σ_v) and plotted (Figure 20). There is a notable improvement in relating σ_y to down wind travel (time, here); 75% of the data lie within 40% of the mean. However, there are several outlying tests that certainly do not fit the scheme.

The availability of a reasonably dependable method for estimating σ_y from source point meteorological data created hope that a physically consistent model for diffusion over South Vandenberg was possible. However, the success of such a model would be limited by the fraction of data remaining as unexplained outliers.

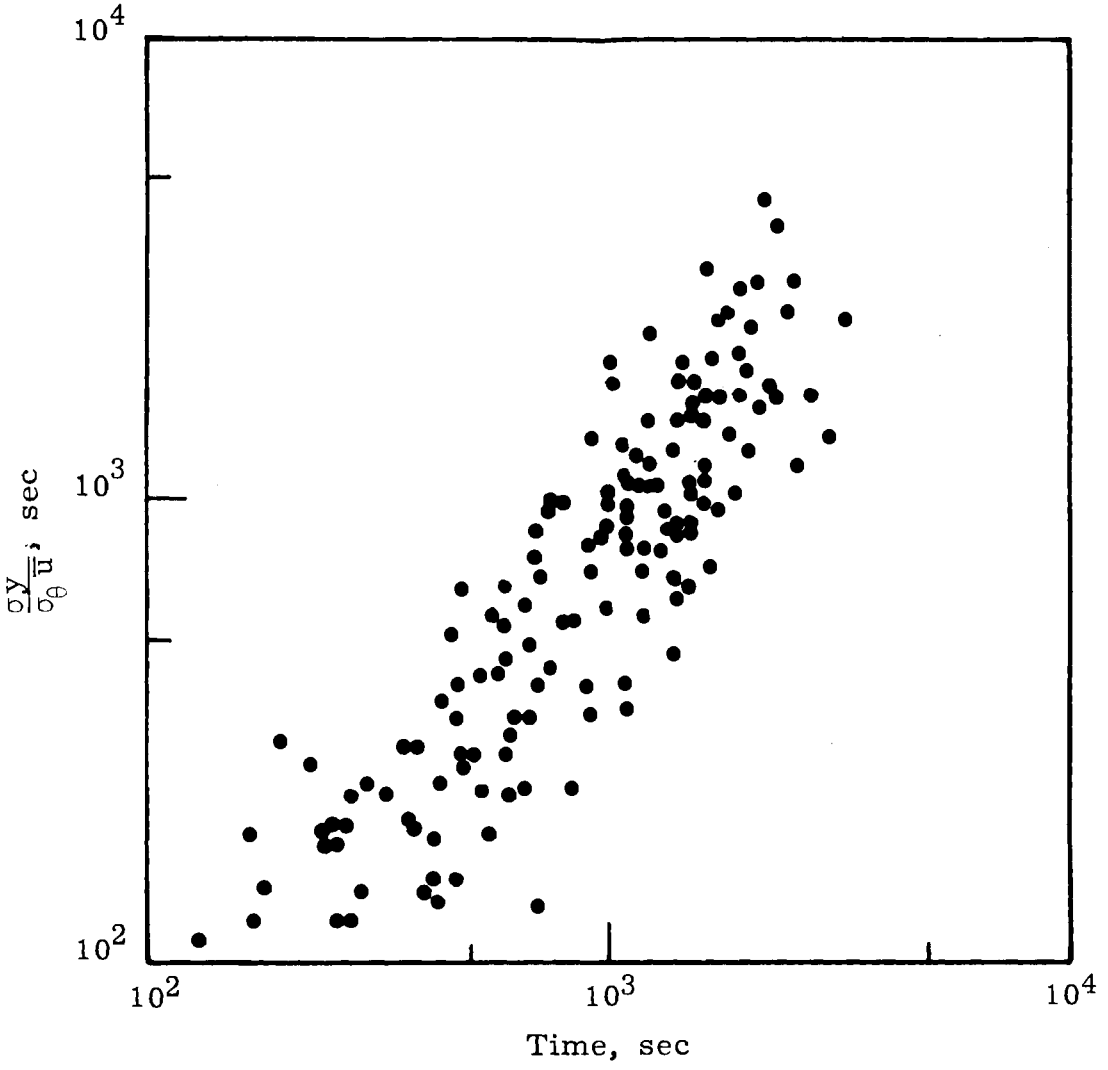

FIGURE 20. Normalized Crosswind Plume Standard Deviation Versus Travel Time

CHAPTER 6.
DEVELOPMENT OF MODELS FOR DIFFUSION OVER SOUTH VANDENBERG

The data presentation in Chapter 5 can be used directly for estimating exposures at various distances over South Vandenberg; however, the dependence on distance alone is not likely to yield the most accurate estimates attainable because no meteorological variables would be used to categorize the various tests. The method of integrating atmospheric variations into the diffusion data to yield a straight-forward equation, rather than a set of graphs, is sometimes termed "modeling" of the diffusion results. Two approaches were followed in developing a workable model: one follows directly from the theoretical discussion in Chapter 3, the other from the work that led to the North Vandenberg WIND equation. These two models will be discussed* in that order so that the surprisingly close relationship between a purely statistical result and the result of semiphysical reasoning will be clear.

THE QUASI-PHYSICAL MODEL

The fundamental theory of diffusion chosen as a framework for the development of a physically meaningful model derives from Taylor's theorem (as discussed in Chapter 3). Of first importance to this theory is the determination of the proper averaging interval to be applied to the source point wind direction fluctuations so that a wind variance calculation will yield an accurate estimation of plume spread. The method of determining the proper averaging interval relies directly upon the travel time to the point in question. Therefore, in essence, diffusion is treated as a time dependent process, with σ_θ and $\bar{u}$ as variables indicating the rate of horizontal plume spread. The theoretical approach to estimating the rate of plume spread in the vertical is analogous, but no measurements of wind fluctuations in the vertical were made during this series of tests.

---

* The units used in this chapter are cgs.

However, the turbulence in the vertical wind component is generally closely related to stability, so a direct dependence of vertical plume growth on temperature stratification was postulated.

Because the exposure data decreased approximately as t^{-2} and since σ_y, as a function of $(\sigma_\theta)_\beta$, is nearly linear in time, it appears that the linear transformation $X = \bar{u}t$ is sufficiently accurate to allow the straightforward substitution of X for t as the independent variable. Thus, considering plume growth in the lateral direction to be a function of $(\sigma_\theta)_\beta$ and X, and in the vertical direction to be a function of ΔT and X the equation of continuity, Equation 7, takes the form

$$E_p \bar{u}/Q_T = f[X, (\sigma_\theta)_\beta, \Delta T] \tag{10}$$

Determining the power function relationship for the above dependence that best fits the data, we have

$$E_p \bar{u}/Q_T = 1.26\, X^{-1.83}\, (\sigma_{\theta_\beta})^{-0.368}\, (\Delta T_6^{54} + 5)^{1.43} \tag{11}$$

The predictions fall within a factor of two of the observed data, 68% of the time; within a factor of four, 96% of the time (Figure 21).

The dependence on σ_θ, shown in Equation (11), is much smaller than expected. This is perhaps due to using a σ_θ at a single point (which may be nontypical) to describe the diffusion over terrain of such differing character as found in South Vandenberg. Indications were found, in the few tests available with the full complement of WIND system sensors in operation, that σ_θ varied considerably over South Vandenberg and that using downwind values of σ_θ may well improve the dependability of the predictions. Further study of the relation between lateral plume spread and wind variability would be expected to improve prediction capabilities.

Thus, the usefulness of the "quasi-physical" model is limited, even though good estimates of plume width are available for a substantial fraction of the cases. However, the relatively successful predictions

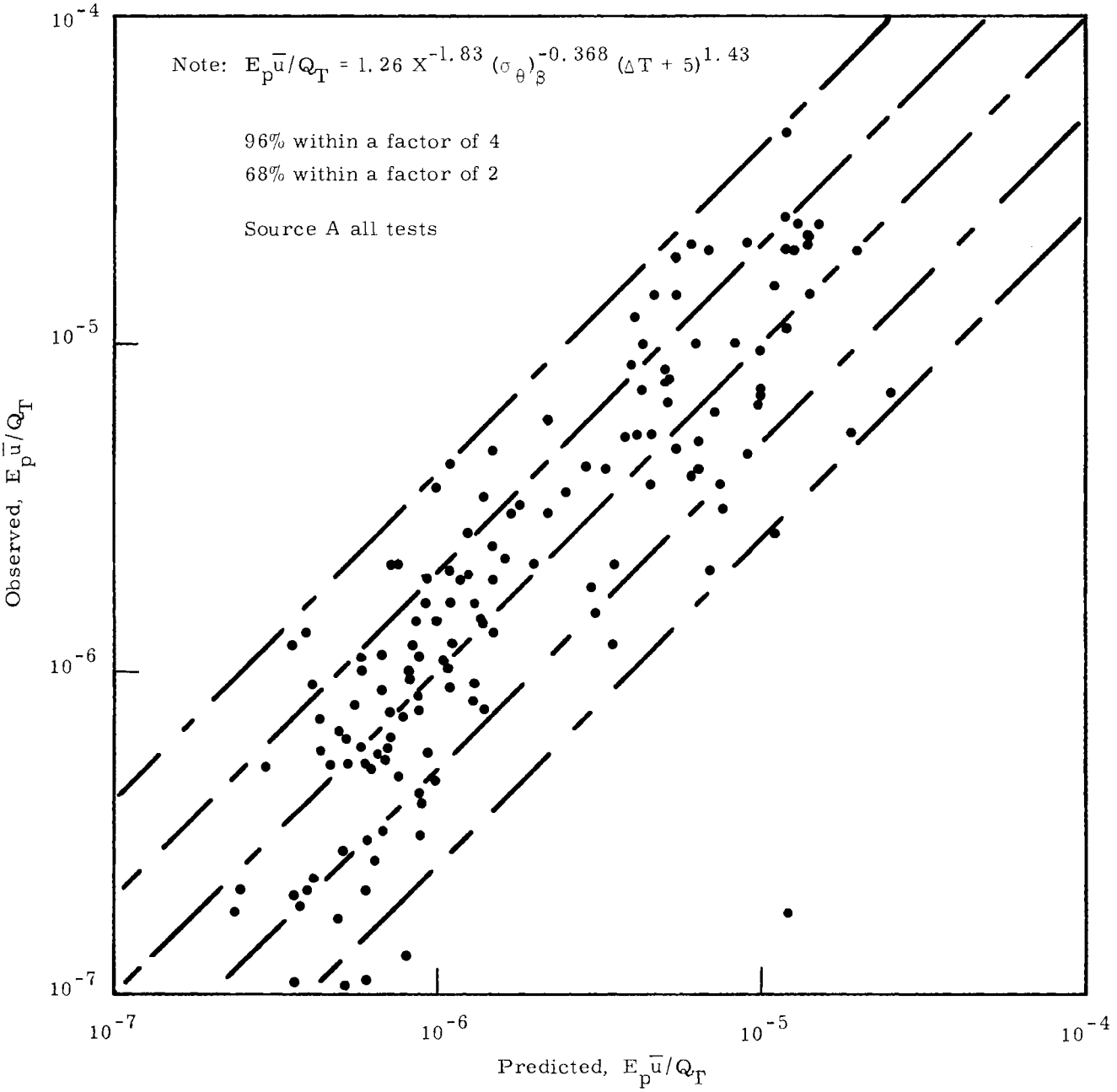

FIGURE 21. Observed Exposures Versus Predictions as a Function of Distance, Running-Mean-Average σ_θ, Wind Speed and Temperature Difference.

achieved by this model provides confidence that a model resulting from data completely divorced from an dependence on calculated travel time (such as is developed in the following section) will be equally successful.

STATISTICAL MODELING

In spite of the advantages that a physically based model possesses, some serious flaws sometimes prevent such a model from being truly useful. An important complication which can accrue to a physical model is complexity caused by the myriad interrelated factors that must be at least partially accounted for. Another and simpler approach, adopted for use in the earlier WIND system installations, is to form a product of relevant parameters with statistically determined exponents on each of the factors.[7] Since the determination of the exponents is based on a least-squares analysis, the best (statistical) fit of the equation to the data yields the least variance of the predicted values about the observed values. The drawback to this sort of analysis is precisely in the exponents for best fit which may well have little physical meaning--not allowing for confident extrapolation either in distance or geography. Nevertheless, a statistical approach can yield a useful and simple result for immediate application--a fitting criterion for any engineering study. This section will detail the results of the statistical analysis of the Mountain Iron data and discuss the reliability of the final equation.

The Mountain Iron series of tests included two source points having little in common. Because Source A was of primary importance, the data from its tests will be treated in considerably more detail than those from Source B. This is doubly necessary because of difficulties encountered in acquiring data from Source B.

In this analysis, some sort of benchmark is required so that relative improvement of various forms of "best-fit" equations can be seen. A reasonable choice is the simple dependence of exposure on distance alone because distance from the source has the greatest single bearing on dilution. In truth, the results of a simple distance-dependent statistical

fit are surprisingly good. Figure 22 shows the observed exposure data plotted against the predicted exposures for the Source A data, by use of the equation

$$E_p/Q_T = 0.390\, X^{-1.66} \quad , \tag{12}$$

with 63% within a factor of 2 of the mean, and 92% within a factor of 4. In contrast, the data forming the original WIND equation for North Vandenberg had corresponding values of 36% and 78%.[7] The implications of the large fraction of Mountain Iron data well predicted by the simple distance dependence are not obvious, but the rough terrain characterizing South Vandenberg seems to overwhelm the meteorological variability most of the time, so that only a few cases are strongly dependent upon the atmosphere's nature at the time.

The addition of the parameter σ_θ, an obvious step, yielded the equation

$$E_p/Q_T = 0.582\, X^{-174}\, \sigma_\theta^{-0.128} \tag{13}$$

Curiously enough, this fit, including σ_θ, is not as good as using distance alone (Figure 23); although 64% of the points were within a factor of 2, only 91% were within a factor of 4. Of course, this is not a significant reduction but it is an indication of the difficulty found in working with the Mountain Iron data.

Addition of a temperature difference to make the equation format identical with the North Vandenberg equation gave the results shown in Figure 24 and the equation

$$E_p/Q_T = 0.0536\, X^{-1.79}\, \sigma_\theta^{0.0983}\, (\Delta T_6^{54} + 5)^{2.23} \tag{14}$$

The fit is slightly improved, with 93% within a factor of 4 and 68% within a factor of 2. Even so, the form adequate for North Vandenberg will not provide predictions of comparable quality over South Vandenberg. The one remaining source point datum is of course the wind speed. Inserting this

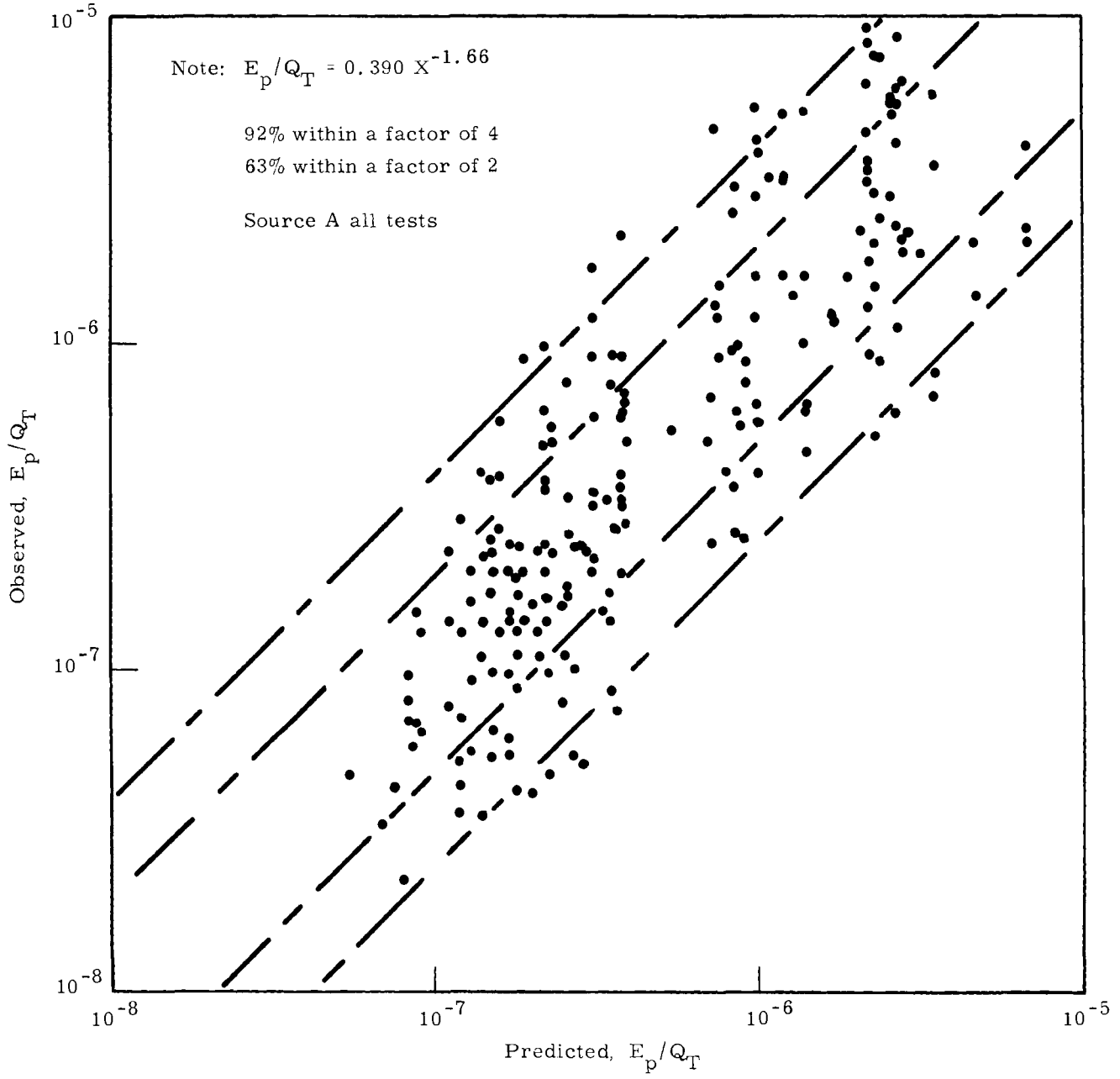

FIGURE 22. Observed Exposures Versus Predictions as a Function of Distance Only

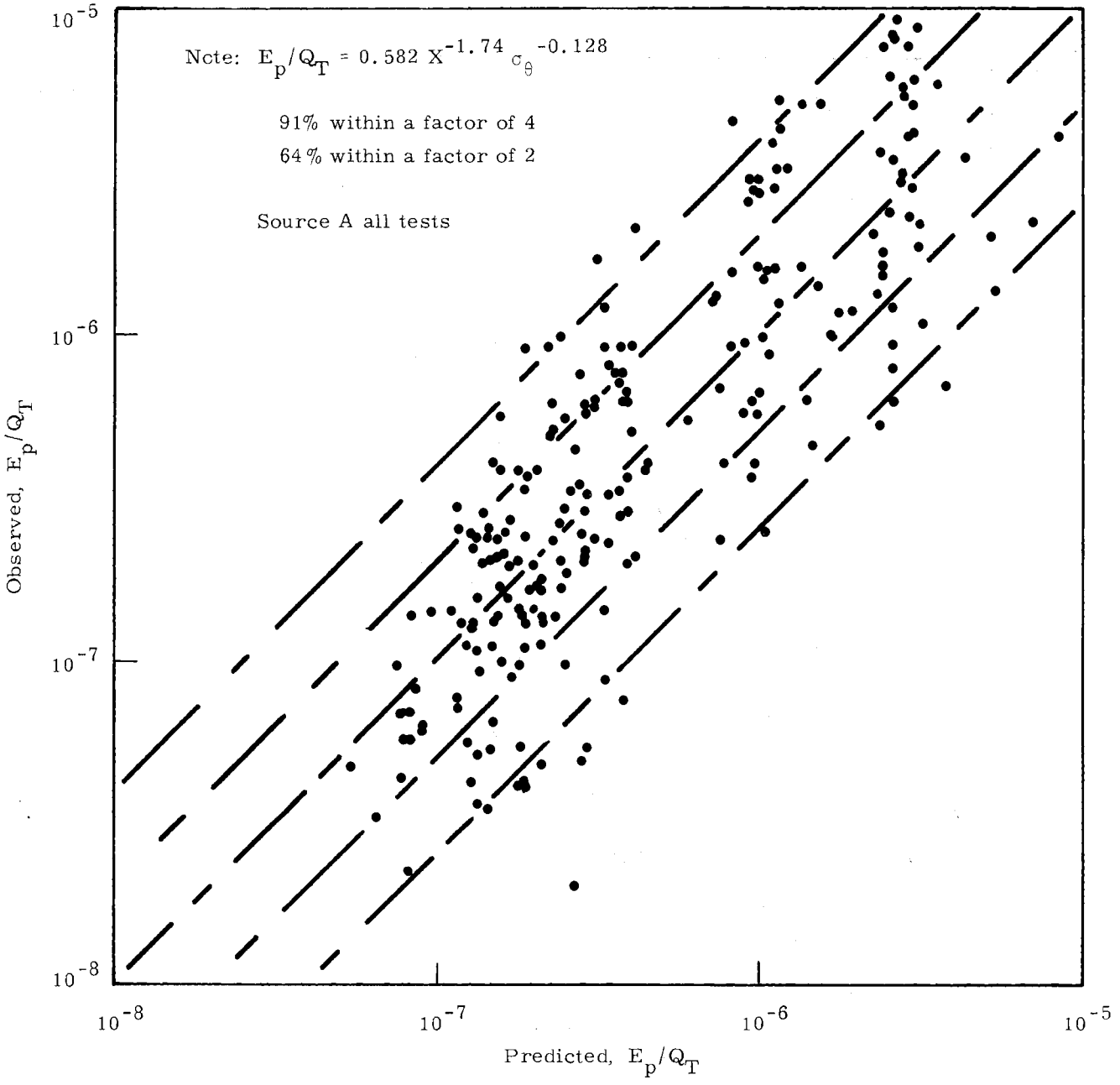

FIGURE 23. Observed Exposures Versus Exposures Predicted as a Function of Distance and σ_θ

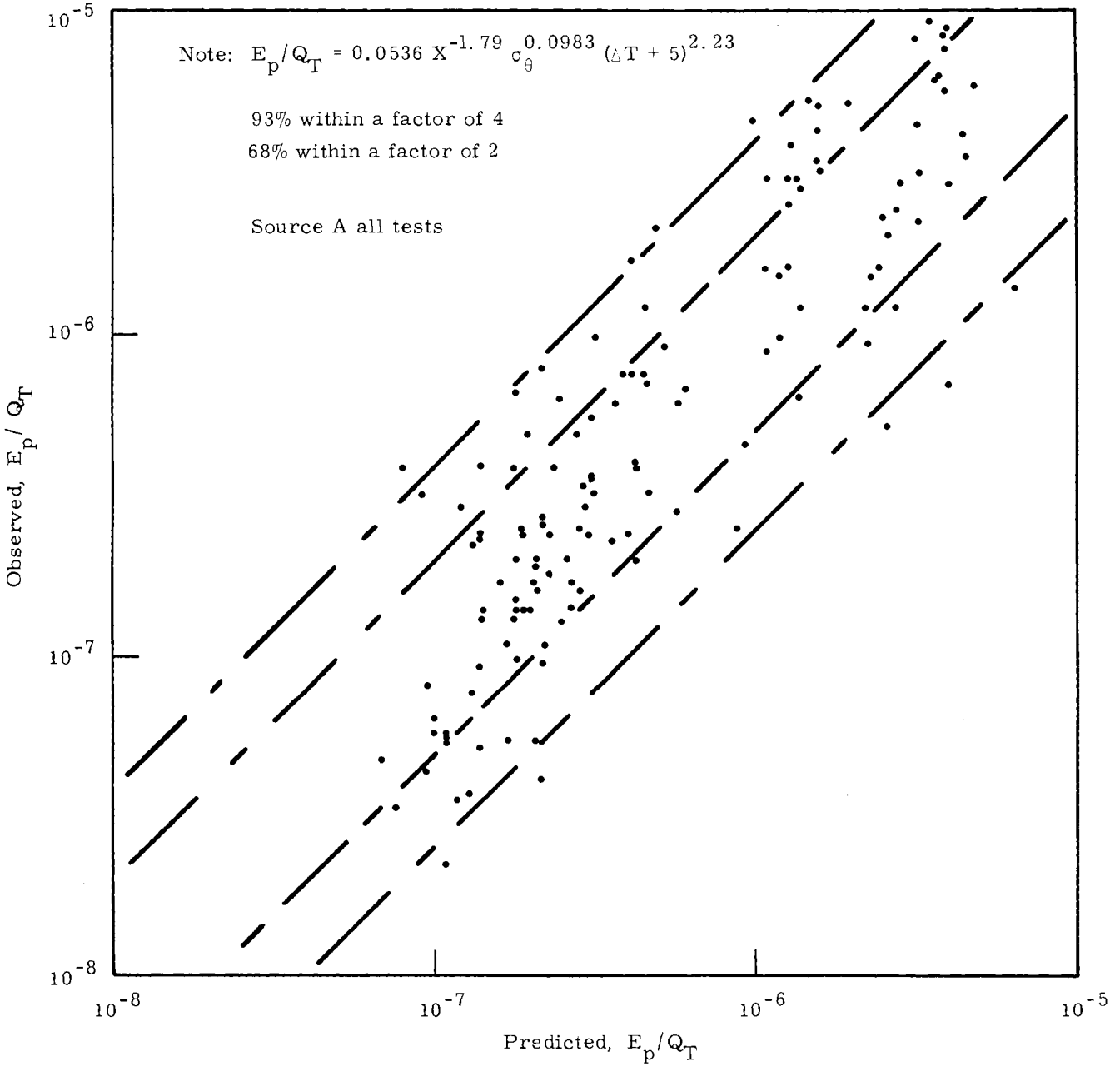

FIGURE 24. Observed Exposures Versus Predictions as a Function of Distance, σ_θ, and Temperature Difference

into the fit yielded the equation

$$E_p/Q_T = 0.248\ X^{-1.82}\ \sigma_\theta^{-0.417}\ \bar{u}^{-1.03}\ (\Delta T_6^{54} + 5)^{1.55} \quad (15)$$

for which 73% of the data were within a factor of 2 and 97% within a factor of 4, shown in Figure 25, which is probably adequate. However, the temperature stratification through a thicker layer than the 54 feet used in the WIND equation measureably improved the predictions of South Vandenberg data. By including the temperature difference between 6 and 300 feet, the equation

$$E_p/Q_T = 0.529\ X^{-1.85}\ \sigma_\theta^{-0.355}\ \bar{u}^{-0.868}\ (\Delta T_6^{300} + 6)^{1.14} \quad (16)$$

was found for best fit, which predicted 75% within a factor of 2 and 97% within a factor of 4 (Figure 26). This is the equation recommended for use, and is altered to operational form for use with the WIND system in Volume I.

Some interesting information is hidden in Figure 26. Equation (7) was derived from all Source A data, without discrimination according to day or night conditions. A difference in the predictions for these two conditions is readily apparent in Figure 27 where daytime and nighttime data are separated. Of most importance is the systematic error indicated for the daytime tests: at the lower exposures, (greater distances) the predictions are low and the error appears to increase as exposures decrease. If the data are separated into groups for day and night, the resulting equations yield predictions with 80% within a factor of 2 at night and 83% during the day, with the portion within a factor of 4 remaining at 95%. However, this increase in success is not outstanding enough to recommend itself because of the operational advantage of simply using a single equation for all conditions.

It is significant to note that the forms of both Equations (15) and (16) are physically reasonable. The proportionality between concentration and

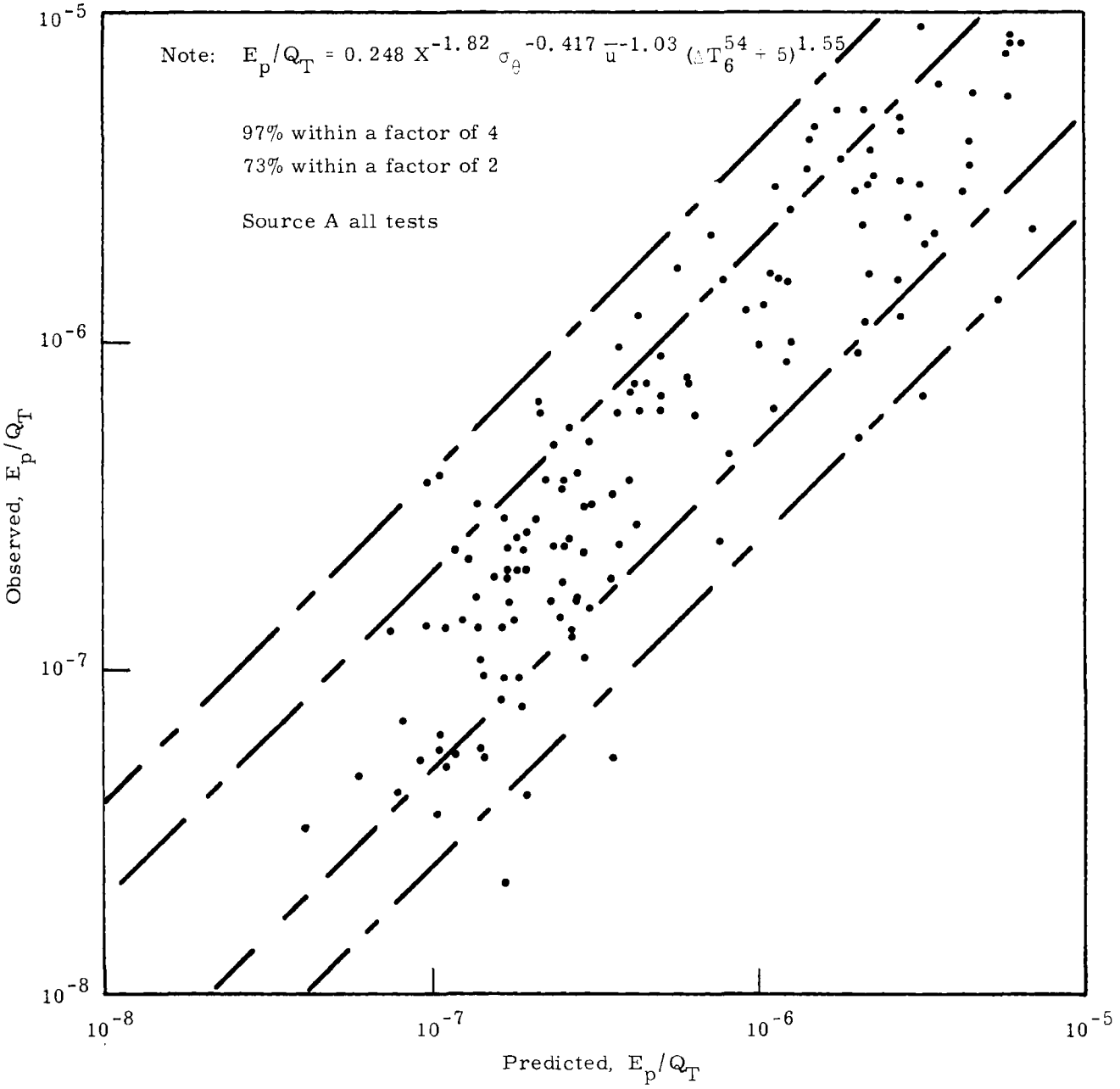

FIGURE 25. Observed Exposures Versus Predictions as a Function of Distance, σ_θ, Wind Speed and Temperature Difference

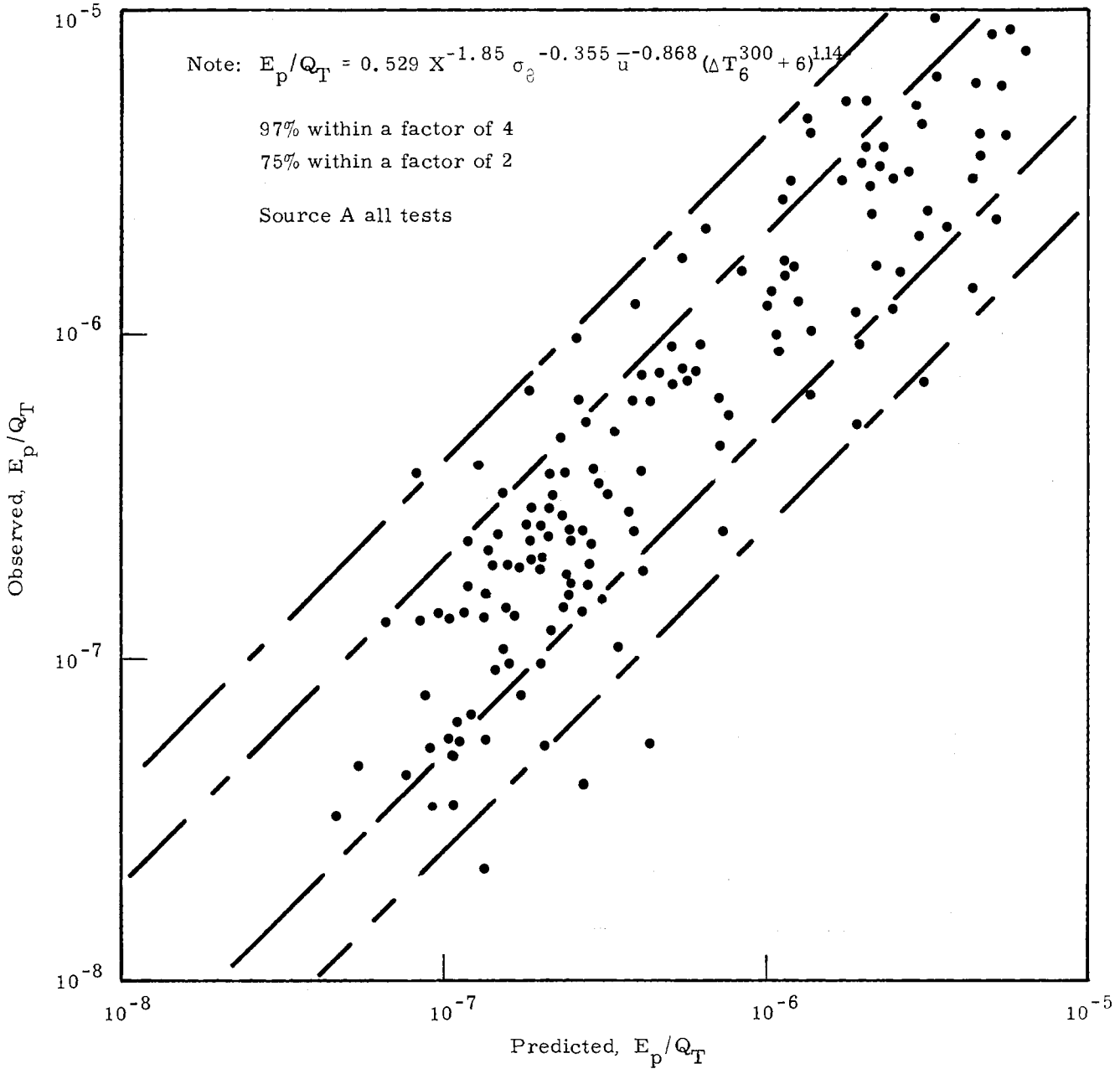

FIGURE 26. Observed Exposures Versus Predictions as a Function of Distance, σ_θ, Wind Speed and Temperature Difference

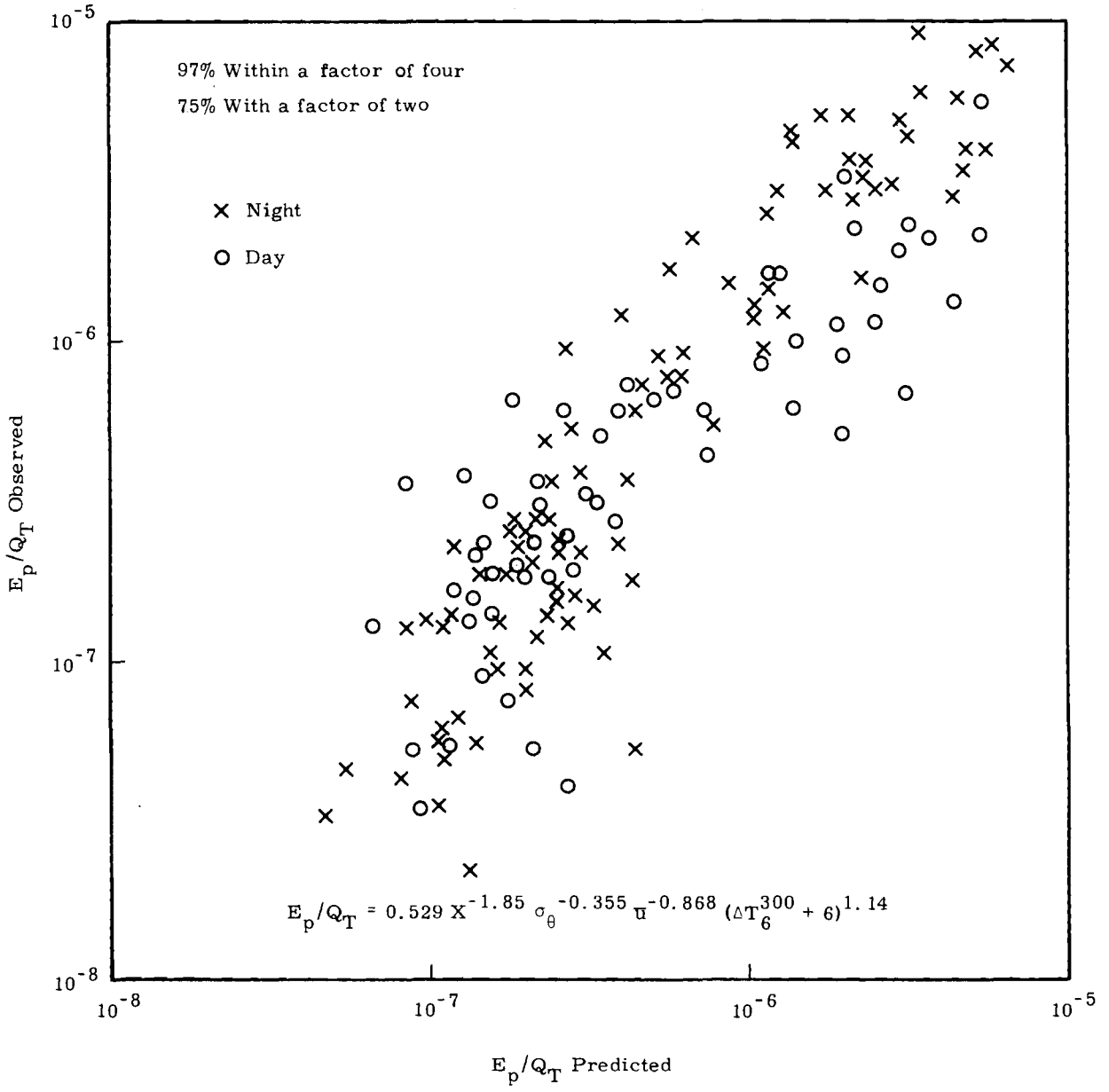

FIGURE 27. Illustration of Systematic Error in Prediction of Daytime Exposures

$\bar{u}^{-1}$ expected from the continuity equation is very closely approached. The inverse dependence on σ_θ was also expected* as was the increase in dilution with increasing instability, indicated by the exponent for temperature difference.

SOURCE B EQUATIONS

The equations found for best fit to the Source B data will be presented here, but no further use will be made of them because so little confidence can be attached to the slope of the exposure versus distance curves. An additional factor complicating the analysis of Source B data is the indication that in some, but not all, cases the plume from Source B was bodily lifted from the canyon floor and well into the atmosphere by large eddies generated by airflow over the two ridges that almost converge at the source point. Brief visual observations of wind patterns over, through, and along gullies on South Vandenberg revealed a persistent spiral flow. This flow lifts material from the ground up and along the downwind side of the depression. No reason is apparent why the same pattern should not be characteristic of larger scale wind flow, which in the case of Source B at the mouth of Honda Canyon would provide the strong upwelling implied by occasional very low exposures quite near the source. If, indeed, the plume is sometimes lifted above the samplers so that only the bottom edge is sampled, the effective source height must be variable in the extreme; this, coupled with the difficulty found in defining the certerline, precludes recommending the equation derived from Source B data.

The equation for best fit for the Source B data is similar in format to that for Source A. However, because less data went into finding the Source B equation, there is less confidence that other parameters will not improve matters. The equation,

---

* The exponent on σ_θ is somewhat smaller than expected, apparently because the mountainous terrain reduces the importance of lateral diffusion in relation to vertical diffusion.

$$E_p/Q_T = 0.00913\, X^{-1.20}\, \sigma_\theta^{-0.140}\, \bar{u}^{-1.00}\, (\Delta T_6^{54} + 5)^{-0.57} \qquad (17)$$

predicts 75% within a factor of 2 and 97% within a factor of 4. By separating the tests into day and night classes, prediction success of 100% within a factor of 4 could be attained. With only about 40 points available for testing, however, (about a dozen for night tests) little importance is attached to the success.

It is worth noting that the dependence on temperature stratification in Equation (17) is inverse to that physically plausible and to that found for the Source A equation. Whether this is a meaningful result of some interrelation between stability and wind flow patterns, or a fiction resulting from a severely truncated set of data, is not known.

The difficulty involved in deriving an equation for use from Source B, and the physically reasonable form of Equations (15) and (16) for Source A, led to a test of the hypothesis that the two sources could be modeled by the same equation. The meteorological data from Tower 300 were used in conjunction with data from Source B tests and the best Source A equation to yield the results shown in Figure 28. The tendency for overprediction at high exposures (short distances) is obvious, and is related to uncertainty in short range centerline exposures for Source B tests. At lower exposures, the predictive success increases. In no case does the Source A equation underpredict by a factor of four, and only 1 of the 27 test points lies outside the 95% upper limit of the Source A equation.

A particularly significant test of the Source A equation applied to diffusion from Source B was offered by Test 72. This test gave the highest concentrations observed in the entire test series at distances of five to seven miles from the source. Even for these most extreme concentrations, the prediction equation gave acceptable results. Thus, the Source A equation appears to be adequately representative of the diffusion over the rugged terrain of South Vandenberg and, therefore, can be used for both source points.

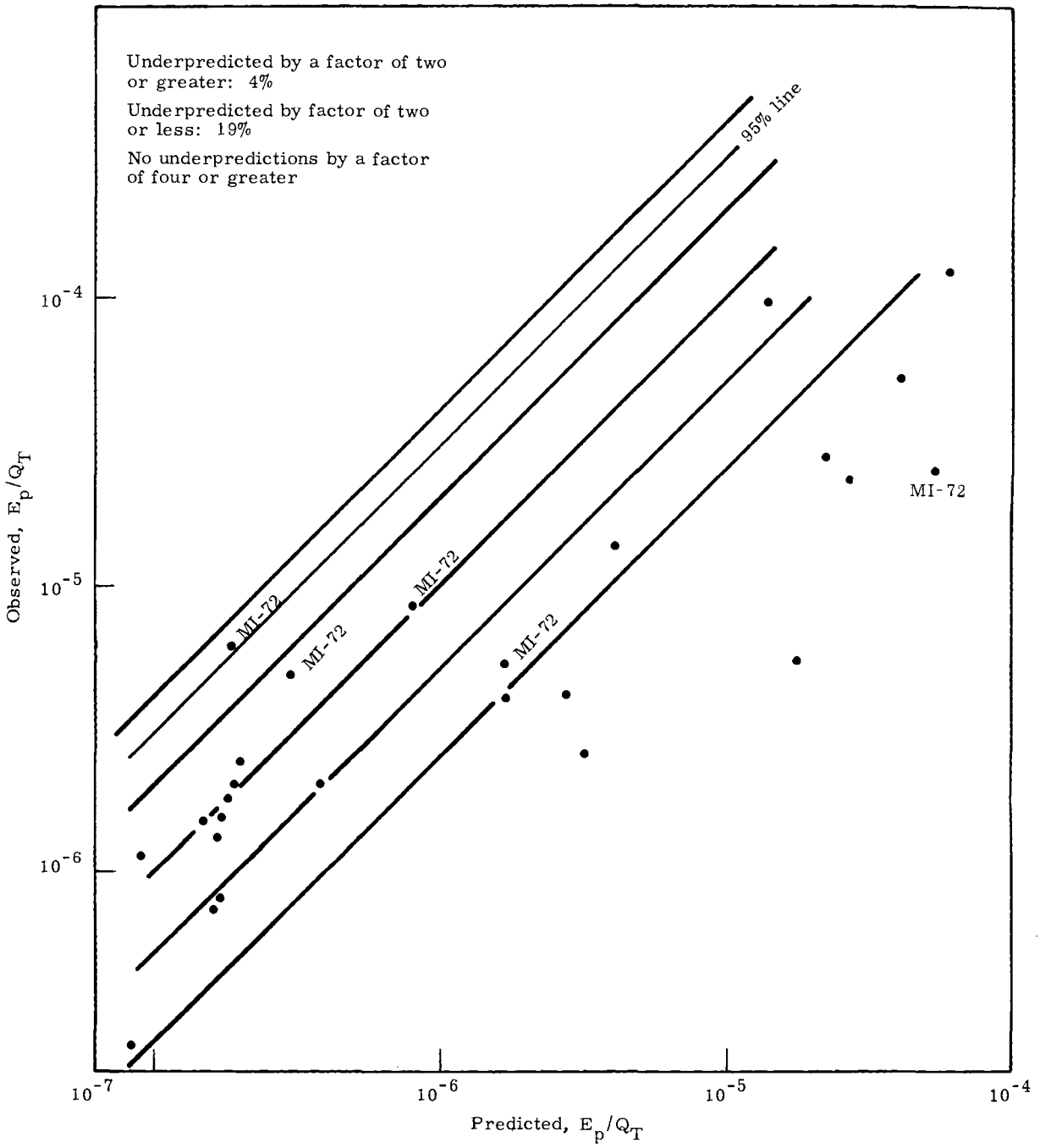

FIGURE 28. Source "B" Diffusion Data Predicted by Recommended Source "A" Equation with "300" Tower Meteorological Data

OPERATIONAL EQUATIONS

A detailed discussion of the derivation of prediction equations is given in Volume I. Here the equations are presented in forms directly useful for prediction.

The engineering units used in this section are as follows:

- x/Q is normalized concentration in ppm NO_2/lb per minute release
- X is distance in feet
- σ_θ is standard deviation of wind direction fluctuations in degrees, measured at 12 feet and averaged over 10-second intervals
- $\bar{u}$ is mean wind speed in knots, measured at 12 feet
- ΔT_1^2 is temperature difference in degrees Fahrenheit, between heights 1 and 2 (heights in feet)

These units are common to all equations in this chapter unless explicitly noted.

Limitations On The Use Of The South Vandenberg Equation(s)

Results from any empirical study are limited in their usefulness, and the statistical-fit equations developed from the Mountain Iron data are no exceptions. To offer some guidance in the judicious use of the equations, the limits imposed by test conditions are briefly examined here.

Source Point Limitations

Although the equation applies specifically to the VIP-1 area, the equation should also be applicable to source points resembling the Source A area: near the ocean, with unobstructed upwind fetch, and with a fairly rough downwind region over which diffusion takes place (which assures a level of mixing more or less comparable to that observed from Source A). These restrictions mean that the equation must not be expected to apply to diffusion from a source in Honda Canyon, for example, nor a source in the Santa Ynez Valley, especially in westerly winds. Likewise, a source in the Sudden Ranch area can not be reliably simulated from the Phase I Mountain Iron equation. Source points that are reasonable extrapolations from the Source A area lie between Palc I, Palc II, Pad A and

Pad D--a fairly generous portion of South Vandenberg. Probably any departure from the immediate area of Source A will probably result in degrading the accuracy and reliability of the predictions. However, in this respect, comparisons of the Source B tests with predictions from the Source A equation and tower 300 data are encouraging. The Source B tests show that exposures from this release point can be expected to be comparable to those from Source A over moderate distances.

Distance Limits

All Mountain Iron tests were confined to distances less than about 10 miles, with only a very few tests successful in providing data at that distance. The majority of the tests terminated at 5 miles or so, since the sampling was restricted to the South Vandenberg area. For this reason, confident use of the equations must be restricted to perhaps 10 or 11 miles. The systematic error pointed out in the statistical fit portion of this chapter means that extreme caution is required even at that distance because underprediction is almost assured during daytime conditions beyond some 8 or 9 miles. There is no help for this unless a quite artificial correction is applied to daytime tests to reduce the error, and such a practice is not recommended. More work would be required, and substantially different testing programs carried out, to provide a real basis for prediction of exposures at distances exceeding 10 miles.

Source Type Restrictions

Most of the Mountain Iron tests were of 15 or 30 minute duration, with a constant and continuous release rate, while 9 tests were only 5 minutes long. Since no discernible difference exists between 15 and 30 minute tests, these were treated in the analysis as a homogeneous group. The 5-minute tests presented a slightly different result: they indicated a more rapid decrease in exposure with distance than the other tests, in agreement with theoretical predictions, and, for that reason, are not strictly within the domain of the equations recommended for use.

The most severe restriction on source type is the height of release, with only ground level releases being pertinent. If any substantial elevation from ground level is postulated, the Mountain Iron results are not applicable. Thus, bouyant plumes--as from a conflagration--are among the excluded types of sources; so are simple elevated sources. Some use of the equation can be made as a limit which slightly elevated sources will soon approach, but there is little possibility of accurately predicting the position or magnitude of the maximum exposure from any elevated source. It seems probable that the equation will not serve even as a limiting case if the source is high (such as a couple hundred feet), or if the elevated release is into a stable atmosphere. Only a substantially modified testing program will yield results pertaining to bouyant or elevated sources. As in the case with the North Vandenberg WIND equation, the South Vandenberg equation applies most accurately to a cold spill situation; especially one with a limited horizontal extent, since the tests were conducted with essentially point sources.

Puffs, even if not bouyant, are not correctly handled by the recommended equation, because of the great difference in the mechanism governing diffusion of puffs and plumes (the 5-minute tests approach puffs in behavior). In particular, puffs during a portion of their history diffuse faster than plumes, leading to somewhat lower exposures for a given release rate. Without data, no guidance is possible other than theoretical developments beyond the scope of this report.

Recommended Equations

In the development of the statistical model, two equations of almost identical format were finally chosen to provide the best available predictions. The recommended equation uses the temperature difference between 6 and 300 feet; the deeper layer parameter produces a slightly improved reliability of prediction within a factor of 2 when compared to the results from a 6 to 54 foot temperature difference.

The median equation for the centerline concentration, averaged over the time of plume passage, is

$$\chi/Q = 7.35 \times 10^4 X^{-1.85} \sigma_\theta^{-0.355} \bar{u}^{-0.868} (\Delta T_6^{300} + 10.8)^{1.14} \quad (18)$$

The 95% confidence level equation is

$$\chi/Q = 2.13 \times 10^5 X^{-1.85} \sigma_\theta^{-0.355} \bar{u}^{-0.868} (\Delta T_6^{300} + 10.8)^{1.14} \quad (19)$$

The distance to a given average concentration is

$$X = 444(\chi/Q)^{-0.54} \sigma_\theta^{-0.192} \bar{u}^{-0.470} (\Delta T_6^{300} + 10.8)^{0.616} \quad (20)$$

for the median prediction, while for the 95% level, the distance is

$$X = 790(\chi/Q)^{-0.54} \sigma_\theta^{-0.192} \bar{u}^{-0.470} (\Delta T_6^{300} + 10.8)^{0.616} \quad (21)$$

These equations refer to average concentration of NO_2 only, in parts per million. The release rate, which was used to normalize the concentration, is in units of pounds per minute.

An Alternate Equation

Since only a small difference was found between the two equations and since 6 to 300 foot temperature differences are available at very few sites on South Vandenberg, the equation developed for 6 to 54 foot temperature difference is used here to form a set of equations for operational use in the same manner as the recommended equation.

The median equation for the average concentration along the centerline of the plume is

$$\chi/Q = 3.79 \times 10^4 X^{-1.82} \sigma_\theta^{-0.417} \bar{u}^{-1.03} (\Delta T_6^{54} + 9)^{1.55} \quad (22)$$

while the 95% level equation is

$$\chi/Q = 1.14 \times 10^5 X^{-1.82} \sigma_\theta^{-0.417} \bar{u}^{-1.03} (\Delta T_6^{54} + 9)^{1.55} \quad (23)$$

The distance to a given concentration level is

$$X = 332(\chi/Q)^{0.55} \sigma_\theta^{-0.229} \bar{u}^{-0.566} (\Delta T_6^{54} + 9)^{0.852} \quad (24)$$

for the median equation; the 95% level distance equation is

$$X = 608(\chi/Q)^{-0.55} \sigma_\theta^{-0.229} \bar{u}^{-0.566} (\Delta T_6^{54} + 9)^{0.852} \quad (25)$$

These equations (just as for the recommended equations in the previous section) refer to parts per million of NO_2 only, and are normalized to a release rate in terms of pounds per minute.

Equations for an Arbitrary Contaminant

When some gas other than NO_2 is expected to be troublesome, the equations must be corrected to allow for variation in molecular weight. If M is the molecular weight of the gas of concern, then the 95% confidence level equation is

$$\frac{\chi M}{Q} = 52.5 \times 10^5 X^{-1.82} \sigma_\theta^{-0.417} \bar{u}^{-1.03} (\Delta T_6^{54} + 9)^{1.55} \quad (26)$$

or, in terms of distance to a concentration,

$$X = 5000\left(\frac{\chi M}{Q}\right)^{-0.55} \sigma_\theta^{-0.229} \bar{u}^{-0.566} (\Delta T_6^{54} + 9)^{0.852} \quad (27)$$

If the contaminant is a particulate rather than a gas, specification of parts per million loses its significance. Rather, the mass of the contaminant per cubic meter is the pertinent measure. At the 95% confidence level, with χ in grams per cubic meter and Q in pounds per minute,

$$\frac{\chi}{Q} = 228 X^{-1.82} \sigma_\theta^{-0.417} \bar{u}^{-1.03} (\Delta T_6^{54} + 9)^{1.55} \quad (28)$$

or, in terms of distance to a concentration,

$$X = 19.8\left(\frac{\chi}{Q}\right)^{-0.55} \sigma_\theta^{-0.229} \bar{u}^{-0.566} (\Delta T_6^{54} + 9)^{0.852} \quad (29)$$

Source B

The recommended equation for diffusion from Source A, Equation (21), is also recommended for Source B by using meteorological data from Site 300 tower. The successful prediction of the exceptionally high concentrations measured in Test 72 (mentioned earlier) gives added confidence in this recommended application.

CHAPTER 7.
SECONDARY INVESTIGATIONS

In conjunction with the work leading to the prediction equation, which was the object of this study, several subsidiary facets of diffusion over South Vandenberg were examined. Generally, these studies were brief and not at all definitive, but were certainly of interest in the conclusions possible. The topics included in this chapter are short-term releases, trajectory analysis of some of the tests, and ways of constructing trajectories. The initial effort made here on trajectory studies indicates that investigation of transport on a mesoscale is particularly promising for future work.

SHORT TERM RELEASES

During the Mountain Iron testing series, a few tests were conducted with release times considerably shorter than the standard. Although such tests were not required to provide the final equation sought, additional confidence in the use of the equation seemed possible if such data were available. In all, nine 5-minute tests were made from Source A, with two being night tests. The exposure data from the 5-minute tests formed a very homogeneous set, with relatively little scatter; comparison with data from 30-minute tests showed that the 5-minute tests resulted in the same level of exposure at moderate distances--one to three miles (Figure 29). The striking difference lay in the dependence on X of the 5-minute tests; whereas, the 30-minute tests decreased with the -1.8 power of distance, the 5-minute tests decreased with the -2.2 power of distance. This is in accordance with theory--at least in principle, if not in magnitude. The 30-minute tests diffuse in two dimensions only, being little affected by longitudinal diffusion, but the 5-minute tests diffuse in three dimensions, because the longitudinal dimension of the short tests is usually comparable with the lateral dimension.

TRAJECTORY STUDIES

Several techniques for estimating the trajectory of the material released during Mountain Iron tests were investigated to determine as accurately as possible the relative usefulness of each.

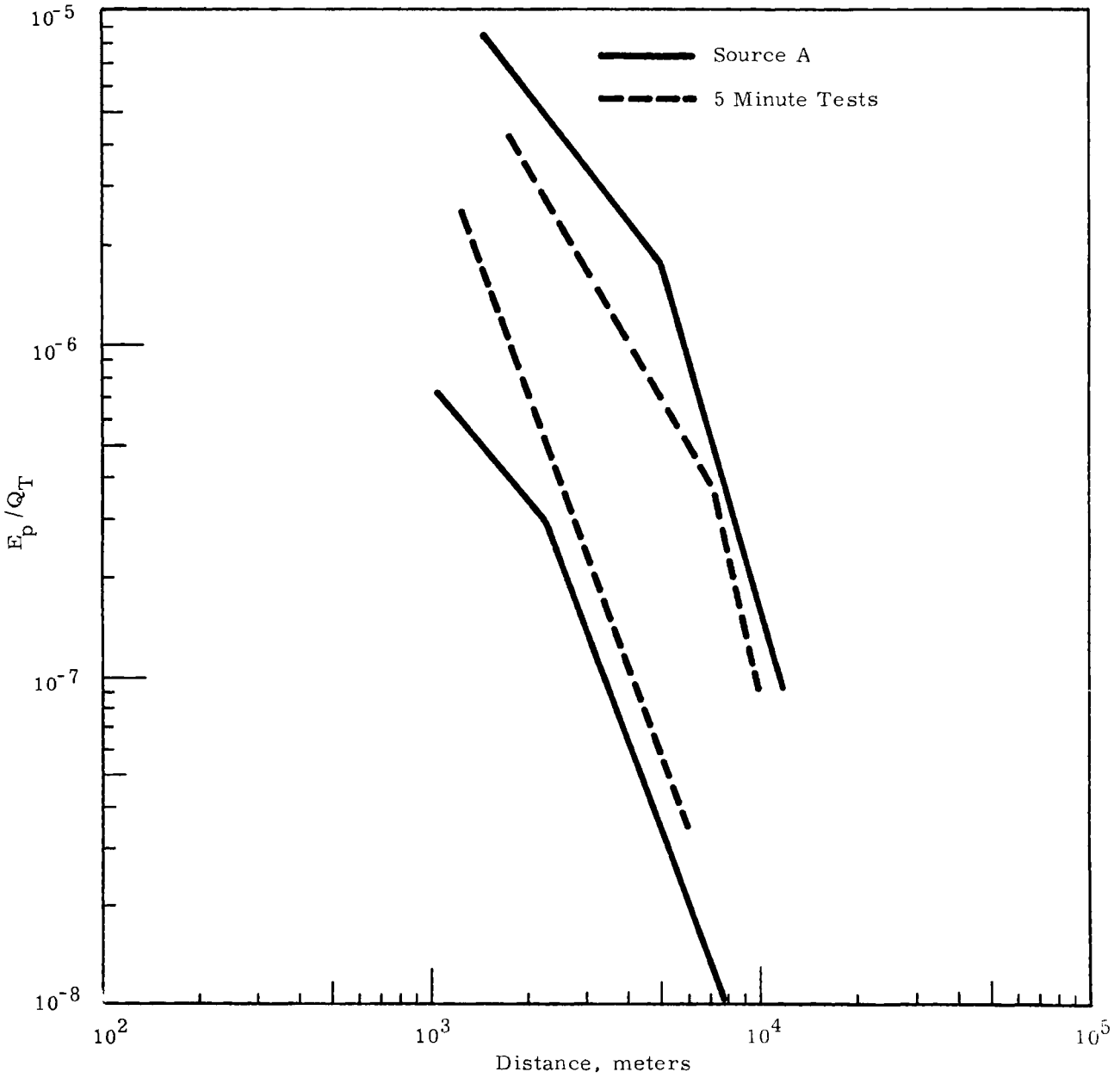

FIGURE 29. Comparison of 30- and 5-Minute Release Times

- The simplest approach involved the use of wind direction from a single WIND sensor to predict the trajectory.
- A more complex method was the use of 100-foot winds wherever available and 54-foot or surface winds at other sites.
- Another method entailed the use of 5-minute averages of surface winds at all possible sites to construct a rather detailed trajectory prediction.

These methods will be discussed individually to provide a basis for operational trajectory predictions.

Trajectories From 30-Minute Average Winds

The possibility of using rather long-term averages of wind direction and speed to estimate plume travel was investigated by using 30-minute average data from the operational WIND sites. Only a few tests were conducted during the brief interval when the entire WIND system was up, prior to the complete shutdown involved in the installation of the new computer during June and July. The tests were MI-67 and MI-69 through 96, of which 14 tests were from Source A and 5 from Source B.

The simplest approach to trajectory forecast is to choose a single wind sensor to indicate the wind field carrying the plume. To determine the success of various choices of wind sensors, the difference in direction between the forecast plume direction and the actual direction was calculated (in degrees azimuth) for all the tests listed above, along with the standard deviation of error was calculated (Table IX). Since the one-sigma limit is tabled for each site, the trajectory forecast from a particular site fell within the listed limits of error 68% of the time.

If only a single site is to be used, it is clear from the table that Site 100 provides the best prediction of plume travel. Thus, for a release at the VIP-1 Pad, a centerline drawn according to Site 100 wind direction would be less than 6 degrees in error 68% of the time. A similar degree of success seems plausible for releases from nearby points (such as Palc II), especially since a quarter of the data involved in deriving Table IX were from Source B releases, rather distant from the VIP-1 pad.

TABLE IX. Plume Centerline Location Error Using Selected Single Wind Observations

Site	Height of Wind Observation	Degrees Error (in 68% of Cases)
Source	Surface	±10
300	300 - 100 foot	±15
300	54 foot	±19
300	Surface	±23
100	100 foot	±6
100	Surface	±17
10	Surface	±28
11	Surface	±84

Nevertheless, the use of a single point for estimating trajectories is to be discouraged, especially in such terrain as found at South Vandenberg, since the probability of strong deviations in direction with increasing distance is high. The 30 minute average wind conditions from all the WIND system sensors, using 100-foot winds where available, provided a much more detailed basis on which to work. To construct the 30-minute trajectories, the wind field indicated by the 30-minute average winds was drawn, and the path of a parcel starting from the source point was drawn according to the field. The next 30 minute average field was drawn, the path of the parcel for the second 30-minute interval deduced, and drawn onto the first 30 minute map. This 1 hour path was then compared with the observed plume.

Two variations were investigated at this time. The 100-foot wind field was drawn both with and without the information received from the source point wind sensor, which is not a WIND site for the Source A releases. Likewise, the wind fields as indicated by the surface winds were drawn with and without the source point wind. The results are shown in Table X. Although the lack of a source point wind is a serious handicap, it is interesting to note that the relative success of this detailed procedure is no better than that of the single-wind process.

For example, at two miles, the best estimate is from the 100-foot winds, but the one-sigma error is still 6 degrees.

TABLE X. Trajectory Errors in Tests MI-67 and MI-69 Through 86 Using Selected Wind Data

Wind Data	Degrees Error 68% of Cases	
	1.8 mi	3.6 mi
100 ft height with source wind	±6	±4
100 ft height without source wind	±12	±10
Surface winds	±8	±13
Surface winds without source wind	±21	±21

The surface winds have a larger error, 8 degrees, which seems to indicate that 100 feet is a better estimate of the transport height of the bulk of the plume. There are no definitive data on this point, so it must be conjectural. It will be shown later (in the Appendix on aircraft sampling) that the plume regularly was sampled at hundreds of feet above the terrain; therefore, a great deal of the plume must be well removed from the surface, at least during daytime conditions to which aircraft sampling was restricted.

Trajectories From 5-Minute Average Winds

A detailed investigation of trajectories, as indicated by the surface winds averaged over 5-minute intervals, was also carried out for one case. The wind field was drawn in detail from the wind information for each 5 minute interval; from this the plume travel was deduced and drawn on a map and, as would be expected, this technique yielded the best estimate of plume travel. The results of the trajectory predicted and observed for Mountain Iron Test 72 is shown in Figure 30. It is worthwhile to note that the curvature on the ground pattern of exposure is, indeed, indicated in the surface wind pattern as well. No attempt was made to relate the spread of the estimated plume segment trajectories to the observed plume spread, but such a relationship would be worthy of future study.

MI-72

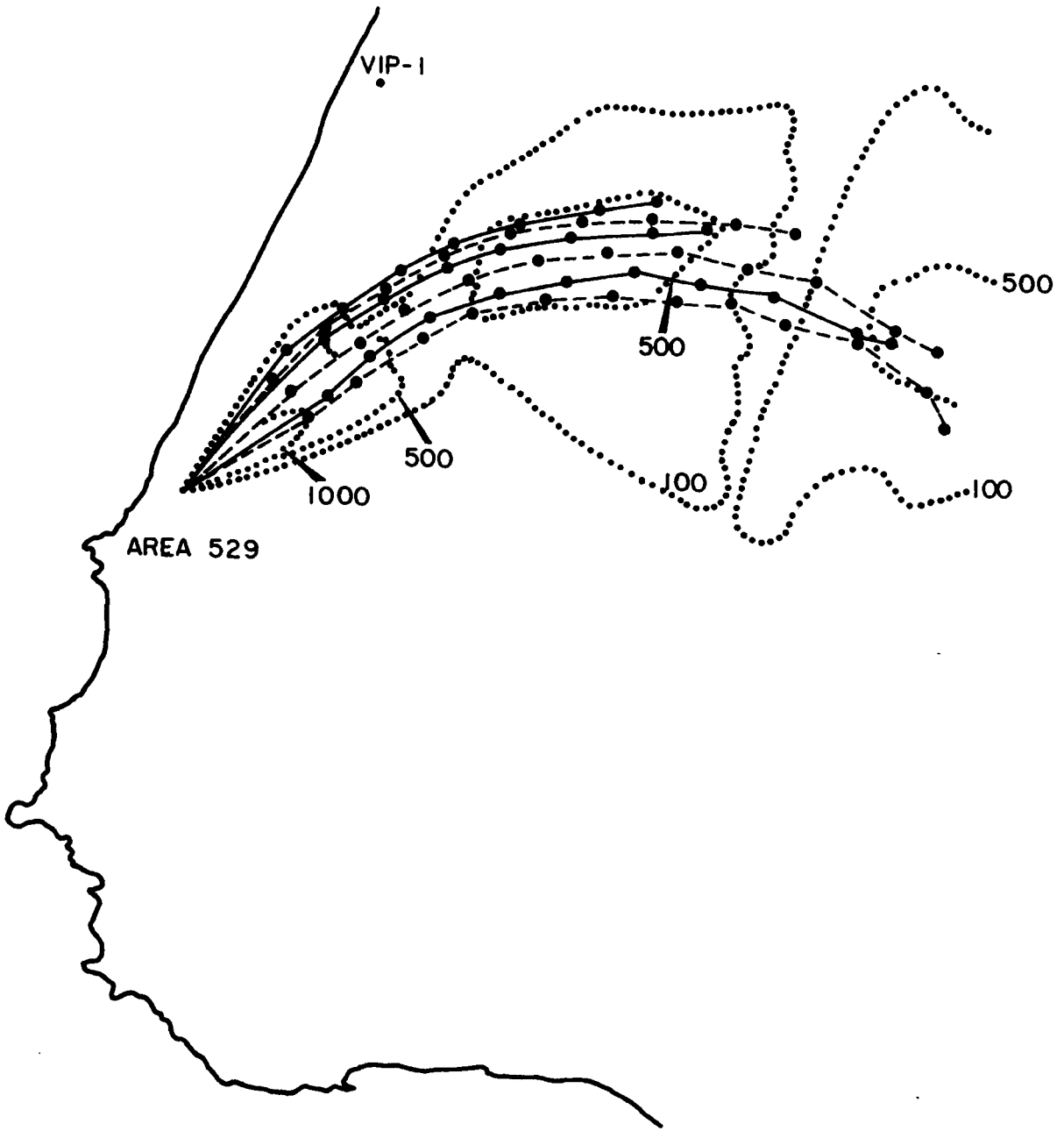

FIGURE 30. Trajectory from 5-Minute Average Winds for MI-72

The success of any trajectory analysis probably lies in accurate and rapid wind information. The WIND system should provide an adequate basis for well estimated plume paths, particularly if the trajectories are constructed by one familiar with the peculiarities of orographically distorted wind fields.

One of the by-products of the trajectory investigation was noting the persistent lack of correlation between the average wind field and the flow indicated by three of the WIND system sensors: 010 in Bear Creek Canyon, 011 in Spring Canyon, and 012 in Honda Canyon. These sites appear to be very strongly influenced by the nearby walls of their respective canyons, so that their information is not at all indicative of the flow only a few hundred yards away. These sensors should be left where they are only if the data from these canyons are of primary importance. If their indications are used uncritically to construct wind fields, severe and erroneous curvature in the wind patterns will often result.

CHAPTER 8.
COMPARISON OF MOUNTAIN IRON DATA WITH OTHER SITES

INTRODUCTION

One important aspect of any large field program in atmospheric diffusion is the relationship between the data gathered and data available from previous experimentation. The importance of comparing new data with older and more familiar data is at least two-fold:

- Anomolous diffusion conditions or sites will be singled out and may provide important contributions to the understanding of diffusion in general.
- If no anomalies are found, the existence of regularities in diffusion at varying sites provides hope that generalized models will indeed be appropriate.

THE NORTH VANDENBERG DIFFUSION EQUATION

The possibility of using the existing North Vandenberg diffusion equation, developed for use over the northern section of Vandenberg, is examined here. Only the Source A data were used for the comparison, with the source point data, not the standard WIND sensor data, being used as input to the equation. The reason for this is that adequate WIND system data from the 300 tower were not available for many of the Mountain Iron diffusion tests.

The results of the comparison are shown in Figure 31. The North Vandenberg equation shows a systematic error. On the average, the equation overpredicts by about a factor of two, but underpredicts 26% of the cases examined. The relative scatter increases as exposures decrease (at greater distances). One of the limiting factors in the use of the North Vandenberg equation is that it was derived from data taken no further than 6 km from the source, a distance which is about the middle of the South Vandenberg sampling grid. The comparison was made with data taken out to about 8 km.

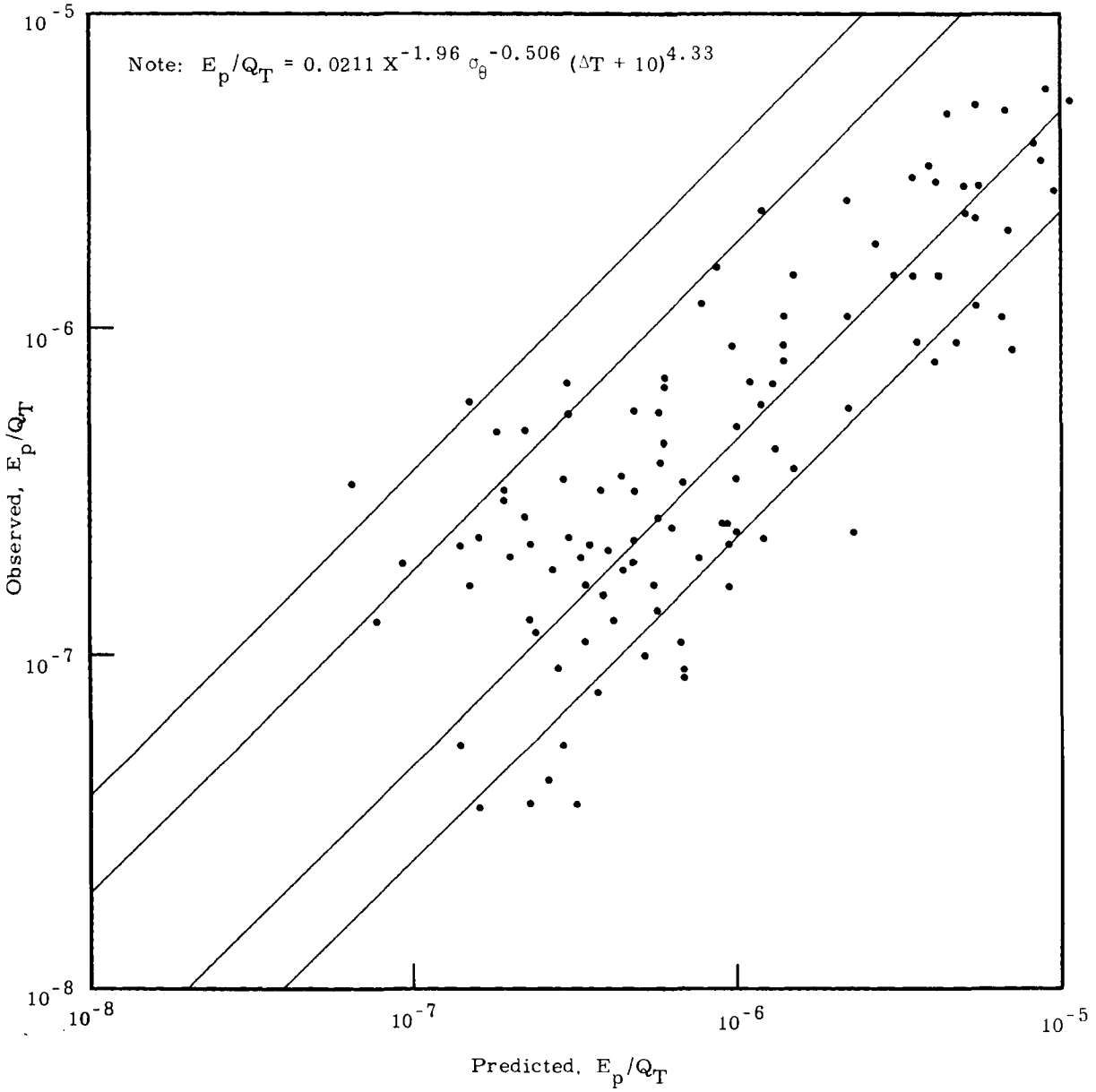

FIGURE 31. Mountain Iron Data Versus Predictions from Weather Information Network and Display (WIND)

The predictions from the North Vandenberg equation are generally rather good. Its major drawback is the too rapid decrease of exposure with distance, which leads to underprediction if pressed beyond several kilometers. Futhermore, wind speed was found not to be an important parameter for the North Vandenberg equation, which, in addition is too sensitive to temperature stratification to be accurate over South Vandenberg. This can be easily seen by comparing the North Vandenberg equation with either the quasi-physical model or the statistical model for South Vandenberg.

COMPARISON OF SOUTH VANDENBERG WITH OTHER SITES

Earlier work integrating diffusion results from several sites is reported by Fuquay and Simpson[8] who used data from many field programs including the Dry Gulch diffusion program at North Vandenberg. The present purposes do not require detailed comparisons of the Mountain Iron data with many other sites because a comparison with the Dry Gulch data will indicate the degree of difference of the South Vandenberg area sufficiently.

Dry Gulch data indicated that, on the average, winter night conditions yielded exposures some two to four times higher than summer night conditions. In contrast, daytime conditions were little different between the seasons, and the daytime tests averaged about a factor of four lower than the night tests. However, the Mountain Iron data do not fall into this same pattern. Over South Vandenberg (on the average), summer nights produced the highest exposures--about a factor of two higher than the winter night tests. Also, the daytime Mountain Iron tests, are only a factor of two lower than the night tests. In fact, the Mountain Iron data indicate a considerable overlap between day and night tests, something not found in all earlier series.

Some important differences between Mountain Iron and Dry Gulch data can be seen in Figure 32, where the day tests from both Dry Gulch and Mountain Iron are plotted as well as the average of all Hanford day

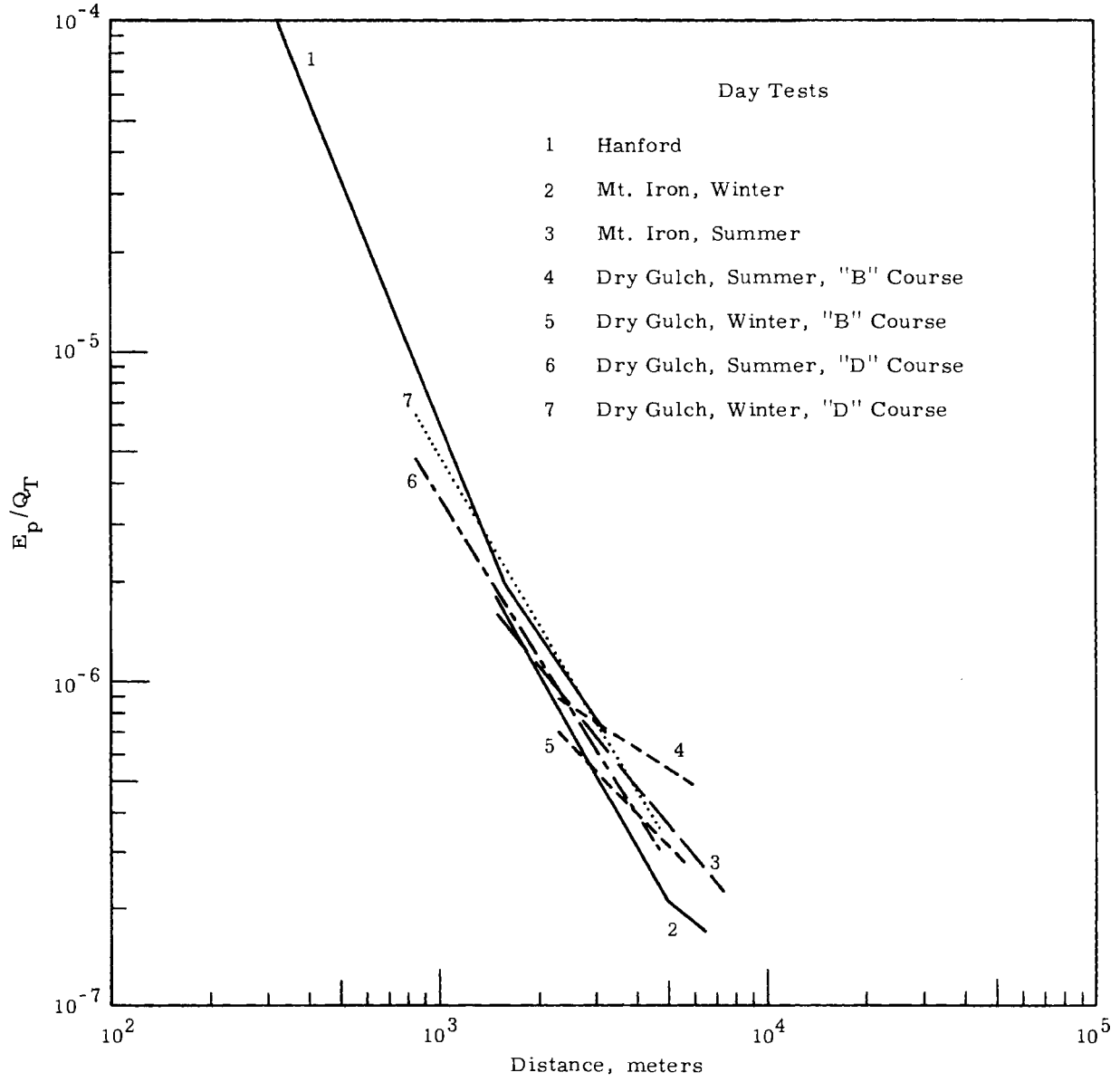

FIGURE 32. Comparison of Day Tests from Dry Gulch, Mountain Iron, and Hanford Series

tests. The overlap is remarkable, with all the data averages found within a factor of two over the range of data. Considering the number of tests included in the average curves, some fair degree of confidence can be felt in the resulting figure. The variance of terrain from flat (at Hanford) to South Vandenberg's ridges and canyons would indicate that terrain effects are minimized during day-light hours; relatively windy days produce similar exposures at all three sites. The restriction to "relatively windy days" is made because the Hanford area, at least, can be subjected to intense convective conditions, and such conditions can yield results considerably different from those found in the windy conditions prevailing during all the tests. There is some question whether South Vandenberg is ever subject to such intense heating because of the proximity of the ocean and adjacent cool air. In any case, no tests have been made at either site in such convective and relatively windless conditions.

Considerably wider scatter between sites for the night tests is shown in Figure 33. As noted before, the Dry Gulch data show winter nights to yield higher exposures than summer nights; whereas, the Mountain Iron data show just the opposite. These are difficult generalizations, though, because the Dry Gulch test series had rather sketchy testing during the night hours, and the Mountain Iron series had only a few tests during the winter nights. Thus, some question may remain whether the results (Figure 33) are completely adequate for representative climatology. The Mountain Iron test series included a generous sampling of nighttime summer tests, a substantially higher proportion than Dry Gulch, or Mountain Iron winter testing, and may be relied upon. The relatively low exposures indicated for Hanford's night tests are from the large proportion of testing in only slightly stable conditions. During very stable conditions at Hanford, the resulting exposures are considerably higher than indicated here; however, very stable conditions near the surface are not at all characteristic of the Vandenberg area, so the more moderate stability shown is more or less comparable to Vandenberg results.

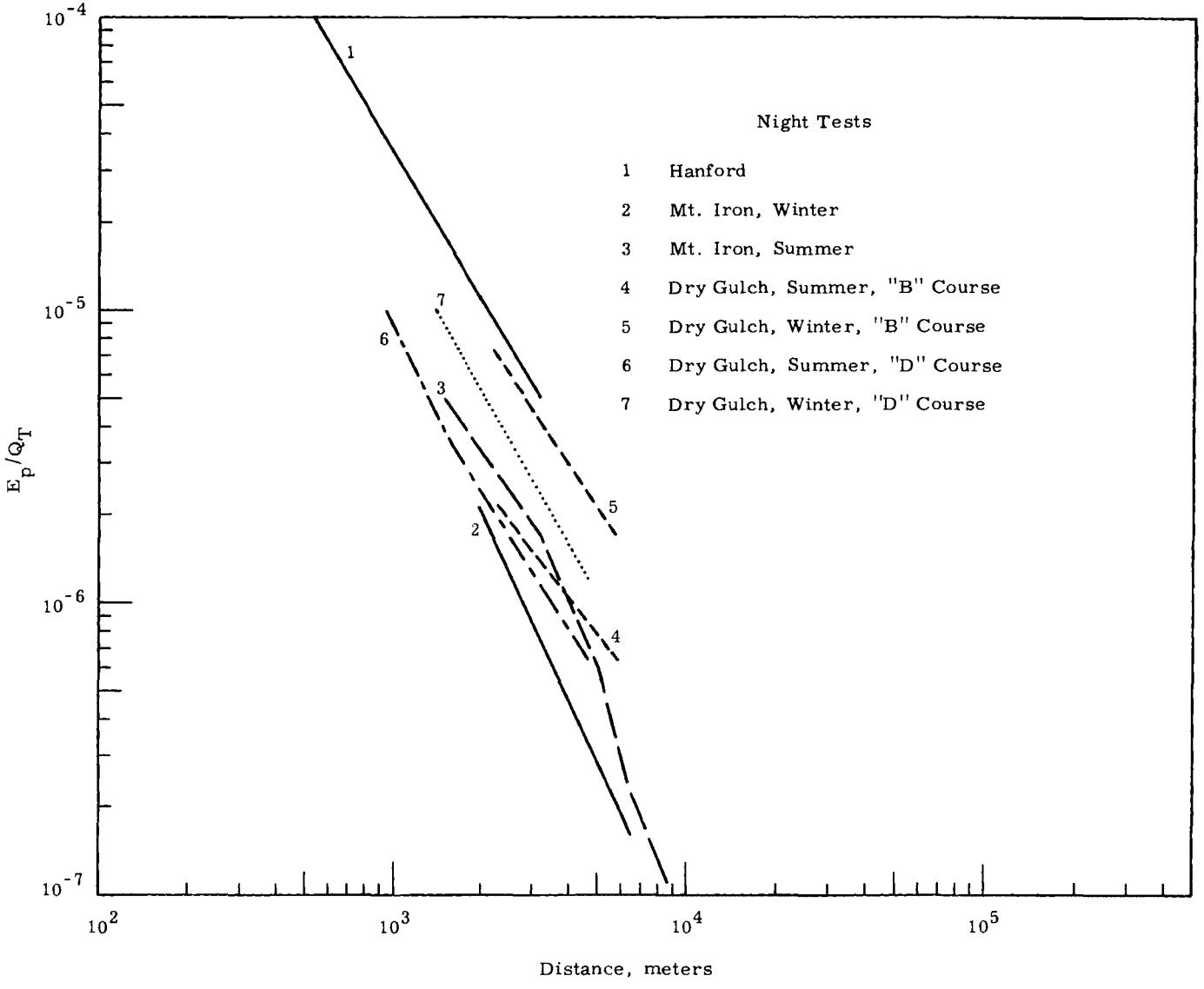

FIGURE 33. Comparison of Night Tests from Dry Gulch, Mountain Iron, and Hanford Series

In spite of the rather close relationship between sites (indicated in Figures 32 and 33), it must be remembered that a great deal of scatter exists around each of the averaged curves. In fact, most of the curves have data that lie a factor of three or more above and below the mean; this precludes any finer comparison between the curves. However, the average slope of the data curves is probably rather well determined and deserves mention. The Mountain Iron data indicate a steeper slope for the night tests than any of the other sites shown here, which seems to be the result of the enhanced mixing caused by the strong vertical motions induced in travel over the ridges of South Vandenberg. The slope of both winter and summer tests over South Vandenberg is steeper than over North Vandenberg, so apparently the rough terrain is influential in causing enhanced diffusion, whether a summer subsidence inversion exists or not. Actually, since the averages of the Mountain Iron data are so closely related, the hilly terrain seems to be the decisive factor in determining diffusion.

APPENDIX A

BASIC DATA FROM MOUNTAIN IRON PHASE I

APPENDIX A

BASIC DATA FROM MOUNTAIN IRON PHASE I

TEST	E_p/Q_T Sec/m^3	X Meters	t Seconds	σ_y Meters	σ_θ Degrees	$\bar{u}$ Meters/sec	ΔT_6^{54} °C	ΔT_6^{300} °C
3	1.75^{-6}	1420	540	142	9.5	2.7	--	--
	9.40^{-7}	2540	940	251	9.5	2.7	--	--
	3.30^{-7}	5130	1250	368	9.5	2.7	--	--
	1.10^{-7}	7820	1600	535	9.5	2.7	--	--
4	3.60^{-7}	2540	590	251	6.0	4.3	--	--
	1.35^{-7}	5640	1200	--	6.0	4.3	--	--
	6.40^{-8}	7210	1500	--	6.0	4.3	--	--
5	1.20^{-6}	1420	270	135	5.5	5.3	--	--
	5.60^{-7}	2480	470	285	5.5	5.3	--	--
	9.70^{-8}	5500	930	--	5.5	5.3	--	--
	4.20^{-8}	6480	1120	--	5.5	5.3	--	--
	4.40^{-8}	8070	1170	--	5.5	5.3	--	--
6	2.80^{-6}	1290	180	109	6.5	7.1	--	--
	1.40^{-6}	1940	270	142	6.5	7.1	--	--
	2.05^{-7}	4080	550	335	6.5	7.1	--	--
7	5.70^{-7}	2300	1350	470	31.3	1.7	--	--
	1.60^{-7}	5300	2590	--	31.3	1.7	--	--
	6.00^{-8}	8700	3810	--	31.3	1.7	--	--
9	1.48^{-6}	2300	790	251	11.0	2.9	--	--
	9.14^{-7}	5560	1940	--	11.0	2.9	--	--
	9.01^{-7}	6130	2150	--	11.0	2.9	--	--
	5.66^{-7}	6800	2410	--	11.0	2.9		
	4.05^{-7}	7400	2640	--	11.0	2.9	--	--
11	7.55^{-7}	2400	--	--	--	--	--	--
	2.32^{-7}	5500	--	--	--	--	--	--
	1.63^{-7}	7820	--	--	--	--	--	--
12	6.20^{-7}	1290	540	201	18.5	2.4	--	--
	4.00^{-7}	2300	960	332	18.5	2.4	--	--
	2.24^{-7}	4600	1660	--	18.5	2.4	--	--
	1.40^{-7}	8700	2680	--	18.5	2.4	--	--

Note: The notation used for all exposure data in Appendix A is such that $2.00^{-6} = 2.00 \times 10^{-6}$

BASIC DATA FROM MOUNTAIN IRON PHASE I

TEST	E_p/Q_T Sec/m^3	X Meters	t Seconds	σ_y Meters	σ_θ Degrees	$\bar{u}$ Meters/sec	ΔT_6^{54} °C	ΔT_6^{300} °C
13	1.32^{-6}	1420	680	167	13.6	2.1	--	--
	6.57^{-7}	2300	1090	135	13.6	2.1	--	--
	1.74^{-7}	5640	1810	--	13.6	2.1	--	--
14	2.13^{-6}	1240	210	167	15.1	5.8	--	--
	4.00^{-7}	2630	450	--	15.1	5.8	--	--
	8.60^{-8}	4280	670	--	15.1	5.8	--	--
	4.70^{-8}	5580	840	--	15.1	5.8	--	--
15	1.15^{-5}	1240	200	142	10.2	--	--	--
	1.46^{-6}	2770	430	--	10.2	--	--	--
	4.59^{-7}	4120	580	--	10.2	--	--	--
	1.24^{-7}	4970	720	--	10.2	--	--	--
16	6.30^{-6}	1240	200	92	8.6	2.1	--	--
	9.08^{-7}	2670	430	109	8.6	2.1	--	--
	2.74^{-7}	4220	660	367	8.6	2.1	--	--
	4.90^{-8}	4950	810	--	8.6	2.1	--	--
	1.10^{-7}	5810	900	--	8.6	2.1	--	--
17	6.30^{-7}	1240	380	142	--	--	--	--
	5.30^{-8}	2630	790	267	--	--	--	--
	3.10^{-8}	4280	1200	318	--	--	--	--
	3.30^{-8}	5260	1450	--	--	--	--	--
18	2.39^{-6}	1340	520	142	15.8	2.6	-0.9	-0.8
	1.60^{-6}	2300	880	226	15.8	2.6	-0.9	-0.8
	3.21^{-7}	4600	1580	546	15.8	2.6	-0.9	-0.8
	2.01^{-7}	6150	2690	670	15.8	2.6	-0.9	-0.8
	2.19^{-7}	7420	3240	879	15.8	2.6	-0.9	-0.8
19	8.71^{-7}	1340	--	--	--	--	-1.3	-1.7
	2.62^{-7}	2540	--	--	--	--	-1.3	-1.7
	1.66^{-7}	4700	--	--	--	--	-1.3	-1.7
	1.58^{-7}	7130	--	--	--	--	-1.3	-1.7

BASIC DATA FROM MOUNTAIN IRON PHASE I

TEST	E_p/Q_T Sec/m^3	X Meters	t Seconds	σ_y Meters	σ_θ Degrees	$\bar{u}$ Meters/sec	ΔT_6^{54} °C	ΔT_6^{300} °C
21	1.52^{-6}	1390	510	167	12.9	2.7	-1.1	-1.4
	1.85^{-7}	5110	1660	836	12.9	2.7	-1.1	-1.4
	1.93^{-7}	6420	1960	930	12.9	2.7	-1.1	-1.4
	5.50^{-8}	7700	2570	--	12.9	2.7	-1.1	-1.4
23	1.18^{-6}	1660	540	134	6.5	3.1	-0.5	-0.9
	3.43^{-7}	5110	1410	268	6.5	3.1	-0.5	-0.9
	2.37^{-7}	6420	1630	286	6.5	3.1	-0.5	-0.9
	9.20^{-8}	7760	1860	--	6.5	3.1	-0.5	-0.9
25	2.28^{-6}	1270	290	92	9.2	4.4	-1.2	-1.6
	6.79^{-7}	2770	600	168	9.2	4.4	-1.2	-1.6
	3.55^{-7}	4080	760	300	9.2	4.4	-1.2	-1.6
	5.30^{-8}	7130	1130	570	9.2	4.4	-1.2	-1.6
26	3.39^{-6}	1420	250	100	5.5	5.7	-1.5	-0.8
	6.21^{-7}	2540	440	201	5.5	5.7	-1.5	-0.8
	5.40^{-8}	5010	700	335	5.5	5.7	-1.5	-0.8
27	9.24^{-7}	1420	280	117	5.8	5.0	-0.9	-1.4
	2.49^{-7}	2430	490	--	5.8	5.0	-0.9	-1.4
	7.80^{-8}	5300	900	--	5.8	5.0	-0.9	-1.4
	3.50^{-8}	7420	1130	450	5.8	5.0	-0.9	-1.4
28	5.75^{-6}	1080	400	100	16.9	2.7	-0.6	+0.8
	7.04^{-7}	4030	1420	351	16.9	2.7	-0.6	+0.8
	4.10^{-8}	6050	1900	838	16.9	2.7	-0.6	+0.8
29	6.16^{-7}	1870	--	--	--	--	-0.9	-1.2
	1.04^{-7}	4970	--	--	--	--	-0.9	-1.2
	6.10^{-8}	6660	--	--	--	--	-0.9	-1.2
30	7.46^{-6}	1340	480	92	5.6	2.8	0.0	+0.2
	5.18^{-6}	2300	820	126	5.6	2.8	0.0	+0.2
	7.97^{-7}	4600	1370	277	5.6	2.8	0.0	+0.2
	1.68^{-7}	7130	1940	--	5.6	2.8	0.0	+0.2
31	1.24^{-6}	2300	350	192	4.7	6.6	-0.1	+0.2
	2.52^{-7}	5600	810	--	4.7	6.6	-0.1	+0.2
	1.09^{-7}	6480	1110	418	4.7	6.6	-0.1	+0.2
	7.70^{-8}	8700	1150	--	4.7	6.6	-0.1	+0.2

BASIC DATA FROM MOUNTAIN IRON PHASE I

TEST	E_p/Q_T Sec/m^3	X Meters	t Seconds	σ_y Meters	σ_θ Degrees	$\bar{u}$ Meters/sec	ΔT_6^{54} °C	ΔT_6^{300} °C
32	4.41^{-6}	1420	260	76	4.5	5.4	-0.1	+0.3
	9.70^{-7}	2480	460	218	4.5	5.4	-0.1	+0.3
	1.65^{-7}	5600	920	293	4.5	5.4	-0.1	+0.3
	9.80^{-8}	7210	1460	--	4.5	5.4	-0.1	+0.3
33	1.60^{-6}	1530	260	76	3.7	5.9	-0.4	-0.5
	2.36^{-7}	4970	960	--	3.7	5.9	-0.4	-0.5
	2.33^{-7}	5850	1180	226	3.7	5.9	-0.4	-0.5
	3.60^{-8}	8110	1790	--	3.7	5.9	-0.4	-0.5
34	3.14^{-6}	1390	240	75	3.8	5.9	-0.2	-0.2
	2.29^{-7}	4750	770	335	3.8	5.9	-0.2	-0.2
	1.92^{-7}	6420	1000	351	3.8	5.9	-0.2	-0.2
35	3.52^{-6}	1080	200	67	3.5	5.5	-0.4	-0.4
	3.78^{-7}	4060	710	218	3.5	5.5	-0.4	-0.4
	1.37^{-7}	6700	1060	335	3.5	5.5	-0.4	-0.4
36	2.87^{-6}	1390	170	84	3.2	8.1	--	--
	3.99^{-7}	4060	490	--	3.2	8.1	--	--
	1.37^{-7}	7500	880	--	3.2	8.1	--	--
38	2.01^{-6}	1660	620	118	10.9	2.7	-1.6	-1.4
	4.89^{-7}	5110	1540	335	10.9	2.7	-1.6	-1.4
	1.94^{-7}	6800	1940	--	10.9	2.7	-1.6	-1.4
39	2.00^{-6}	720	--	--	--	--	-1.4	-1.5
	7.76^{-7}	1080	--	--	--	--	-1.4	-1.5
	3.47^{-7}	4620	--	--	--	--	-1.4	-1.5
	2.21^{-7}	7500	--	--	--	--	-1.4	-1.5
40	4.47^{-6}	1270	260	84	7.0	4.9	-1.7	-0.9
	6.83^{-7}	4080	700	349	7.0	4.9	-1.7	-0.9
	3.07^{-7}	5060	900	488	7.0	4.9	-1.7	-0.9
	8.30^{-8}	7110	1060	--	7.0	4.9	-1.7	-0.9
41	1.17^{-6}	2000	430	84	4.3	4.7	-1.6	-2.0
	2.24^{-7}	5620	1050	502	4.3	4.7	-1.6	-2.0
	2.33^{-7}	6640	1250	316	4.3	4.7	-1.6	-2.0

BASIC DATA FROM MOUNTAIN IRON PHASE I

TEST	E_p/Q_T Sec/m^3	X Meters	t Seconds	σ_y Meters	σ_θ Degrees	$\bar{u}$ Meters/sec	ΔT_6^{54} °C	ΔT_6^{300} °C
42	2.98^{-6}	1240	240	60	31.2	5.2	-0.9	-1.3
	1.52^{-7}	2770	510	--	31.2	5.2	-0.9	-1.3
	1.08^{-7}	4320	690	200	31.2	5.2	-0.9	-1.3
	3.40^{-8}	5810	950	435	31.2	5.2	-0.9	-1.3
	2.30^{-8}	9820	1540	--	31.2	5.2	-0.9	-1.3
43	4.26^{-6}	1290	270	84	6.9	4.7	-0.3	-1.4
	2.51^{-6}	2050	440	151	6.9	4.7	-0.3	-1.4
	9.49^{-7}	2730	560	--	6.9	4.7	-0.3	-1.4
	3.47^{-7}	4080	730	465	6.9	4.7	-0.3	-1.4
	1.82^{-7}	5060	930	--	6.9	4.7	-0.3	-1.4
	6.00^{-8}	5810	960	--	6.9	4.7	-0.3	-1.4
	3.00^{-8}	9600	1470	--	6.9	4.7	-0.3	-1.4
44	3.99^{-6}	1760	340	67	2.9	5.2	-0.7	-1.6
	1.68^{-7}	4750	820	207	2.9	5.2	-0.7	-1.6
	3.50^{-8}	8110	1360	218	2.9	5.2	-0.7	-1.6
45	5.06^{-6}	360	70	42	9.9	3.7	--	--
	1.53^{-7}	4060	1030	335	9.9	3.7	--	--
	1.37^{-7}	5740	1290	502	9.9	3.7	--	--
46	2.54^{-6}	1290	430	100	11.0	3.6	-0.2	+0.1
	1.84^{-6}	2730	880	159	11.0	3.6	-0.2	+0.1
	3.52^{-7}	4080	1120	302	11.0	3.6	-0.2	+0.1
	9.40^{-8}	4950	1350	419	11.0	3.6	-0.2	+0.1
	1.91^{-7}	5810	1490	419	11.0	3.6	-0.2	+0.1
	9.00^{-8}	9820	2830	--	11.0	3.6	-0.2	+0.1
47	2.25^{-6}	1470	--	--	--	--	--	--
	4.99^{-7}	2850	--	--	--	--	--	--
	3.32^{-7}	4060	--	--	--	--	--	--
	1.52^{-7}	4420	--	--	--	--	--	--
	1.09^{-7}	5220	--	--	--	--	--	--
	7.20^{-8}	8130	--	--	--	--	--	--

BASIC DATA FROM MOUNTAIN IRON PHASE I

TEST	E_p/Q_T Sec/m^3	X Meters	t Seconds	σ_y Meters	σ_θ Degrees	$\bar{u}$ Meters/sec	ΔT_6^{54} °C	ΔT_6^{300} °C
48	2.72^{-6}	1340	--	--	--	--	-0.2	+0.2
	1.31^{-6}	2560	--	--	--	--	-0.2	+0.2
	4.27^{-7}	4830	--	--	--	--	-0.2	+0.2
	3.73^{-7}	7110	--	--	--	--	-0.2	+0.2
	6.00^{-8}	9820	--	--	--	--	-0.2	+0.2
49	2.76^{-6}	390	--	--	--	--	-1.4	-1.8
	7.50^{-8}	5620	--	--	--	--	-1.4	-1.8
50	1.00^{-6}	1870	400	100	4.4	4.7	-1.3	-1.3
	2.00^{-7}	5460	1190	302	4.4	4.7	-1.3	-1.3
51	1.81^{-6}	670	--	107	--	--	0.0	+0.4
	2.62^{-7}	1320	--	--	--	--	0.0	+0.4
	1.04^{-7}	7090	--	581	--	--	0.0	+0.4
52	8.04^{-6}	390	--	--	--	--	-1.8	-2.2
	6.60^{-7}	1200	--	235	--	--	-1.8	-2.2
	1.52^{-7}	6090	--	553	--	--	-1.8	-2.2
53	2.20^{-6}	720	690	117	23.9	3.2	-0.6	-1.8
	3.17^{-7}	4080	1190	419	23.9	3.2	-0.6	-1.8
54	1.58^{-7}	7740	2120	158	10.7	3.7	-1.5	-0.5
55	9.59^{-6}	390	--	--	--	--	-5.3	-5.5
	4.02^{-7}	1200	--	--	--	--	-5.3	-5.5
	2.40^{-8}	6090	--	--	--	--	-5.3	-5.5
56	5.37^{-7}	570	200	--	18.7	--	-0.6	0.0
57	1.23^{-6}	670	--	--	--	--	-2.1	-2.7
	7.60^{-7}	1320	--	--	--	--	-2.1	-2.7
	8.40^{-8}	5620	--	--	--	--	-2.1	-2.7
	8.90^{-8}	7050	--	--	--	--	-2.1	-2.7

BASIC DATA FROM MOUNTAIN IRON PHASE I

TEST	E_p/Q_T Sec/m^3	X Meters	t Seconds	σ_y Meters	σ_θ Degrees	$\bar{u}$ Meters/sec	ΔT_6^{54} °C	ΔT_6^{300} °C
58	2.30^{-6}	390	--	--	--	--	-2.1	-2.5
	4.07^{-7}	1230	--	--	--	--	-2.1	-2.5
	1.83^{-7}	5790	--	--	--	--	-2.1	-2.5
59	4.57^{-7}	1870	480	201	12.4	3.9	-1.7	-2.5
	1.42^{-7}	4400	1110	--	12.4	3.9	-1.7	-2.5
	1.70^{-7}	5110	1280	--	12.4	3.9	-1.7	-2.5
	1.30^{-7}	6910	1710	--	12.4	3.9	-1.7	-2.5
60	1.36^{-6}	900	230	84	9.8	3.9	-0.6	-1.5
	1.97^{-7}	4060	1010	402	9.8	3.9	-0.6	-1.5
	1.62^{-7}	6050	1430	637	9.8	3.9	-0.6	-1.5
61	4.27^{-7}	1120	400	--	15.8	--	-0.2	-1.6
	1.03^{-7}	5340	3190	--	15.8	--	-0.2	-1.6
	4.80^{-8}	7660	3860	--	15.8	--	-0.2	-1.6
62	3.52^{-6}	390	100	67	15.8	3.9	-2.2	-2.5
	6.04^{-7}	1320	340	335	15.8	3.9	-2.2	-2.5
63	1.36^{-6}	1120	390	116	8.0	2.9	-2.5	-3.0
	7.80^{-8}	6300	2350	--	8.0	2.9	-2.5	-3.0
64	5.12^{-6}	280	90	--	--	--	-1.2	-1.8
	1.82^{-7}	5380	--	--	--	--	-1.2	-1.8
	1.15^{-7}	7480	--	--	--	--	-1.2	-1.8
65	4.75^{-7}	3910	--	--	27.3	--	--	--
66	2.87^{-6}	390	--	--	--	--	-2.0	-2.2
	9.77^{-7}	670	--	--	--	--	-2.0	-2.2
	1.07^{-7}	5180	--	--	--	--	-2.0	-2.2
67	2.62^{-7}	5320	2080	--	16.3	--	-1.2	-1.5
	2.00^{-7}	5580	1890	386	16.3	--	-1.2	-1.5
	2.44^{-7}	7660	2610	--	16.3	--	-1.2	-1.5
	2.04^{-7}	7480	2690	--	16.3	--	-1.2	-1.5

BASIC DATA FROM MOUNTAIN IRON PHASE I

TEST	E_p/Q_T Sec/m^3	X Meters	t Seconds	σ_y Meters	σ_θ Degrees	$\bar{u}$ Meters/sec	ΔT_6^{54} °C	ΔT_6^{300} °C
68	7.00^{-6}	390	100	67	12.0	4.0	-0.8	-1.3
	2.16^{-6}	670	170	134	12.0	4.0	-0.8	-1.3
	8.56^{-7}	1200	300	201	12.0	4.0	-0.8	-1.3
	1.45^{-7}	5790	1450	502	12.0	4.0	-0.8	-1.3
69	6.91^{-7}	1080	280	--	13.2	3.8	-0.9	-1.3
	5.21^{-7}	1390	370	167	13.2	3.8	-0.9	-1.3
	1.36^{-7}	6050	1590	670	13.2	3.8	-0.9	-1.3
70	6.26^{-7}	1870	550	167	16.4	3.4	-1.1	-0.7
	6.05^{-7}	4620	1430	670	16.4	3.4	-1.1	-0.7
	3.94^{-7}	6800	2210	--	16.4	3.4	-1.1	-0.7
71	5.07^{-6}	260	59	42	47.0	4.4	-0.8	-1.4
	1.30^{-7}	5540	1360	--	47.0	4.4	-0.8	-1.4
	1.14^{-7}	7900	1650	837	47.0	4.4	-0.8	-1.4
72	2.50^{-6}	370	130	100	14.0	2.8	--	--
	5.25^{-7}	2420	860	386	14.0	2.8	--	--
	8.40^{-7}	3600	1290	--	14.0	2.8	--	--
	4.75^{-7}	6130	2140	1120	14.0	2.8	--	--
	5.95^{-7}	7950	2740	1120	14.0	2.8	--	--
73	6.60^{-6}	260	60	33	9.2	4.7	-1.1	-2.7
	3.35^{-7}	1400	300	151	9.2	4.7	-1.1	-2.7
	2.55^{-7}	4090	850	351	9.2	4.7	-1.1	-2.7
	1.99^{-7}	5420	1080	502	9.2	4.7	-1.1	-2.7
74	1.17^{-6}	1660	503	167	14.6	3.3	-0.1	-0.6
	2.77^{-7}	4030	1260	553	14.6	3.3	-0.1	-0.6
	2.36^{-7}	6700	2290	1105	14.6	3.3	-0.1	-0.6
65	1.97^{-6}	720	360	118	--	--	-0.2	0.0
76	2.25^{-6}	720	270	--	--	--	-0.3	-0.2
	5.02^{-7}	4030	1470	--	--	--	-0.3	-0.2
	2.00^{-7}	6050	2120	--	--	--	-0.3	-0.2

BASIC DATA FROM MOUNTAIN IRON PHASE I

TEST	E_p/Q_T Sec/m^3	X Meters	t Seconds	σ_y Meters	σ_θ Degrees	$\bar{u}$ Meters/sec	ΔT_6^{54} °C	ΔT_6^{300} °C
77	3.65^{-6}	1420	260	116	9.4	5.5	-0.4	-0.2
	1.57^{-6}	2300	420	134	9.4	5.5	-0.4	-0.2
	2.90^{-7}	5300	1120	235	9.4	5.5	-0.4	-0.2
	1.30^{-7}	8070	1700	384	9.4	5.5	-0.4	-0.2
	3.30^{-8}	11400	1990	670	9.4	5.5	-0.4	-0.2
78	5.40^{-6}	1270	260	118	13.4	4.9	--	--
	3.20^{-6}	2050	420	140	13.4	4.9	--	--
	5.70^{-7}	4700	930	302	13.4	4.9	--	--
	8.80^{-8}	6400	1540	467	13.4	4.9	--	--
	1.06^{-7}	7420	1350	502	13.4	4.9	--	--
	9.60^{-8}	10200	1560	418	13.4	4.9	--	--
79	8.20^{-6}	1420	570	84	5.2	2.5	+0.2	-0.1
	3.00^{-6}	2540	1010	117	5.2	2.5	+0.2	-0.1
	7.54^{-7}	5130	1470	167	5.2	2.5	+0.2	-0.1
	1.27^{-7}	8010	1930	418	5.2	2.5	+0.2	-0.1
	2.20^{-8}	10500	2100	604	5.2	2.5	+0.2	-0.1
80	8.05^{-6}	1420	590	100	5.1	2.4	--	+0.6
	3.00^{-6}	2540	1050	151	5.1	2.4	--	+0.6
	5.95^{-7}	4830	1400	209	5.1	2.4	--	+0.6
	5.40^{-8}	6620	2090	460	5.1	2.4	--	+0.6
	1.10^{-7}	7420	1730	418	5.1	2.4	--	+0.6
	8.10^{-8}	10200	1920	335	5.1	2.4	--	+0.6
81	9.20^{-6}	1420	300	84	4.9	4.8	0.0	+0.4
	2.97^{-6}	2480	520	163	4.9	4.8	0.0	+0.4
	5.52^{-7}	5500	1060	302	4.9	4.8	0.0	+0.4
	9.60^{-8}	6710	2110	--	4.9	4.8	0.0	+0.4
	2.33^{-7}	8700	1650	511	4.9	4.8	0.0	+0.4
	4.30^{-8}	10800	1690	418	4.9	4.8	0.0	+0.4
82	1.20^{-5}	260	60	34	11.5	4.1	-2.1	+0.4
	1.56^{-7}	6130	1870	502	11.5	4.1	-2.1	+0.4
	1.03^{-7}	7900	2260	753	11.5	4.1	-2.1	+0.4
83	1.49^{-7}	5970	1840	--	24.0	--	-1.2	-2.0

BASIC DATA FROM MOUNTAIN IRON PHASE I

TEST	E_p/Q_T Sec/m^3	X Meters	t Seconds	σ_y Meters	σ_θ Degrees	$\bar{u}$ Meters/sec	ΔT_6^{54} °C	ΔT_6^{300} °C
84	1.60^{-6}	1870	640	167	24.6	2.9	--	--
	3.56^{-7}	5720	1540	435	24.6	2.9	--	--
	2.33^{-7}	7000	1890	486	24.6	2.9	--	--
85	2.01^{-6}	1390	500	184	24.6	2.8	--	--
86	7.59^{-6}	1390	460	84	12.7	3.0	--	--
	6.23^{-7}	4060	1540	334	12.7	3.0	--	--
	2.36^{-7}	5640	3970	--	12.7	3.0	--	--
	1.72^{-7}	6300	3030	418	12.7	3.0	--	--
	7.10^{-8}	7970	3950	--	12.7	3.0	--	--
87	3.97^{-6}	720	140	48	5.7	5.2	--	--
	1.08^{-6}	1260	--	100	5.7	5.2	--	--
	5.39^{-6}	3310	--	418	5.7	5.2	--	--
	3.27^{-7}	4400	--	--	5.7	5.2	--	--
88	6.17^{-6}	1420	360	126	6.3	3.9	+0.1	+0.1
	2.54^{-6}	2560	650	217	6.3	3.9	+0.1	+0.1
	1.21^{-6}	4600	1110	293	6.3	3.9	+0.1	+0.1
	1.43^{-7}	6150	1810	418	6.3	3.9	+0.1	+0.1
89	4.19^{-6}	2270	520	116	5.4	4.4	+0.1	+0.1
	9.78^{-7}	5620	1140	318	5.4	4.4	+0.1	+0.1
	2.66^{-7}	6860	2640	326	5.4	4.4	+0.1	+0.1
	1.96^{-7}	7700	2040	675	5.4	4.4	+0.1	+0.1
	1.41^{-7}	8800	2150	502	5.4	4.4	+0.1	+0.1
	4.70^{-8}	13200	2400	745	5.4	4.4	+0.1	+0.1
90	5.08^{-6}	1870	480	134	7.9	3.9	-0.3	-0.3
	4.90^{-7}	5620	1630	435	7.9	3.9	-0.3	-0.3
91	4.09^{-6}	1270	380	117	8.5	3.3	0.0	+0.4
	1.54^{-6}	2670	780	335	8.5	3.3	0.0	+0.4
	9.11^{-7}	4220	1010	581	8.5	3.3	0.0	+0.4
	2.42^{-7}	4950	1180	670	8.5	3.3	0.0	+0.4
	2.02^{-7}	7130	1400	558	8.5	3.3	0.0	+0.4
	5.70^{-8}	10000	1640	836	8.5	3.3	0.0	+0.4

BASIC DATA FROM MOUNTAIN IRON PHASE I

TEST	E_p/Q_T Sec/m^3	X Meters	t Seconds	σ_y Meters	σ_θ Degrees	$\bar{u}$ Meters/sec	ΔT_6^{54} °C	ΔT_6^{300} °C
92	8.58^{-6}	390	90	174	5.7	4.5	-0.1	+0.2
	1.98^{-6}	670	150	232	5.7	4.5	-0.1	+0.2
	6.11^{-7}	940	210	465	5.7	4.5	-0.1	+0.2
	3.27^{-7}	5260	820	--	5.7	4.5	-0.1	+0.2
93	7.07^{-6}	390	70	--	10.7	5.5	-0.5	0.0
	2.80^{-6}	670	120	226	10.7	5.5	-0.5	0.0
	1.18^{-6}	940	170	268	10.7	5.5	-0.5	0.0
	1.07^{-7}	5260	660	670	10.7	5.5	-0.5	0.0
94	4.98^{-6}	1290	330	100	6.5	3.9	--	--
	2.76^{-6}	2300	590	159	6.5	3.9	--	--
	9.15^{-7}	4600	1040	227	6.5	3.9	--	--
	1.31^{-7}	6400	1510	--	6.5	3.9	--	--
	2.03^{-7}	7130	1530	--	6.5	3.9	--	--
	6.90^{-8}	10200	1950	--	6.5	3.9	--	--
95	5.98^{-7}	5320	3920	627	18.1	2.2	-1.3	-1.0
	2.35^{-7}	7480	5120	--	18.1	2.2	-1.3	-1.0
96	6.99^{-6}	390	140	--	16.2	2.8	-1.6	-1.4
	2.55^{-6}	860	310	--	16.2	2.8	-1.6	-1.4
	5.35^{-7}	1200	430	--	16.2	2.8	-1.6	-1.4
	3.60^{-7}	5790	1380	418	16.2	2.8	-1.6	-1.4
	5.50^{-8}	15100	2420	--	16.2	2.8	-1.6	-1.4
97	2.10^{-7}	7480	3320	--	11.0	--	-3.0	-4.2
98	5.96^{-6}	1270	400	93	7.8	3.2	-0.4	-0.1
	7.49^{-7}	4320	1220	402	7.8	3.2	-0.4	-0.1
	1.32^{-7}	5810	1460	465	7.8	3.2	-0.4	-0.1
	6.30^{-8}	9600	2080	--	7.8	3.2	-0.4	-0.1
99	8.67^{-6}	1270	470	76	6.0	2.7	-0.2	-0.1
	4.55^{-6}	2730	980	169	6.0	2.7	-0.2	-0.1
	2.13^{-6}	4088	1510	297	6.0	2.7	-0.2	-0.1
	3.76^{-7}	7110	1880	--	6.0	2.7	-0.2	-0.1

BASIC DATA FROM MOUNTAIN IRON PHASE I

TEST	E_p/Q_T Sec/m^3	X Meters	t Seconds	σ_y Meters	σ_θ Degrees	$\bar{u}$ Meters/sec	ΔT_6^{54} °C	ΔT_6^{300} °C
100	5.40^{-6}	1290	--	136	--	--	-0.4	-0.3
	3.08^{-6}	2050	--	187	--	--	-0.4	-0.3
	7.05^{-7}	4080	--	678	--	--	-0.4	-0.3
	1.54^{-7}	9840	--	--	--	--	-0.4	-0.3
101	2.76^{-6}	2300	1920	--	18.8	--	-0.4	0.0
102	5.61^{-6}	1290	640	109	11.4	2.0	-0.3	0.0
	3.25^{-6}	2170	1080	184	11.4	2.0	-0.3	0.0
	1.69^{-6}	4600	1580	293	11.4	2.0	-0.3	0.0
	2.48^{-7}	7130	1880	--	11.4	2.0	-0.3	0.0
	5.70^{-8}	10000	2320	419	11.4	2.0	-0.3	0.0
103	4.04^{-6}	1240	680	134	14.9	2.0	--	-0.1
	1.25^{-6}	2730	1290	302	14.9	2.0	--	-0.1
	9.15^{-7}	4080	1510	441	14.9	2.0	--	-0.1
	1.82^{-7}	5060	1800	710	14.9	2.0	--	-0.1
	2.80^{-7}	7110	2090	418	14.9	2.0	--	-0.1
	6.80^{-8}	9920	2510	754	14.9	2.0	--	-0.1
104	498^{-6}	2000	1000	142	8.4	2.0	-0.5	+0.1
	3.81^{-6}	2270	1140	177	8.4	2.0	-0.5	+0.1
	6.16^{-7}	5620	2270	419	8.4	2.0	-0.5	+0.1
	1.53^{-7}	6680	2980	--	8.4	2.0	-0.5	+0.1
	2.93^{-7}	8330	2630	--	8.4	2.0	-0.5	+0.1
106	2.89^{-6}	1270	510	136	14.3	2.5	-0.4	-0.2
	1.30^{-6}	2730	1070	--	14.3	2.5	-0.4	-0.2
	1.67^{-7}	5700	1860	560	14.3	2.5	-0.4	-0.2
	1.33^{-7}	9620	2540	--	14.3	2.5	-0.4	-0.2
107	1.56^{-6}	2000	620	102	9.4	3.2	-0.7	0.0
	5.02^{-7}	5480	1580	--	9.4	3.2	-0.7	0.0
109	5.00^{-7}	4030	1460	--	8.8	2.8	-1.9	-1.9
	3.24^{-7}	6260	2350	627	8.8	2.8	-1.9	-1.9

BASIC DATA FROM MOUNTAIN IRON PHASE I

TEST	E_p/Q_T Sec/m^3	X Meters	t Seconds	σ_y Meters	σ_θ Degrees	$\bar{u}$ Meters/sec	ΔT_6^{54} °C	ΔT_6^{300} °C
110	1.53^{-6}	2230	830	144	15.4	2.7	-0.6	-0.7
	7.37^{-7}	4060	1400	254	15.4	2.7	-0.6	-0.7
	3.75^{-7}	5740	1700	507	15.4	2.7	-0.6	-0.7
111	1.99^{-6}	900	280	101	11.5	3.2	-2.1	-2.8
	6.65^{-7}	4030	1180	--	11.5	3.2	-2.1	-2.8
	3.75^{-7}	6260	1550	--	11.5	3.2	-2.1	-2.8
112	2.16^{-6}	1200	380	102	10.3	3.2	-0.9	-0.9
	6.06^{-7}	4060	1210	336	10.3	3.2	-0.9	-0.9
113	8.73^{-7}	2400	560	152	4.6	4.3	-0.4	-0.8

BASIC DATA FROM MOUNTAIN IRON, PHASE I

DISTANCE FROM VIP-1 (SOURCE A) TO SAMPLES IN METERS

Arc	Sample	X	Sample	X	Sample	X	Sample	X
01	010	701	02 010	1420	03 010	4120	04 010	4930
	020	693	020	1340	020	4220	020	4950
	030	725	030	1290	030	4280	030	5030
	040	799	040	1270	040	4320	040	4950
	050	913	050	1240	050	4280	050	4850
	060	880	060	1240	060	4220	060	4970
	070	880	070	1270	070	4180	070	5200
	080	929	080	1470	080	4080	080	5100
	090	717	090	1450	090	4080	090	4950
	100	538	100	2960	100	4180	100	5060
	110	375	110	2730	110	4270	110	5150
	120	261	120	2770	120	4340	120	5500
	130	408	130	2670	130	4500	130	5620
	140	570	140	2630	140	4600	140	5830
	150	717	150	2590	150	4700	150	5950
	160	896	160	2420	160	4750	160	6150
	170	1076	170	2640	170	4830	170	6400
	180	1222	180	2850	180	4890	180	6620
	190	1386	190	3280	190	5010	190	6850
	200	1532	200	3690	200	5130	200	6710
	210	1663	210	4060	210	5300	210	6580
	220	1760	220	4380	220	5500	220	6480
	230	1874	230	4340	230	5500	230	6680
	240	2005	240	4320	240	5560	240	6800
	250	2119	250	4420	250	5640	250	7000
	260	2266	260	4520	260	5640	260	6990
	270	2298	270	4600	270	5600	270	7210
	280	2396	280	4520	280	5620	280	7400
	290	2478	290	4440	290	5660	290	7700
	300	2543	300	4360	300	5790	300	8030
	310	2559	310	4280	310	5870	310	8440
	320	2429	320	4200	320	5720	320	8570
	330	2298	330	4080	330	5560		
	340	2168						
	350	2054						
	360	1940						

DISTANCE FROM VIP-1 (SOURCE A) TO SAMPLES IN METERS (contd)

Arc	Sample	X	Sample	X	Sample	X	Sample	X
05	010	5220	06 010	4090	07 010	5420	09	
	020	5260	020	4090	020	5540	020	7210
	030	5460	030	4090	030	5580	030	8030
	040	5640	040	4090	040	5740	040	8130
	050	5580	050	4060	050	5830	050	8720
	060	5700	060	4030	060	6050	060	9270
	070	5810	070	4010	070	6210	070	9620
	080	5810	080	4010	080	6260	080	9600
	090	6010	090	4030	090	6050	090	9820
	100	6340	100	4030	100	6300	100	9840
	110	6620	110	4060	110	6500	110	9920
	120	6910	120	4080	120	6500	120	9820
	130	7110	130	4060	130	6700	130	10020
	140	7130	140	4060	140	6800	140	10210
	150	7170	150	4090	150	6910	150	10470
	160	7190	160	4220	160	7190	160	10820
	170	7210	170	4400	170	7500	170	11410
	180	7420	180	4520	180	7860	180	12180
	190	7580	190	4620	190	7990	190	12780
	200	7820	200	4690	200	8070	200	13220
	210	8010	210	4750	210	8110	210	13350
	220	8170	220	4830	220	7970	220	13810
	230	8070	230	4970	230	7760	230	14340
	240	8330	240	5110	240	7540	240	14790
	250	8620	250	5240	250	7210	250	15140
	260	8700	260	5400	260	6860	260	15360
	270	8800	270	5480	270	6640	270	15630
	280	8820	280	5620			280	16220
			290	5850			290	16790
			300	5970			300	17420
(Resurrected Jeep			310	6130			310	18010
Trail Samplers)			320	6280			320	18660
			330	6400				
05	500	5540	340	6420				
	510	5400	350	6400				
	520	5680	360	6520				
	530	6110	370	6540				
	540	6340	380	6660				
	550	7110	390	6800				

BASIC DATA FROM MOUNTAIN IRON, PHASE I

DISTANCE FROM AREA 529 (SOURCE B) TO SAMPLES IN METERS

Arc	Sample	X	Sample	X	Sample	X	Sample	X
01	010	5400	02 010	3870	03 010	1380	04 010	260
	020	5400	020	3790	020	1490	020	390
	030	5420	030	3710	030	1630	030	670
	040	5460	040	3650	040	1790	040	860
	050	5520	050	3570	050	1940	050	1120
	060	5440	060	3500	060	2060	060	1450
	070	5320	070	3460	070	2200	070	1750
	080	5240	080	3240	080	2280	080	1940
	090	5130	090	3260	090	2420	090	2220
	100	4970	100	2690	100	2570	100	2480
	110	4970	110	2710	110	2750	110	2770
	120	4730	120	2570	120	2890	120	3040
	130	4730	130	2420	130	3020	130	3300
	140	4730	140	2240	140	3160	140	3690
	150	4750	150	2140	150	3300	150	3950
	160	4770	160	2260	160	3460	160	4260
	170	4690	170	2080	170	3590	170	4540
	180	4600	180	1870	180	3710	180	4830
	190	4540	190	1450	190	3850	190	5200
	200	4460	200	1020	200	3990	200	5220
	210	4360	210	650	210	4160	210	5380
	220	4240	220	470	220	4300	220	5480
	230	4140	230	370	230	4440	230	5700
	240	4120	240	370	240	4560	240	5970
	250	4080	250	260	250	4710	250	6130
	260	4010	260	280	260	4810	260	5990
	270	3870	270	390	270	4850	270	6110
	280	3750	280	570	280	4950	280	6300
	290	3600	290	770	290	5070	290	6580
	300	3460	300	900	300	5200	300	6860
	310	3360	310	1040	310	5380	310	7050
	320	3320	320	1160	320	5340	320	7010
	330	3300	330	1280	330	5340		
	340	3280						
	350	3260						
	360	3260						

BASIC DATA FROM MOUNTAIN IRON, PHASE I (contd)

Arc	Sample	X	Sample	X	Sample	X	Sample	X
05	010	550	06 010	7290	07 010	8350	09	
	020	670	020	7190	020	8310	020	2530
	030	940	030	7070	030	8170	030	3360
	040	1200	040	6950	040	8070	040	3520
	050	1320	050	6780	050	7900	050	4160
	060	1610	060	6660	060	8010	060	4730
	070	1890	070	6500	070	8050	070	5180
	080	2120	080	6380	080	7950	080	5260
	090	2510	090	6280	090	7600	090	5620
	100	3000	100	6130	100	7600	100	5790
	110	3280	110	6030	110	7660	110	6090
	120	3650	120	5910	120	7460	120	6400
	130	3910	130	5810	130	7480	130	6640
	140	4200	140	5700	140	7350	140	7090
	150	4380	150	5600	150	7250	150	7600
	160	4500	160	5600	160	7380	160	8070
	170	4660	170	5620	170	7660	170	8580
	180	4930	180	5600	180	7990	180	9370
	190	5220	190	5580	190	7880	190	10000
	200	5580	200	5540	200	7740	200	10550
	210	5770	210	5480	210	7660	210	10840
	220	5990	220	5380	220	7420	220	11330
	230	6050	230	5320	230	7070	230	11920
	240	6230	240	5320	240	6860	240	12430
	250	6640	250	5340	250	6560	250	12750
	260	6990	260	5420	260	6150	260	13060
	270	7130	270	5400	270	5790	270	13280
	280	7010	280	5500			280	13900
			290	5720			290	14510
			300	5790			300	15120
(Resurrected Jeep			310	5910			310	15770
Trail Samplers)			320	6030			320	16440
			330	6150				
05	500	1220	340	6320				
	510	1280	350	6400				
	520	1670	360	6620				
	530	2870	370	6720				
	540	3060	380	6930				
	550	4320	390	7110				

APPENDIX B

AIRBORNE TRACER MONITORING

APPENDIX B

AIRBORNE TRACER MONITORING

INTRODUCTION

The Battelle-Northwest Queen Air 80 aircraft was used in an attempt to monitor tracer at locations and elevations not accessible to the ground-based bulk filters. The aircraft was instrumented with a device capable of monitoring the emitted zinc sulfide tracer on a real-time scale. A minimal crew consisted of a pilot, an instrument operator, and a position observer. When possible, radar tracking of the aircraft was undertaken to aid in the specification of aircraft location during tracer sampling.

The zinc sulfide real-time sampler mounted on the Queen Air aircraft has been dubbed the Queen Air Real-Time Sampler (QARTS). A similar ground-based device is described by Nickola et. al.[9] Briefly, the device consists of a chamber into which air is continuously drawn and irradiated by an ultraviolet lamp. The air and phosphorescing zinc sulfide (if any) pass through a light trap, then by a photomultiplier which monitors the glowing particles. The photomultiplier anode current is recorded on a strip chart moving at (generally) 6 inches per minute. The chart is calibrated in terms of air concentration of the zinc sulfide tracer.

During the flights, it was the duty of the position observer to make notes as to aircraft location, altitude, and heading at convenient landmarks, and to activate an event marker on the QARTS chart as the aircraft passed over these landmarks.

Theoretically, a very precise location of the aircraft should have been possible during radar tracking; unfortunately, this was seldom the case. Frequent problems included the loss of tracking due to the low level of flights, imprecise time coordination between aircraft QARTS charts and radar tracks, and internal inconsistencies in timing on supplied radar charts. Consequently, most tracer intercept positions were determined visually.

The aircraft was operated during 25 field experiments. Tracer generation and flight duration data applicable to these tests are listed in Table B-1. Maps are also presented for each field experiment. The dashed lines emanating from the generation source show the limits of the tracer as found on the ground-based bulk filters. The double line with an arrowhead at the end specifies the "centerline" of exposure for these ground samples. The individually numbered dots and x's show the projection to the surface of intercepts of the aircraft with the tracer. The intercepts are numbered in their order of occurrence.

Further information concerning each intercept is tabled on the pages facing each map. Normalized Peak Concentration is derived from the highest point reached by the pen on the QARTS recorder during the duration of the intercept. The peak concentration is a near instantaneous value, and thus embraces only a small fraction of the time listed in the Duration column. Since generation rate did vary from test to test (Table B-1), peak concentrations have been normalized to a common unit emission rate so that between test comparisons will be valid.

Unfortunately, sampling during tests MI-57 through 69 was carried out during a time when a change in the electronics caused the QARTS system to be relatively insensitive and caused the calibration in terms of absolute concentration (g/m^3) to be in error. The peak concentration values listed for these runs have been normalized to a common emission rate, but the values are relative only. That is, peak concentrations for runs MI-57 through 69 are relative values and may be compared only among these tests. The absolute concentration is unknown.

At times, the concentration at plume intercept was so high that the peak value was off scale on the QARTS recorder. In such instances the peak concentration was listed as greater than the recorder full scale concentration. The "greater than" values are not always identical, because several spans of concentration are available to the instrument operator. His choice of span depended on the approximate peak concentration expected.

TABLE B-I. Tracer Generation and Flight Duration Data

Test No.	Date	Site[a]	Generation				Aircraft Sampling		
			Emission Rate, g/sec	Duration, min	Start, PST	Stop, PST	First Intercept, PST	Last Intercept, PST	Sampling Terminated, PST
9	17 Dec 65	A	2.94	30	1435	1505	1439	1618	1620
10	20 Dec 65	A	3.15	30	1200	1230	1207	1321	1328
19	24 Jan 66	A	3.16	30	1040	1110	1046	1118	1131
20	25 Jan 66	A	2.94	30	1156	1226	1157	1300	1301
21	27 Jan 66	A	2.98	30	1155	1225	1200	1405	1415
22	28 Jan 66	A	5.90	15	1147	1202	1152	1358	1400
23	31 Jan 66	A	5.96	15	1145	1200	1145	1200	1309
24	3 Feb 66	A	6.27	15	1130	1145	1130	1145	1255
57	25 Apr 66	B	3.24	30	1055	1125	1100	1153	1235
58	25 Apr 66	B	3.24	30	1407	1437	1408	1515	1535
59	26 Apr 66	A	4.04	48	1213	1301	1218	1253	1320
60	27 Apr 66	A	3.37	29	1255	1324	1256	1318	1324
63	4 May 66	B	3.17	30	1302	1332	1306	1452	1500
64	5 May 66	B	3.24	30	1328	1358	1335	1409	1445
65	5 May 66	B	3.17	30	1645	1715	1645	1729	1805
66	6 May 66	B	3.24	30	1323	1353	1329	1434	1440
67	10 May 66	B	3.24	30	1014	1044	1020	1055	1146
68	11 May 66	B	3.14	30	1007	1037	1012	1127	1209
69	12 May 66	A	3.14	30	1005	1035	1011	1057	1113
108	20 Jul 66	A	3.24	30	1110	1140	1128	1218	1235
109	21 Jul 66	A	3.24	30	1157	1227	1202	1254	1256
110	22 Jul 66	A	3.24	30	1055	1125	1111	1207	1209
111	25 Jul 66	A	3.26	30	1400	1430	1408	1458	1715
112	26 Jul 66	A	3.26	30	1400	1430	--	--	1657
113	27 Jul 66	A	3.24	30	1345	1415	1425	1425	1427

(a) Site A is VIP No. I; Site B is Area 529

Since the aircraft travels at about 60 mps during sampling, a multiplication of the duration (in seconds) by 60 will give the distance in meters that the aircraft traversed during an intercept. Because the aircraft did not always fly--or even always attempt to fly--normal to the expected tracer plume, this distance cannot be interpreted as a crosswind instantaneous plume width. For that matter, even if each aircraft traversal had been normal to the plume axis, each intercept and accompanying concentration and width is a sample of a plume whose instantaneous values at a given distance would have a high variance (with the likely exception of extremely stable atmospheres). An attempt to define mean instantaneous plume widths and concentrations at different distances and elevations would (for statistical significance) require a series of crosswind traverses at each of the desired locations to obtain statistical significance. Such a procedure was not attempted during Mountain Iron, Phase I.

It must be admitted that some subjectivity was required in interpretation of the QARTS recorder charts. Unfortunately, the atmosphere frequently contained contaminants which phosphoresce or in some other manner simulated the phosphorescent effect of the zinc sulfide tracer in the QARTS system. This "noise" varied from day to day, and from location to location. For instance, in flying close to and downwind of the Johns-Manville plant, frequently considerable noise was observed. An idea of the noise to be expected was obtained by pregeneration QARTS operation and an occasional in-between test flight. In any event, some subjectivity was involved in chart interpretation. Some positive signals could be discarded immediately by an experienced chart reader as being "nontypical" in appearance. Other signals were debatable, and still others were unquestionably zinc sulfide. Both the debatable and sure intercepts are tabled and plotted on the maps. The questionable intercepts are noted with x's on the maps. The confident intercepts are shown as solid dots on the maps.

The aircraft altitude and its distance from the source at each intercept are listed on the tables under Sampling Location. An attempt was made to plot each intercept location at the midpoint of its duration--not where the aircraft first or finally detected the tracer. Aircraft elevation above mean sea level (with MSL subheading) and above the mean surface elevation in the vicinity of the aircraft traverse (with Above Surface subheading) are listed under Altitude. In the text, altitudes are reported in MSL unless otherwise noted.

The last two columns in the tables accompanying each map list the minimum and maximum speeds with which a puff of tracer would have had to move to arrive at the point of aircraft intercept when it did. The Min column represents the assumption that the sampled aircraft intercept was the first puff out of the generator (e.g., was emitted at 1435 for Test MI-9). A knowledge of the time the intercept was detected, and its distance from the source permits this speed computation. Obviously, any puff of the tracer emitted from the generator after the initial puff would have to travel at a greater mean speed to get to the intercept point at the time of measurement. The puff which would have to move the fastest to get to the point of intercept would be the last puff from the generator. The Max column lists the speed which this last puff would have had to travel to qualify as the tracer intercepted by the aircraft. The Max Tracer Speed computation results in infinite or absurdly high speeds being required if the aircraft intercept takes place before, at, or shortly after the last puff has been generated. As time after generation increases, the Max speed value becomes more meaningful and, with the accompanying Min value, can closely specify the mean speed required for the sampled tracer to get from source to intercept location.

MI-9

During this field test, tracer was generated between the hours of 1435 and 1505 PST. The aircraft QARTS sampling equipment was in operation at 1434 PST and continued to function until 1620 PST. Intercept No. 1 occurred at 1439 and Intercept No. 19, the last for this test, was made at 1618 PST.

Measured surface winds at the tracer source, at VHF, and at Range Operations were in agreement with the plume centerline as shown on the accompanying map for test MI-9. They were 305 to 315° at 2 to 3 mps. Speeds aloft, as measured by upper air soundings at Building 22, were 1 to 3 mps throughout the period of aircraft tracer intercepts. Thus, the computed Min Tracer Speeds listed in the accompanying table appear in good agreement with the measured winds.

Note that most of the aircraft tracer intercepts were south of the centerline of the ground-level tracer plume. This observation is consistent with observed upper winds at Building 22. These winds veered from about 310° throughout the surface to 1000 ft MSL layer to 30 to 80° at the 3000 foot MSL elevation. Intercept 12 is an apparent anamoly in in location but, admittedly, the coordination between aircraft location and QARTS chart was less than ideal during this first test. Plotted Intercept 12 (and others, for that matter) may be somewhat displaced from its true location.

Temperature soundings at Building 22 showed an unstable atmospheric layer (-1.2F°/100 ft) from the surface up to about 700 ft MSL. From 700 to 1700 ft MSL, the atmosphere was relatively stable (-0.2F°/100 ft), although there was no temperature inversion. Above 1700 ft MSL, the atmosphere had a near adiabatic lapse rate throughout the layer of aircraft sampling. We find, then, an atmosphere unstable to 700 ft, relatively stable from 700 ft to 1700 ft, and adiabatic above 1700 ft MSL. If the Building 22 soundings were typical of the aircraft sampling zone, an

examination of Sampling Altitude in the accompanying table shows that the tracer penetrated readily into the relatively stable layer--even as close to the source as Intercept 4 at 2.3 km.

Intercepts 17, 18, and 19 were made during traverses up and down Honda Canyon. The lengthy Duration (see table) on these intercepts suggests that Honda Ridge provided a barrier to "trap" some tracer along Honda Canyon despite the unstable atmosphere at lower elevations.

Several traverses at greater than 1500 ft MSL were made between Intercepts 9 and 10, with no tracer interception. It would seem the maximum extent of the tracer at about 3 km was 1500 ft MSL. Between Intercepts 11 and 13, traverses of 2100 and 2200 ft MSL were flown with negative results. This suggests a maximum vertical tracer extent of 2000 ft MSL at about 5 to 7 km. As evidenced by significant Intercept 14, tracer extended to at least 2500 ft MSL at a distance of 11 km.

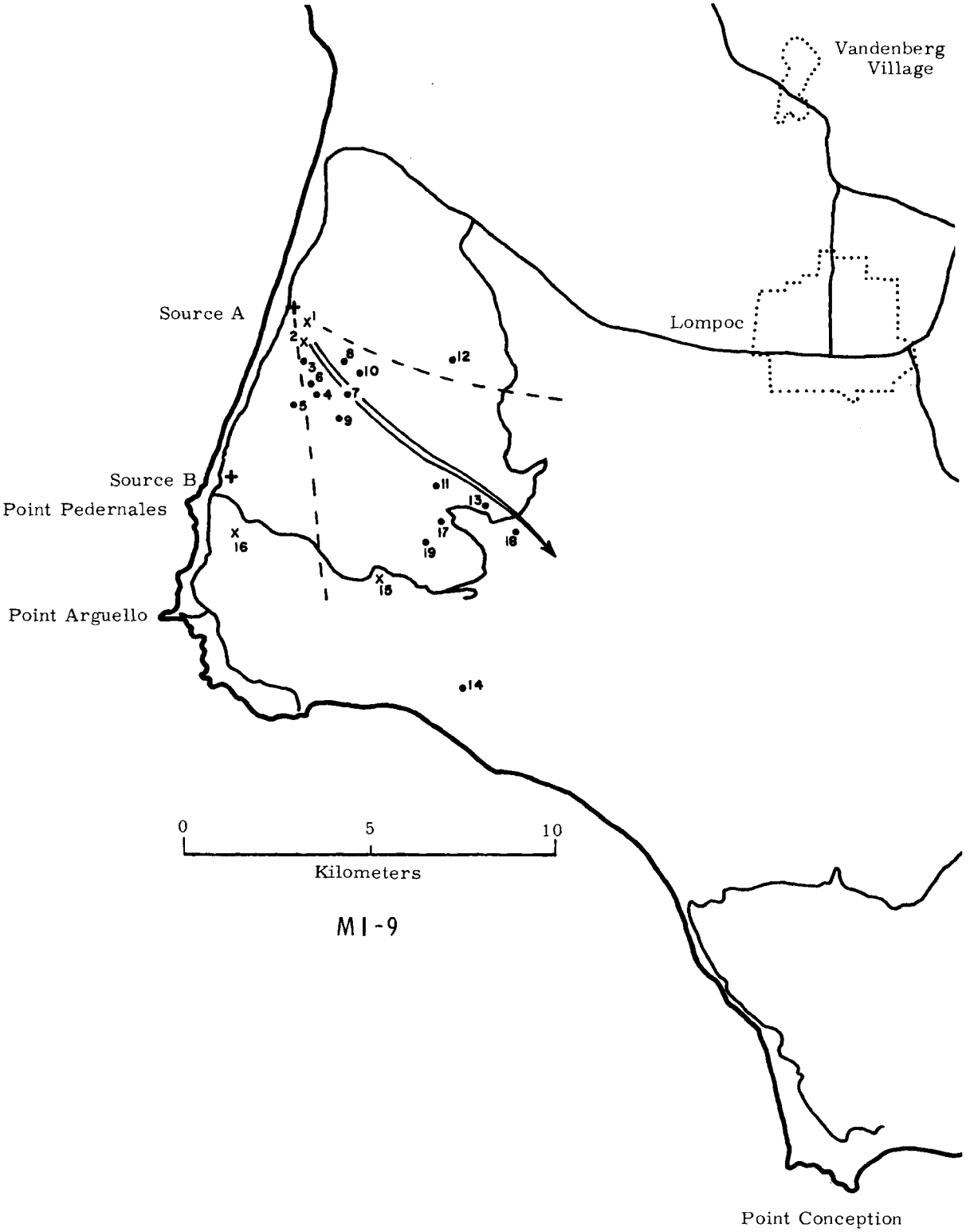
Vandenberg
Village
Lompoc
Source A
Source B
Point Pedernales
Point Arguello
Point Conception
0
5
10
Kilometers
MI-9

FIELD TEST MI-9

Tracer Intercept Number	Normalized** Peak Concentration g/m^3	Duration in Seconds	Sampling Location: Altitude, ft MSL	Sampling Location: Altitude, ft Above Surface	Sampling Location: Distance from Source, km	Tracer Speed: Min, mps	Tracer Speed: Max, mps
1*	2.6	2	500	250	0.5	2.2	∞
2*	>5.4	4	500	200	0.9	3.1	∞
3	9.9	5	620	220	1.3	3.0	∞
4	>20	9	1100	600	2.3	3.4	∞
5	2.7	6	1500	1100	2.5	2.9	∞
6	> 6.2	32	1100	650	2.0	2.0	∞
7	3.9	12	1500	800	2.6	2.0	∞
8	> 6.6	26	1500	1050	1.9	1.3	∞
9	8.1	5	1500	850	3.0	1.8	∞
10	4.3	12	1500	1050	2.4	1.0	3.4
11	> 6.7	38	1600	500	6.0	2.3	7.9
12	3.5	63	1500	600	4.5	1.5	3.7
13	2.8	13	2000	1250	7.2	2.1	4.5
14	0.79	9	2500	1900	10.9	3.1	6.3
15*	0.60	41	3000	1500	7.3	1.9	3.8
16*	1.1	36	1500	750	6.0	1.4	2.3
17	> 2.0	82	1500	800	6.8	1.4	2.3
18	5.3	115	1000	250	8.2	1.6	2.6
19	3.4	96	800	100	7.0	1.1	1.6

* Questionable tracer intercept.

** Normalized to 1 g/sec emission rate. Concentrations listed must be multiplied by 10^{-6} for true concentration. Comparable among Tests MI-9 through 24 and MI-108 through 111 inclusive.

MI-10

Tracer generators were operated during the interval 1200 to 1230 PST. Aircraft sampling began at 1157 and continued until approximately 1328, with plume intercepts occurring between 1207 and 1321.

Winds at the source averaged about 240° at 2 mps during generation, and became 270 to 295° at 1 mps between 1230 and 1313 PST. At 1313, the wind shifted abruptly to 60° at 2 mps. All surface winds on SVAFB were westerly during generation. Winds south of Range Operations remained westerly throughout the period of aircraft sampling, while VHF showed a shift to the northeast between 1230 and 1300, and Range Operations direction became northeasterly between 1300 and 1330.

Pretest upper winds from Building 22 showed winds from 330° at 400 ft through west to 180° at 1000 ft MSL. Winds at 1400 PST were 80° backing to 360° through the same height interval. Thus, the upper winds veered with time as did the surface winds.

Only a minimal number of "ground" samplers were operated during MI-10 (indicated on the accompanying map). With the extreme shift in wind, the double plume centerline and smear of tracer over the entire limited ground ampling grid is reasonable. By the same token, the aircraft samples observed over a wide range in directions from the source are reasonable. The tabled Max and Min Speeds for tracer intercepts during this test are quite low--not only because of low wind speeds during transport, but because of the unusually indirect trajectories from source to point of intercept.

Minimal information is available from the 1100 PST Building 22 radiosonde, and that reported is open to some conjecture. Temperatures reported were 48.2 °F at the surface (370 ft MSL); 56.6 °F at 660 ft; 57.2 °F at 2500 ft; and 47.1 °F at 6400 ft. We find, then, a strong inversion from the surface to near 660 ft. The precise character of the temperature stratification between 660 and 2500 ft is not known, but the temperature at the top and bottom of the layer are nearly the same.

The next reported Building 22 temperatures were at 1400 PST. Here a superadiabatic lapse rate existed from the surface to 500 ft. An inversion of about 1.4F° was found between 500 and 950 ft. Above 950 ft, a lapse rate of roughly -0.3F°/100 ft applied.

Examination of the heights of plume intercept on the table accompanying test MI-10 shows that more than half the intercepts reported were above 500 ft MSL, the base of the inversion at the 1400 PST sounding. If the 1400 PST sounding is representative, then there was frequent penetration of the inversion layer to an elevation 300 ft above its base. Only two intercepts (No. 9 and 26) were made above 800 ft MSL.

There is considerable evidence specifying limits on the vertical extent of the tracer:

1) Between Intercepts 14 and 15, the aircraft flew at elevations above 800 ft MSL for 6 minutes without intercepting plume.
2) Between Intercepts 26 and 27, the aircraft flew at elevations of 900 to 1000 ft for 7 minutes without interception.
3) Subsequent to and in the vicinity of Intercept 36, the aircraft flew for 6 minutes at an elevation of 1000 ft without further intercepts.

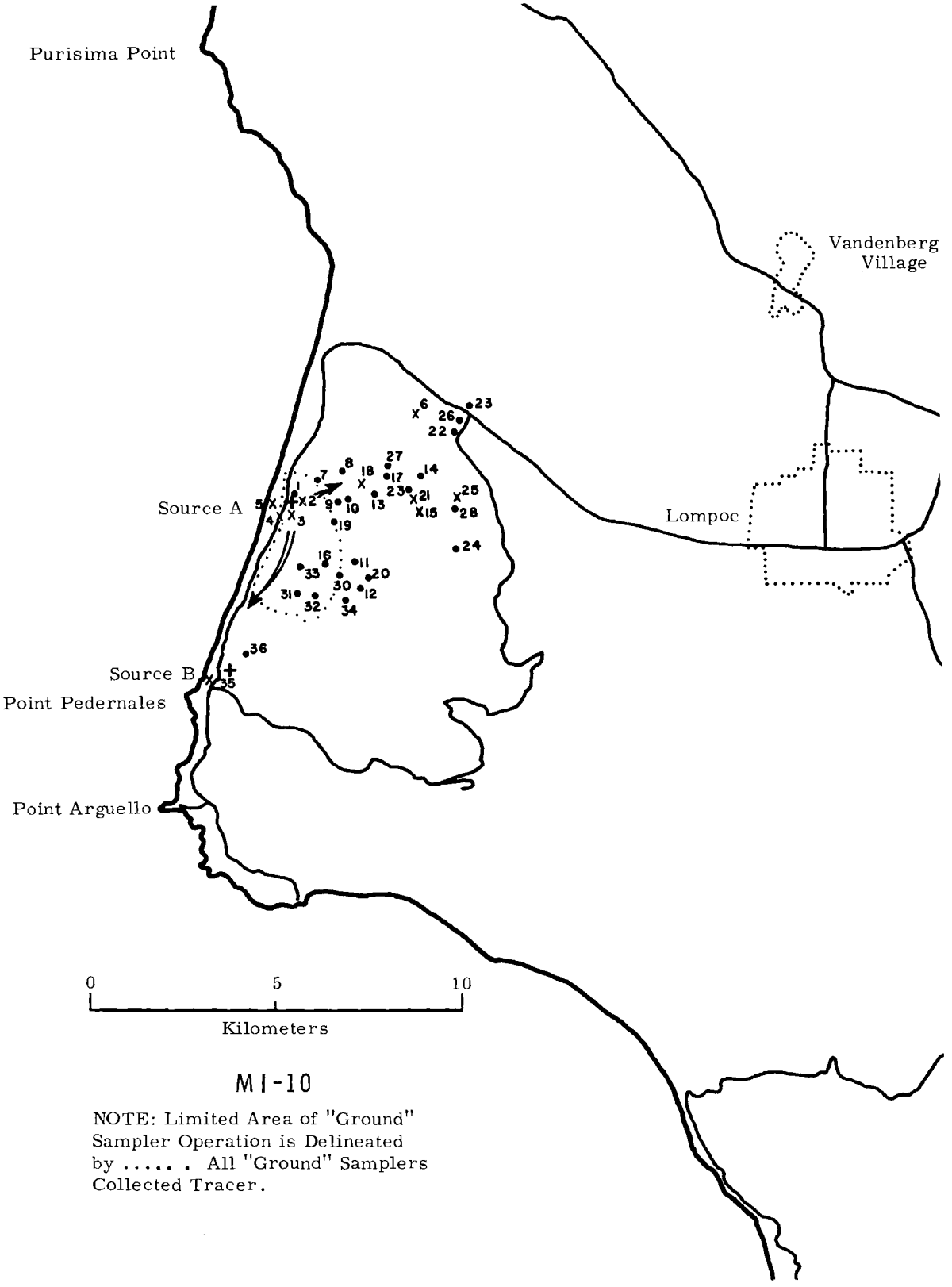

MI-10

NOTE: Limited Area of "Ground" Sampler Operation is Delineated by ..... . All "Ground" Samplers Collected Tracer.

FIELD TEST MI-10

Tracer Intercept Number	Normalized Peak Concentration g/m^3	Duration in Seconds	Sampling Location: Altitude, ft MSL	Sampling Location: Altitude, ft Above Surface	Sampling Location: Distance from Source, km	Tracer Speed: Min, mps	Tracer Speed: Max, mps
1	> 1.4	18	500	300	0.3	0.7	∞
2*	6.4	9	500	300	0.4	0.8	∞
3*	1.4	1	500	250	0.2	0.4	∞
4*	3.5	2	500	300	0.4	0.7	∞
5*	1.3	2	580	480	0.4	0.5	∞
6*	1.2	62	500	350	4.1	4.3	∞
7	> 6.0	23	500	300	1.0	1.0	∞
8	> 1.5	9	500	200	1.8	1.6	∞
9	> 6.0	23	1000	700	1.3	1.0	∞
10	19.0	23	500	200	1.6	1.1	∞
11	>19	38	500	100	2.3	1.3	∞
12	18.1	17	500	100	2.8	1.5	60
13	8.9	8	500	150	2.3	1.2	21
14	4.4	15	500	250	2.6	1.3	14
15*	1.3	3	800	450	3.5	1.4	4.8
16	3.1	48	800	300	1.8	0.7	2.1
17	3.8	29	800	250	2.7	0.9	2.7
18*	0.67	3	800	500	2.0	0.7	1.9
19	> 6.4	51	700	350	1.3	0.4	1.1
20	10.0	48	650	100	2.8	0.9	2.2
21*	3.5	39	600	250	3.3	1.0	2.4
22	> 6.4	41	700	550	4.9	1.5	3.4
23	4.1	23	700	550	5.6	1.7	3.6
24	1.3	7	700	300	4.6	1.3	2.8
25*	1.5	2	700	400	4.5	1.3	2.7
26	4.4	26	900	750	5.1	1.5	3.0
27	3.5	36	800	450	2.8	0.7	1.3
28	3.8	21	800	500	4.5	1.1	1.9
29	3.8	20	800	450	3.2	0.8	1.3
30	5.1	64	600	100	2.2	0.5	0.9
31	5.1	76	500	100	2.3	0.5	0.9
32	4.4	59	500	100	2.5	0.5	0.9
33	6.4	19	800	400	1.6	0.3	0.5
34	4.8	41	800	200	2.8	0.6	1.0
35*	1.8	3	600	500	5.1	1.1	1.7
36	6.0	61	600	300	4.0	0.8	1.3

* Questionable tracer intercept.

MI-19

Generation occurred between 1040 and 1110 PST. Tracer was intercepted during the interval 1046 to 1118 PST, and sampling continued until 1131. It is likely that sampling past 1121 was between the generation site and the "tail" of the tracer plume.

All plume intercepts occurred within 2.6 km of the source and at heights of 1600 ft MSL and less. These heights were well below the base of the inversion, 2200 ft. Unfortunately, flight notes do not make it clear whether the aircraft flew above 1600 ft and did not find tracer, or whether it merely flew above 1600 ft.

Two minutes after the last plume intercept (No. 18), a traverse was made at an elevation of 1800 ft along the path indicated by the dotted line on the accompanying map; no tracer was found. All previous traverses had been at elevations of 1600 ft or less. The last puff of tracer emitted from the generator at 1110 PST would have had to travel at a speed of 4.8 mps to have arrived at the expected intercept location near Spring Canyon during the aircraft traverse. Previously emitted tracer would have had to travel at a slower mean speed to be at the expected intercept location. Since Intercept 18--just 2 minutes previous and 200 ft lower--had traveled at a speed of 4.2 mps or less and since upper winds showed no speed shear at these elevations, it is unlikely that the lack of intercept at 1800 ft was due to the tracer moving at greater than an average speed of 4.8 mps (and thus being beyond the expected intercept). It is much more likely that the vertical extent of the plume at this distance of 3 km was less than 1800 ft, but at least 1600 ft. This elevation is about 1000 ft above the land surface in the Spring Canyon area.

Continued traverses along the dotted line at 1600 ft showed the tracer had passed Spring Canyon before 1123 PST. The last puff from the generator would have had to have moved at least 4.0 mps to have passed by this time. Intercept 18 shows that the tracer traveled at most at 4.2 mps in arriving at a distance of 2.1 km. It can be concluded

that the mean tracer speed at 1600 ft to a distance of 2 to 3 km was about 4.1 mps. Upper winds from Building 22 and Scout Pad D suggest speeds during the period under consideration as follows:

- Surface - 2 mps
- 300 ft - 3 mps
- 660 ft - 4 mps
- 980 ft - 5 mps
- 1310 ft - 6 mps
- 1970 ft - 6 mps.

In this case the wind at about 700 ft indicates the mean speed of the plume at the 1600 ft elevation.

Intercept 16 looks extremely dubious. Since there was some veering of the wind with height on the Building 22 and Scout Pad D winds, Intercepts 1, 2, 4, and 11 are not unreasonable. Trace movement at lower levels, as indicated by significant Intercept 2, was possible at speeds of at least 2.5 mps.

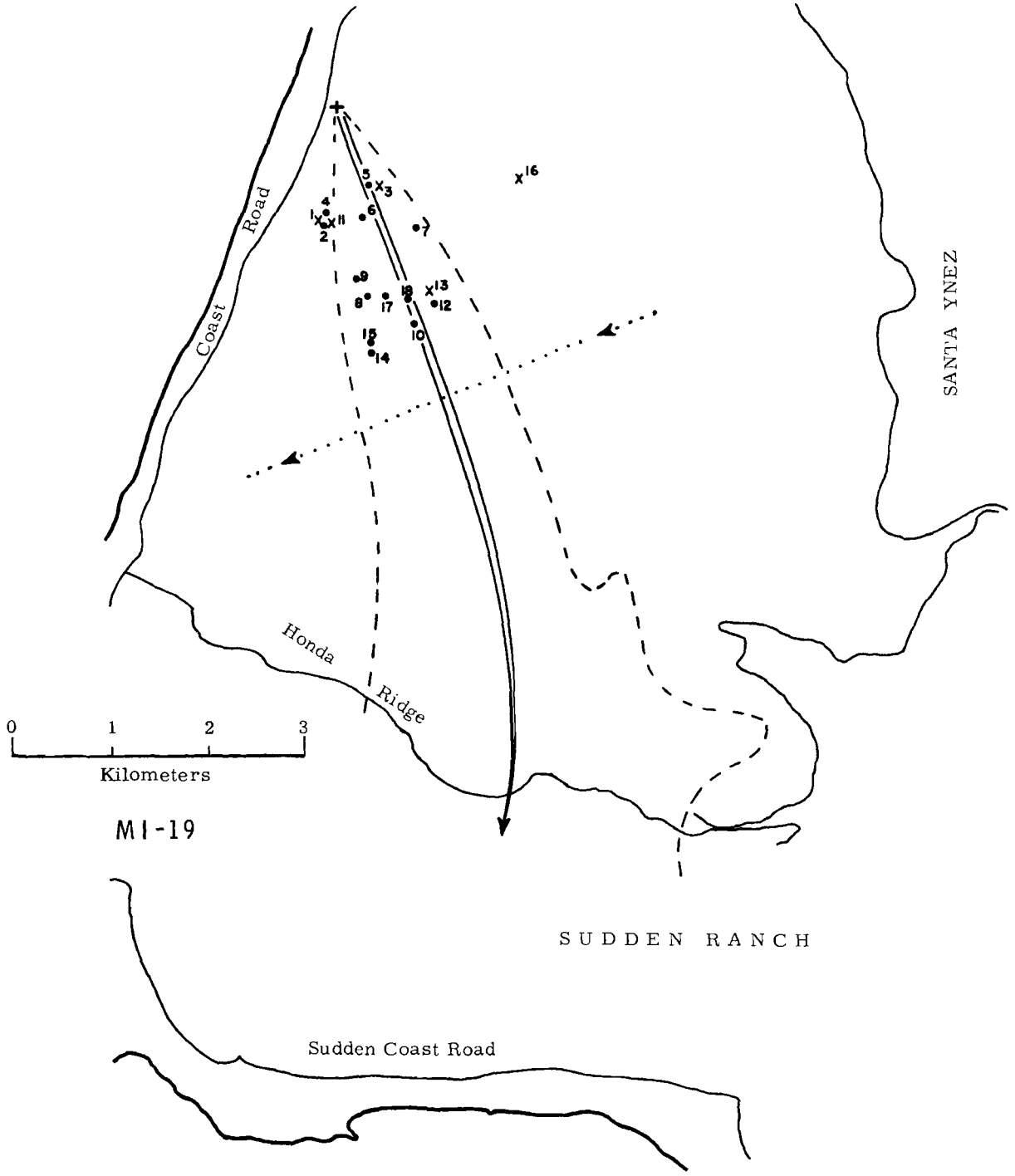
Coast Road
SANTA YNEZ
Honda Ridge
0 1 2 3
Kilometers
MI-19
SUDDEN RANCH
Sudden Coast Road

FIELD TEST MI-19

Tracer Intercept Number	Normalized Peak Concentration g/m^3	Duration in Seconds	Sampling Location: Altitude, ft MSL	Sampling Location: Altitude, ft Above Surface	Sampling Location: Distance from Source, km	Tracer Speed: Min, mps	Tracer Speed: Max, mps
1*	0.92	1	500	200	1.1	3.1	∞
2	2.8	2	500	200	1.1	2.5	∞
3*	0.66	1	Missing		0.8	1.6	∞
4	> 1.9	8	500	200	1.1	1.8	∞
5	> 6.4	6	700	350	0.8	1.6	∞
6	13.0	4	700	300	1.2	1.5	∞
7	13.2	6	700	250	1.4	1.6	∞
8	> 6.4	10	1000	950	1.9	1.8	∞
9	11.9	6	1000	900	1.8	1.6	∞
10	10.4	8	1300	650	2.1	1.7	∞
11*	2.1	2	1200	900	1.1	0.6	110
12	3.0	9	1200	600	2.1	1.1	22
13*	0.92	2	1200	600	2.1	1.1	16
14	6.0	5	1300	700	2.6	1.2	12
15	3.9	5	1200	600	2.4	1.1	8.8
16*	1.4	4	1400	1000	2.0	0.9	5.0
17	> 2.0	12	1400	800	1.9	0.9	4.4
18	4.8	17	1600	1000	2.1	0.9	4.2

* Questionable tracer intercept.

MI-20

Tracer generation during test MI-20 was from 1156 to 1226 PST. The first tracer was intercepted at 1157, and the last tracer was found at 1300--only a minute before the sampling flight was terminated.

Surface winds were 180 to 210° at the generation site and Scout Pad A during the generation and associated aircraft sampling. Aloft winds measured at Building 22 just prior to generation showed backing from 175° at 300 ft to 140° at 2000 ft. Unfortunately, additional aloft winds were not obtained at Building 22 until about 45 minutes after aircraft sampling ceased. However, backing with increasing height was found in winds at both Scout Pad D and Ionospheric Sounder. With these backing winds, the interception of the plume somewhat to the west of the suggested ground-level centerline is reasonable.

If on the tabled MI-20 data, we ignore Tracer Speed computations based on the first 2 intercepts (questionable chart records and possible relatively large timing errors in the first few minutes of sampling), we find the movement of the tracer can be at least 3.7 mps at 900 ft (Intercept 7). This rate of movement is commensurate with the ground level speed of from 2 to 5 mps and the aloft winds of 3.0, 4.7, and 5.2 mps measured at 330, 660, and 990 ft, respectively.

The base of the temperature inversion was at about 3000 ft during this run. Although no tracer was intercepted above 2100 ft, sampling was pursued to an elevation of 2300 ft near the mouth of the Santa Ynez River. The maximum vertical extent of the plume, then, at 5 km from the source was about 2100 ft.

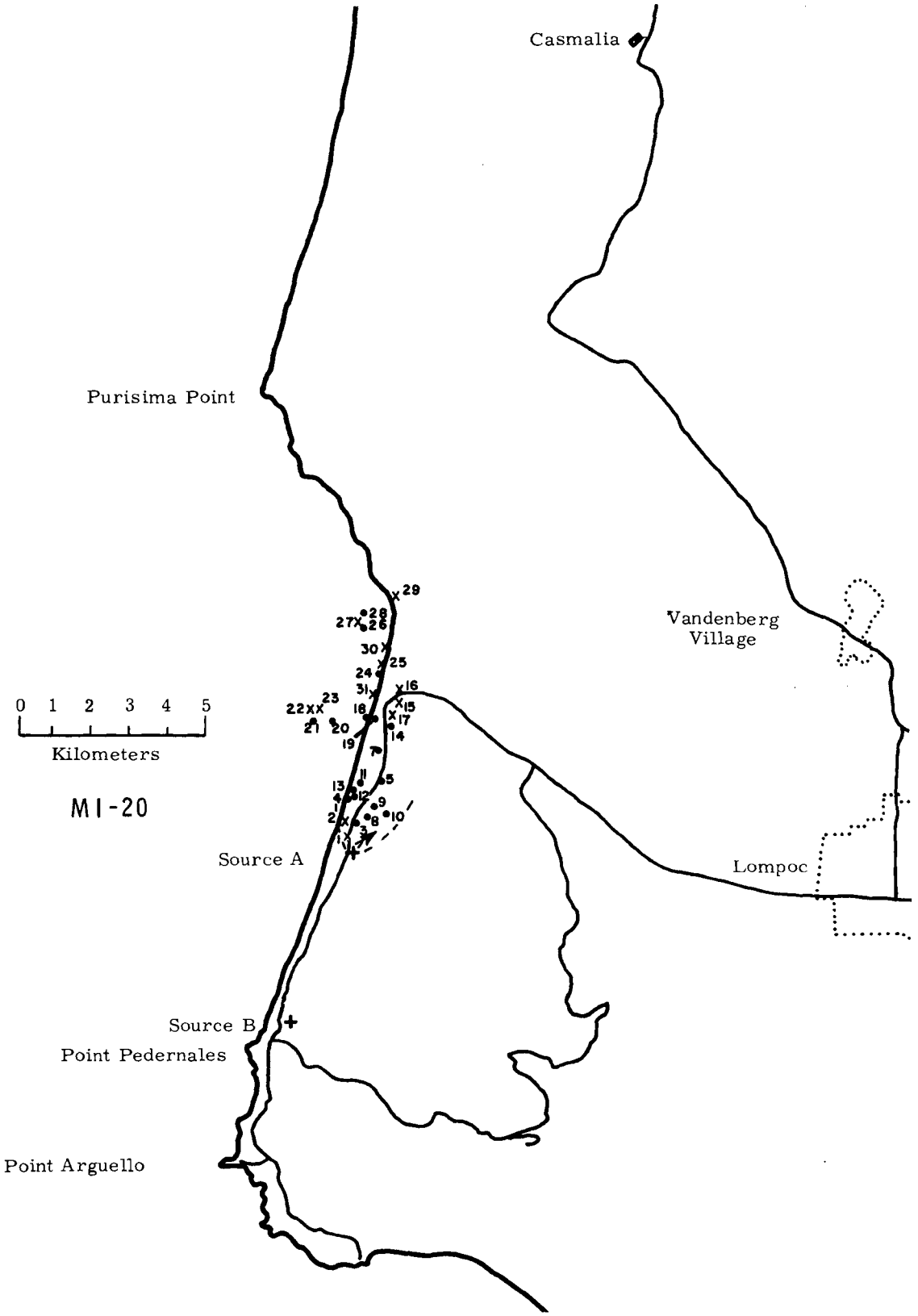
Casmalia
Purisima Point
Vandenberg Village
0 1 2 3 4 5
Kilometers
MI-20
Source A
Lompoc
Source B
Point Pedernales
Point Arguello

FIELD TEST MI-20

Tracer Intercept Number	Normalized Peak Concentration g/m^3	Duration in Seconds	Sampling Location: Altitude, ft MSL	Sampling Location: Altitude, ft Above Surface	Sampling Location: Distance from Source, km	Tracer Speed: Min, mps	Tracer Speed: Max, mps
1*	2.1	2	400	200	0.4	4.5	∞
2*	0.71	2	400	250	0.8	5.2	∞
3	>6.8	6	500	300	0.8	3.4	∞
4	1.5	4	700	600	1.7	3.6	∞
5	3.4	8	700	600	2.1	3.8	∞
6*	0.51	9	700	Uncertain Location			∞
7	>1.9	16	900	850	2.8	3.7	∞
8	1.6	8	900	700	0.8	1.0	∞
9	1.9	3	700	500	0.8	0.8	∞
10	4.7	14	500	300	1.4	1.4	∞
11	2.9	9	700	600	1.8	1.6	∞
12	>6.8	11	900	750	1.5	1.2	∞
13	0.92	4	1100	950	1.5	1.1	∞
14	4.6	23	1100	1000	3.5	2.4	∞
15*	2.4	2	1100	1000	4.2	2.7	∞
16*	1.6	8	1100	1000	4.4	2.8	∞
17*	1.7	18	1300	1200	3.9	2.4	∞
18	>1.9	19	1500	1500	3.6	2.1	∞
19	1.2	2	1700	1700	3.6	2.0	∞
20	0.78	12	1900	1900	3.5	1.8	31
21	0.78	21	2000	2000	3.8	2.0	29
22*	0.58	3	2100	2100	3.8	1.9	19
23*	0.31	2	2100	2100	3.8	1.9	18
24	1.5	3	1900	1900	4.8	2.0	7.2
25*	0.37	2	1500	1500	5.0	1.9	6.4
26	>1.9	7	1500	1500	6.0	2.3	7.4
27*	.31	7	1300	1300	6.1	2.2	6.4
28	1.4	10	1300	1300	6.3	2.2	6.0
29*	0.08	2	1100	1000	6.8	2.3	6.2
30*	0.78	2	900	900	5.4	1.6	3.5
31*	0.14	2	1100	1100	4.2	1.1	2.1

* Questionable tracer intercept.

MI-21

The tracer generators were operated during the interval 1155 to 1225 PST during Test MI-21. Aircraft sampling took place from shortly before generation until 1415 PST.

Based on the surface winds, tracer was intercepted generally where one might expect it. There was generally a veering of surface wind (up to 60°) with time during the period of sampling. Upper winds taken from the Ionospheric Sounder site showed minimal direction shear at the time the tracer should have been in that vicinity.

Measured surface winds in the zone traversed by the ground level plume averaged 3 to 4 mps. Winds up to 3000 ft measured at Ionospheric Sounder did not exceed 4 mps until 1445. Yet, there is considerable evidence (Intercepts 7, 11, 13, 15, and 27) that some of the tracer traveled at speeds of at least 4 mps to distances between 4 and 14 km.

No temperature inversion was in evidence during this field experiment. The temperature sounding at Ionospheric Sounder showed a lapse rate of -0.2F° /100 ft at the start of generation throughout the layer of aircraft sampling. The lapse rate became adiabatic by 1245 PST.

Confident tracer intercepts (No. 35) were made at elevations as high as 3000 ft, and more questionable intercepts (No. 39 and 43) were found at elevations up to 3400 ft. During a 7 minute interval between Intercepts 38 and 39, aircraft sampling was conducted near the east end of Sudden Ranch to elevations as high as 4000 ft; no tracer was found. Thus, the plume top at a distance of about 14 km was in the vicinity of 3000 to 3400 ft.

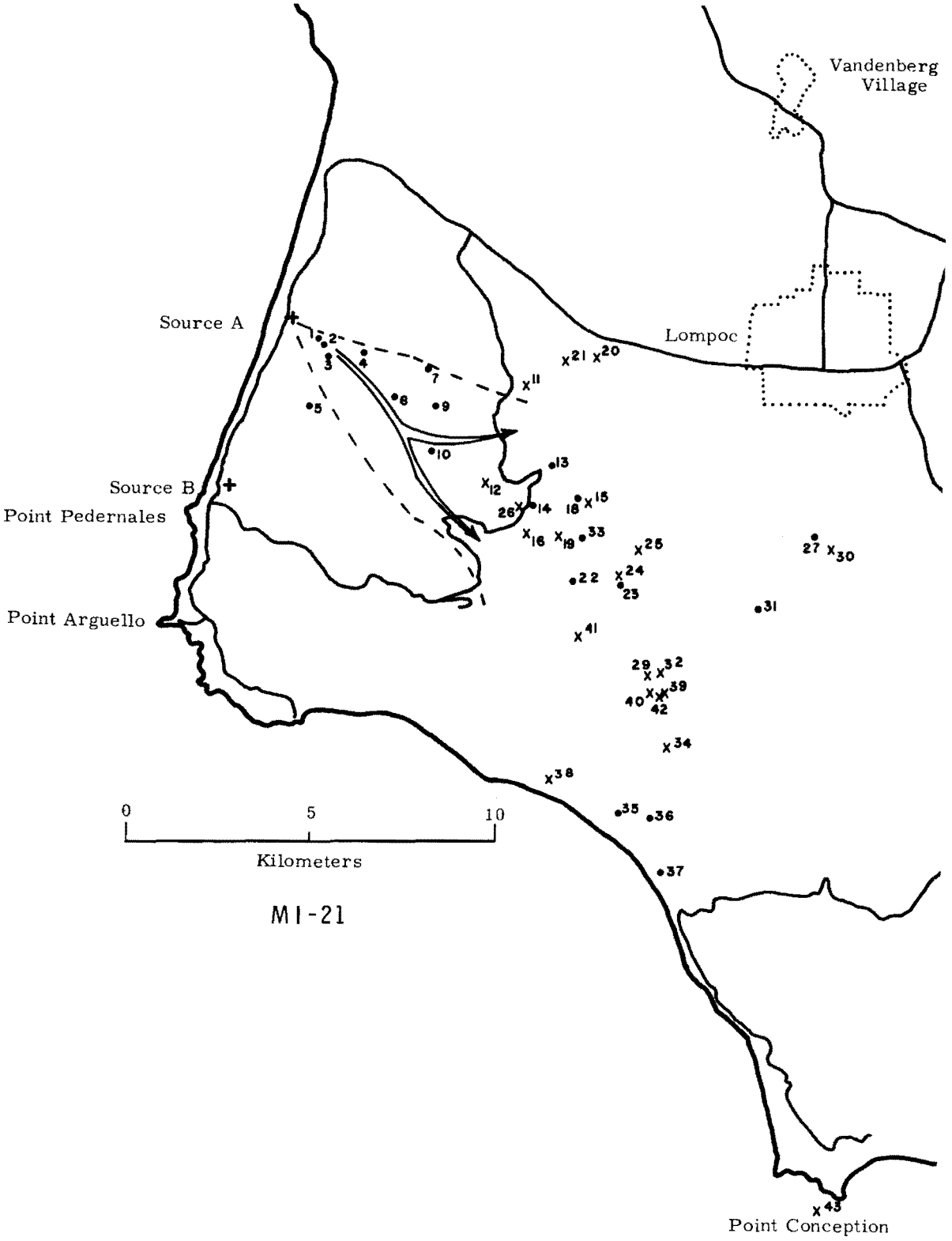
Vandenberg Village
Lompoc
Source A
Source B
Point Pedernales
Point Arguello
Point Conception
0
5
10
Kilometers
MI-21

FIELD TEST MI-21

Tracer Intercept Number	Normalized Peak Concentration g/m^3	Duration in Seconds	Sampling Location: Altitude, ft MSL	Sampling Location: Altitude, ft Above Surface	Sampling Location: Distance from Source, km	Tracer Speed: Min, mps	Tracer Speed: Max, mps
1	2.3	4	700	350	0.8	2.8	∞
2	0.77	7	700	350	1.0	2.5	∞
3	3.3	6	900	500	1.3	2.6	∞
4	3.7	7	900	500	2.2	3.6	∞
5	2.3	21	1000	300	2.4	3.2	∞
6	4.2	7	900	500	3.3	3.8	∞
7	2.7	14	1100	600	3.9	4.0	∞
8	4.0	22	1100	500	3.4	3.1	∞
9	0.97	21	1300	650	4.5	3.6	∞
10	0.84	5	1300	550	5.1	3.7	∞
11*	0.71	3	1500	1000	6.6	4.2	∞
12*	0.57	15	1500	400	6.7	3.9	∞
13	> 1.9	5	1700	700	7.9	4.2	78
14	1.8	16	1700	700	8.0	3.9	33
15*	0.27	2	1800	600	9.2	4.2	24
16*	0.71	2	1900	1100	8.4	3.6	15
17*	0.71	2	1900	Uncertain location			
18	> 1.9	5	1900	700	9.2	3.7	13
19*	0.67	13	1900	1000	9.2	3.5	11
20*	0.24	2	2100	1900	8.1	2.9	8.3
21*	0.44	9	2100	1850	7.3	2.5	6.5
22	0.97	27	2100	1300	10.2	3.2	7.3
23	1.6	3	2100	800	11.3	3.4	7.3
24*	0.77	12	2100	800	11.3	3.3	7.1
25*	0.44	2	2100	700	11.3	3.2	6.1
26*	0.54	2	2300	1300	7.8	2.1	4.2
27	1.6	4	2300	1550	15.0	4.0	7.9
28*	0.27	1		Uncertain location			
29*	0.47	18	2600	900	13.5	3.4	6.3
30*	0.71	5	2700	1950	15.7	3.8	6.7
31	1.5	2	2700	1700	14.6	3.5	6.1
32*	0.84	32	2800	1100	13.7	3.0	5.0
33	1.4	15	2800	1800	9.6	2.0	3.3
34*	0.71	31	2900	1200	15.1	3.1	5.0
35	1.6	3	3000	2500	15.7	3.0	4.9
36	1.6	4	2900	2400	16.5	3.0	4.5
37	> 2.0	3	2900	2650	17.7	3.2	4.7
38*	0.54	2	2900	2400	13.9	2.3	3.3
39*	0.97	60	3400	1700	14.1	2.3	3.3
40*	0.71	2	3300	1600	13.8	2.2	3.1
41*	0.13	1	3100	1900	11.3	1.8	2.5
42*	0.97	19	3000	1300	14.1	2.2	3.0
43*	0.30	2	3400	3400	24.9	3.2	4.1

* Questionable tracer intercept.

MI-22

Generators were operated only 15 minutes during this field experiment--from 1147 to 1202 PST. Aircraft sampling began prior to generation and continued until 1420. The first plume intercept occurred south of the source at 1152. The last intercept occurred about 40 km northwest of the source at 1358. Sampling was discontinued at 1400 PST.

Few surface wind records for this test have been reduced, since it was basically "off course" insofar as ground samplers were concerned. However, at the source, surface winds were 300° at 3 mps at the start of the run. By the end of the 15 minute generation period, the generator operator noted that "the wind came back in our face for 5 to 7 minutes." Since generators faced east, this remark indicates a wind with an easterly component from about 1156 to at least 1202 PST. At 1215, winds were back to 280° at 2 mps; at 1245, the surface wind was 100° at 1 mps; and at 1345, it was 110° at 3 mps.

Tracer collected on ground samples show a maximum at an azimuth of about 200° at a distance of 1.5 km. Before tracer proceeded much further southward, it must have been blown seaward because no tracer was apparent on ground samplers beyond 3.5 km. The computed mean Tracer Speeds for intercepts up to No. 21 can be low because of erratic trajectories prior to their intercept, as well as low wind speeds at near surface levels.

Speeds computed for Intercepts 23 to 34 compare more favorably to upper winds of 4 to 6 mps from Scout Pad D and Building 22. Directions were southeasterly--from 110° at lower levels veering to about 170° at 2000 ft. Thus, winds (aloft or surface) were measured that could explain all tracer intercept speeds and locations.

No temperature inversion was in evidence during this field run. At Building 22, the 1145 PST sounding showed a lapse rate of -0.3F° / 100 ft from near the surface to 1600 ft MSL, an isothermal layer from

1600 to 2000 ft, and back to the -0.3F° lapse rate above 2000 ft. The 1245 PST sounding showed superadiabatic conditions up to 1500 ft, with the relatively stable -0.3F° /100 ft above.

Some definition of the maximum vertical extent of the plume is possible from the observation that between Intercepts 18 and 19, an 8 minute search at elevations from 1900 to 3000 ft MSL produced negative results. It is possible, however, that tracer was nearly all beyond this relatively close-to-source location despite minimal surface winds and tracer "meandering". Further evidence on the vertical extent of the plume can be deduced from the fact that between Intercepts 22 and 31 (20 to 30 km), several traverses were made at 1500 ft without finding tracer (with the exception of No. 22 whose areal location was ill defined). Yet dropping the aircraft 50 to 100 ft resulted in numerous tracer intercepts. More distant traverses (30 to 40 km) at 1500 ft did result in tracer intercepts (Nos. 31 to 34).

It appears that there was considerable mixing up to the base of the isothermal (at 1145 PST) or relatively stable (at 1245 PST) layer, but minimal mixing above the 1500 foot elevation--even to distances of 20 km or more.

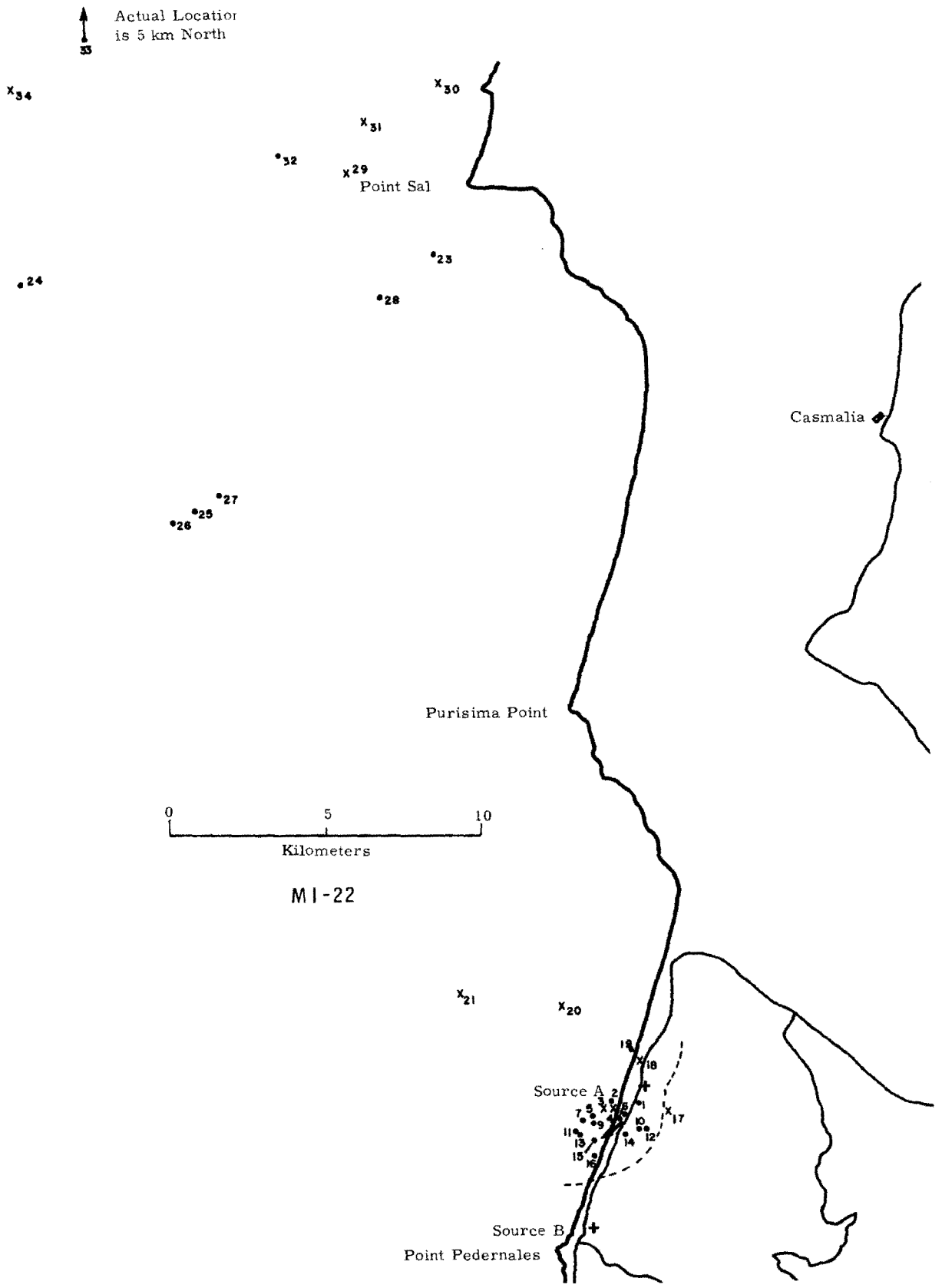
Actual Location
is 5 km North
33
34
30
31
32
29
Point Sal
23
24
28
27
25
26
Casmalia
Purisima Point
0
5
10
Kilometers
MI-22
21
20
19
18
Source A
17
16
15
14
13
12
11
10
9
8
7
6
5
4
3
2
1
Source B
Point Pedernales

FIELD TEST MI-22

Tracer Intercept Number	Normalized Peak Concentration g/m^3	Duration in Seconds	Sampling Location: Altitude, ft MSL	Sampling Location: Altitude, ft Above Surface	Sampling Location: Distance from Source, km	Tracer Speed: Min, mps	Tracer Speed: Max, mps
1	>3.5	13	600	450	0.4	1.3	∞
2	4.8	23	700	700	1.0	1.8	∞
3*	0.84	1	900	900	1.0	1.5	∞
4*	0.84	1	900	900	1.0	1.2	∞
5	1.1	28	900	900	1.6	1.7	28
6	1.7	32	900	875	1.2	1.1	5.8
7	>3.5	58	1100	1025	2.6	2.1	7.5
8	2.6	56	1100	900	1.0	0.7	2.2
9	3.9	58	1100	1025	1.8	1.1	2.6
10	3.1	37	1300	900	1.4	0.8	1.6
11	5.2	39	1300	1200	2.5	1.3	2.4
12	3.4	50	1300	925	1.4	0.7	1.2
13	1.5	35	1300	1200	2.5	1.1	1.8
14	0.93	26	1300	1175	1.5	0.6	0.9
15	1.4	10	1500	1500	2.3	0.9	1.3
16	1.0	12	1450	1325	2.5	0.9	1.3
17*	2.0	3	1450	1050	1.4	0.4	0.6
18*	1.7	2	1200	1100	0.8	0.2	0.3
19	1.2	20	900	900	1.1	0.3	0.4
20*	0.22	1	1200	1200	3.6	0.9	1.2
21*	1.6	34	1200	1200	6.3	1.5	2.0
22*	0.07	8	1500	1500	Uncertain Location		
23	0.54	66	1400	1400	27.0	5.2	6.3
24	0.17	38	1400	1400	31.9	5.4	6.4
25	0.35	45	1400	1400	22.9	3.9	4.6
26	0.29	20	1400	1400	23.0	3.8	4.5
27	0.42	33	1400	1400	22.9	3.8	4.3
28	0.87	82	1450	1450	26.0	4.2	4.9
29*	0.39	2	1450	1450	30.2	4.7	5.5
30*	0.35	4	1450	1450	32.2	5.0	5.8
31*	0.22	2	1500	1500	35.3	5.2	6.0
32	0.78	50	1500	1500	31.5	4.5	5.1
33	0.39	2	1500	1500	42.0	5.5	6.2
34*	0.25	2	1500	1500	37.2	4.8	5.4

* Questionable tracer intercept.

MI-23

The 15 minute generation during Test MI-23 gave a relatively narrow and well defined pattern on the ground samples. Generation was between 1145 and 1200 PST. The QARTS was activated intermittently between 1030 and 1145 for background level. Tracer was first intercepted at 1149, and the final intercept occurred at 1303. Sampling was discontinued at about 1309 after tracking tracer to the vicinity of Point Conception.

Wind directions and speeds, both surface and aloft, were quite steady during this test. Source and near source surface winds were about 300°. Surface winds veered slightly as the tracer moved inland until they were 340 or 350° near Intercepts 17 and 19. There was also a veering from about 310 to 340° in aloft winds through the interval from near surface to 2500 ft. The steadiness and veering of the wind throws doubt on the plotted location of Intercepts 7 and 8.

Surface speeds averaged about 3.5 mps in the vicinity of the plume traverse. Speeds averaged about 5 mps at 700 ft and 7.5 mps at 2500 ft. These speeds are in good agreement with the range of speeds computed for tracer moving to the points of intercept. In general, Intercepts 1 to 17 (tracer found at elevations less than 1000 ft above the surface) moved at speeds approximating the surface wind. Intercepts 20 to 25, occurring at 1500 to 2800 ft above the surface, required tracer to have moved at speeds of about 7 mps. Thus, the wind speeds in the 2000 to 2500 ft level (MSL) would have been forecast with these intercepts.

There was a continuous decrease in temperature with height during this field test. Its magnitude was about -1F°/100 ft in the first 300 ft above the surface, and changed to roughly -0.6F°/100 ft throughout the next 2500 ft.

Specification of vertical plume extent is not easy from the data recorded during this run. For about 5 minutes after Intercept 16, no

tracer was found during flight at elevations above 1500 ft MSL. Continuing searching at 2000 to 2200 ft MSL resulted in Intercept 17. Rugged terrain in this area makes specification of heights above surface subject to considerable question, but it appears that all intercepts through No. 17 were obtained at elevations less than 1000 ft above the underlying surface.

While flying in the vicinity of Point Conception, 13 minutes of sampling between Intercepts 22 and 23 revealed no tracer above 3000 ft MSL.

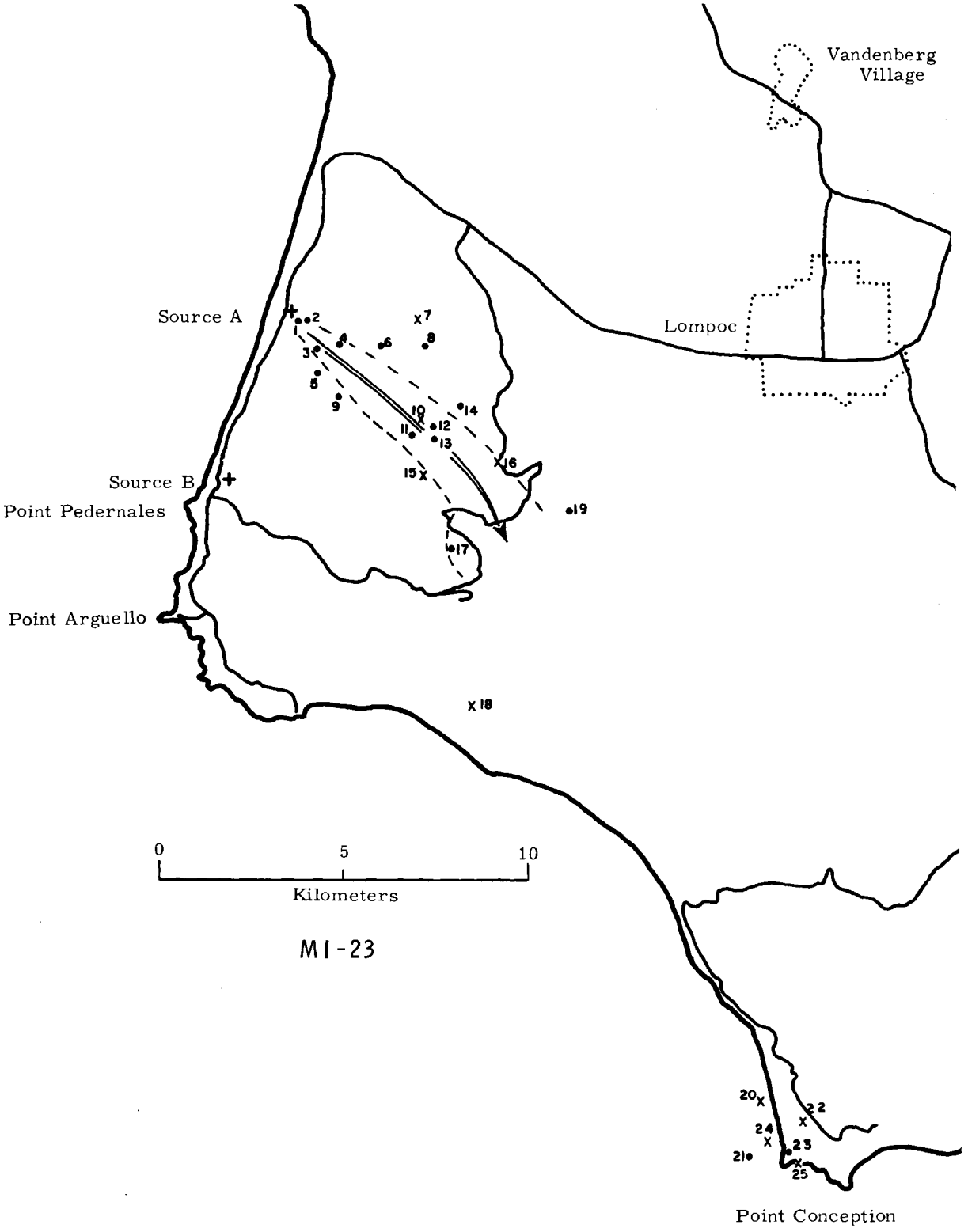
Vandenberg Village
Lompoc
Source A
Source B
Point Pedernales
Point Arguello
Point Conception
0
5
10
Kilometers
MI-23

FIELD TEST MI-23

Tracer Intercept Number	Normalized Peak Concentration g/m^3	Duration in Seconds	Sampling Location: Altitude, ft MSL	Sampling Location: Altitude, ft Above Surface	Sampling Location: Distance from Source, km	Tracer Speed: Min, mps	Tracer Speed: Max, mps
1	3.5	3	700	500	0.2	0.8	∞
2	8.0	3	800	450	0.4	1.2	∞
3	5.1	7	900	550	1.1	2.4	∞
4	4.0	8	1100	750	1.6	2.8	∞
5	3.2	12	1300	700	1.7	2.5	∞
6	2.1	6	1200	700	2.5	3.1	∞
7*	0.74	13	1300	850	3.4	3.6	120
8	2.3	10	1300	850	3.6	3.3	18
9	1.8	5	1300	550	2.5	2.0	7.5
10*	0.49	2	1300	550	4.6	3.4	10
11	1.2	8	1300	550	4.6	3.1	7.7
12	1.9	16	1300	550	4.8	2.9	6.5
13	1.1	30	1300	550	5.1	2.9	6.0
14	1.6	17	1500	750	5.2	2.7	5.2
15*	1.1	27	1500	500	5.6	2.7	4.9
16*	0.07	2	1500	500	6.8	3.1	5.2
17	0.99	10	2200	700	7.5	2.6	3.7
18*	0.39	16	2400	1650	11.3	3.6	5.0
19	0.74	3	2600	1300	9.1	2.8	3.9
20*	0.29	10	2600	2600	24.3	7.3	9.9
21	0.92	49	2800	2800	25.4	7.1	9.5
22*	0.25	26	3000	2800	25.3	6.8	8.9
23	>1.1	8	2500	2500	25.9	5.7	7.4
24*	0.99	3	2400	2400	25.3	5.5	6.8
25*	0.77	3	1500	1500	26.2	5.6	6.9

* Questionable tracer intercept.

MI-24

Generation took place from 1130 to 1145 PST during this test, while aircraft tracer intercepts occurred between 1137 and 1238. QARTS equipment was activated at 1119, and sampling was completed at 1255. Radar coverage materially aided in specifying the aircraft location during this overwater test.

Surface winds at the source were approximately 140° at 5.5 mps during generation. Winds at Scout Pad D near generation time were 160° at 9 mps in the layer 600 to 1000 ft MSL. In this layer at Building 22, winds were 200 to 150° at 4.5 mps. The appearance of intercepts (such as No. 1, 2, and 3) to the north of the position which would have been expected from source surface winds is, no doubt, due to the winds in this intermediate level. Winds above 1000 ft were 140 to 150° at both Building 22 and Scout Pad D at the start of the experiment, and veered about 10° in the next hour. The intercept locations are in good agreement with these winds of from 140 to 165°.

Wind speeds aloft at 1230 PST were 6, 8, and 10 mps at elevations of 1000, 1500, and 2000 ft, respectively. Tracer speeds computed for Intercepts 8 through 18 suggest that the wind speed specifying transport was that at 1500 ft MSL or higher although these intercepts were found between 1100 and 1400 ft.

Although no inversion was evident at Building 22 before or after this field test, the radiosonde from Scout Pad D did show a temperature inversion of 0.5 F° between 2000 and 2600 ft MSL at 1130 PST. This inversion was gone at the 1230 PST sounding. A near adiabatic lapse rate existed below 2000 ft MSL at both Building 22 and Scout Pad D.

The pattern of the aircraft flight did not permit the specification of the vertical extent of the tracer. Minimal difficulty in intercepting the tracer plume was encountered until after Intercept 17. Then, repeat traverses at 1300 to 1400 ft for 18 minutes showed no tracer until the minor and questionable Intercept 18 was made. Ten more minutes of searching west of Point Sal at 1300 ft failed to locate more tracer.

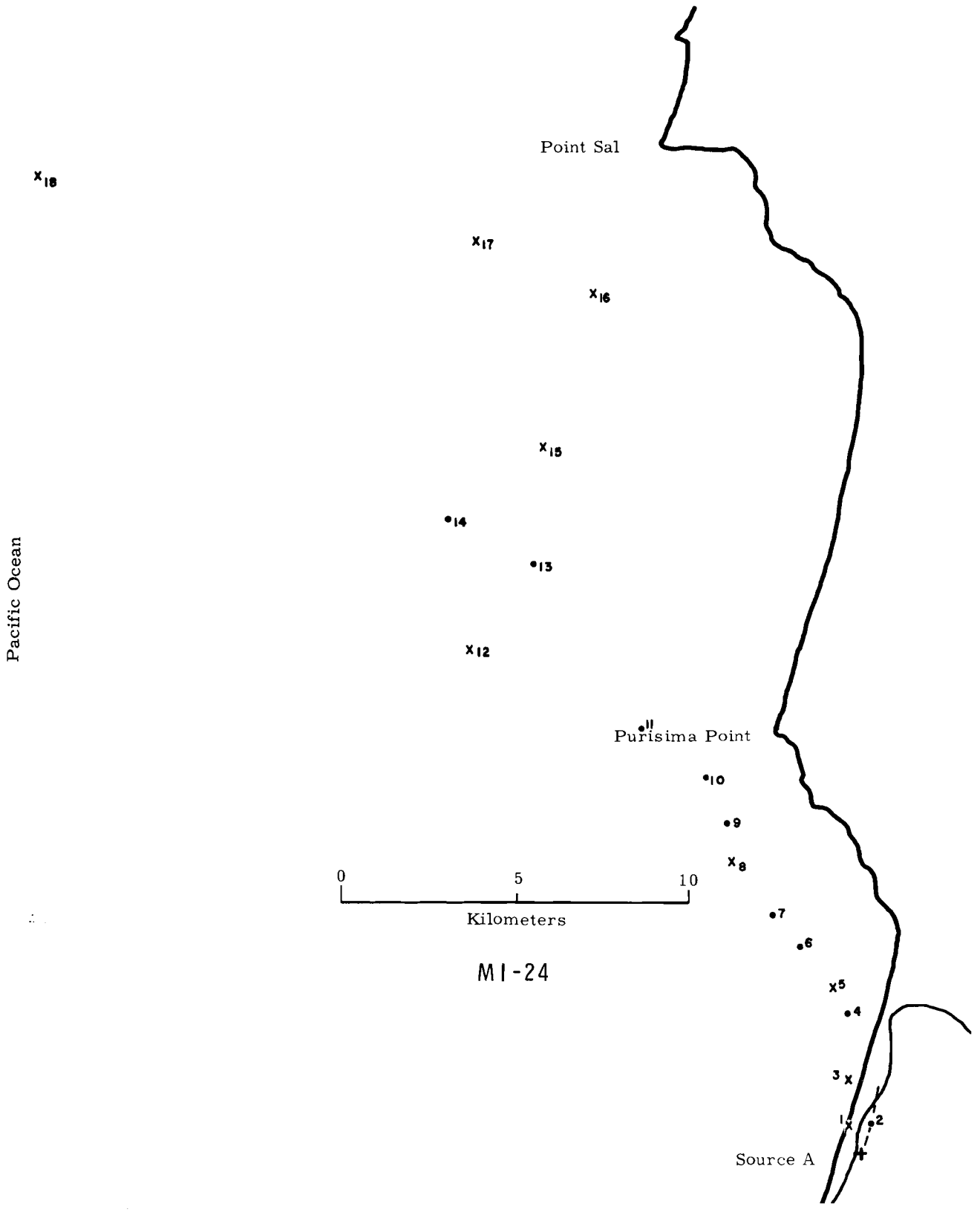
Point Sal
Pacific Ocean
Purisima Point
0
5
10
Kilometers
MI-24
Source A

FIELD TEST MI-24

Tracer Intercept Number	Normalized Peak Concentration g/m^3	Duration in Seconds	Sampling Location: Altitude, ft MSL	Sampling Location: Altitude, ft Above Surface	Sampling Location: Distance from Source, km	Tracer Speed: Min, mps	Tracer Speed: Max, mps
1*	1.2	2	700	700	0.9	2.2	∞
2	>6.2	8	700	550	0.9	1.9	∞
3*	4.5	6	700	700	2.2	3.9	∞
4	3.6	3	900	900	3.8	4.3	∞
5*	1.2	6	1000	1000	4.7	4.7	47
6	2.4	10	1100	1100	6.0	5.4	27
7	3.2	15	1100	1100	7.1	5.9	23
8*	1.8	2	1300	1300	8.9	6.6	20
9	1.6	8	1100	1100	10.1	6.8	17
10	1.2	2	1300	1300	11.5	7.1	16
11	0.68	19	1400	1400	13.4	7.7	16
12*	0.40	2	1300	1300	18.0	8.8	16
13	1.1	10	1300	1300	19.0	8.6	14
14	1.4	18	1300	1300	21.3	9.1	15
15*	0.56	16	1300	1300	21.9	8.9	14
16*	0.18	1	1300	1300	25.4	8.9	13
17*	0.25	9	1360	1360	27.9	9.4	13
18*	0.21	2	1300	1300	35.9	8.7	11

* Questionable tracer intercept.

MI-57

As was mentioned in the introduction to this section on airborne tracer monitoring, Test MI-57 is the first of a series of eleven tests, (MI-57 to 69) where the QARTS did not function well. Sensitivity was low and absolute calibration was lacking. Much higher concentrations of tracer were required to give significant QARTS recorder indications than was the case before or after this series. Thus, the apparent number of intercepts is reduced, and those that were recorded tend to be located in the higher tracer concentrations near the generator.

Tracer Generation occurred for 30 minutes during MI-57. The time interval was 1055 to 1125 PST. Sampling was pursued from 1100 to 1235, but only 5 intercepts with the tracer were made--the last at 1153 PST.

Surface winds near the source were at 315° during generation and the same or slightly more northerly at 500 ft MSL. This direction appears to have been conducive to the split of the plume into two lobes as evidenced by the ground samples and suggested by the meager aircraft samples.

Surface winds in and along Honda Canyon were westerly during generation, and Ionospheric Sounder upper winds were west to southwest through elevations of 2000 ft at 1100 and 1200 PST. These winds transported the one "finger" of the tracer. Intercepts 1, 2, 3, and 5 were made with this finger.

Surface winds at Station 301 on Sudden Ranch were 310 to 330° throughout the period 1100 to 1230 PST. Boathouse surface winds, easterly through the generation period, were 305 to 320° from 1130 to 1230. Upper winds at the Boathouse were easterly to elevations of 1300 ft MSL at 1100 PST, but were 305 to 320° from the surface to 3000 ft at 1200 PST. Thus, the winds necessary to transport the south to southeast finger of the tracer were also in evidence. Intercept No. 4 confirms the southerly movement of tracer aloft.

Measured wind speeds in and about Honda Canyon were 1 to 3 mps. It is difficult to explain the Min Speed of 6 computed for Intercepts 1 and 3 found in the canyon. Speeds at Station 301 were 4 mps, and at Boathouse were 3 to 6 mps. These speeds offer no contradiction to the Min of 3.7 mps computed for Intercept 4 on the southerly finger.

The low sensitivity of the QARTS system during this test makes any statement concerning vertical extent of the tracer open to considerable doubt, but the plume was not intercepted at elevations greater than 700 ft above the underlying surface. This observation is compatible with the low level of the inversion base (it reached to the surface) at Pad D at 1100 PST. The base had lifted to about 700 ft MSL by 1200 PST. Ionospheric Sounder showed an isothermal layer from the surface to 1300 ft MSL and a steep inversion above that at 1100 PST. The isothermal layer had been transformed into a lapse of -3 °F through this 1300 ft layer at the 1200 PST sounding. The Boathouse soundings showed a superadiabatic layer from the surface to 400 ft, a layer with a lapse rate of -0.2F° per 100 ft from 400 to 1000 ft MSL, and a temperature inversion above 1000 ft MSL.

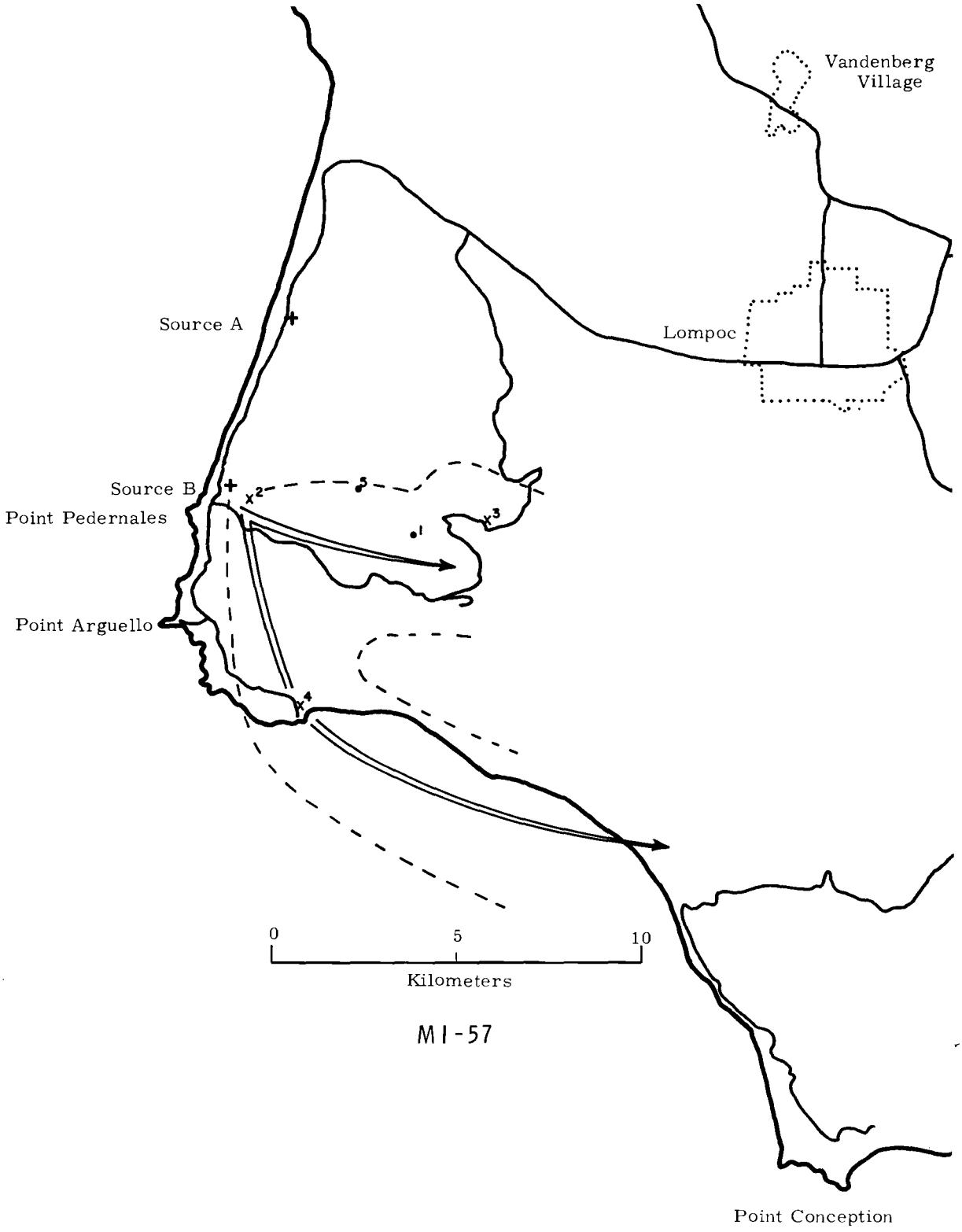
Vandenberg Village
Lompoc
Source A
Source B
Point Pedernales
Point Arguello
Point Conception
0
5
10
Kilometers
MI-57

FIELD TEST MI-57

Intercept Number	Peak Relative** Concentration	Duration in Seconds	Sampling Location Altitude, ft MSL	Sampling Location Altitude, ft Above Surface	Sampling Location Distance from Source, km	Tracer Speed Min, mps	Tracer Speed Max, mps
1	> 82	6	1200	700	5.1	6.3	∞
2*	163	2	600	350	0.8	0.8	∞
3*	167	1	1000	250	7.0	5.8	∞
4*	110	1	500	400	6.1	3.7	∞
5	> 84	13	1300	300	3.5	1.0	2.1

* Questionable tracer intercept.

** Relative concentration only. Comparable among Tests MI-57 through 69 inclusive.

MI-58

Generation began at 1407 and ended at 1437 PST. The aircraft sampled until 1535, although the last intercept was at 1515 PST.

This field experiment took place on the same day (April 25, 1966) as test MI-57. The Min Speed of 71 mps required for Intercept 1 to reach its indicated location suggests the tracer intercepted was a remnant remaining from the preceding test.

Intercepts 2 through 7 are so near the generator and so close to the surface that they offer minimal information of interest. The base of the inversion at Pad D was at least 600 ft MSL on the 1400 and 1500 PST soundings. Since a lapse rate of 10 F° was in evidence through this 600 ft layer, it is not surprising to find Intercept 4 at an elevation 600 ft MSL (500 ft above terrain) only 0.4 km from the source.

Surface winds at Station 301 and the Boathouse were 320 to 350° at 5 to 9 mps for the 1 1/2 hours after initiation of generation. Scout Pad D surface winds were 305 to 340° at 3 mps. Winds to 3000 ft at Scout Pad D and the Boathouse were approximately 320° at 4 mps. There is nothing unexpected, then, in the Distance from Source of Intercept 8 or its computed speed.

The altitude of Intercept 8 is another matter. Both Ionospheric Sounder and Scout Pad D show strong inversions at 1400 and 1500 PST between about 700 and 1700 ft MSL. Although the Boathouse inversion of +3 F° through the layer 300 to 1300 ft is not as strong as the Ionospheric Sounder or Scout Pad D inversions, it still would seem unlikely that the tracer at Intercept 8 could have penetrated to its specified heights of 3000 ft MSL. It is likely a noise signal on the QARTS.

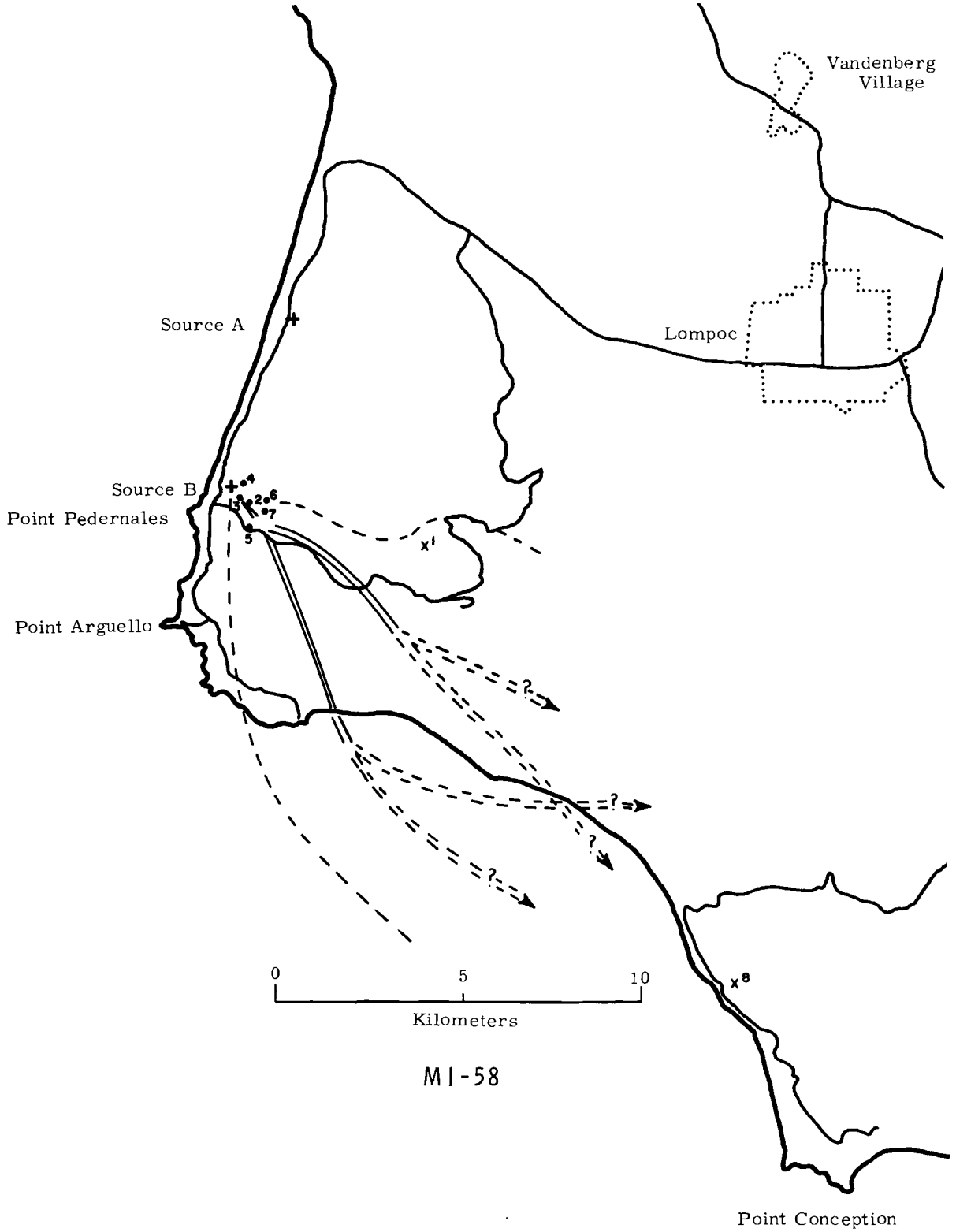
Vandenberg
Village
Lompoc
Source A
Source B
Point Pedernales
Point Arguello
Point Conception
0
5
10
Kilometers
MI-58

FIELD TEST MI-58

Intercept Number	Peak Relative Concentration	Duration in Seconds	Sampling Location: Altitude, ft MSL	Sampling Location: Altitude, ft Above Surface	Sampling Location: Distance from Source, km	Tracer Speed: Min, mps	Tracer Speed: Max, mps
1*	10	2	500	100	5.6	71	∞
2	73	4	500	400	0.7	5.0	∞
3	>85	12	300	200	0.4	1.7	∞
4	>85	5	600	500	0.4	0.4	∞
5	>82	6	400	100	1.2	1.2	∞
6	66	2	200	100	1.0	0.8	∞
7	68	2	200	100	1.1	0.7	∞
8*	3	1	3000	2750	19.0	4.6	8.3

* Questionable tracer intercept.

MI-59

During field run MI-59, generators were operated for 48 minutes--from 1213 to 1301 PST. Aircraft intercepts with tracer were made between 1218 and 1253, although sampling continued until about 1320.

Surface wind direction at the source was about 320° at 4 mps during generation, and was slightly more westerly at 3 to 5 mps at VHF, WIND Station 054, Range Operations, Telemetery, and Honda East. Aloft winds at Ionospheric Sounder and Building 22 were roughly 285° from near the surface to 700 ft, and veered to 295° at 1000 ft MSL. Speeds varied from 3 to 13 mps. Ground plume and aircraft intercepts were at locations one could anticipate from the previous wind information.

A lapse of -10 F° was evident from the surface (400 ft) to 1000 ft MSL at Ionospheric Sounder with an inversion above. No tracer was intercepted above 1000 ft MSL. Building 22 and Scout Pad D soundings showed lapse rates of similar magnitude to that at Ionospheric Sounder, but they extended about 300 ft farther aloft before intercepting the inversion base.

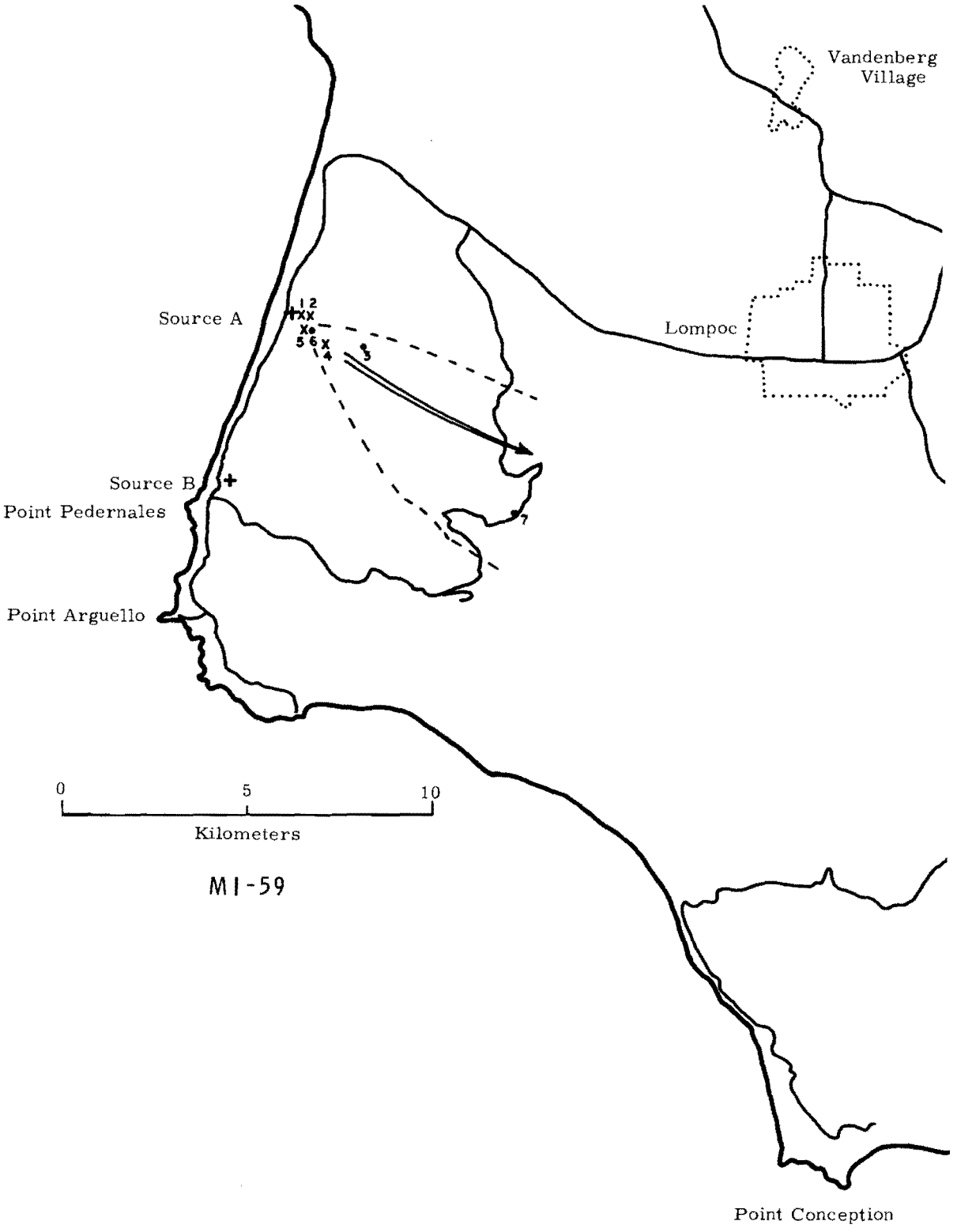
Vandenberg Village
Lompoc
Source A
Source B
Point Pedernales
Point Arguello
Point Conception
0
5
10
Kilometers
MI-59

FIELD TEST MI-59

Intercept Number	Peak Relative Concentration	Duration in Seconds	Sampling Location: Altitude, ft MSL	Sampling Location: Altitude, ft Above Surface	Sampling Location: Distance from Source, km	Tracer Speed: Min, mps	Tracer Speed: Max, mps
1*	5	1	250	100	0.3	0.7	∞
2*	5	1	300	100	0.3	0.4	∞
3	>67	9	700	325	2.0	1.9	∞
4*	37	2	500	200	1.3	1.1	∞
5*	24	2	500	250	0.5	0.4	∞
6	>67	2	400	150	0.6	0.4	∞
7	58	2	1000	350	8.0	3.0	∞

* Questionable tracer intercept.

MI-60

Aircraft sampling during Test MI-60 was restricted to the period of generation, 1255 to 1324 PST. Furthermore, sampling was restricted to near generator traverses.

All plume intercepts were in the direction dictated by surface and lower level upper winds. Surface and upper winds to 650 ft MSL were 3 to 5 mps.

An inversion was in evidence at the four stations collecting upper air data. The inversion base was at its lowest (650 ft) at Building 22, and at its highest (1300 ft) at the Ionospheric Sounder. The temperature lapse rate below the inversion at Building 22 was -6 F° through the interval from the surface (370 ft) to 650 ft MSL.

No tracer intercepts were made above 500 ft MSL or above 250 ft above terrain. Perhaps the only significant information to come from aircraft data during this run was this lack of intercepts at 600 ft MSL and above in the vicinity of Intercepts 5 through 7--0.4 to 0.8 km from the source.

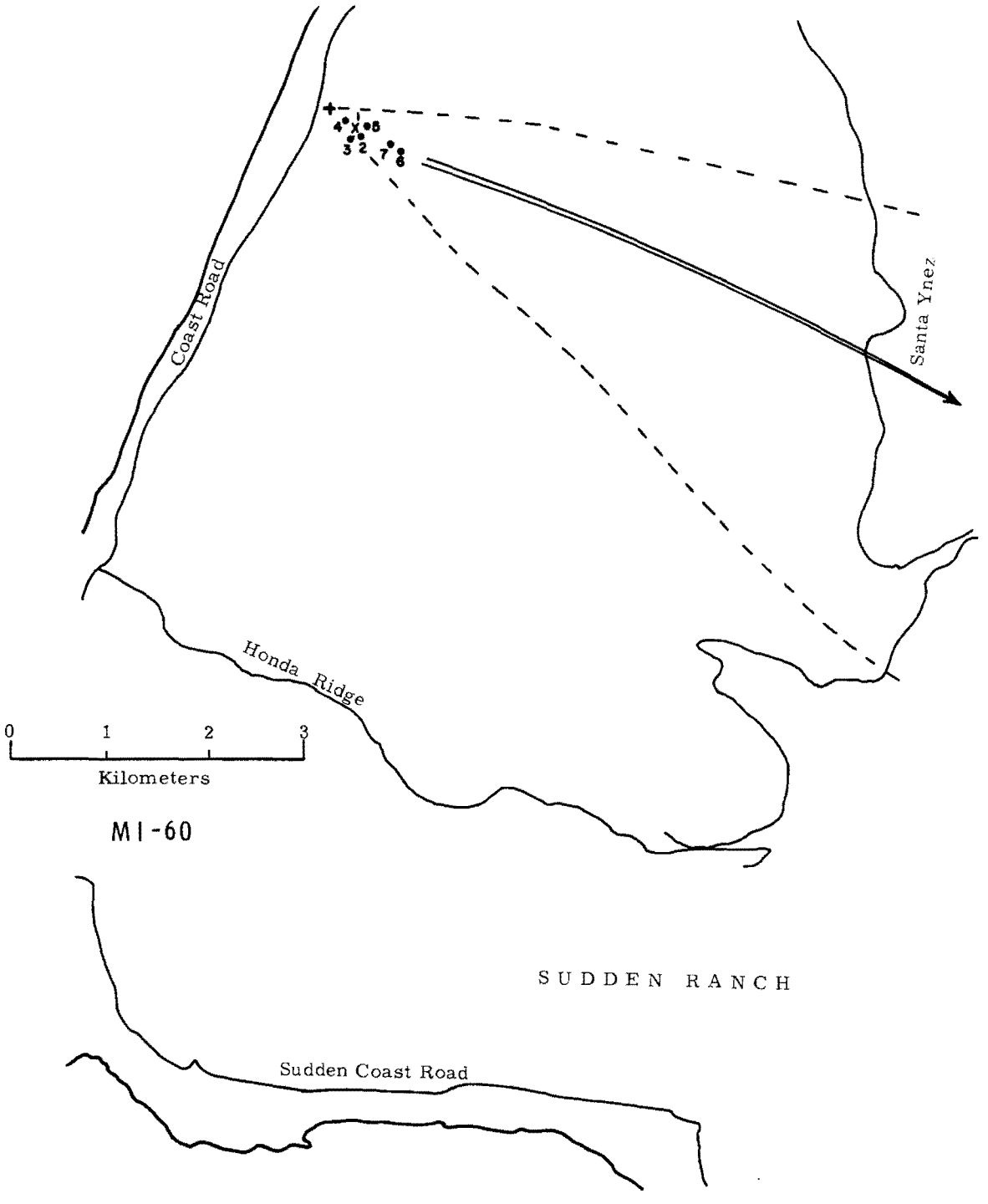
Coast Road
Santa Ynez
Honda Ridge
0 1 2 3
Kilometers
MI-60
SUDDEN RANCH
Sudden Coast Road

FIELD TEST MI-60

Intercept Number	Peak Relative Concentration	Duration in Seconds	Sampling Location Altitude, ft MSL	Sampling Location Altitude, ft Above Surface	Sampling Location Distance from Source, km	Tracer Speed Min, mps	Tracer Speed Max, mps
1*	6	2	500	250	0.3	4.1	∞
2	>81	4	500	250	0.4	1.6	∞
3	>81	4	500	250	0.3	0.8	∞
4	>80	5	400	150	0.2	0.3	∞
5	>81	2	300	50	0.4	0.4	∞
6	>81	2	400	100	0.8	0.6	∞
7	290	2	350	100	0.7	0.5	∞

* Questionable tracer intercept.

MI-63

Tracer generation began at 1302 and ended at 1332 PST. Aircraft plume intercepts were made from 1306 to 1452, and sampling was ended at 1500.

Surface winds at and very near the source were 240 and 290° during generation at 1 to 3 mps. In Honda Canyon (Ionospheric Sounder) they were 240° at 2 mps for a 1 1/2 hour interval starting at generation. In the area north of the Canyon, surface winds were 270 to 290° at 3 to 6 mps. The surface plume, according to these winds, should have traveled the canyon. One lobe appeared to do so. Winds south of Honda Canyon showed northerly components--especially Remote Radar with 340° at 7 mps. Station 301 showed 310° at 4 mps, and the Boathouse 290 to 305° (speed missing).

Winds throughout the layer from the surface to 3000 ft MSL were 260 to 350° at the 1300 and 1400 PST soundings. The upper winds tended to back with time. Speeds were in the 4 to 10 mps range.

With the exception of Intercept 9, the plume intercept locations are in agreement with the wind field. No. 9 was likely either mislocated or was not tracer.

Upper air temperature soundings showed a steep lapse condition (about 3F°/100 ft) up to 500 or 600 ft MSL. A less steep lapse (about 0.3F°/100 ft) continued to 3000 ft MSL at Ionospheric Sounder and to greater than 3000 ft MSL at the Boathouse. Scout Pad D showed an isothermal layer from 500 to 3000 ft at 1300 PST, and a slight lapse in the same interval at 1400 PST.

All intercepts up to and including No. 11 were within the steep lapse layer or had penetrated only one or two hundred feet into the isothermal (Pad D) or slight lapse (Ionospheric Sounder and Boathouse) layer. Intercepts 12, 13, and 14 were found much higher in the slight lapse layer, but not higher than the inversion base.

Two aircraft traverses were made at 900 and 1000 ft MSL between Intercepts 4 and 5. No tracer was found. Probably no tracer penetrated above 800 ft MSL at a distance of about 1 km.

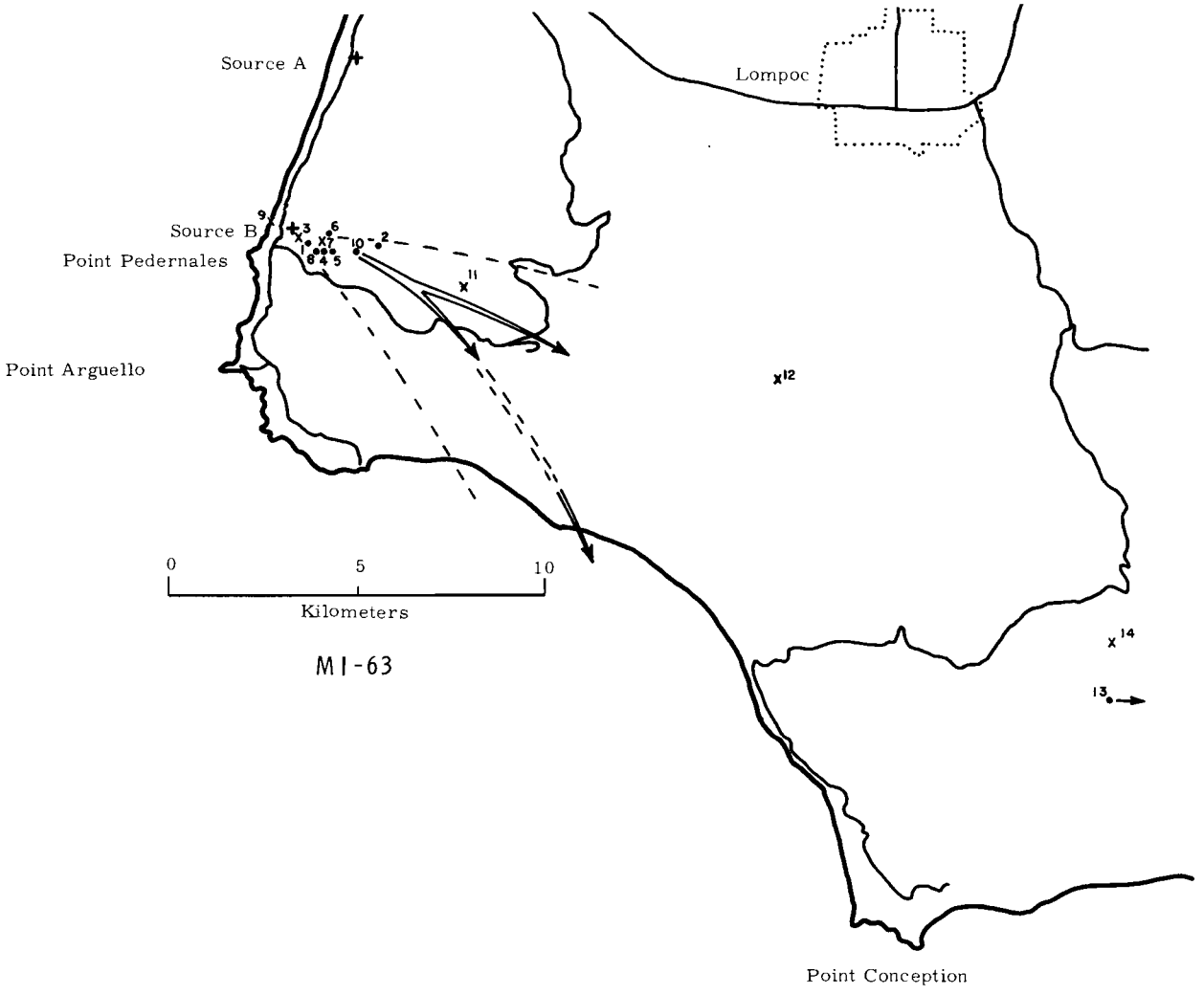
Source A
Source B
Point Pedernales
Point Arguello
Lompoc
Point Conception
0
5
10
Kilometers
MI-63

FIELD TEST MI-63

Intercept Number	Peak Relative Concentration	Duration in Seconds	Sampling Location: Altitude, ft MSL	Sampling Location: Altitude, ft Above Surface	Sampling Location: Distance from Source, km	Tracer Speed: Min, mps	Tracer Speed: Max, mps
1	64	2	700	500	0.6	2.3	∞
2	>86	4	400	150	2.3	3.7	∞
3*	20	1	700	500	0.3	0.4	∞
4	73	2	800	600	1.0	1.2	∞
5	>85	8	500	300	1.2	1.0	∞
6	>88	7	700	400	0.9	0.7	∞
7*	32	1	700	500	0.9	0.6	∞
8	46	1	600	400	0.9	0.6	∞
9*	16	1	500	500	0.5	0.3	∞
10	>85	10	400	150	1.8	0.8	5.3
11*	17	5	600	200	4.7	2.1	9.6
12*	4	1	2100	700	13.4	3.2	5.3
13	49	2	2900	1900	31.0	5.0	7.0
14*	9	2	3000	2100	28.7	4.3	6.0

* Questionable tracer intercept.

MI-64

Tracer emission began at 1328 and ended at 1358 PST. Tracer was intercepted during the interval 1335 to 1409. Sampling was concluded at 1445 PST.

Winds at the surface were about 260° at 2 mps at the source throughout generation, and did not vary much directionwise up to 2000 ft MSL. Speeds in the surface to 2000 ft layer were 2 to 5 mps, and winds at Building 22 were similar. Position of aircraft intercepts occurring below 2000 ft MSL agree with these winds.

A shear in wind direction occurred between 2000 and 2600 ft MSL. Building 22 winds were 255° at 5 mps at 2000 ft, and 215° at 3 mps at 2600 ft--a backing of 40° over a 600 ft interval. Winds at the source backed 20° over the same height interval. Above 2600 ft wind directions were 205 to 220°. These more southerly upper winds explain the location of Intercepts 7, 8, and 9 which were found above 2000 ft MSL and north of the ground level plume.

Temperature soundings at Scout Pad D and Building 22 showed surface temperatures about 15F° warmer than temperatures at 3000 ft, with about half the 15° difference found in the lowest 400 ft. The level 3000 ft MSL marked the lowest elevation of the base of a shallow inversion layer observed at these two stations. So, even the highest observed intercepts, No. 8 and 9, were below the base of the inversion.

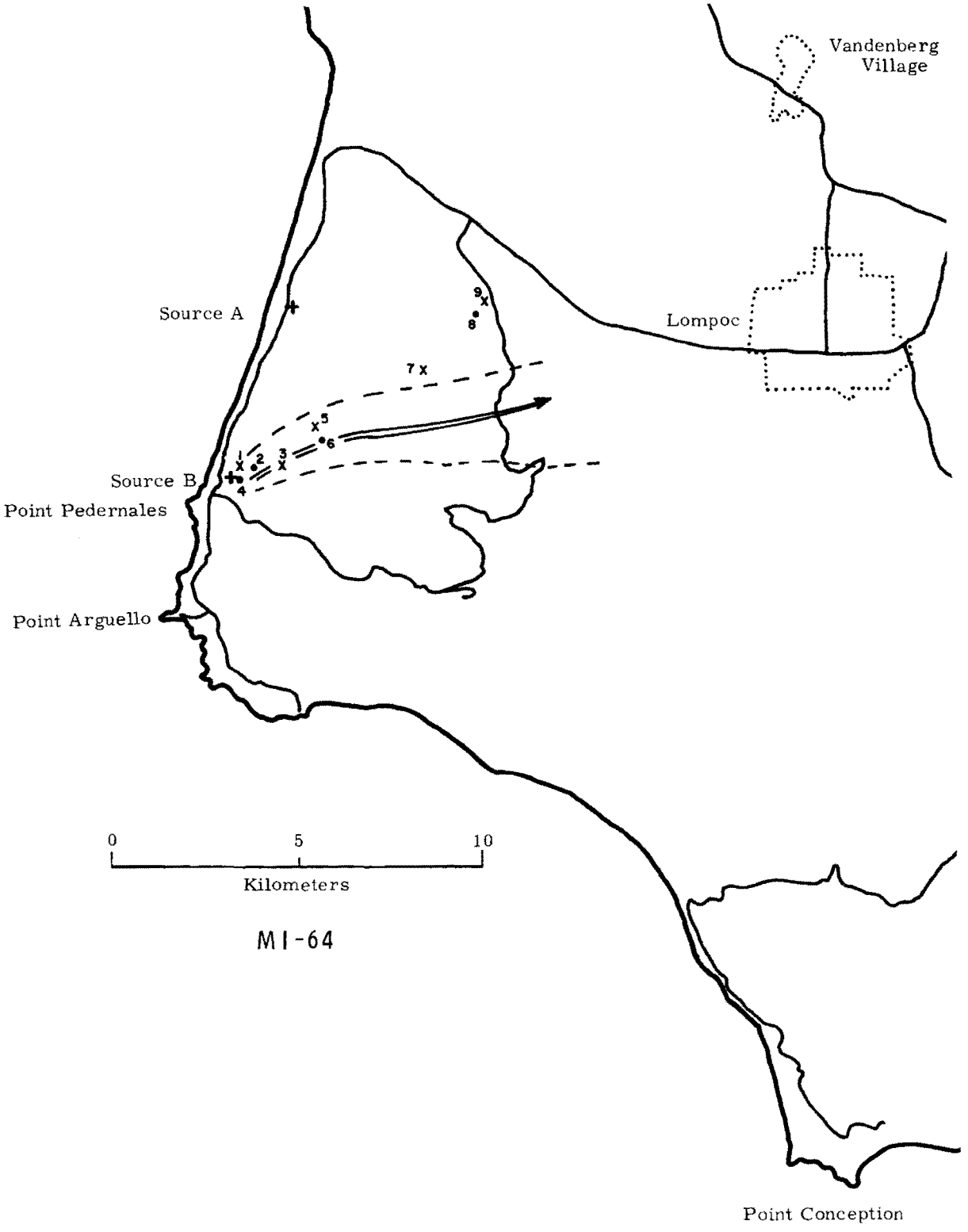
Vandenberg Village
Lompoc
Source A
Source B
Point Pedernales
Point Arguello
Point Conception
1
2
3
4
5
6
7
8
9
0
5
10
Kilometers
MI-64

FIELD TEST MI-64

Intercept Number	Peak Relative Concentration	Duration in Seconds	Sampling Location: Altitude, ft MSL	Sampling Location: Altitude, ft Above Surface	Sampling Location: Distance from Source, km	Tracer Speed: Min, mps	Tracer Speed: Max, mps
1*	2	2	400	100	0.5	0.6	∞
2	>82	5	500	200	0.7	0.8	∞
3*	7	7	600	100	1.4	1.1	∞
4	66	2	300	175	0.2	0.2	∞
5*	1	1	1200	450	2.6	1.7	∞
6	>84	3	1100	200	2.6	1.3	14
7*	5	1	2500	1800	6.0	2.4	8.8
8	79	2	2800	2500	7.9	3.0	9.7
9*	2	1	2800	2500	8.3	2.9	8.0

* Questionable tracer intercept.

MI-65

Test MI-65 was held in the late afternoon on May 5, 1966--following the early afternoon test MI-64. Generation for MI-65 continued from 1645 to 1715 PST. Aircraft sampling began at 1640 and continued till 1805. Intercepts were made between 1645:15 and 1729.

Surface winds at Scout Pad D were 290 to 300° at about 2 mps. Winds between the surface and 2600 ft were nearly the same as the surface in direction, 300 to 310°, but had speeds of 2 to 6 mps. Boathouse and Ionospheric Sounder winds were quite similar to those at Pad D. With the possible exception of questionable Intercept 4, intercepts are where one could expect to find them. The high Min Speed computed for Intercept 2 was likely the result of poor time coordination between generator operator and aircraft. Field notes indicate it was detected less than 2 minutes after generation. The time interval was likely greater.

The 1700 PST temperature soundings at Scout Pad D, Ionospheric Sounder, and the Boathouse were unusually similar. The base of the inversion was very near 3100 ft at all three stations. Temperature lapse rate was nearly a constant -0.4F°/100 ft throughout the layer beneath the inversion. All tracer intercepts were well below the base of the inversion.

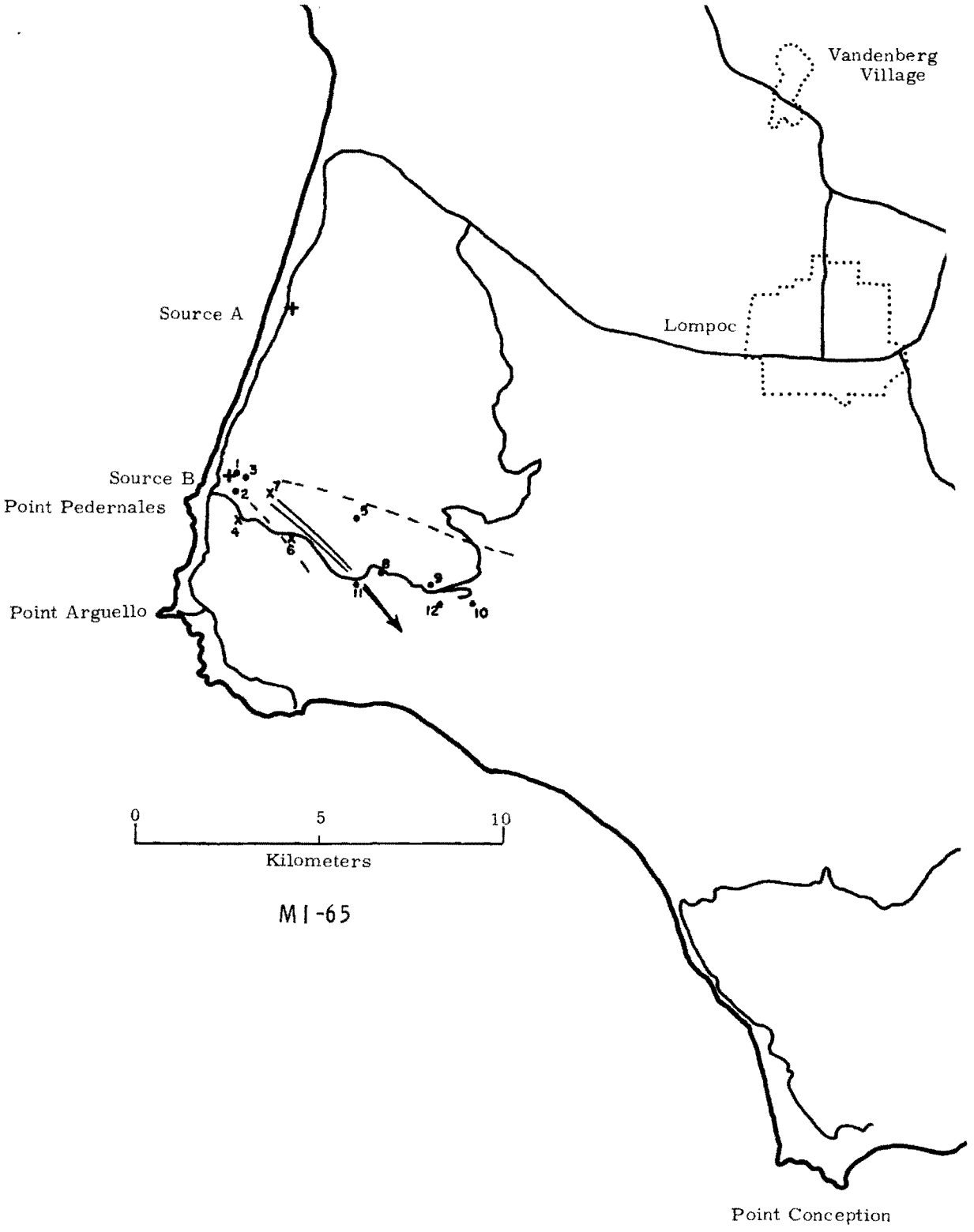
Vandenberg Village
Lompoc
Source A
Source B
Point Pedernales
Point Arguello
Point Conception
0
5
10
Kilometers
MI-65

FIELD TEST MI-65

Intercept Number	Peak Relative Concentration	Duration in Seconds	Sampling Location: Altitude, ft MSL	Sampling Location: Altitude, ft Above Surface	Sampling Location: Distance from Source, km	Tracer Speed: Min, mps	Tracer Speed: Max, mps
1	>310	1	500	300	0.0	0	∞
2	157	2	500	300	0.8	6.6	∞
3	>310	3	500	250	0.5	1.2	∞
4*	110	1	700	250	1.2	1.9	∞
5	> 86	2	800	400	3.6	4.1	∞
6*	12	1	1200	450	2.4	2.5	∞
7*	67	1	800	550	1.2	1.2	∞
8	33	2	1500	200	5.0	3.7	∞
9	34	2	1700	200	6.1	4.4	∞
10	37	1	1700	200	7.4	4.3	∞
11	31	1	1700	200	4.5	2.8	∞
12	> 87	2	1800	300	6.6	2.5	8.0

* Questionable tracer intercept.

MI-66

Tracer generation began at 1323 and ended at 1353 PST. The aircraft sampling equipment was in operation from 1316 to 1440, with tracer intercepts occurring between 1329 and 1434.

This test is a poor one because all but one of the intercepts were of the questionable variety.

The location of Intercepts 5, 7, and 8 are acceptable on the basis of Boathouse wind directions of 5 to 40° between 1300 and 2000 ft. Intercepts 9 and 10 are not unreasonable in that near surface winds were 340° at the Boathouse and more westerly at points farther inland. Additionally, the tendency for a curved trajectory over the ocean near the Boathouse and back over land near Jalama Beach was observed on several other tests. Evidence to the converse is that no tracer was found on ground-based bulk filters which extended as far south as Jalama Beach.

Possible Intercepts 5, 7, and 8 were made at elevations of 2400, 2500, and 1800 ft MSL respectively. These elevations are well above the base of the inversion, 1300 ft, at Scout Pad D at 1400 PST, the time nearest these intercept occurrances. Thus, although wind directions are not in conflict with these more distant intercepts, their deep penetration of the inversion is. That these intercepts were truly tracer released from Source B is considered very unlikely.

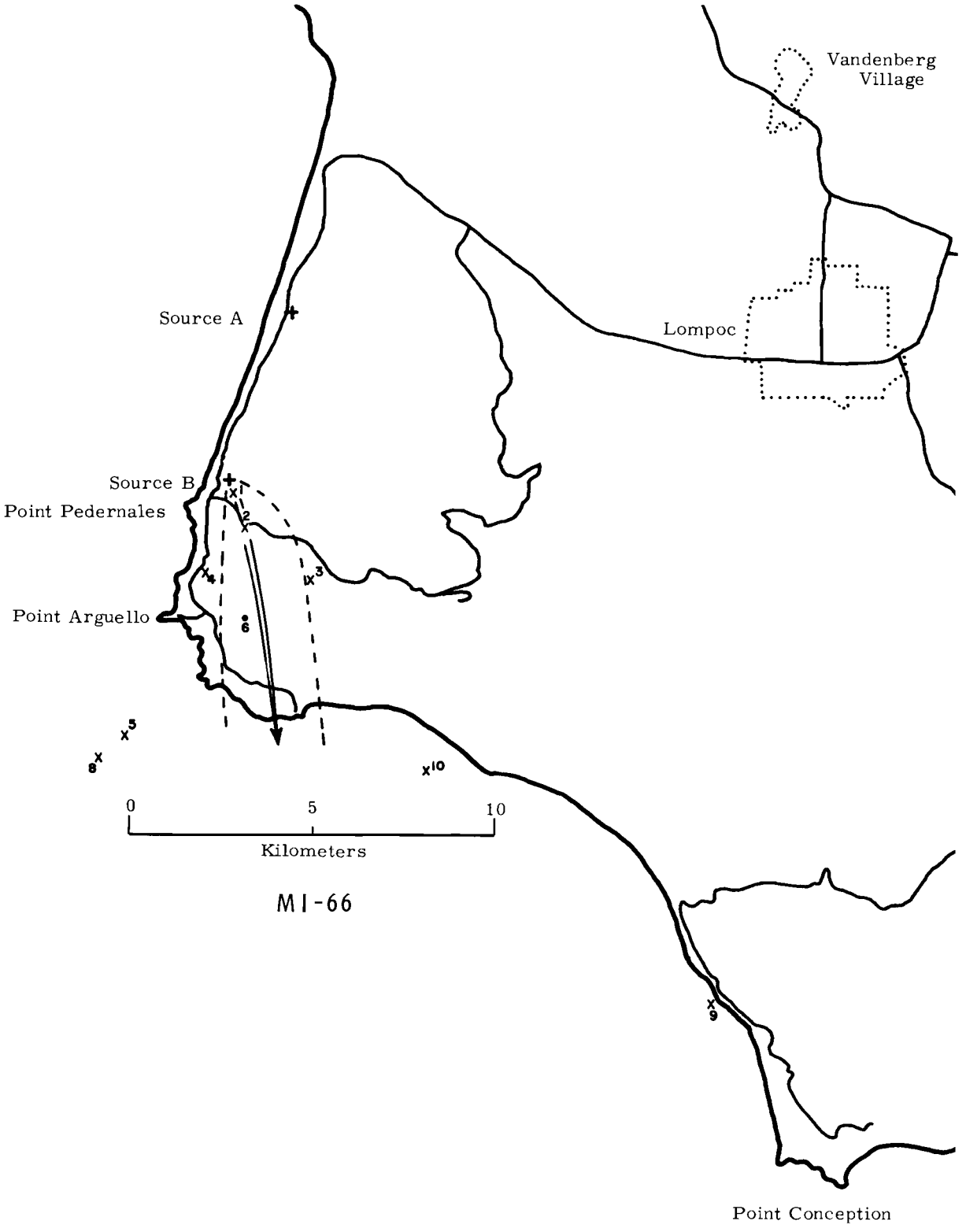
Vandenberg Village
Source A
Lompoc
Source B
Point Pedernales
Point Arguello
0
5
10
Kilometers
MI-66
Point Conception

FIELD TEST MI-66

Intercept Number	Peak Relative Concentration	Duration in Seconds	Sampling Location: Altitude, ft MSL	Sampling Location: Altitude, ft Above Surface	Sampling Location: Distance from Source, km	Tracer Speed: Min, mps	Tracer Speed: Max, mps
1*	2	1	300	100	0.4	1.1	∞
2*	9	2	1100	600	1.3	2.5	∞
3*	2	1	1500	250	3.4	5.9	∞
4*	8	2	700	500	2.6	2.0	∞
5*	5	1	2400	2400	7.3	4.5	∞
6	49	2	1100	350	3.6	2.0	∞
7*	2	1	2500	2500	17.5	6.4	18
8*	1	1	1800	1800	8.1	2.8	7.6
9*	2	1	500	500	19.0	4.6	8.3
10*	6	1	700	700	9.3	2.1	3.8

* Questionable tracer intercept.

MI-67

Tracer generation proceeded from 1014 to 1044 PST. Aircraft sampling began at 0956 and ended at 1146. Tracer intercepts occurred between 1020 and 1055.

Intercepts between aircraft and tracer plume were difficult to come by during this field test. In fact, some doubt even existed after sampling was begun that the QARTS system was in operation. That it was indeed operative was confirmed by passes near the generator--resulting in Intercepts 1 to 4. Doubtful Intercept 5 is acceptable on the basis of winds as far southwest as 230° at 4 mps at Building 22 from the surface up to 650 ft.

Perhaps the reason for the difficulty in finding tracer during this run was that the atmosphere was unstable throughout the layer up to 900 ft. The lapse rate was -0.6F°/100 ft throughout this layer and about -0.5F°/100 ft for several thousand feet above that. No inversion layer was in evidence. The instability likely led to high mixing rates and, consequently, low tracer concentration. The low sensitivity of the QARTS system at this time contributed to the difficulty.

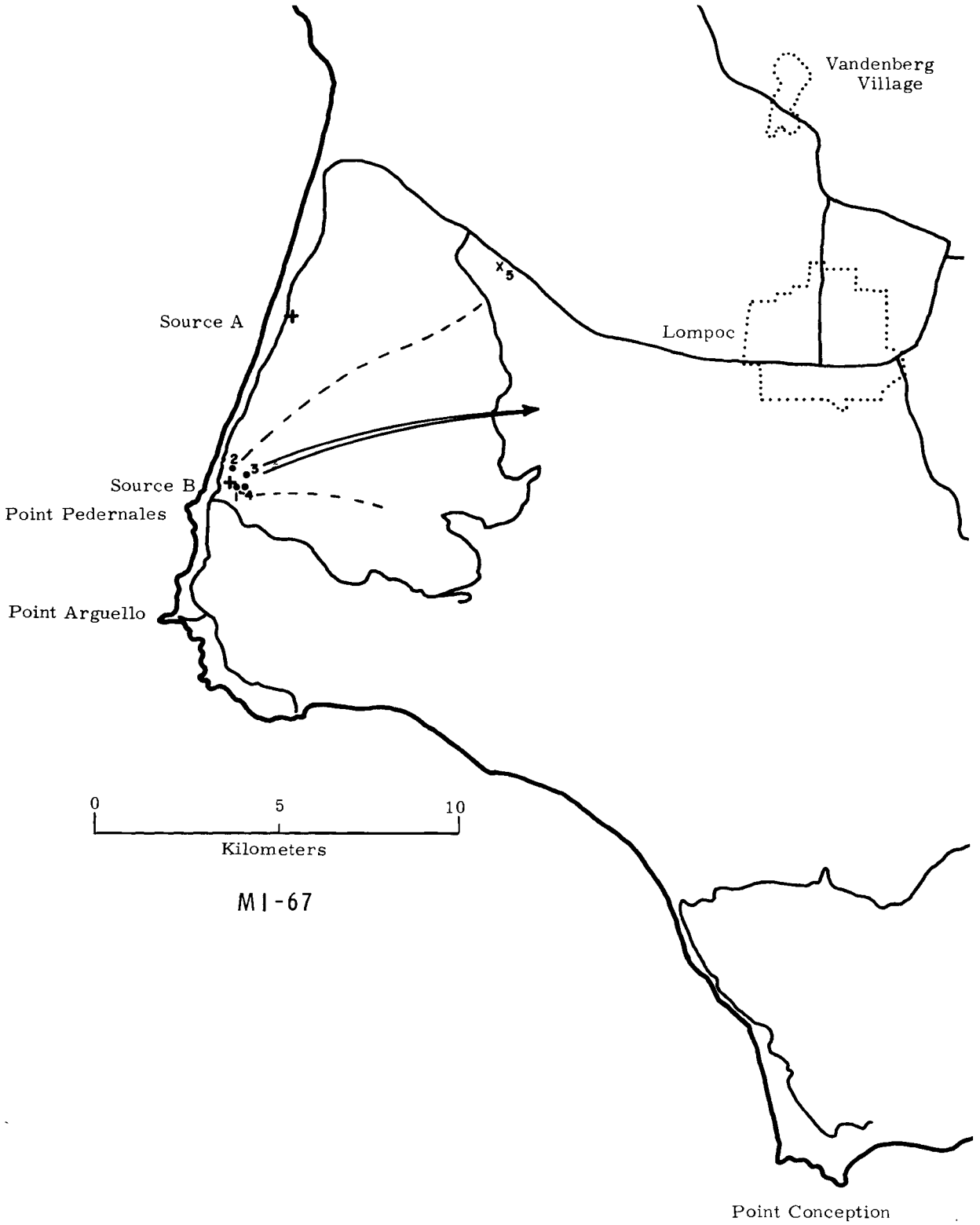
Vandenberg
Village
Lompoc
Source A
Source B
Point Pedernales
Point Arguello
Point Conception
0
5
10
Kilometers
MI-67

FIELD TEST MI-67

Intercept Number	Peak Relative Concentration	Duration in Seconds	Sampling Location: Altitude, ft MSL	Sampling Location: Altitude, ft Above Surface	Sampling Location: Distance from Source, km	Tracer Speed: Min, mps	Tracer Speed: Max, mps
1	> 84	6	400	200	0	0	∞
2	206	3	500	300	0.3	0.5	∞
3	266	2	1000	700	0.4	0.6	∞
4	296	2	400	200	0	0	∞
5*	2	1	500	375	0.3	3.3	14

* Questionable tracer intercept.

MI-68

Tracer generation occurred from 1007 to 1037 PST. Aircraft sampling occurred between 0959 and 1209, with intercepts made from 1012 to 1127.

Location of the intercepts is in good agreement with measured winds. Winds near the source were 330 to 350° from 2 to 4 mps up to a level of 650 ft during Intercepts 1 to 4. Winds at the Boathouse showed 310 to 350° in the layer 650 to 2300 ft at 4 to 9 mps.

At the start of the test, the base of the inversion was at about 2300 ft MSL at both the Boathouse and Scout Pad D. It remained at this level at the Boathouse during the 1100 PST sounding. The temperature lapse rate from the surface to 650 ft MSL was about -0.9F° /100 ft, and from 650 ft to the base of the inversion at 2300 ft, it was about 0.4F° /100 ft.

Although no tracer was intercepted above the inversion base, very little flight time was expended above this level.

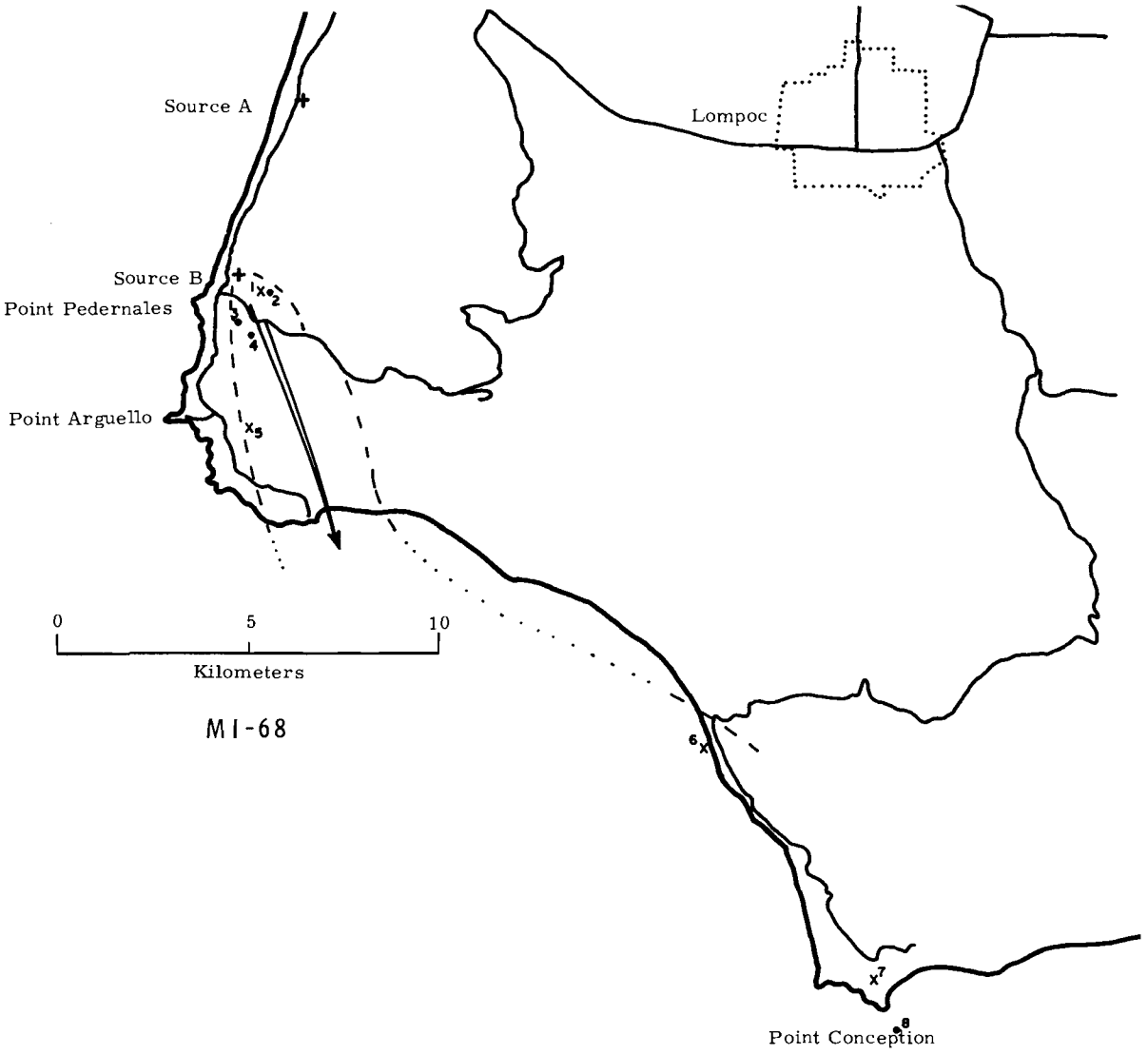
Source A
Lompoc
Source B
Point Pedernales
Point Arguello
0
5
10
Kilometers
MI-68
Point Conception

FIELD TEST MI-68

Intercept Number	Peak Relative Concentration	Duration in Seconds	Sampling Location: Altitude, ft MSL	Sampling Location: Altitude, ft Above Surface	Sampling Location: Distance from Source, km	Tracer Speed: Min, mps	Tracer Speed: Max, mps
1*	43	1	300	100	0.8	2.5	∞
2	>88	2	300	100	0.9	1.2	∞
3	46	2	450	100	1.2	1.1	∞
4	31	1	450	100	1.6	1.2	∞
5*	5	1	1100	500	3.9	2.1	71
6*	7	34	2300	2300	17.1	4.3	8.0
7*	4	1	1400	1200	24.3	5.7	9.7
8	70	2	1700	1700	26.0	6.0	10
9	60	2	1100	1100	32.4	6.8	11
10*	7	1	1000	1000	33.7	7.0	11

* Questionable tracer intercept.

MI-69

Generators were operated from 1005 to 1035 PST. The aircraft flew from 1002 to 1113, with intercepts made from 1011 to 1057.

Winds were light during this field test. All measured surface winds averaged less than 4 mps during generation. Winds aloft were even lower up to levels well above the zone of sampling. Measured surface wind directions agreed with the ground level trajectory, and as can be seen on the accompanying map, all plume intercepts lay relatively close to the ground plume centerline. Aloft soundings at Building 22 showed directions of 220° through north to 50°, and, as mentioned, very low speeds through the layer surface to 1100 ft MSL. The low speeds are in agreement with the computed Tracer Speeds in the Tabled MI-69 data.

The inversion base, as measured at Building 22 and Ionospheric Sounder, was between 2000 and 2500 ft MSL during this test. The Building 22 average gradient over the surface to 2000 ft interval was 0.8°F/100 ft. No tracer was found above 1100 ft MSL, but minimal sampling was done above that level--only a traverse at 1200 ft and one at 1400 ft in the vicinity of Intercept 10.

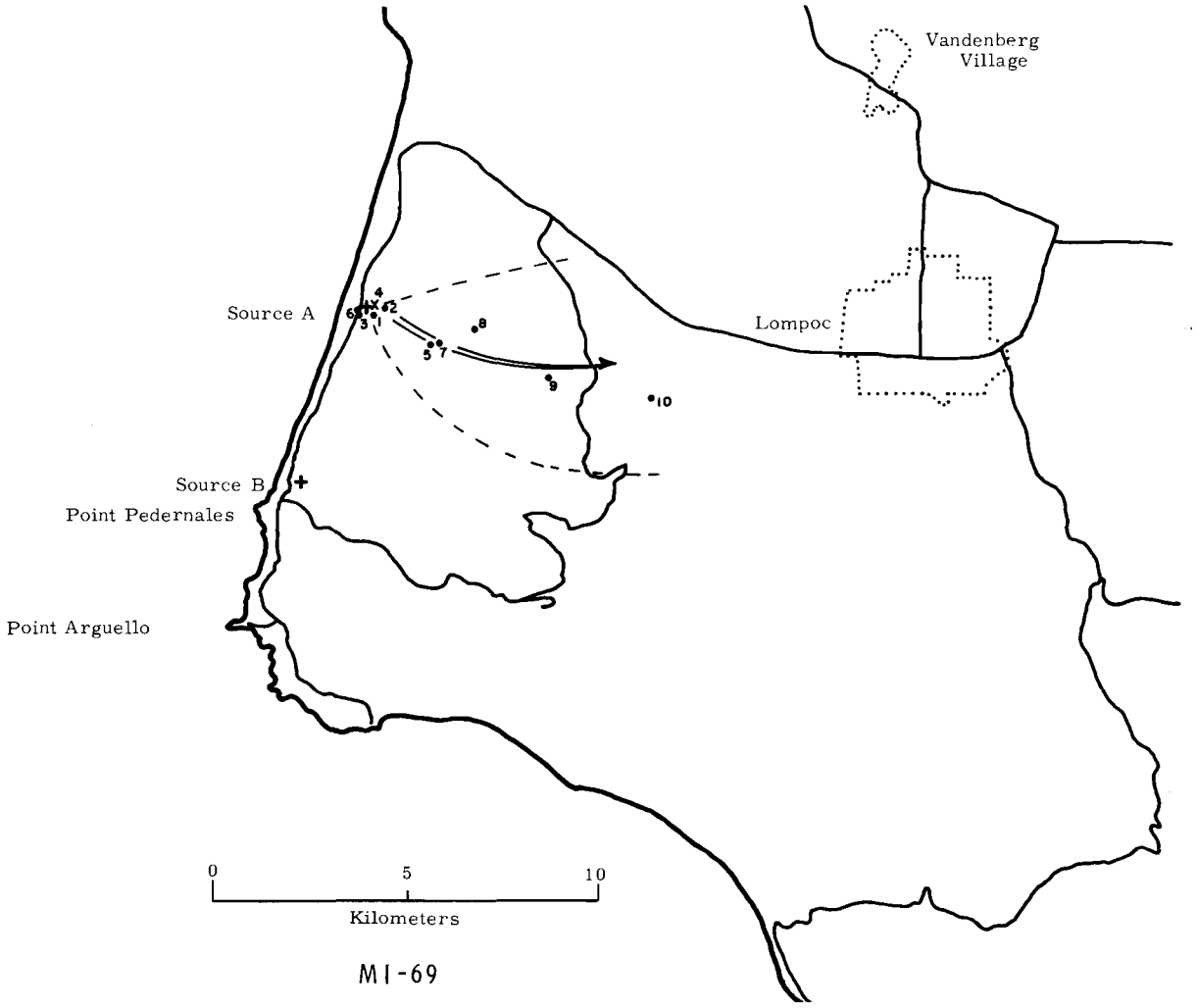
Vandenberg
Village
Source A
Lompoc
Source B
Point Pedernales
Point Arguello
0
5
10
Kilometers
MI-69

FIELD TEST MI-69

Intercept Number	Peak Relative Concentration	Duration in Seconds	Sampling Location: Altitude, ft MSL	Sampling Location: Altitude, ft Above Surface	Sampling Location: Distance from Source, km	Tracer Speed: Min, mps	Tracer Speed: Max, mps
1	>85	2	300	80	0.1	0.3	∞
2	>88	2	300	80	0.3	0.7	∞
3	>87	3	250	50	0	0	∞
4*	2	1	600	380	0.2	0.2	∞
5	>87	2	450	100	2.0	1.9	∞
6	37	1	300	80	0	0	∞
7	18	1	450	100	2.0	1.1	∞
8	>85	1	600	200	2.7	1.0	3.2
9	>86	2	1100	550	5.0	1.7	4.2
10	>87	2	1100	500	8.1	2.6	6.0

* Questionable tracer intercept.

MI-108

The generation period during this field run was 1110 to 1140 PST. All aircraft sampling took place at distances greater than 10 km from the source between 1120 and 1235 PST. The first possible tracer intercept occurred at 1128, and the last at 1218.

Note that all intercepts during this test are of the questionable variety. Intercepts 4 and 6 were of such lengthy duration that the path of the aircraft during intercept is shown on the map rather than reducing the intercepts to a midpoint location. Data tabled for these two intercepts apply to the beginning and end of the lengthy intercepts.

With regard to thermal stability, the soundings during this test at Building 22, Ionospheric Sounder, and the Boathouse all show a strong inversion whose base was at about 2000 ft MSL. Since reported flight elevation was restricted to 1500 ft MSL and lower, no significance can be attached to the fact that no intercepts above that level were reported.

The interpretation of agreement or disagreement between measured winds and intercept locations is complicated by the unusually large distances between meteorological measurement sites and sampling locations. If Intercepts 4, 5, and 6 are valid, there would have to be a more westerly wind than is indicated by the ground plume path. Since the most westerly wind reported at the three sounding stations mentioned in the previous paragraph was 317°, no such wind was in evidence. Furthermore, speeds were nearly all 6 mps or less through the layer up to 600 ft. This leaves the intercepts open to question on the basis of the Min Tracer Speeds computed. It is felt that the aircraft sampling was done downwind of the tracer plume, and that the noted intercepts are likely noise on the QARTS system.

During this test, a series of membrane filters were exposed to the free atmosphere during the sampling period from a sampling system accessible from within the aircraft. Absence of tracer on these filters bolsters the conclusion that none of the questionable intercepts were tracer.


Purisima Point
Vandenberg Village
Source A
Lompoc
Source B
Point Pedernales
Point Arguello
0
5
10
Kilometers
MI-108
Point Conception
Rt. 101
Rt. 1

FIELD TEST MI-108

Tracer Intercept Number	Normalized Peak Concentration g/m^3	Duration in Seconds	Sampling Location: Altitude, ft MSL	Sampling Location: Altitude, ft Above Surface	Sampling Location: Distance from Source, km	Tracer Speed: Min, mps	Tracer Speed: Max, mps
1*	0.19	5	600	600	11.1	10.3	∞
2*	0.16	28	400	400	13.5	9.5	∞
3*	0.14	∿ 60	900	650	18.9	8.3	50
4*	>0.27	∿120	1200	300	23.8	7.2	18
			800	100	22.8	6.8	15
5*	>0.27	∿ 60	800	425	21.5	6.1	13
6*	0.77	∿300	1500	300	35.5	9.3	18
			1200	600	43.8	11	19

* Questionable tracer intercept

MI-109

Tracer was generated throughout the interval 1157 to 1227 PST. Active aircraft sampling began at 1200 and ended at 1343. However, difficulties with noise in the QARTS system developed after 1256 such that the useable period of tracer intercepts occurred between 1202 and 1254 PST.

The majority of intercepts on the QARTS chart appear valid. Furthermore, bulk samples were collected during aircraft flight on filters exposed outside the aircraft. These were changed periodically. These filters confirmed that tracer was indeed in the atmosphere during the periods of reported intercepts.

Surface wind directions in the general vicinity of the ground plume were in agreement with the location of that plume and the aircraft intercepts. The aloft soundings at Building 22 and Ionospheric Sounder at 1200 and 1300 PST were 250 to 305° up to an elevation of 1000 ft and backed above that level. Aloft wind directions were also in agreement with noted plume intercepts--with the exception of questionable Intercept 3.

Measured wind speeds were 2 to 4 mps at the source, at surface wind stations south of the ground plume centerline, and at the Ionospheric Sounder upper wind site. These speeds are lower than the bulk of the Min Speeds computed for the aircraft intercepts. However, surface speeds at VHF were greater than 6 mps, and winds at Building 22 were 3 to 6 mps from the surface to the top of the layer of tracer detection. These winds appear to have been more indicative of the true speed of travel of the aloft tracer.

This field test poses some questions on the ability of the tracer to penetrate into a layer characterized by a temperature inversion. The Building 22 soundings at 1200 and 1300 PST are similar, with a lapse rate of about -2.2F°/100 ft in the layer from the surface (370 ft MSL) to 820 ft MSL, the base of the inversion. The strong inversion layer, with a temperature increase of about 5F° in the first 130 ft, extended to at least 3000 ft.

At the Ionospheric Sounder, however, the 1200 and 1300 PST soundings showed the base of the inversion to be at 1400 ft MSL. The layer below the inversion was approximately -0.9F°/100 ft throughout the entire layer at 1200 PST. At 1300 PST, the layer was more unstable from surface to 700 ft, and about -0.2F°/100 ft from 700 to 1400 ft, but the base of the strong inversion still was at 1400 feet MSL.

If one accepts the soundings at Building 22 and its inversion base at 820 ft MSL as representative of the air in which the tracer moved, then one accepts the fact that some of the intercepts penetrated into the very stable layer. Intercept 12, for instance, was made at an elevation of 1400 ft MSL. Conversely, if one accepts the inversion base of 1400 ft MSL found at Ionospheric Sounder then all intercepts are below the stable layer. (Aircraft traverses were made at elevations up to 1800 ft MSL between Intercepts 11 and 12 without tracer interception.) Recall, though, that the aloft tracer appeared to travel at the higher speeds typical of the Building 22 Sounding. But again conversely, the Min Speed computed for the intercept found at the highest elevation, Intercept 12, was quite low--2 mps. This speed, and the actual location of Intercept 12, suggest better agreement with the Ionospheric Sounder.

It is felt that the superadiabatic lapse rate existing below the inversion permitted rapid tracer mixing to the base of the inversion, and that there was some diffusion of the tracer (perhaps 200 ft) into the stable layer beyond 4 km from the source. The inversion base in the vicinity of the tracer path was likely somewhere between the 820 and 1400 ft levels found off the opposite edges of the plume.

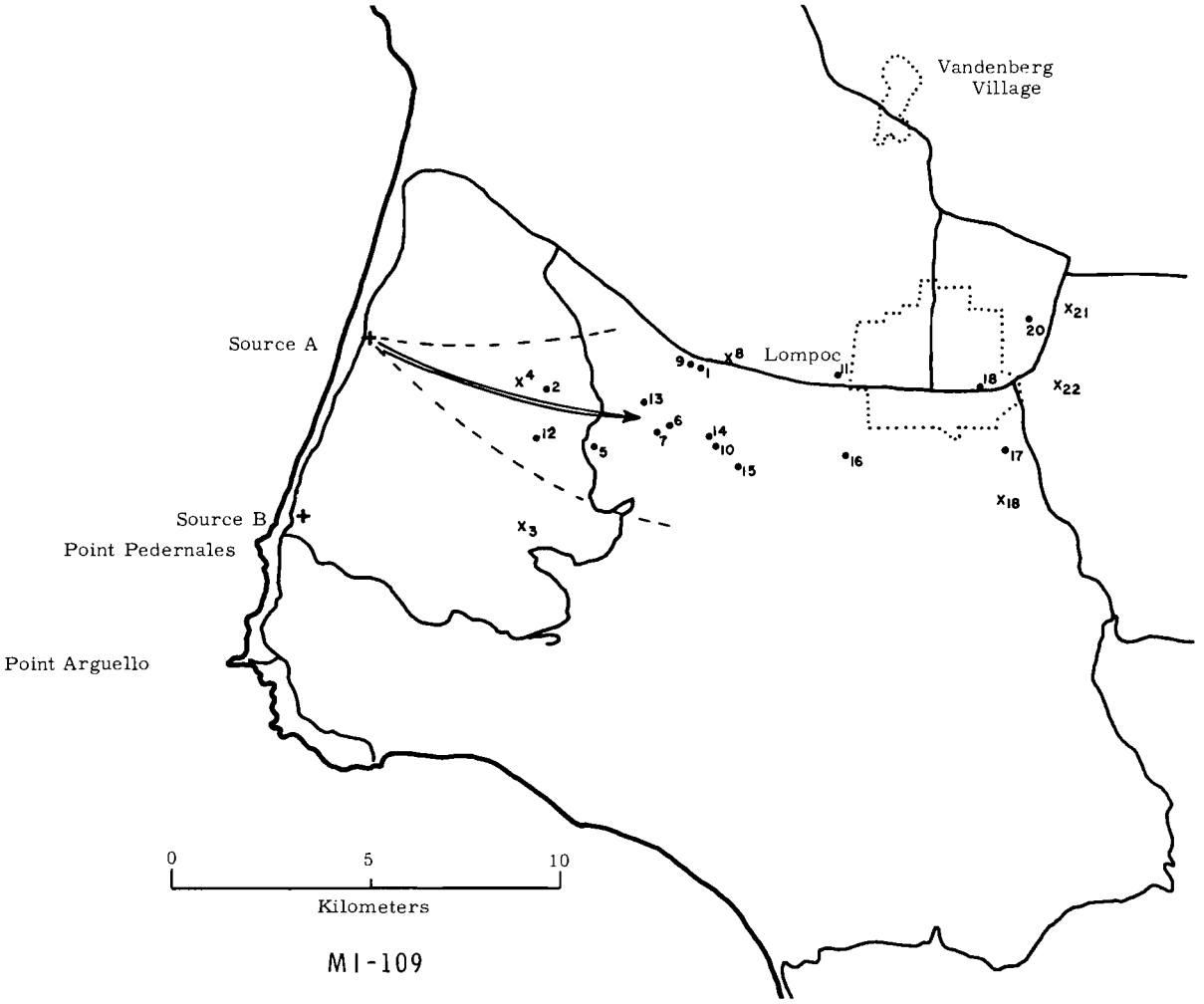
Vandenberg
Village
Source A
Lompoc
Source B
Point Pedernales
Point Arguello
0
5
10
Kilometers
MI-109

FIELD TEST MI-109

Tracer Intercept Number	Normalized Peak Concentration g/m^3	Duration in Seconds	Sampling Location: Altitude, ft MSL	Sampling Location: Altitude, ft Above Surface	Sampling Location: Distance from Source, km	Tracer Speed: Min, mps	Tracer Speed: Max, mps
1	0.20	35	1000	875	8.3	6.8	∞
2	0.65	32	1200	850	4.6	3.7	∞
3*	0.30	1	1300	300	6.0	4.5	∞
4*	0.59	12	1200	825	3.8	2.7	∞
5	>1.2	65	900	150	6.2	4.1	∞
6	>1.2	29	500	100	7.8	4.8	∞
7	0.31	30	900	400	7.6	4.5	∞
8*	0.60	14	1000	875	9.0	4.7	950
9	>1.2	43	700	575	8.0	4.0	43
10	1.2	39	1050	550	9.1	4.4	36
11	1.2	38	850	725	11.9	5.5	32
12	>1.2	29	1400	900	4.9	2.0	7.0
13	>1.2	35	1000	625	7.1	2.7	8.2
14	1.1	37	1100	500	8.9	3.2	9.2
15	0.84	30	1000	200	9.8	3.4	9.3
16	1.2	45	1000	500	12.4	4.3	11
17	>1.2	15	1100	725	16.3	5.5	14
18	0.67	20	1100	975	15.5	5.2	13
19	>1.2	41	1100	725	16.5	5.1	13
20	0.68	7	800	675	16.7	5.2	12
21*	1.1	2	900	700	17.7	5.3	12
22*	0.47	26	1050	850	17.5	5.3	11

* Questionable tracer intercept.

MI-110

Tracer was emitted from 1055 to 1125 PST during test MI-110. Aircraft sampling began at 1055 and continued until 1424. However, noise in the QARTS system coupled with low tracer concentrations resulting from sampling at distances of greater than 20 km made reducing of chart data after 1209 PST unreliable. The last reliable tracer intercept was observed at 1207. As in Test MI-109, bulk filters on the aircraft confirmed the presence of tracer during the period of reported tracer intercepts.

Measured surface wind directions showed no significant deviation from the ground tracer plume centerline or the aircraft intercepts. Soundings at Building 22 and Ionospheric Sounder through the tracer intercept layer indicated directions of 280 to 295° at 1100 PST, and 230 to 275° at 1200. All upper air wind speeds were 1 or 2 mps except for 6 to 8 mps at the 1100 PST Building 22 sounding.

As in test MI-109, the highest wind speeds (about 5 mps) at the surface were found at VHF and Building 22.

Also as in Test MI-109, the inversion base was lower at Building 22 than at Ionospheric Sounder. At Building 22, the base was at about 800 ft MSL while at Ionospheric Sounder, it was at 1000 ft MSL. At the start of the test, a near isothermal layer extended to the surface from the base of the inversion at Ionospheric Sounder. This layer became superadiabatic by the 1200 PST sounding. Building 22 soundings were superadiabatic beneath the inversion at both the 1100 and 1200 soundings.

If we discard questionable Intercept 1, and assume that the inversion base is at a mean of the values found at the two radiosonde stations, we see that no intercept was found above the inversion base. Even if we accept the lower value for this base (800 ft MSL), the table for MI-110 shows no intercepts penetrating beyond 100 ft into the stable layer. Traverses at 1000 ft were made before and after Intercept 14.

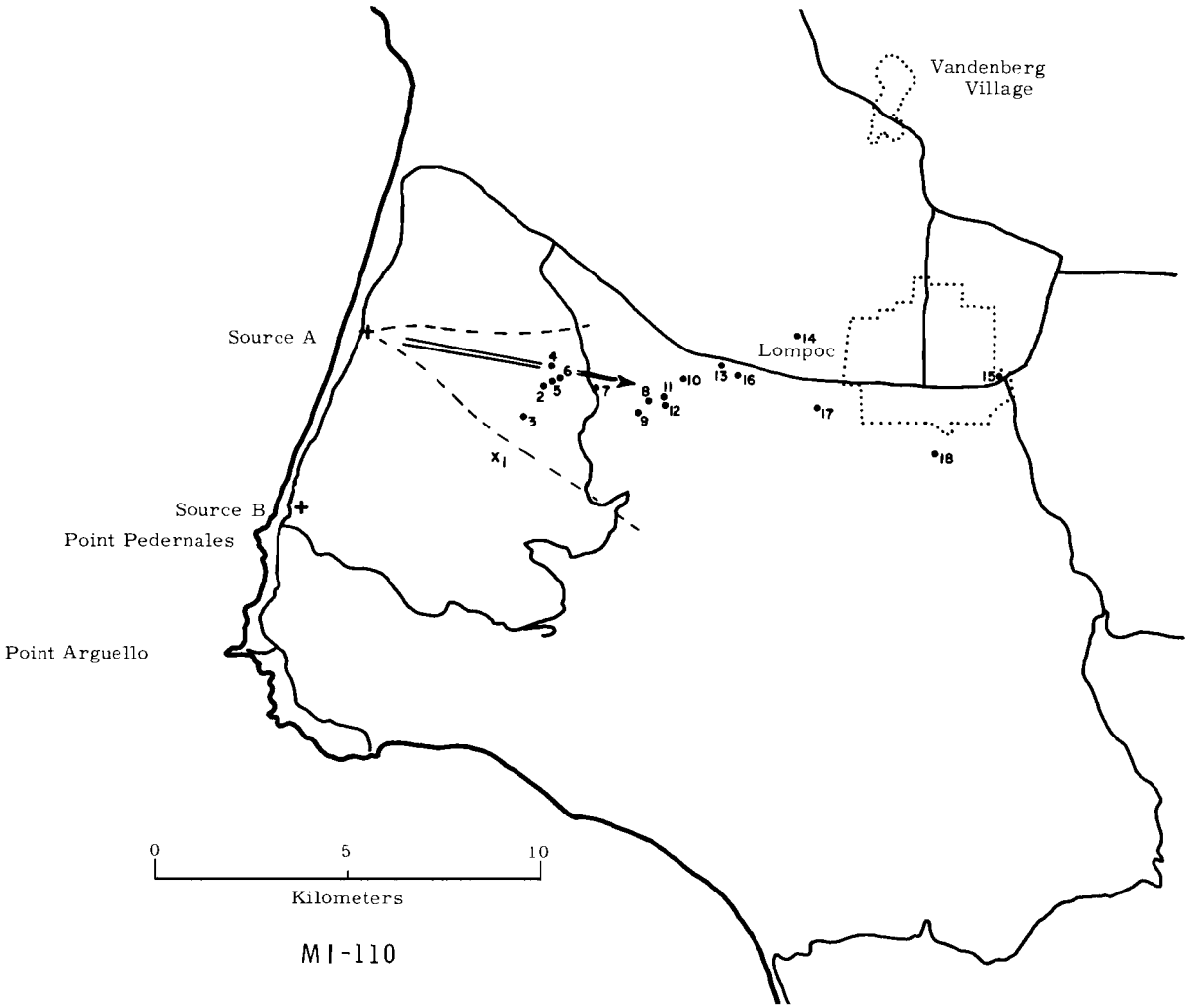
Vandenberg
Village
Source A
Lompoc
Source B
Point Pedernales
Point Arguello
0
5
10
Kilometers
MI-110

FIELD TEST MI-110

Tracer Intercept Number	Normalized Peak Concentration g/m^3	Duration in Seconds	Sampling Location: Altitude, ft MSL	Sampling Location: Altitude, ft Above Surface	Sampling Location: Distance from Source, km	Tracer Speed: Min, mps	Tracer Speed: Max, mps
1*	1.3	1	1100	300	4.4	4.5	∞
2	2.3	37	700	350	4.6	4.1	∞
3	3.6	19	800	200	4.4	3.4	∞
4	>10	25	400	100	4.8	3.1	∞
5	11.9	25	700	350	4.8	2.8	∞
6	9.3	18	700	350	5.0	2.6	39
7	4.6	25	800	350	6.0	2.9	20
8	8.1	26	400	100	7.3	3.3	17
9	4.0	17	900	400	7.1	3.0	12
10	10.0	23	700	500	8.1	3.2	11
11	4.6	18	800	500	7.7	2.9	9.3
12	12.0	44	900	600	7.8	2.8	8.1
13	5.5	20	900	750	9.0	3.2	8.9
14	5.7	13	900	775	11.0	3.2	6.7
15	1.5	13	800	675	16.1	4.4	8.8
16	4.6	16	700	550	9.5	2.3	4.2
17	6.8	15	800	600	11.7	2.8	4.9
18	1.6	15	900	525	14.8	3.4	5.8

* Questionable tracer intercept.

MI-111

Tracer generation occurred from 1400 to 1430 PST. QARTS equipment was activated at 1400, and continued in operation until 1715. Tracer was intercepted during the interval 1408 to 1458. Filters exposed from the aircraft showed significant amounts of tracer on those exposed to 1500; subsequent filters showed background amounts of tracer. Aircraft sampling after 1500 proceeded to the east southeast to distances as great as Santa Barbara.

Wind directions at the surface in the neighborhood of the ground plume agreed with the actual plume location. Speeds were 2 to 3 mps south of the plume centerline and 4 to 6 mps to the north. Building 22 and Ionospheric Sounder winds up to 1300 ft were all within the range 260 to 280° at the 1400 and 1500 soundings. Speeds at Building 22 were 4 to 5 mps, and 1 to 2 mps at Ionospheric Sounder. Wind speeds, then, offer no contradiction to the computed Min Tracer Speeds.

The base of the inversion at Building 22 was at 1000 ft MSL at both the 1400 and 1500 PST soundings, and there was a superadiabatic lapse rate from the surface up to 700 ft MSL. The intermediate level, 700 to 1000 ft, was stable at both soundings, being -0.3F°/100 ft at 1400 PST, and isothermal at 1500 PST. At Ionospheric Sounder at 1400 PST, a superadiabatic lapse rate existed up to the base of a steep inversion at 1300 ft MSL. At 1500 PST, a more complicated picture existed. A superadiabatic layer was indicated from the surface to 700 ft MSL. An inversion of 1.3F° was found from 700 to 1000 ft. From 1000 to 1300 ft, there was no change in temperature. The steep inversion of about 14F° in the lowest 400 ft began at 1300 ft MSL.

In this test we find a considerable number of intercepts in the 700 to 1300 ft MSL layer. This layer was stable, in both Building 22 soundings and in the 1500 PST Ionospheric Sounding. There is the possibility that the superadiabatic lapse rate to 1300 ft, which was in existance at Ionospheric Sounder at 1400 PST, better described the

atmosphere during plume traversal until near 1500 PST. If this had been the case, then mixing to about 1300 ft could have taken place before the atmosphere became stable. To give an idea on the timing on the intercepts, Intercept 6 was observed at 1415 PST, Intercept 14 at 1530, Intercept 20 at 1446, and Intercept 24 at 1458.

Note that no tracer was observed above 1300 ft MSL, the highest level at which the inversion base was observed on any of the four soundings considered.

Resolution of how much penetration (if any) there was by tracer into the stable atmosphere is difficult because of the conflicting meteorological evidence. The author's judgment is that the major penetration occurred while the atmosphere was unstable to near neutral.

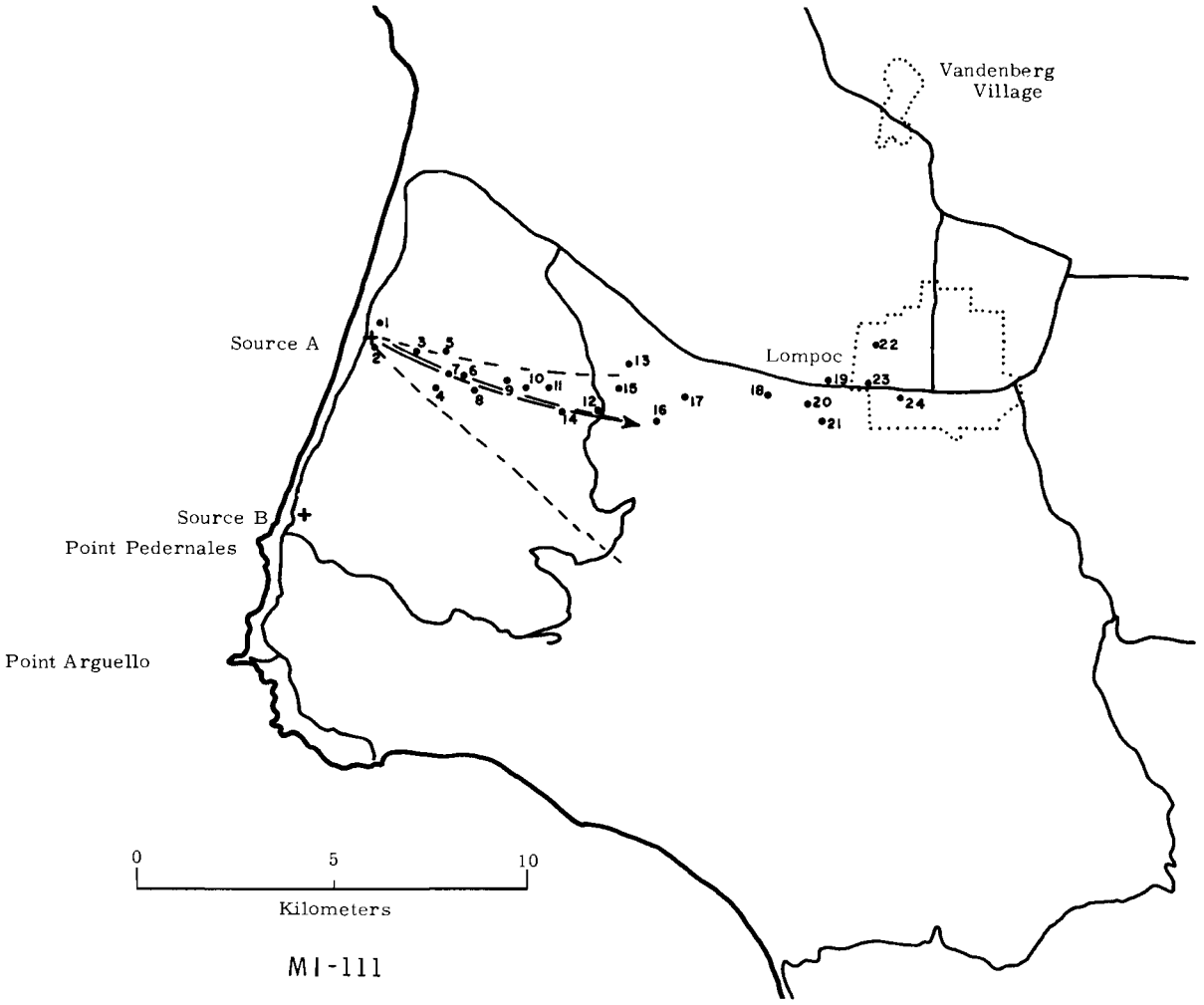
Vandenberg
Village
Source A
Lompoc
Source B
Point Pedernales
Point Arguello
0
5
10
Kilometers
MI-111

FIELD TEST MI-111

Tracer Intercept Number	Normalized Peak Concentration g/m^3	Duration in Seconds	Sampling Location: Altitude, ft MSL	Sampling Location: Altitude, ft Above Surface	Sampling Location: Distance from Source, km	Tracer Speed: Min, mps	Tracer Speed: Max, mps
1	> 1.2	11	400	275	0.6	1.4	∞
2	8.9	5	500	375	0.2	0.4	∞
3	9.1	5	700	450	1.1	1.9	∞
4	1.4	8	800	425	2.0	2.9	∞
5	1.6	8	800	425	1.9	2.4	∞
6	3.2	9	800	425	2.4	2.7	∞
7	6.2	6	600	225	2.1	2.2	∞
8	2.1	14	800	400	2.8	2.5	∞
9	2.2	13	800	400	3.5	2.9	∞
10	2.0	18	800	400	4.1	3.4	∞
11	> 0.35	25	800	400	4.6	3.2	∞
12	1.8	27	1000	400	6.0	3.8	∞
13	1.8	11	900	525	6.6	3.8	∞
14	0.65	18	1300	700	5.1	2.8	390
15	1.9	40	1000	600	6.4	3.3	49
16	1.3	36	1000	600	7.5	3.7	27
17	1.7	35	800	600	8.0	3.6	18
18	2.2	32	1100	950	10.2	4.5	21
19	2.0	42	800	675	11.7	4.6	15
20	0.74	42	1000	850	11.2	4.1	12
21	> 1.2	25	1000	800	11.7	4.2	12
22	0.48	68	1000	875	12.8	4.4	12
23	0.77	45	1000	875	12.7	4.1	9.9
24	1.7	23	900	775	13.6	3.9	8.1

* Questionable tracer intercept.

MI-112

Aircraft sampling from 1401 to 1657 PST during this field test was fruitless. Low stratus clouds prevented any low level sampling over the base. A scan of a wide area embraced roughly by Lompoc, Jalama Beach, Carpinteria, the Santa Barbara Reservoir, and Route 154 back to Lompoc revealed no certain intercepts with the plume. Posttest analysis of winds suggests that the aircraft was sampling downwind of the most distant portion of the tracer plume.

MI-113

Severe turbulence was encountered in the Sudden Ranch area during one-half hour of pretest background sampling, and continued during the initial attempts at plume interception. The aircraft run was aborted shortly after the first intercept of the tracer, due to airsickness of a crew member.

ANALYSIS AND CONCLUSIONS

Vertical Extent of Tracer with Respect to Thermal Stability

In attempts to analyze the data from these aircraft tests, it seemed reasonable to categorize the tests on the basis of thermal stabilities. It was found that both wiresonde data from near the tracer source and WIND Station 300 data showed superadiabatic conditions for all tests during which they and the aircraft were operated. (Wiresonde was operated during 20 of the 23 successful aircraft runs; the WIND network gave data for 12 of the 23.) Thus, these systems showed an atmosphere which was unstable from the surface to about 300 ft. This common characteristic, superadiabatic conditions, made differentiation of field tests on the basis of WIND or wiresonde temperature lapse rates impossible.

Examination of radiosonde data generally confirmed a temperature decrease with elevation at low levels, with the exception of test MI-10--one of the tests for which neither WIND nor wiresonde data were available. (In test MI-10, the prerun sounding showed a temperature inversion reaching to the surface). At levels above those monitored by the WIND system or by the wiresondes, there were considerable differences in thermal stratification from test to test. It is on the basis of the radiosonde data that some classification of the aircraft runs has been attempted. For each test, Figure B-1 depicts the thermal stratification felt to be most representative of the atmosphere during aircraft sampling.

The first category of stability includes tests where temperature at least decreased at the adiabatic rate (-0.5F°/100 ft) throughout the lower 3,300 ft of the atmosphere. Tracer diffusion would be expected to proceed at a high rate and to relatively high elevations during such tests.

The second category includes tests where no temperature inversion was present, but which included a layer whose temperature lapse rate was between isothermal and adiabatic (0 to -0.5F°/100 ft). Such layers would be expected to somewhat inhibit vertical motions.

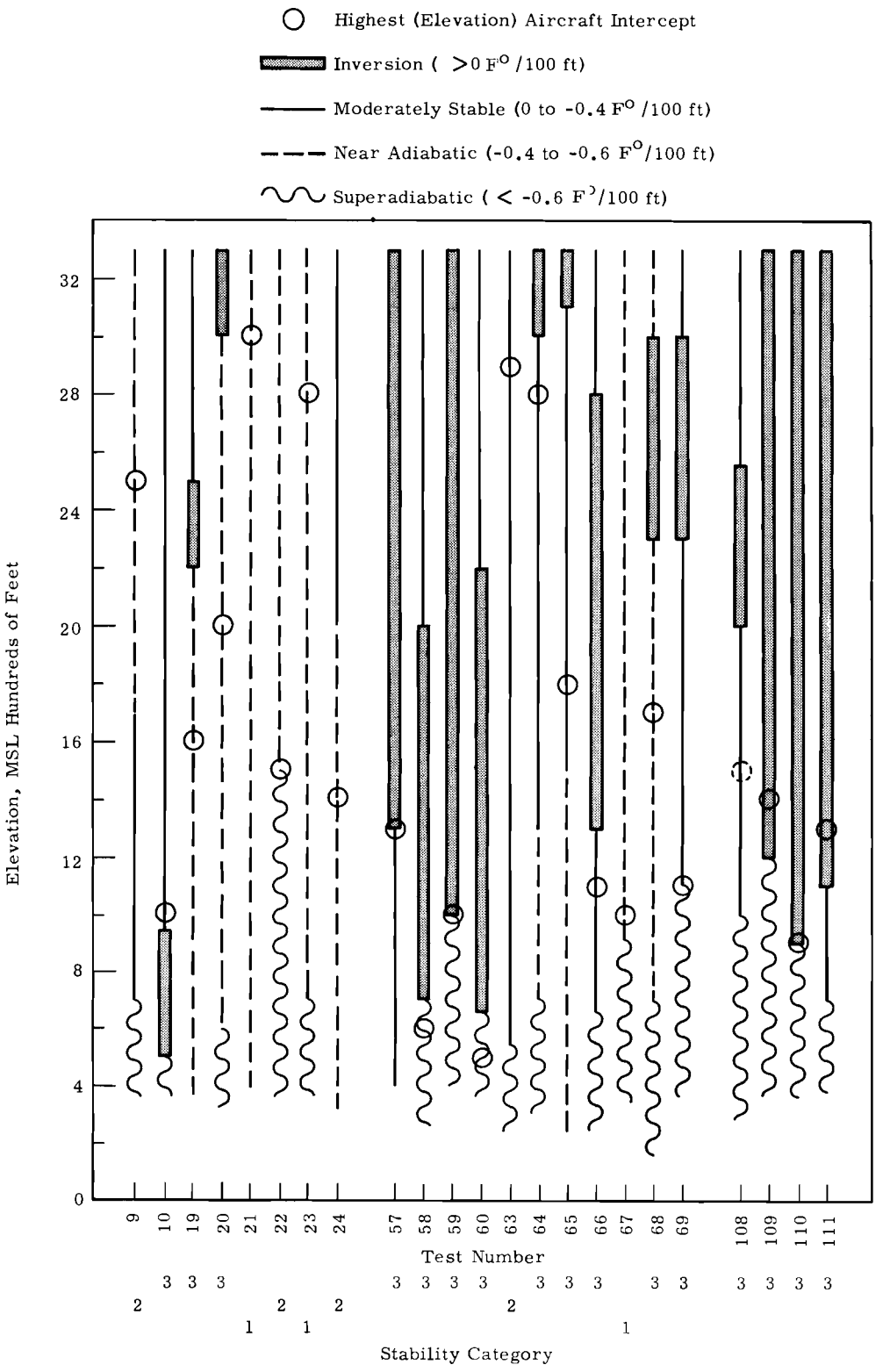

FIGURE B-1. Thermal Stratification During Aircraft Field Tests

The final classification, which claims 16 of the 23 aircraft tests, includes those where a temperature inversion was observed below 3,300 ft. MSL. Such an increase in temperature with height would, of course, be expected to greatly suppress vertical atmospheric motions.

Before listing the field tests by category, it should be mentioned that time and spatial differences in vertical thermal structure frequently complicated the selection of the proper category for a field test. The temperature soundings at the four radiosonde stations were not necessarily in agreement, nor were successive soundings taken at the same station identical. In an area so near to the seacoast, in terrain as rugged as the South Vandenberg area, and throughout sampling periods of up to 3 hours, such differences in soundings are not unexpected. However, it did complicate the classification procedure, and the significant differences are mentioned in the individual discussions of each field test. An attempt was made to categorize on the basis of the soundings most representative of the time and location of aircraft sampling.

One more point should be noted before proceeding with the thermal classification. Only the confident aircraft tracer intercepts were considered in specifying vertical extent of tracer. These are the intercepts shown on Figure B-1 (with the exception of MI-108 where no confident intercepts were made).

Three tests were included in the first or adiabatic to super-adiabatic category. These tests were MI-21, 23, and 67. Both tests MI-21 and 23 show confident intercepts as high as 2,800 ft MSL and are among the highest confident intercepts encountered. No such high elevation intercepts were found during MI-67, but QARTS insensitivity coupled with low concentrations precluded much successful sampling during this run.

It is difficult to draw conclusions on expected concentrations since too few measurements were made at or near a given distance from the source to insure statistical significance. For instance, it is possible to traverse through a given spatial location with the aircraft and find a significant amount of tracer, but repeat traverse would likely

reveal a much different concentration -- possibly zero. There is no assurance that the peak observed on a given traverse is representative of the peak possible at that location. If peak concentrations on a distance versus height graph are plotted, relatively high and low concentration values plotted side by side are found. If the peak concentrations (defined here as the highest expected instantaneous concentration), are sought then the low values should be ignored. In such a graph, a plotting of, say, 20 points may result in the use of only the three or four highest values for isoplething peak concentrations.

After pointing out the difficulties involved in drawing conclusions concerning concentration, we point out with some reservation that there is a tendency for isopleths of extreme concentration for the unstable runs to be lower at a given elevation and distance than for the other two stability categories.

The second category of field runs includes tests MI-9, 22, 24, and 63. Tests MI-9 and 63 showed that there could be significant penetration of the slightly stable layer, i.e., the layer with a lapse rate between isothermal and adiabatic. However, the lack of sampling in this slightly stable layer during MI-24 precludes drawing any such conclusion. MI-22 differs from other runs because no vertical mixing was apparent beyond the base (1500 ft MSL) of the slightly stable layer (-0.3F°/100 ft). Mixing into such a layer, below a layer of greater stability, was evident in tests MI-10, 57, 64, 66, 68, and 109 as well as the just mentioned tests, MI-9 and 63. Perhaps the soundings made during MI-22 differed significantly from the temperatures actually in existence at the tracer sampling locations.

The third category of tests are those where a temperature inversion existed with a base at an elevation less than 3,300 ft MSL. Tests MI-10, 19, 20, 57, 58, 59, 60, 64, 65, 66, 68, 69, 108, 109, 110, and 111 fall into this class. As just mentioned, tracer was found to penetrate significant depths into layers whose lapse rate was between isothermal and adiabatic. The question is can tracer penetrate into an

inversion layer to any great depth. No penetration beyond about 100 ft was found, with the exception of test MI-10 and possibly MI-109 and 111.

As noted in the MI-109 and MI-111 sections, a difference in inversion height between sounding stations leaves some doubt as to the representative inversion height to choose. However, one of the choices, which is most likely the case, places the inversion base near or above the elevation of aircraft tracer intercepts.

Furthermore, even if the soundings with inversion bases at their lowest levels are considered representative, the results are not startling. If surface parcels of air were lifted adiabatically and minimal mixing with the ambient air were assumed, the parcels would come to thermal equilibrium within 300 ft of the highest intercept elevation observed by the aircraft.

In test MI-10, if the post test radiosonde (taken at Building 22) is accepted as representative, frequent penetration occurred through 300 ft of the inversion layer—one penetration of 400 ft, and one through the entire 450 ft thick inversion layer. However, deeper penetrations would have occurred if the pretest radiosonde is accepted as representative.

Lifting and adiabatic warming of a surface air parcel of the 1400 PST sounding would have brought the parcel to equilibrium at less than 600 ft MSL. It is unfortunate that the frequency of soundings during this relatively early-in-the-series test was not higher, so soundings could have been nearer to generation time. Generation began at 1200 PST, and the last aircraft sampling occurred at 1321. It is probable that the inversion in existence during sampling was more like that found at 1400 PST (when a 1.3F° increase from 500 to 950 ft was observed) than at 1100 PST (when a strong surface inversion extended to 660 ft or more).

Horizontal Distribution of Tracer Intercepts with Respect to Ground Plume

The measured or predicted ground-level plume can be used as a basis for specifying the expected location of the aloft plume. Figure B-2

displays a plot of tracer intercept locations (projected to the ground) with respect to the ground plume centerline. Only confident tracer intercepts are plotted. The points plotted include those generated during the same seven tests used in the section on the comparison of peak-to-mean concentrations (MI-9, 19, 21, 23, 109, 110, and 111). Since the absolute value of concentration was not a criterion during this plotting, intercepts from eleven more tests could be used (MI-57, 58, 59, 60, 63, 64, 65, 66, 67, 68, and 69). Since the technique of plotting involved specification of a distance from the ground plume centerline, the specification could only be made within or near the area where ground samplers were exposed. The total number of intercepts plotted on this composite is 137.

At first glance, the figure suggests that a bias of the intercepts exists counterclockwise from the plume centerline. In fact, if only frequency is considered, there is nearly an even split--50.7% of the points being counterclockwise of the centerline and 49.3% found clockwise.

The percentages at the right of Figure B-2 show that a bit of a bias does exist toward counterclockwise displacement if distance from centerline is considered. The inner envelope embraces 50% of the points but of the 50% remaining outside the envelope, 23% are in a clockwise direction. A similar bias is evident beyond the 83% envelope. The uncertainties in plotting of the original aircraft location and the small number of points (especially beyond 1 km from the source) leave the significance of this observed bias in doubt. Furthermore, the question becomes relatively unimportant in the suggested application of the data.

If the centerline of the ground plume is known or predicted, then Figure B-2 provides a means for estimating locating of the aloft plume at distances up to 10 km from the source. For instance, at a distance of 6 km from the source, the aloft plume would be found within 1 km of the ground-plume centerline about 50% of the time, and within 2 km of the centerline 83% of the time. (The "within" distances refer to the projection of the aloft plume to the ground.)

Although the graph in Figure B-2 does not extend beyond 10 km an extrapolation suggests that at a distance of 20 km from the source,

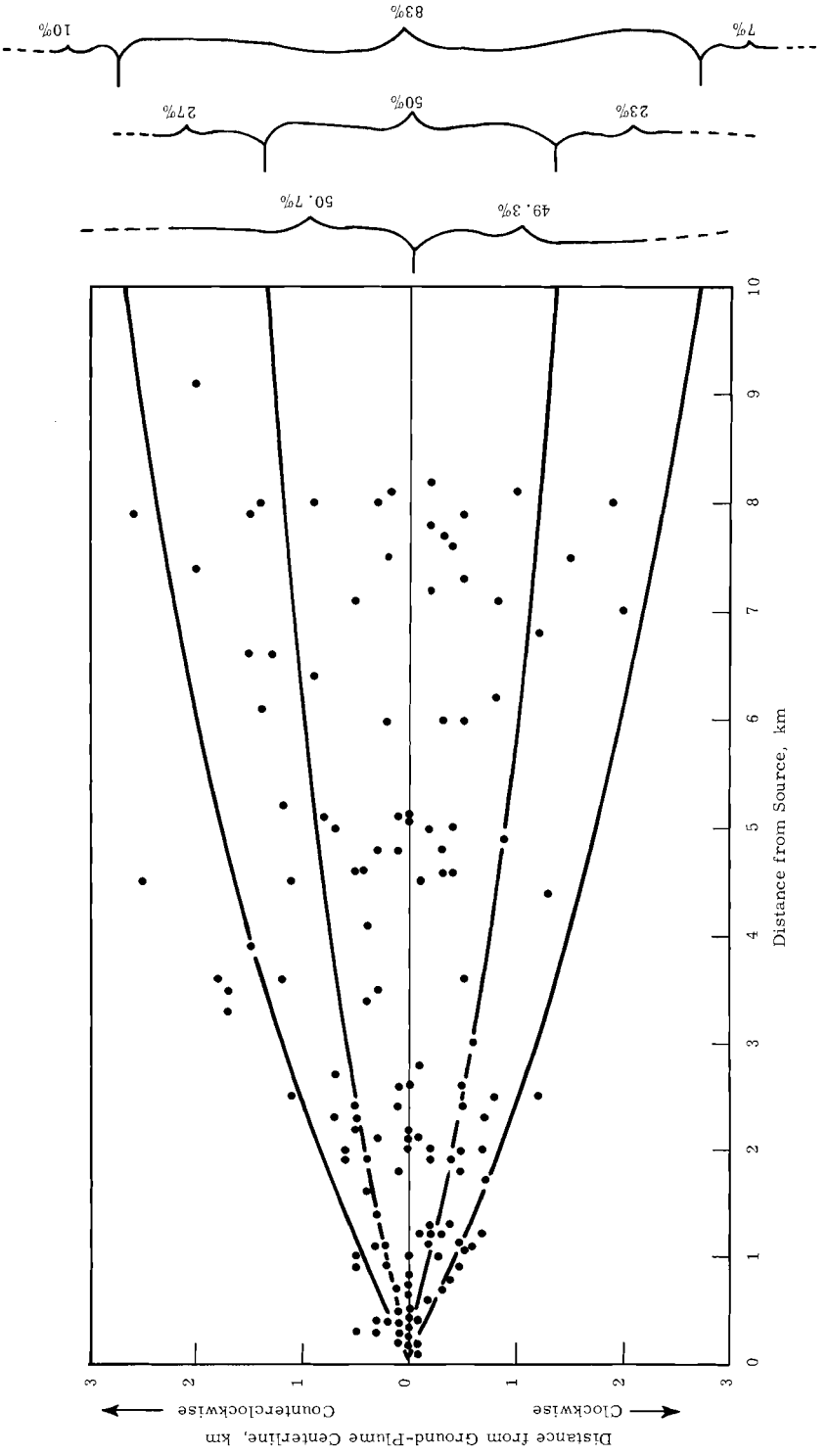

FIGURE B-2. Location of Aloft Tracer with Respect to Ground Level Centerline

the aloft plume will be within 2 km of the ground plume centerline 50% of the time, and within 4 km 83% of the time.

A second statistical approach was made to the specification of aloft tracer intercepts with respect to the ground plume. In this case, the extremities (rather than the centerline) of the ground plume were considered. These extremities (the dashed lines on the maps in the section on airborne tracer monitoring) were extrapolated when aircraft sampling was at distances beyond the extent of ground sampling. It was found that 85% of all aircraft intercepts fall within the boundaries of these ground exposures. If the questionable intercepts (x's) are ignored, the figure goes up to 90%. If the intercepts considered are restricted to those found beyond 10 km, the total and "confident only" figures become 91% and 94%.

It is seen that the ground level tracer patterns were a good indicator of where the aloft tracer could be found; however, the aircraft was flown primarily in areas where tracer was expected. It is less likely, but possible, that tracer could have been found at other more unexpected locations. The aircraft intercept is, though, biased to some (hopefully) small degree toward reporting tracer at expected locations.

Location of Tracer Intercepts with Respect to Measured Winds

With the exception of a few anomolous intercepts, almost all field test found tracer intercepts in locations that were explainable on the basis of measured winds--surface or aloft. Computed tracer speeds (tabled with each test) and intercept areal locations agreed with measured wind speeds as well as directions. The only run with significant disagreement was MI-21, and here the disagreement was in speed only. As noted in the detailed discussion of MI-21, the minimum speed computed for several tracer intercepts was greater than any measured winds.

Comparison of Peak Aloft Concentrations to Peak Ground Concentrations

Of interest in a hazard analysis associated with a ground-level release is the relationship between "ground" concentrations of a contaminant and concentrations expected aloft. In the current study, this

relationship was investigated by comparing the peak instantaneous concentration, observed by the aircraft at a given distance from the source, to the mean centerline concentration measured at the ground at the same distance.

Concentration measurements made by the aircraft were normalized to a unit emission rate by dividing the measured concentration (g/m^3) by the tracer emission rate (g/sec). The resulting units are sec/m^3. Ground exposures ($g\text{-}sec/m^3$) were normalized to unit mass by dividing by the mass emitted (g); the resulting units are also sec/m^3. Thus, the ground normalized exposures, E/Q, may be considered as concentrations normalized to unit emission rate. It is possible to compare the near instantaneous concentrations, χ_i, measured aloft by the aircraft to the mean centerline concentration, $\overline{\chi}_p$, measured at the ground. If, somehow, one is able to specify that the concentration measured by the aircraft at a given distance is the highest concentration occurring at that distance, then the ratio $\chi_{ip}/\overline{\chi}_p$ can be formed for that distance, where χ_{ip} is near instantaneous peak concentration observed aloft.

Before proceeding with a description of the analysis, it should be stated that the method necessary to develop the aloft-to-ground comparison entails use of techniques and data that are less than ideal. Yet, the comparison should offer some "feel" for the magnitude of the aloft concentrations that can be associated with the predicted ground concentrations.

On the ground, the large number of samples obtained close to and concurrent with the centerline sample build confidence in its validity. The data are restricted to a single plane 1.5 meters above the surface. The "plane" may be badly warped by terrain, but it is an easily defined surface. The aircraft intercepts with tracer are a series of relatively random intercepts with a plume, no two of which are concurrent in time. As previously noted, a repeat traverse of a zone showing a high tracer concentration may result in finding no tracer at all.

The aircraft has an infinite number of planes through which it must search out tracer, and yet the total number of tracer intercepts throughout all aircraft tests is of the same order of magnitude as the number of samplers exposed on one ground test.

The peak aloft concentrations employed in forming the aloft-to-ground ratio are those reported in the data already tabulated for each field test. These values are the farthest upscale point reached by the QARTS system recorder pen during each intercept. It is unfortunately true that the magnitude of this pen excursion across the chart is to some degree a function of the sensitivity adjustment of the recorder. Although an attempt was made to maintain a constant sensitivity adjustment, this may not have been always possible. (The possibility of using a mean signal level for a short - say, one second - increment of time to define peak concentration was considered, but the problem of defining the area under a near instantaneous up and down pen motion would have arisen frequently.)

At the ground, the plume centerline is relatively easily defined within the area embraced by the ground samplers. However, as pointed out in the ninth paragraph under "Analysis and Conclusions, Vertical Extent of Tracer with Respect to Thermal Stability," perhaps only 3 or 4 aircraft intercepts from an entire field test may be available to specify the extreme or peak concentrations on a graph embracing tens of kilometers in the horizontal and 3000 ft in the vertical. Even if one can select the few near-peak aircraft concentrations available from each field run, problems arise if the intercepts occur beyond the zone where ground samplers provide data with which to compare them.

Despite the problems mentioned in the preceeding paragraphs, it was felt that some comparison of aloft-to-ground concentrations was in order. Of the 23 tests when the aircraft was operated successfully, eleven (MI-57 to 69) were eliminated because the concentrations obtained were relative only--not absolute. Four more tests (MI-10, 20, 22, 24) were eliminated because the tracer went offshore or in some direction where very few ground samplers were available for

specifying ground centerline concentration. Since Test MI-108 entailed only questionable intercepts, it was eliminated by the decision to consider only confident intercepts. Seven tests remained (MI-9, 19, 21, 23, 109, 110, and 111).

The problem of lack of plume centerline definition below some of the more distant tracer intercepts was solved by plotting the centerline $\overline{\chi}_p$ (i.e. E/Q) values versus distance and extrapolating the curve as far as necessary.

The ratio $\chi_i / \overline{\chi}_p$ was computed for each QARTS tracer intercept. These ratios were plotted versus distance from the source. The points plotted on Figure B-3 from test MI-23 include ratios for all confident intercepts. However, only the highest ratios were selected as a guide in the plotting of the peak aloft concentration ratio, $\chi_{ip}/\overline{\chi}_p$. This curve is labeled "MI-23 (Typical)" on Figure B-3.

Although the points for individual aloft-to-ground ratios for other runs are not plotted, the other curves on Figure B-3 were determined in the same manner as the one for MI-23. The extent of the curves along the distance axis is dictated by the range of distances over which aircraft intercepts occurred, except that the curves were not extended closer to the source than 0.5 km. The proximity of the plume to the ground would limit the ability of the aircraft in finding χ_{ip} at short distances.

Although it is debatable whether to draw the curves as the straight lines indicated, the paucity of data and approximations used in obtaining the data make the question somewhat academic. In any event, it is true that the curve can never go below a ratio of one. The temptation to draw the curve for MI-23 points in a concave upward fashion is not evident in points plotted from the other six tests.

The curve for test MI-23 has been designated "typical" because it falls in the middle of the group of curves, it has a slope reasonably typical of the others, and the data extends over a relatively wide range of distances. The equation for this curve is $\chi_{ip}/\overline{\chi}_p = 2.0\ X^{1.2}$, where

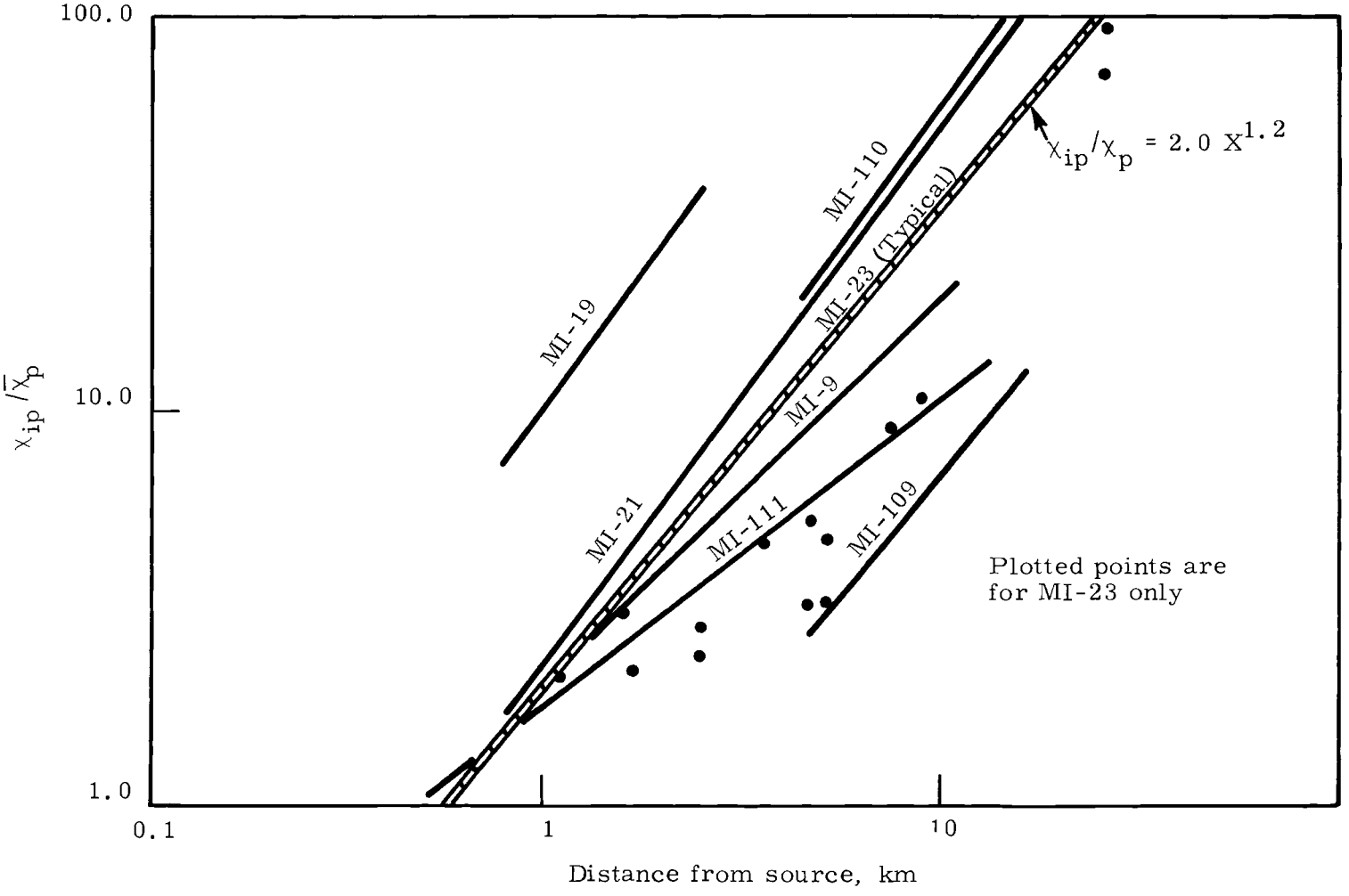

FIGURE B-3. $\chi_{ip}/\bar{\chi}_p$ Versus Distance from Source

X is the distance from the source in kilometers. The curves derived from aloft-to-ground concentration ratios from the other six tests range from about 5 times the "typical" values to 1/5 these values.

As previously stated, the data and techniques are not flawless, but the curves do give some guidance in terms of the relationship between the centerline mean concentration expected at the ground and the peak instantaneous concentration which may be expected aloft. It is very unlikely that ground-level peak instantaneous concentration will exceed those expected aloft, since diffusion aloft is considerably slower than at ground level.

SUMMARY

Appendix B results are summarized as follows:

- Where superadiabatic and/or adiabatic conditions existed, tracer was found at relatively high elevations and at relatively low concentrations.
- Where thermal stratifications between isothermal and adiabatic existed, tracer was frequently found well within or at the top of these relatively stable layers.
- Where a temperature inversion was found, tracer penetration into the inversion layer was minimal. The one exception involved penetration through a relatively weak inversion layer (1.4F° through 450 ft).
- Tracer intercepts were found at locations and distances consistent with measured surface and/or aloft wind directions and speeds.
- Approximately 90% of the aircraft tracer intercepts were made above the area swept by the ground-level plume.
- The relationship between the mean ground-level plume centerline ($\overline{\chi}_p$) concentration and the instantaneous aloft peak concentration (χ_{ip}) can be approximated by the expression $\chi_{ip}/\overline{\chi}_p = 2.0\ X^{1.2}$, where X is the distance from the ground source in kilometers.

APPENDIX C

LIST OF ABBREVIATIONS, TERMINOLOGY, AND UNITS

APPENDIX C

LIST OF ABBREVIATIONS, TERMINOLOGY, AND UNITS

The terminology of the various symbols used throughout the body of the text are given here. Unless otherwise noted, the units to be associated with the variables are in terms of meters, grams, seconds, radians, and Fahrenheit degrees.

E	Exposure (time--averaged concentration)
E_p	Centerline exposure
Q	Rate of release of tracer
Q_T	Mass of tracer released during test period
χ	Concentration
M	Molecular weight of gases (used in prediction equations)
$\bar{u}$	Mean wind speed
θ	Wind direction
v'	Fluctuation speed of lateral component of wind
X	Downwind distance from release point, along mean wind, usually in meters
y	Crosswind distance
z	Height above surface
t	Travel time downwind from release point
σ_y	Standard deviation of crosswind plume distribution
σ_z	Standard deviation of vertical plume distribution
σ_θ	Standard deviation of crosswind wind fluctuations
σ_v	Standard deviation of lateral wind speed
ΔT	Temperature difference $T_{z2} - T_{z1}$
β	Ratio of Lagrangian to Eulerian time scales
R_ξ	Lagrangian correlation coefficient between events at time t and $t + \mathcal{E}$
χ_i	Instantaneous aloft concentration
χ_{ip}	Peak instantaneous aloft concentration

The engineering units used in the operational equations are:

χ/Q	Normalized concentration in ppm NO_2/lb per minute release
X	Distance in feet
σ_θ	Standard deviation of wind direction fluctuations in degrees, measured at 12 feet and averaged over 10-second intervals
$\bar{u}$	Mean wind speed in knots, measured at 12 feet
ΔT_1^2	Temperature difference in degrees Fahrenheit, between heights 1 and 2 (heights in feet)

These units are common to all equations unless explicitly noted.

APPENDIX D

LOCATOR MAP

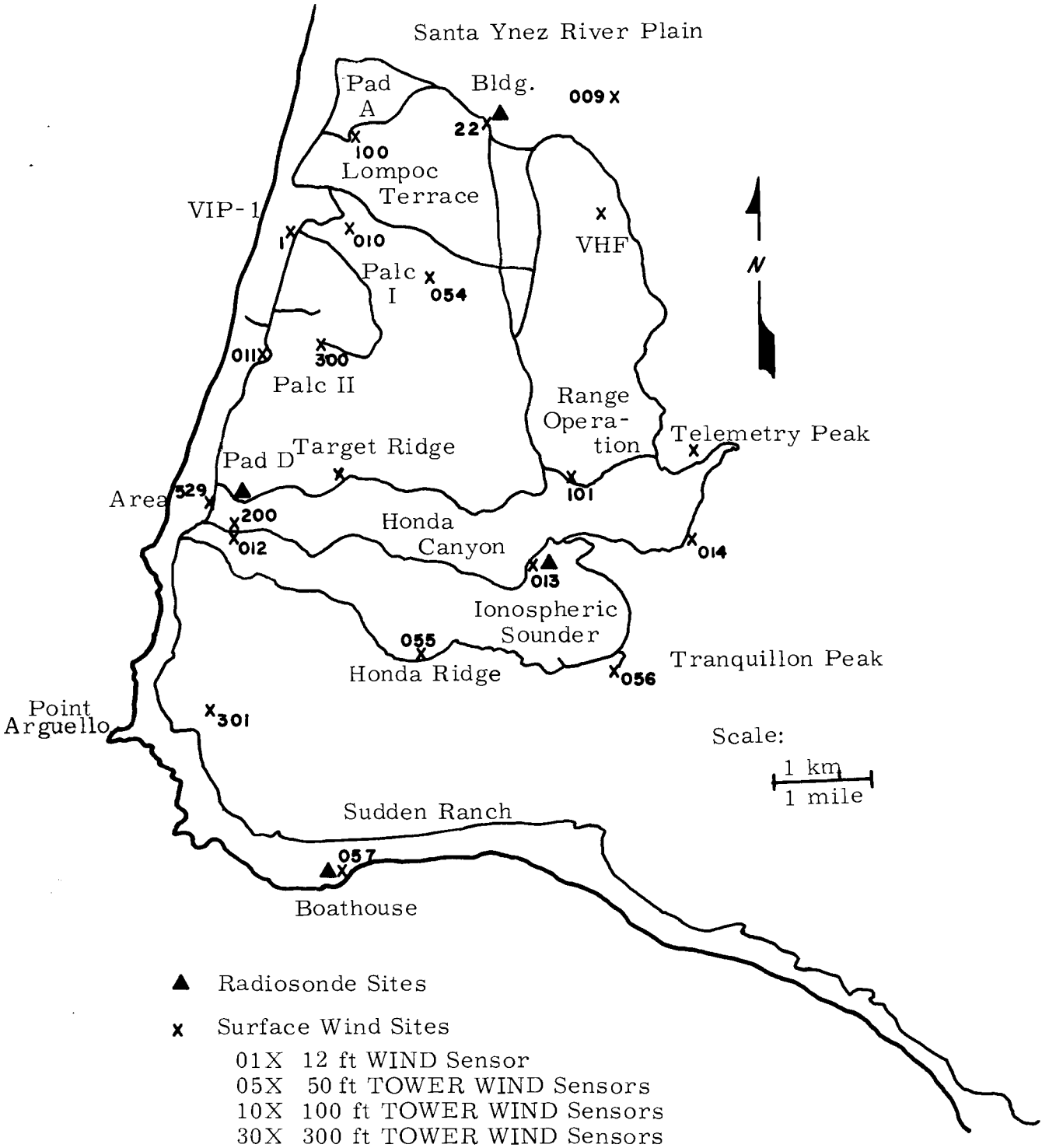

FIGURE D-1. Locater Map

REFERENCES

1. T. B. Smith, E. K. Kauper, S. Berman and F. Vukovich. Micrometeorological Investigation of Naval Missile Facility, Point Arguello, California, vol I, Meteorology Research, Inc. 2420 North Lake Avenue, Altadena, California. 1964

2. G. A. Demarrais, G. C. Holzworth and C. R. Hosler. Meteorological Summaries Pertinent to Atmospheric Transport and Dispersion Over Southern California, Tech. Paper 54, Weather Bureau (ESSA) Dept. of Commerce, Washington, D.C. 1965.

3. M. L. Barad and J. J. Fuquay. The Green Glow Diffusion Program, Vol I. AFCRL-62-251(I) Geophysics Research Directorate, Air Force Cambridge Research Laboratories, Bedford, Massachusetts. 1962.

4. G. I. Taylor. "Diffusion by Continuous Movements," Proceedings of the London Mathematical Society, ser. 2, vol. 20. 1921.

5. F. Pasquill. Atmospheric Diffusion, Van Nostrand, London. 1962.

6. R. E. Munn. Descriptive Micrometeorology, Academic Press, New York. 1966

7. D. A. Haugen and J. H. Taylor (editors). The Ocean Breeze and Dry Gulch Diffusion Programs, Air Force Cambridge Research Laboratories. 1963

8. J. J. Fuquay and C. O. Simpson. "Atmospheric Diffusion Experiments and Prediction Models," Nuclear Safety, vol. 5, No. 4, pp. 403-407. 1964.

9. P. W. Nickola, M. O. Rankin, M. F. Scoggins, and E. M. Sheen. "A System for Recording Air Concentrations of Zinc Sulfide Fluorescent Pigment on a Real Time Scale," Journal of Applied Meteorology, vol. 6, No. 2. pp. 430-433. 1967.

DISTRIBUTION

Number of Copies	
2	AEC Chicago Patent Section G. H. Lee R. K. Sharp
5	AEC Library, Washington J. Z. Holland
3	AEC Richland Operations Office L. C. Brazley C. L. Robinson Technical Information Library
1	Battelle Memorial Institute, Columbus
20	Division of Technical Information Extension
300	U.S. Air Force, Vandenberg Air Force Base, California Col. Robert F. Durbin
324	Battelle-Northwest C. E. Elderkin J. J. Fuquay W. T. Hinds (316) P. W. Nickola R. S. Paul C. L. Simpson Technical Information Files (2) Technical Publications